Effects of proteasome inhibition on cisplatin-induced DNA damage responses in human cells

by

Kathleen Gallagher, B.Sc.
Centre for Chromosome Biology
School of Natural Sciences
National University of Ireland, Galway

Head of School: Dr. Heinz-Peter Nasheuer
Head of Biochemistry: Dr. Michael P. Carty
Research Supervisor: Dr. Michael P. Carty

Acknowledgments

I would like to sincerely thank my research supervisor, Dr Michael Carty, for his support, guidance, encouragement and inspiring discussions about RPA.

Thank you to the present and past members of the DDR team Séverine, Elaine, Aine, Mitra, Ania and Sarah for making the lab such an enjoyable place to be. A big thank you to Séverine for all your help and expertise over the past four years. A special thank you to Sarah and Laura for all of our wine sessions and for keeping me sane though the final stages of this thesis. Thank you to Aga for all the fun we had living together and for your delicious tomato soup. And thank you to Ania for just being Polish!

A special thank you to my family for all of their support during my studies. Their encouragement and belief, has led me to be where I am today.

Table of Contents

S. Cruet-Hennequart, **K. Gallagher**, A. Zielezny, S.Villalan., A. Prendergast and MP. Carty, DNA polymerase η, a key protein in translesion synthesis in human cells. Review. In *'Genome Stability and Human Diseases'* Subcell Biochem, 2010: 50, (189-209).

Abbreviations

APC/C	Anaphase-promoting compolex/cyclosome
AT	Ataxia telangiectasia
ATM	Ataxia telangiectasia-mutated
ATR	ATM and Rad3 related
ATRIP	ATR-interacting protein
BRCA2	Breast cancer type 1 susceptibility protein
BRCA1	Breast cancer type 1 susceptibility protein
BrdU	Bromodeoxyuridine
BSA	Bovine Serum Albumin
CDK	Cyclin-dependent kinase
Chk1	Checkpoint kinase 1
Chk2	Checkpoint kinase 2
CPD	Cyclobutane pyrimidine dimer
CTR1	Copper transporter
DAPI	4, 6 diamidino-2-phenylindole
DDR	DNA damage response
DMSO	Dimethyl sulfoxide
DBD	DNA binding domain
DNA-PKcs	DNA protein kinase catalytic subunit
DSB	Double-stranded DNA break
dsDNA	Double-stranded DNA
DTT	Dithiothreitol
DUB	Deubiquitinating enzyme
EDTA	Ethylenediamminetetraacetic acid
ERCC2	Excision repair cross-complementing rodent repair deficiency, complementation group 2
FA	Fanconi anaemia
FANCD2	Fanconi anaemia, complementation group D2
FBS	Foetal bovine serum
FHA	Forkhead-associated
FITC	Fluorescein iso-thiocyanate

GGR	Global genome repair
γH2AX	H2AX pSer139
HECT	Homologous to E5-AP Carboxyl Terminus
HJ	Holliday junction
HR	Homologous recombination
HRP	Horse radish peroxidise
HU	Hydroxyurea
ICL	DNA interstrand crosslink
IR	Ionising radiation
MCM	Minchromosome maintenance 2
MDC1	Mediator of DNA damage checkpoint protein-1
MDM2	Murine double minute
MMC	Mitomycin C
Mre11	Meiotic recombination 11
MRN	Mre11-Rad50-Nbs1
mTOR	Mammalian target of rapamycin
Nbs1	Nijmegen breakage syndrome protein 1
NER	Nucleotide excision repair
NHEJ	Non-homologous end joining
OB fold	Oligonucleotide binding fold
PBS	Phosphate-buffered saline
PCNA	Proliferating cell nuclear antigen
PFA	Paraformaldehyde
PI	Proteasome inhibitor
PIKK	Phosphoinositide 3-kinase-like kinase
PIP	PCNA-interacting peptide
PMSF	Phenylmethylsulfonyl fluoride
Polη	DNA polymerase eta
PTM	Post-translational modification
PVDF	Polyvinylidene fluoride
RING	Really Interesting New Gene
ROS	Reactive oxygen species
RNA	Ribonucleic acid
RPA	Replication Protein A

Rtp	Regulatory particle
SDS-PAGE	Sodium dodecyl sulphate-polyacrylamide gel electrophoresis
SSB	Single-stranded DNA break
ssDNA	Single-stranded DNA
SUMO	Small Ubiquitin-like modifier
SV40	Simian virus 40
TCR	Transcription coupled repair
TIPIN	Timeless interacting protein
TLS	Translesion synthesis
Ub	Ubiquitin
UBA	Ubiquitin associated domain
UBC	Ubiquitin conjugating enzyme
UBL	Ubiquitin like domain
UV	Ultra-violet
XP	Xeroderma pigmentosum
XPV	Xeroderma pigmentosum variant

Abstract

The proteasome is the main site of protein degradation in human cells, and plays a major role in the regulation of cellular processes including cell cycle progression, DNA repair and the DNA damage response. Proteasome inhibition is emerging as a new anti-cancer strategy, with the development of bortezomib for the treatment of patients with multiple myeloma. Proteasome inhibitors can be used either as single agents or in conjunction with other cancer treatments. Proteasome inhibitors can sensitise cancer cell lines to routinely-used cancer treatments including the platinum-based anti-cancer drug, cisplatin. The aim of this research was to investigate the effect of proteasome inhibition on cisplatin-induced DNA damage responses in human cells, including cell viability, cell cycle arrest and the phosphorylation of DNA damage response proteins.

The proteasome inhibitor MG132 sensitised the pol η-deficient human fibroblast cell line XP30RO to cisplatin. MG132 treatment induced strong cell cycle arrest, and prevented cisplatin-induced accumulation of XP30RO cells in S phase. As determined by western blotting, proteasome inhibition alone did not induce phosphorylation of the DNA damage response proteins, H2AX or Chk1. However, a novel phosphorylated form of the RPA2 subunit the trimeric, single-stranded DNA binding protein replication protein A (RPA), RPA2-pS4S8* was identified in MG132-treated cells. RPA2-pS4S8* is phosphorylated but is not hyperphosphorylated, based on gel mobility and western blotting following SDS-PAGE. RPA2-pS4S8* induction is independent of DNA damage but dependent on proteasome inhibition and was detected in all cell lines examined. Co-treatment of cells with MG132 did not alter levels of cisplatin-induced γH2AX, pChk1 or RPA2-pS4S8. Removal of cisplatin and MG132 led to the identification of novel, slow mobility forms of RPA2 by western blotting. Western blotting analysis, using an anti-ubiquitin antibody, of RPA2 immunoprecipitated from native and denatured cell extracts following provided evidence that slow mobility forms of RPA2 represented ubiquitinated forms of RPA2. The dependence of FANCD2 monoubiquitination on pol η was also investigated. FANCD2 is required for the repair of ICLs. Results showed an

increase of FANCD2 monoubiquitination in pol η-deficient cells compared to pol η-proficient cells.

In this study two novel forms of RPA2 have been identified: a DNA damage-independent RPA2-pS4S8* and DNA damage-dependent form which is consistent with ubiquitination of RPA2. These novel forms of RPA2 may be important in regulation of the cellular functions of RPA. This provides new insights into the relationship between proteasome function and the DNA damage response, in particular following cisplatin treatment.

Chapter 1
Introduction

1.1 Cancer

Recent statistics show that cancer is responsible for 25% of all deaths in Ireland and is one of the leading causes of death in the developed world. In a report issued by National Cancer Registry, Ireland, in 2006, cancer accounted for 3869 deaths among females and 4303 deaths among males in Ireland. On a global level the World Health Organisation (WHO) reported that 7.6 million people died worldwide as a result of cancer in 2008 (http://www.who.int/cancer/en/). The proliferation of human cells is a highly regulated process. Cancer occurs when cells evade the normal regulatory mechanisms which normally control cell division, leading to the rapid and uncontrolled growth of genetically abnormal cells resulting in the formation of a tumour. This can occur sporadically or as a result of genetic predisposition. Tumours can be classed as either malignant or benign. Malignant tumours have the ability to metastasise, where cells migrate through the circulatory or lymphatic system and invade other tissues. Malignant tumours pose a severe risk to the patient and are often fatal. Benign tumours are not able to metastasise and therefore pose relatively low risk.

There are six capabilities that distinguish cancer cells from normal cells (Hanahan and Weinberg, 2000). These are referred to as the six 'hallmarks' of cancer and were proposed by Hanahan and Weinberg, (2000). The six hallmarks include: (i) self-sufficiency in growth signals, (ii) insensitivity to growth inhibitory signals, (iii) evasion of apoptosis, (iv) acquisition of limitless replicative potential, (v) sustained angiogenesis, and (vi) tissue invasion and metastatic potential (Hanahan and Weinberg, 2000).

The characteristics of cancer cells which allow for uncontrolled growth and evasion of cellular regulatory mechanisms, which would normally prevent such uncontrolled growth, result from mutations in the genome (discussed in Loeb, *et al.*, 2003). The rate of spontaneously occurring mutations in human cells is approximately 1 per 10^9 nucleotides generated (Loeb *et al.*, 2003; Kunkel 2004) which is too low to account for the frequency of mutations in cancer cells. Loeb (1994) described the 'mutator hypothesis' which proposed that mutations that

occur in the early stages of tumour development occur in genes encoding proteins responsible for the maintenance of genome stability which would account for the high rate of mutations in cancer cells (Loeb *et al.,* 1974; Loeb 1994; Bielas *et al.,* 2006). Mutations, for example, may result from from errors generated by DNA polymerases during DNA replication or the failure to repair DNA damage. Analysis of a number of inherited cancer-prone disorders, are due to mutations in genes required for detecting DNA damage, cell cycle checkpoints and DNA repair (Cleaver 1968; Masutani *et al.,* 1999; Taniguchi *et al.,* 2006; Mavrou *et al.,* 2008), details of which will be described in later sections.

A number of agents used in cancer treatment act through the induction of DNA damage which can inhibit DNA replication and cell division, resulting in cell death through apoptosis or necrosis (Lawley *et al.,* 1996; Kartalou *et al.,* 2001; Chaney *et al.,* 2005). As many cancers have mutations in genes responsible for the repair of DNA damage, cancer cells may be more sensitive to these agents compared to normal cells. However, DNA damaging agents are themselves carcinogenic and can lead to the formation of secondary tumours in surviving cells. Anti-cancer agents targeting cellular processes including regulation of protein levels through the proteasome have been developed (Section 1. 4. 2) (Adams 2004; Adams *et al.,* 2004; Kropff *et al.,* 2006; Adams *et al.,* 2009). Inhibition of the proteasome leads to the disruption of cellular pathways, including cell cycle progression and DNA repair (Jacquemont *et al.,* 2007; Murakawa *et al.,* 2007).

Other anti-cancer treatments have been developed which target cellular signalling pathways. Tyrosine kinases are major mediators of signalling cascades which are classed as non-receptor tyrosine kinases and receptor tyrosine kinases which are activated by extracellular ligands binding to receptors on the cell surface (discussed in Paul *et al.,* 2004). Tyrosine kinases are required for signalling in cell proliferation, metabolism and apoptosis. Tyrosine kinases have been found to be overexpressed in some cancers leading to dysreguation of cellular processes. Inhibitors of the tyrosine kinases, eg. Gleevec, have been used successfully as anti-cancer treatments (discussed in Paul *et al.,* 2004). Monoclonal antibodies (mAbs) are also used in cancer therapy. Specific antigens

on the surface of tumour cells can be targeted by mAbs. Conjugation of mAbs to a toxin or cytotoxic agent can deliver the treatment directly to the tumour cells through the interaction of the antibody with a specific antigen displayed by tumour cells (discussed in Dalle *et al.,* 2008). mAbs have been shown to enhance the host immune response against cancer, induce apoptosis, block growth factor receptors and inhibit the proliferation of tumour cells (discussed in Dalle *et al.,* 2008).

1.2 The DNA Damage Response.

The DNA damage response (DDR) is the name given to the network of signalling pathways that monitor and protect the integrity of the genome (Zhou *et al.,* 2000; Harper *et al.,* 2007). Any un-repaired DNA damage can have detrimental effects on genetic stability. Cells deficient in components of this pathway are more sensitive to DNA damaging agents, and deficiencies in key repair pathways are the basis for a number of cancer prone human disorders. Thus, the DDR functions as a barrier against cancer (Zhou *et al.,* 2000; Bartkova *et al.,* 2005; Niida *et al.,* 2006; Bartek *et al.,* 2007; Harper *et al.,* 2007).

Cells are constantly exposed to DNA damage from both endogenous and exogenous sources (Friedberg *et al.,* 2004). Endogenous DNA damage can result from DNA replication error or can also be the result of reactive oxygen species (ROS) which are the by-products of biochemical reactions in metabolic pathways. ROS can cause oxidative damage to DNA leading to single- and double-strand breaks (SSBs and DSBs) (Kikugawa *et al.,* 2005). Exogenous damage can arise from exposure to environmental agents such as ultraviolet radiation from sunlight and cigarette smoke (Kier *et al.,* 1974; Kraemer 1997) or exposure to therapeutic agents used in the treatment of cancers including chemotherapeutic drugs and ionising radiotherapy induce DNA damage (Stein 1967; Chaney *et al.,* 2005). Several anti-cancer agents, including the chemical crosslinkers cisplatin and mitomycin C (MMC), kill cells by inducing DNA damage which interferes with DNA replication and cell division (Chaney *et al.,* 2005; Wang *et al.,* 2005a).

The DDR is a co-ordinated, highly regulated signalling cascade involving numerous proteins which detect DNA lesions and transduce signals to downstream effector proteins that determine the response to resolve the induced DNA damage (Zhou *et al.,* 2000; Harper *et al.,* 2007). The consequences of DDR activation include cell cycle arrest by induction of cell cycle checkpoints, DNA repair, or apoptosis where the DNA damage is too severe to repair (Zhou *et al.,* 2000; Harper *et al.,* 2007). Signalling in the DDR is mediated in large part through the post-translational modification (PTM) of downstream effector proteins, which leads to the recruitment of a plethora of proteins to the sites of damage. PTMs include phosphorylation, ubiquitination, SUMOylation, glycosylation, ADP-ribosylation, and methylation (Huen *et al.,* 2008).

1.3 PIKK mediated protein phosphorylation in the DNA damage response.

The phosphatidylinositol 3-kinase related kinases (PIKKs) are a family of proteins that include ataxia telangiectasia mutated (ATM), ataxia telangiectasia and Rad-3-related (ATR), DNA-dependent protein kinase catalytic subunit (DNA-PK_{cs}), mammalian target of rapamycin (mTOR; also known as FRAP), and SMG1 homolog, phosphatidylinositol 3-kinase-related kinase (hSMG1) (Abraham 2004). ATM, ATR and DNA-PKcs are activated following DNA damage (Bakkenist *et al.,* 2004; Cimprich *et al.,* 2008). PIKK substrates have been identified through the fact that PIKKs phosphorylate proteins at the consensus sequence, serine or threonine followed by glutamine (S/T-Q) (Kim *et al.,* 1999). However DNA-PK_{cs} also phosphorylates serine and threonines which are not followed by glutamine (Kim *et al.,* 1999). The ability of PIKKs to phosphorylate S/T-Q sites has led to the identification of a large number of PIKK substrates. Mass spectrometry analysis of phosphoproteins from IR-treated Hela cells identified 700 proteins that were phosphorylated on S/TQ sites and were therefore likely to be PIKK substrates (Matsuoka *et al.,* 2007). In response to UV-radiation in Hela cells, 464 proteins were identified that were phosphorylated on S/T-Q sites (Stokes *et al.,* 2007).

ATM is mutated in the autosomal recessive disorder, ataxia telangiectasia (AT) (reviewed in Mavrou *et al.,* 2008). AT is characterised by loss of Purkinje cells

leading to cerebellar degeneration, increased risk of respiratory disorders and cancer pre-disposition (Mavrou *et al.,* 2008). Ataxia refers to loss of co-ordination and telangiectasia to the appearance of small dilated blood vessels in AT patients (Mavrou *et al.,* 2008). AT is characterised at a cellular level by genomic instability and IR sensitivity (Savitsky *et al.,* 1995; Mavrou *et al.,* 2008). ATM protein is found in the nucleus as an inactive homodimer. In response to DNA damage, ATM undergoes autophosphorylation on Ser1981, Ser367 and Ser1893 leading to dimer dissociation and activation of kinase activity (So *et al.,* 2009; Kozlov *et al.,* 2011). ATM is recruited to sites of DSBs through its interaction with the Mre11/Rad50/Nbs1 (MRN) complex which tethers the ends of the DSB (Uziel *et al.,* 2003). Following activation, ATM phosphorylates a number of mediator and effector proteins in the DNA damage response, including H2AX, Chk2, p53, FANCD2 and BRCA1 (Banin *et al.,* 1998; Matsuoka *et al.,* 2000; Nakanishi *et al.,* 2002; Bakkenist *et al.,* 2004).

ATR plays a vital role in all stages of the cell cycle and in signalling in the DNA damage response (Cliby *et al.,* 1998; Wright *et al.,* 1998; Zhou *et al.,* 2000). ATR exists in a stable complex with its binding partner ATR interacting protein (ATRIP) (Zou *et al.,* 2003; Dart *et al.,* 2004; Itakura *et al.,* 2004a; Itakura *et al.,* 2004b). ATR/ATRIP is recruited to DNA following DNA damage through its interaction with the ssDNA binding protein replication protein A (RPA) which coats ssDNA generated at stalled replication forks (Zou *et al.,* 2003). ssDNA generated during the processing and resection of DSBs also recruits ATR to DNA (Zou *et al.,* 2003). Active ATR phosphorylates downstream DDR mediator and effector proteins including RPA (Olson *et al.,* 2006), Chk1 (Zhao *et al.,* 2001), p53 (Tibbetts *et al.,* 1999) and BRCA1 (Tibbetts *et al.,* 2000) .

DNA-PK is a large heterotrimeric protein consisting of the 460kDa catalytic subunit (DNA-PK_{cs}) and the Ku heterodimer (p70/p80) (Gottlieb *et al.,* 1993; Gottlieb *et al.,* 1994). DNA-PK is involved in the repair of DSBs through the non-homologous endjoining repair (NHEJ) pathway (Kurimasa *et al.,* 1999). DNA-Pk_{cs} is recruited to sites of DSBs through the Ku complex which binds to the ends of the DSB. Interaction with Ku stabilises DNA-PK_{cs} which otherwise has weak DNA binding affinity (Yaneva *et al.,* 1997; Falck *et al.,* 2005).

Following recruitment, DNA-PK$_{cs}$ is autophosphorylated on threonine 2609 by another DNA-PK$_{cs}$ molecule on the opposite side of the DSB (Chan *et al.,* 2002). DNA-PK$_{cs}$ phosphorylates other compontents of NHEJ machinery including XRCC4 (Yu *et al.,* 2003) and Artemis (Ma *et al.,* 2005). The RPA2 subunit of RPA is also phosphorylated in a DNA-PK dependent manner in response to DNA damage (Cruet-Hennequart *et al.,* 2006; Cruet-Hennequart *et al.,* 2008)

PIKK activation is required for efficient DNA repair. In these repair processes, the activation of PIKKs is often linked to subsequent substrate ubiquitination. A screen for potential ATM/ATR substrates was carried out using phospho-specific antibodies raised against already known ATM/ATR substrates which recognise phospho-SQ motifs. Antibodies were used to immunoprecipitate potential new protein substrates from lysates of IR or HU-treated HeLa cells (Mu *et al.,* 2007). This screen for ATM and ATR substrates identified proteins from the ubiquitin-proteasome pathway that contain an S/T-Q motif allowing these proteins to be phosphorylated by PIKKs (Mu *et al.,* 2007). Proteins identified in this way included members of the E3 ubiquitin ligases, deubiquitinating enzymes and many ubiquitin interacting proteins (Mu *et al.,* 2007). Functional analysis of some of these PIKK substrates revealed that they played a role in the regulation of cell cycle checkpoints following DNA damage (Mu *et al.,* 2007). In a number of DNA repair pathways phosphorylation of target proteins by PIKKs is required for further modification of the protein by ubiquitination. An example of this is in the Fanconi anemia pathway, in which the FANCI protein must be phosphorylated by ATR in order for the monoubiquitination of FANCD2 and activation of the pathway (Ishiai *et al.,* 2008) as described in Section 1.7.2.

1.4 The ubiquitin-proteasome pathway.

1.4.1 Ubiquitination

In addition to phosphorylation, one of the major post-translational modifications in the DDR and other cellular processes is ubiquitination. Ubiquitin is a 76 amino acid, 8kDa protein that can be attached to lysine residues on its target protein leading to protein ubiquitination (Huen *et al.,* 2007; Mailand *et al.,* 2007). The multi-step process that allows this to occur is highly regulated, and involves the

co-ordination of a series of enzymes including a ubiquitin-activating enzyme (E1), ubiquitin-conjugating enzyme (E2) and ubiquitin ligase (E3) (Hershko *et al.*, 2000; Pickart 2001; Fang *et al.*, 2004).

The first enzyme in the pathway is the ubiquitin-activating enzyme, E1, which forms a thiol-ester bond between its active site cysteine and the carboxyl-terminal glycine of ubiquitin (Fig. 1.1) (Ciechanover *et al.*, 1982). In mammalian cells there are two E1 enzymes, which are able to activate ubiquitin, namely, UBE1L2 and Uba6 (Chiu *et al.*, 2007; Jin *et al.*, 2007; Pelzer *et al.*, 2007). The activated ubiquitin on E1 is then transferred to the active site cysteine of an E2 ubiquitin-conjugating enzyme (UBC), by a transesterification reaction (Fig. 1.1) (Hershko *et al.*, 2000). The human genome encodes over 40 ubiquitin conjugating enzymes (UBCs), which contain a conserved 150-amino acid core domain that includes the cysteine which accepts an activated ubiquitin from E1 (Fang *et al.*, 2004; Ye *et al.*, 2009). Finally, an E3 ubiquitin ligase binds the E2 complex and facilitates the transfer of ubiquitin from E2 to a lysine residue on the target protein (Fig. 1.1) (Fang *et al.*, 2004; Robinson *et al.*, 2004). E3 ubiquitin ligases contain the signature motifs, HECT (Homologous to E6-AP Carboxyl Terminus), RING (Really Interesting New Gene) finger and RING-like motifs (Huibregtse *et al.*, 1995; Freemont 2000; Joazeiro *et al.*, 2000). There are more than 600 proteins in mammalian cells that contain the E3 ubiquitin ligases signature motifs (Yang *et al.*, 2009).. Ubiquitination is a reversible process, and ubiquitin can be removed from target proteins through the action of deubiquitinating enzymes (DUBs) (Wilkinson 2000; Fang *et al.*, 2004).

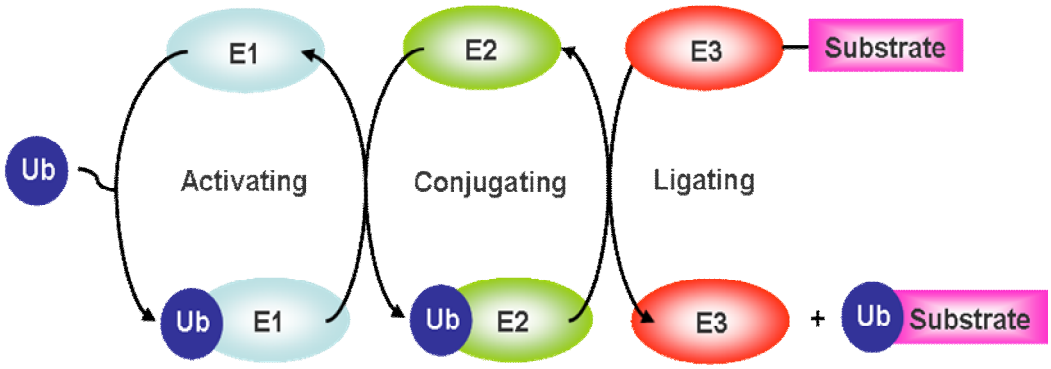

Figure 1.1: The enzyme cascade leading to protein ubiquitination. The multi-step process is highly controlled involving the co-ordination of a series of enzymes including a ubiquitin-activating enzyme (E1), ubiquitin-conjugating enzyme (E2) and ubiquitin ligase (E3). (adapted from Dikic et al, 2009)

Addition of one ubiquitin to a protein is termed monoubiquitination (Hicke 2001; Sigismund *et al.*, 2004). However a single ubiquitin on a substrate protein can be further modified through the addition of more ubiquitin molecules through one of seven lysines in ubiquitin. Polyubiquitnation though lysine 48 (K48) targets the substrate protein to the proteasome for degradation (Thrower *et al.*, 2000). However, polyubiquitination through lysine 63 (K63) on ubiquitin is involved in localisation and signalling of proteins in a proteasome independent manner (Varadan *et al.*, 2002; Varadan *et al.*, 2004). K48 polyubiquitinated proteins are recognised by subunits of the 19S regulatory particle of the proteasome, which contain ubiquitin-binding domains (Deveraux *et al.*, 1994; Elsasser *et al.*, 2005). Polyubiquitinated proteins may also be escorted to the proteasome through ubiquitin receptor proteins which contain one ubiquitin-like (UBL) domain that is recognized by the proteasome and one or more ubiquitin-associated (UBA) domains that bind ubiquitinated proteins (Hofmann *et al.*, 1996; Hiyama *et al.*, 1999; Elsasser *et al.*, 2002; Schmidt *et al.*, 2005)

In addition to ubiquitin, a number of related proteins have been identified in mammalian cells (Kerscher *et al.*, 2006). These include a family of ubiquitin-like protein modifiers including SUMO, Nedd8, FAT10 and ISG15 which can be conjugated to lysine residues on specific substrate proteins in a process similar to that of ubiquitination (Kerscher *et al.*, 2006). These modifications also modify

protein function, however, these modifications do not target proteins for degradation (Kerscher *et al.,* 2006).

1.4.2 The proteasome.

The proteasome is a large multi-subunit protein complex that is found both in the nucleus and cytoplasm of eukaryotic cells (Etlinger *et al.,* 1977). Many proteins are degraded by the ubiquitin-proteasome pathway which is responsible for the regulation of proteins involved in cellular processes including cell cycle, DNA damage signalling, DNA repair and apoptosis (Krogan *et al.,* 2004; Jacquemont *et al.,* 2007; Murakawa *et al.,* 2007; Motegi *et al.,* 2009). One critical element in the development of cancer is loss of cellular protein homeostasis. Because several cancers also result from defects in one or more DNA repair pathways, modulating proteasomal activity is a target in the treatment of cancer.

The 26S proteasome consists of two subunits: the 20S catalytic core particle and the 19S regulatory subunit (Fig. 1.2) (Voges *et al.,* 1999; Bedford *et al.,* 2010). The 20S core partcle which consists of four stacked heptameric rings, containing α- and β- subunits, that form a barrel-shaped protein complex with the two rings of β- subunits sandwiched between two rings of α-subunits (Fig. 1.2) (Gallastegui *et al.,* ; Lowe *et al.,* 1995). The proteolytic activity of the proteasome is found in the β-subunits (Marques *et al.,* 2009). Three of the seven different β subunits are proteolytically active: the β-1, β-2 and β-5 subunits (Groll *et al.,* 1997). The proteolytic activity of the proteasome can be classed into three different types (i) caspase-like or pepitdyl-glutamyl peptide-hydrolyzing-like (PGPH), (ii) trypsin-like and (iii) chymotrypsin-like activities, which are associated with β-1, β-2 and β-5 subunits, respectively (Fig. 1.3) (Marques *et al.,* 2009). The 20S core subunit is capped at each end by two 19S regulatory subunits (Fig. 1.2) (Murata *et al.,* 2009). The lower 19S subunit is composed of six different ATPase subunits known as regulatory particle triple A (Rpt1-6) proteins, and by three non-ATPase subunits referred to as regulatory particle non-ATPase (Rpn1, 2, 13) proteins (Glickman *et al.,* 1998; Rubin *et al.,* 1998). The upper 19S subunit is composed of Rpn3, 5, 6, 7, 8, 9, 11, 12, and 15. The upper and lower 19S regulatory subunits are linked by the Rpn10 protein forming

the 19S regulatory particle (Glickman *et al.*, 1998; Rubin *et al.*, 1998). The 19S subunit recognises and regulates the entry of polyubiquitinated proteins into the 20S catalytic core where ubiquitin residues are removed in an ATP-dependent manner from the protein and recycled (Fig. 1.2) (Voges *et al.*, 1999).

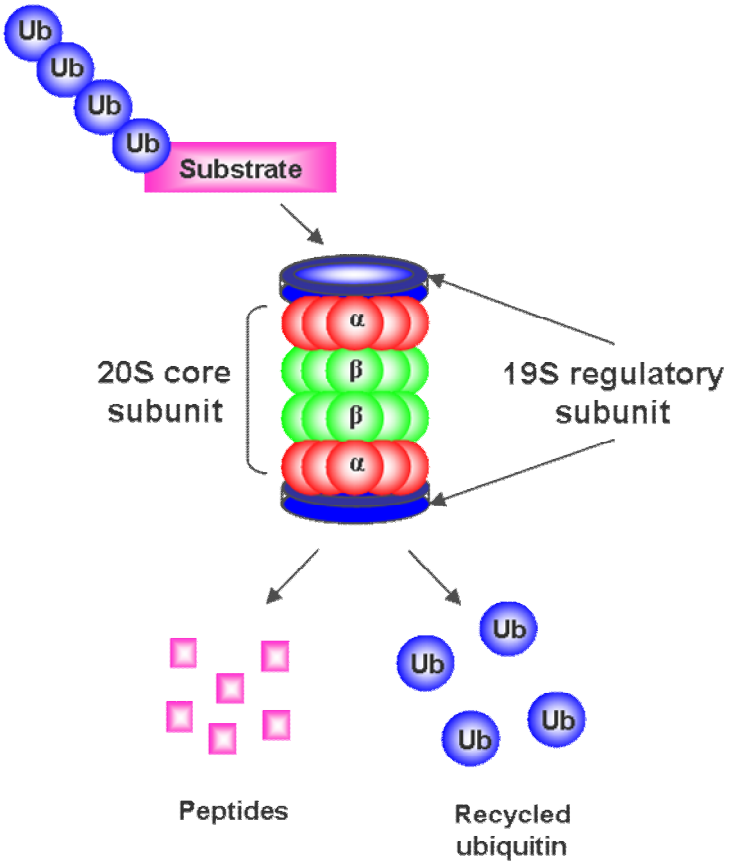

Figure 1.2: The 26S proteasome. The 26S proteasome is composed of the 20S core and 19S regulatory subunits. Polyubiquitinated proteins are targeted to the proteasome and degraded yielding small peptides and free ubiquitin. Ub-Ubiquitin. (Adapted from Almond *et al.*, 2002)

As the proteasome regulates the levels of key proteins involved in cell cycle progression, DNA repair and other cellular processes, anti-cancer drugs that act by targeting the proteasome have been developed (Voorhees *et al.*, 2006; Jacquemont *et al.*, 2007; Murakawa *et al.*, 2007). Bortezomib, a dipeptide boronic acid derivative, is the most widely used proteasome inhibitor and has been used successfully in the treatment of patients with multiple myeloma

(Adams 2004; Adams *et al.*, 2004; Kropff *et al.*, 2006; Adams *et al.*, 2009). Bortezomib inhibits the chymotryptic-like activity of the proteasome (Adams *et al.*, 1999). Bortezomib and other proteasome inhibitors have been shown to sensitise cancer cells to conventional chemotherapies in culture (Mimnaugh *et al.*, 2000; Mitsiades *et al.*, 2003; Pajonk *et al.*, 2005). There are naturally occurring and synthetic proteasome inhibitors (PIs). Naturally-occurring PIs include lactacystin and epoxomicin derived from the bacteria *Streptomyces* and *Actinomycetes* species respectively (Orlowski *et al.*, 2005). Synthetic PIs include the peptide aldehyde MG132. MG132 is commonly used to investigate the effects of proteasome inhibition. MG132 readily enters the cell and binds to and inhibits the active β-subunits of the 26S proteasome (Lee *et al.*, 1998). The effects of MG132 are rapidly reversed upon its removal from cells (Tsubuki *et al.*, 1993; de Bettignies *et al.*, 2010).

Bortezomib

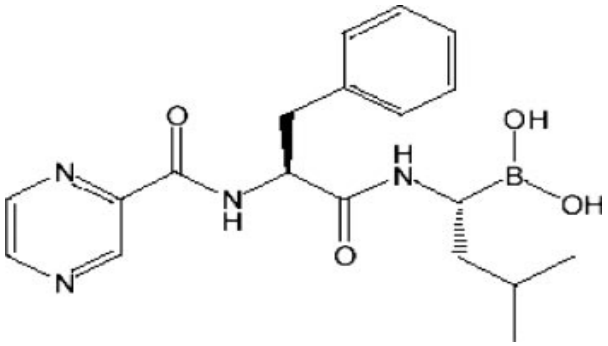

MG132

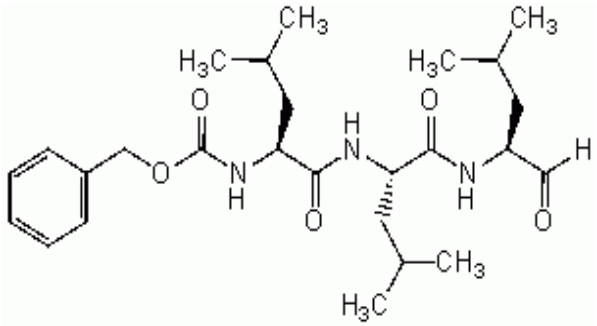

Figure 1.3: Molecular structure of the proteasome inhibitors Bortezomib and MG132 (taken from de Bettignies *et al.*, 2010)

1.5 Proteasomal regulation of cell cycle progression.

Cell cycle progression provides an example of the regulatory function of the proteasome. Regulated protein turnover plays a key role in cell cycle progression in eukaryotic cells. The cell cycle is a highly regulated process which requires the protein kinase activity of the cyclin-dependent kinases (CDKs). Activation of CDKs requires their association with a cyclin regulatory partner (Pines *et al.,* 1991; Pines 1993; Nigg 1995). The levels of cyclins rise and fall as cells progress through each stage of the cell cycle. The levels of cyclins are regulated through periodic polyubiquitination and degradation by the proteasomal machinery (Minshull *et al.,* 1989; King *et al.,* 1996a; King *et al.,* 1996b; Yu *et al.,* 1996). For example, entry of cells into mitosis depends on the activation of the CDK1-cyclin B complex. Exit from mitosis requires inactivation of CDK1-cyclin B which occurs following the proteasome–dependent degradation of cyclin B, mediated by the ubiquitination of cyclin B by the anaphase-promoting complex/cyclosome (APC/C) ubiquitin ligase (Glotzer *et al.,* 1991; Sudakin *et al.,* 1995; Hershko 1999).

Cell cycle checkpoints play an important role in preventing genome instability. Cell cycle arrest following DNA damage allows time for DNA repair to occur prior to complete replication of the genome or entry into mitosis (Hartwell *et al.,* 1989; Ishikawa *et al.,* 2006). Following DNA damage, checkpoint activation can lead to the arrest of the cell cycle in G1 in order to prevent cells from entering S-phase. S phase checkpoints detects DNA damage encountered during ongoing DNA replication (Ishikawa *et al.,* 2006). Checkpoint activation in G2 prevents cells progressing from G2 to mitosis to prevent the segregation of damaged chromosomes. The cell cycle arrest induced by the S-phase checkpoint is in part dependent on the PIKKs.

DNA damage encountered at the G1 checkpoint leads to the activation of ATR and ATM which phosphorylate the checkpoint kinases Chk1 on Ser317 and Ser 345, and Chk2 on Thr68 respectively (Liu *et al.,* 2000; Matsuoka *et al.,* 2000; Gatei *et al.,* 2003; Buscemi *et al.,* 2004; Cai *et al.,* 2009). Chk1 and Chk2 then phosphorylate the cell cycle division protein CDC25A phosphatase leading to

exclusion of CDC25 from the nucleus and its proteasomal degradation (Mailand *et al.*, 2000). The lack of CDC25A inhibits activation of the CDK2-cyclin E complex by preventing removal of an inhibitory phosphorylation on CDK1, preventing cells from progressing from G1 into S (Arata *et al.*, 2000; Li *et al.*, 2005).

The maintenance of G1 arrest involves prevention of the proteasomal degradation of the transcription factor p53. p53 levels are regulated by its interaction with the E3 ligase MDM2, which is responsible for the ubiquitination of p53. ATM phosphorylates MDM2, reducing its interaction with p53, leading to increased levels of p53 in the nucleus (Falck *et al.*, 2001; Bartek *et al.*, 2003; Sancar *et al.*, 2004a). p53 is also regulated by phosphorylation, preventing proteasomal degradation of p53 (Taylor *et al.*, 2001; Zhang *et al.*, 2001). p53 is phosphorylated on serine 15 by ATM, ATR and DNA-PK, and on serine 20 by Chk1 or Chk2 (Banin *et al.*, 1998; Canman *et al.*, 1998; Tibbetts *et al.*, 1999; Hirao *et al.*, 2000; Shieh *et al.*, 2000; Zhang *et al.*, 2001). Increased levels of p53 induce p21 which inhibits CDK2-cyclin E (Sherr *et al.*, 1999; Ekholm *et al.*, 2000). Mu *et al,*. (2007) demonstrated that proteins involved in the ubiquitin-proteasome pathway are involved in G1 arrest following DNA damage, and are required for the maintenance of the checkpoint (Mu *et al.*, 2007). This demonstrates that protein turnover is an important aspect of the activation of the G1 checkpoint (Mu *et al.*, 2007).

S phase checkpoints play a vital role in preventing replication of damaged DNA. During S phase, DNA damage can result from exogenous agents but also from errors during replication leading to DNA strand breaks (Lopes *et al.*, 2001; Li *et al.*, 2005). S-phase checkpoints can be classed into three different types: (i) the replication checkpoint, (ii) the intra-S checkpoint and (iii) the S-M checkpoint. S-phase checkpoints are interlinked and share some control mechanisms (Bartek *et al.*, 2004; Sancar *et al.*, 2004a). The replication checkpoint is activated in response to stalled replication forks which can occur when the replication machinery encounters lesions in the DNA or in response to stresses such as the depletion of deoxyribonucleotide pools (Lopes *et al.*, 2001; Mirkin *et al.*, 2007). Extensive regions of ssDNA generated by replication stalling leads to the

ATRIP/ RPA- dependent activation of ATR/Chk1, phosphorylation of CDC25A, and inhibition of CDK2/cyclin E (Sorensen *et al.,* 2003; Xiao *et al.,* 2003). The replication checkpoint prevents CDC45 loading at replication origins and inhibits the firing of late origins of replication (Bartek *et al.,* 2004).

In contrast to the replication checkpoint, the intra-S phase checkpoint is replication-independent (Bartek *et al.,* 2004). The intra-S phase checkpoint functions by preventing the firing of new origins of replication, by inhibiting loading of replication factors at origins of replication. However, actively replicating forks remain unaltered (Falck *et al.,* 2002; Bartek *et al.,* 2004; Merrick *et al.,* 2004). Inactivation of CDC25A through ATM/Chk2 and ATR/Chk1 activation leads to the inhibition of new origin activation (Costanzo *et al.,* 2000; Falck *et al.,* 2001; Falck *et al.,* 2002). A number of DNA repair proteins co-ordinate cell cycle arrest and a recovery process through recombination, including NBS1, BRCA1, BRCA2 and SMC1 (Lim *et al.,* 2000; Zhao *et al.,* 2000; Nyberg *et al.,* 2002; Yazdi *et al.,* 2002; Sancar *et al.,* 2004a).

The S-M checkpoint prevents premature cell division before completion of correct replication of the entire genome (Bartek *et al.,* 2004). The S-M checkpoint inhibits CDK1-cyclin B required for entry of cells into mitosis (Bartek *et al.,* 2004). This is an ATR-dependent process which prevents premature chromatin condensation and delays entry into mitosis (Bartek *et al.,* 2004; Niida *et al.,* 2005; Ishikawa *et al.,* 2006).

The G2/M checkpoint prevents the cell from entering mitosis in the presence of DNA damage Depending on the type of damage encountered at the G2/M checkpoint, ATR and/or ATM can phosphorylate and inactivate CDC25C through the activation of Chk1 and Chk2 (Donzelli *et al.,* 2003). Inhibition of CDC25C prevents the dephosphorylation and activation of CDK1-cyclin B which is required for progression into mitosis (Furnari *et al.,* 1997; Zhao *et al.,* 2001; Boutros *et al.,* 2006). Upregulation of p53 also plays a role in the maintenance of G2 arrest (Taylor *et al.,* 2001).

1.6 Cisplatin

Agents that inhibit DNA replication are used in the treatment of cancer. Cis-diammine platinum (II) dichloride or cisplatin is a platinum based chemotherapeutic drug which can react with DNA, RNA and proteins (Perez 1998; Berndtsson *et al.,* 2007). Following its accidental discovery, its potential as an anti-cancer drug was first described in the 1960s following experiments treating sarcomas in rats (Rosenberg 1965; Rosenberg 1969; Rosenberg 1975). Cisplatin has been used very successfully in the treatment of testicular and ovarian cancers, as well as being used regularly but less successfully in the treatment of head, neck and non-small cell lung cancers (Boulikas *et al.,* 2004; Kelland 2007). Other cisplatin analogues have been synthesised, including carboplatin (cyclobutane-1, 1-dicarboxylic acid) and oxaliplatin ((*trans-R, R*) 1, 2 diaminocyclohexaneoxalatoplatinum (II)) (Chaney *et al.,* 2005; Wang *et al.,* 2005a). Carboplatin is used in the treatment of non-small cell lung cancer (Belani *et al.,* 2008) while oxaliplatin used for treatment of colon cancers (Andre *et al.,* 2004)

On administration cisplatin enters the cell, mainly by passive diffusion through the plasma membrane (Binks *et al.,* 1990; Wang *et al.,* 2005a). However, more recent evidence has also suggested a relationship between the levels of copper and platinum inside cells (Komatsu *et al.,* 2000; Ishida *et al.,* 2002; Holzer *et al.,* 2004). Experiments in S.*cerevisiae* have shown that mutation or deletion of the high-affinity copper transporter Ctr1 results in a decrease in the levels of platinum inside cells leading to an increase in resistance to cisplatin (Ishida *et al.,* 2002). Overexpression of human CTR1 also led to an increase in platinum levels in cultured ovarian carcinoma, A2780, cells (Komatsu *et al.,* 2000; Holzer *et al.,* 2004). Upon entering the cell, cisplatin undergoes the process of aquation, in which the chlorine ions of cisplatin are replaced by water, due to the lower concentration of chlorine inside the cell compared outside the cell (Wang *et al.,* 2005a). This gives cisplatin a positive charge, allowing it to interact with DNA, RNA and proteins inside the cell (Perez 1998; Berndtsson *et al.,* 2007).

Cisplatin interacts with DNA by covalently by binding to the N^7 positions of purine bases, forming monoadducts, intrastrand crosslinks, and a lower number of interstrand crosslinks (ICLs) (Fig. 1.4) (Kartalou *et al.,* 2001; Chaney *et al.,* 2005). Approximately 60-65% of crosslinks formed by cisplatin are intrastrand GG adducts, 25-30% are intrastrand AG adducts, and 5-10% are intrastrand GNG adducts (Fichtinger-Schepman *et al.,* 1985a; Fichtinger-Schepman *et al.,* 1985b; Eastman 1987). ICLs are formed to a lower extent (1-3%); however these are considered to be the major cytotoxic lesion induced by cisplatin (Huang *et al.,* 1995). Intrastrand crosslinks distort the DNA helix by bending it by 35°. Intrastrand adducts can interfere with the DNA replication and transcription machinery by preventing strand separation (Bellon *et al.,* 1991; Huang *et al.,* 1993; Ferguson *et al.,* 2000). ICLs distort the DNA helix to a greater extent than intrastrand crosslinks by bending and unwinding DNA, preventing DNA replication and transcription (Huang *et al.,* 1995). ICLs encountered during DNA replication can lead to the formation of DSBs (Frankenberg-Schwager *et al.,* 2005).

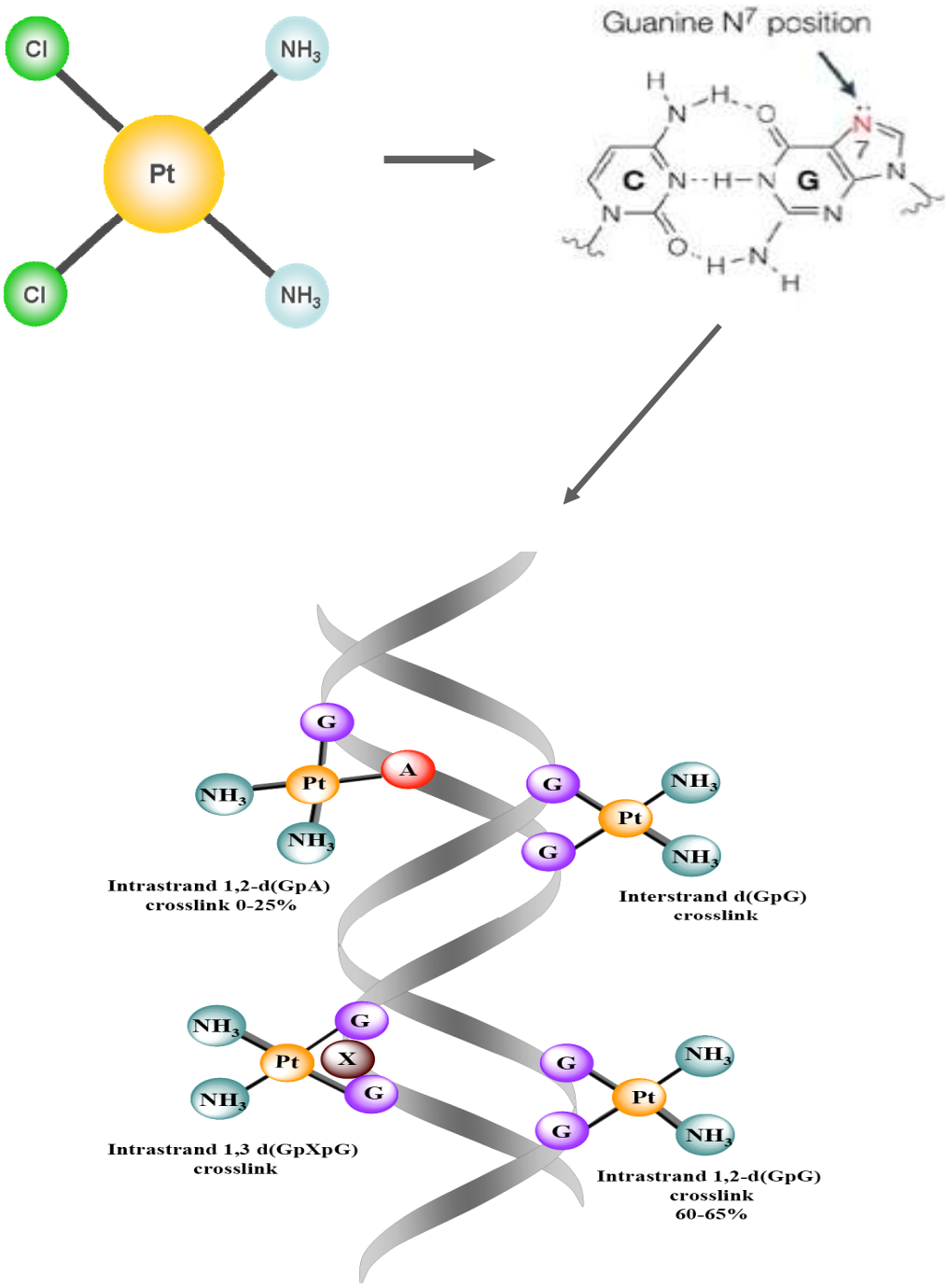

Figure 1.4: Cisplatin-DNA interactions. Cisplatin reacts with DNA by covalently interacting with the N^7 positions of guanine forming intrastrand crosslinks, monoadducts and interstrand crosslinks (ICLs) (adapted from Boulikas *et al*., 2007, Wang and Lippard *et al*, 2005).

1.7 DNA Repair.

In human cells cisplatin-induced DNA damage is repaired by a number of repair pathways. Cisplatin induced intrastrand crosslinks can be repaired by nucleotide excision repair (NER) or bypassed by translesion synthesis (TLS). ICLs are repaired by the co-ordinated action of proteins from different repair pathways including nucleotide excision repair (NER), homologous recombination (HR), the Fanconi anemia (FA) pathway and translesion DNA synthesis (TLS) (Hinz 2010; Ho *et al.,* 2010; Wood 2010). Proteasome inhibition prevents the removal of cisplatin adducts from DNA in A2780/CP70 human ovarian carcinoma cells. This indicates the function of the proteasome is required for effective repair of these lesions (Mimnaugh *et al.,* 2000)

1.7.1 Nucleotide Excision Repair (NER)

Nucleotide excision repair (NER) is a DNA repair pathway which is responsible for the removal of bulky, helix-distorting lesions in DNA that interfere with normal DNA replication and transcription. Lesions repaired by NER include UV-induced cyclobutane pyrimdine dimers (CPDs) and (6-4) photoproducts, and cisplatin-induced intrastrand DNA crosslinks. Approximately 30 proteins are involved in NER (Sancar *et al.,* 2004b). Mutations in genes encoding these proteins provide the molecular basis of the genetic disease xeroderma pigmentosum (XP), complementation groups (A-G), which are characterised by increased sun sensitivity and skin cancer predisposition (Cleaver 1968; de Boer *et al.,* 2000; Lehmann 2003). NER consists of two different pathways: transcription coupled repair (TCR) which repairs DNA damage in transcribed genes (Fousteri *et al.,* 2008) and global genome repair (GGR) which repairs damage in all other genomic DNA (Shuck *et al.,* 2008). The two subpathways differ in the way repair is initiated. TCR is initiated by stalling of RNA polymerase II at the site of damage. GGR is initiated by recogunition of damage by the XPC-HR23B complex and by UV-damaged DNA binding protein (UV-DDB) (Sugasawa *et al.,* 2001; Wittschieben *et al.,* 2005).

Binding of the UV-DDB and XPC-HR23B complexes to damaged DNA allows recruitment of other repair factors to the site of damage, including XPA, RPA and TFIIH (Araujo *et al.,* 2001; Thoma *et al.,* 2003). The DNA is then unwound at the lesion site by the helicase activity of the XPB and XPD subunits of TFIIH. Incisions in the damaged strand are made on the 3' and 5' sides of the damage by the endonucleases XPG and ERCC1-XPF respectively (Evans *et al.,* 1997) . The oligonucleotide containing the damage is released, followed by DNA synthesis to repair the gap, and ligation of the remaining single-stranded gap (Shivji *et al.,* 1995; Moser *et al.,* 2007).

NER is regulated in part by the ubiquitination of key proteins. UV-DDB is a heterodimer composed of DDB1 and DDB2 (Keeney *et al.,* 1993). Mutations in the *DDB2* gene are responsible for xeroderma pigmentosum group E (XPE) (Chu *et al.,* 1988; Rapic-Otrin *et al.,* 2003). DDB2 interacts with the DNA containing the lesion, while DDB1 binds to and stabilises DDB2, but does not bind to DNA (Chu *et al.,* 2008; Scrima *et al.,* 2008). UV-DDB is part of an E3 ubiquitin ligase complex which polyubiquitnates DDB2 leading to its proteasomal degradation (Groisman *et al.,* 2003; Matsuda *et al.,* 2005; Sugasawa *et al.,* 2005). This E3 ligase complex also polyubiquitinates XPC, but in this case, the modification does not target the protein for degradation (Sugasawa *et al.,* 2005; Sugasawa 2006). Instead, ubiquitination stabilises XPC and also enhances its binding affinity for DNA (Sugasawa 2006). The E3 ligase complex also ubiquitinates histone proteins, which may alter their structure allowing NER proteins to access the damaged DNA (Wang *et al.,* 2006). Treatment of cells with proteasome inhibitors leads to the retention of DDB2 at sites of DNA damage, and prevents XPC from being recruited to these sites (El-Mahdy *et al.,* 2006). This demonstrates that the proteasome functions as a positive regulator of NER, as it is required for the degradation of DDB2 which allows the subsequent steps of NER to proceed. Consistent with this proteasome inhibitors reduce the rate at which UV-induced lesions are removed from DNA human fibroblast, OSU-2, cells (Wang *et al.,* 2005b).

1.7.2 The Fanconi Anemia (FA) pathway

While the majority of cisplatin-induced lesions are intrastrand crosslinks, the small percentage of ICLs formed are higly cytotoxic. The Fanconi anemia (FA) pathway plays a vital role in the repair of interstrand crosslinks in human cells (Moldovan *et al.,* 2009b; Moldovan *et al.,* 2009a). FA is a rare autosomal rescessive disorder, characteristed by bone marrow failure, developmental abnormalities and increased risk of cancer (Moldovan *et al.,* 2009b). At a cellular level, mutations in components of the FA pathway leads to hypersensitivity to DNA crosslinking agents such as mitomycin C (MMC) and cisplatin, the formation of chromosome breaks and radial chromosomes (Poll *et al.,* 1985; German *et al.,* 1987; Ho *et al.,* 2006). Fourteen complementation groups of FA have been described to date: FANCA, -B, -C, -D1, -D2, -E, -F,-G, -I, -J, -L, -M, -N, -P. In addition, one FA-like complementation group (FA-O) has been described (reviewed in Kee *et al.,* 2010). Some FA proteins are identical to other proteins involved in DNA repair. For example, FANC -D1 (BRCA2), - J (BACH1/BRIP1), -N (PALB2), -O (RAD51C) and- P (SLX4)) (Bagby 2003; Taniguchi *et al.,* 2006; Moldovan *et al.,* 2009b; Kee *et al.,* 2010; Somyajit *et al.,* 2010; Cybulski *et al.,* 2011).

Eight of the FA proteins (FANCA, FANCB, FACC, FANCE, FANCF, FANCG, FANCL, and FANCM) form a core complex that has E3 ubiquitin ligase activity (Meetei *et al.,* 2003; Meetei *et al.,* 2004). The FA-associated proteins (FAAP), FAAP24 and FAAP100 also play a role in complex formation. The core complex monoubiquitinates FANCD2 on K561, and FANCI on K523 (Dorsman *et al.,* 2007; Sims *et al.,* 2007; Smogorzewska *et al.,* 2007). FANCL is the E3 ligase within the core complex which monoubiquitinates FANCD2 and FANCI (Meetei *et al.,* 2003; Seki *et al.,* 2007; Cole *et al.,* 2010; Hodson *et al.,* 2011). The other proteins of the core complex are involved in recruitment of FANCL to FANCD2 and FANCI. FANCM and FAAP24 are not constantly associated with the core complex and it has been suggested that the FANCM-FAAP24 complex functions in recognising and recruiting the core complex to sites of damage (Ciccia *et al.,* 2007; Kim *et al.,* 2008). Monoubiquitination of FANCD2 is an essential step in the FA pathway, whereas FANCI monoubiquitination is not (Ishiai *et al.,* 2008).

However, FANCI is phosphorylated in an ATR dependent manner, and phosphorylated FANCI is required for FANCD2 monoubiquitination and FA pathway activation (Ishiai *et al.,* 2008). Phosphorylation of FANCI may facilitate the recruitment of the FANCD2/FANCI complex to the FA core complex for monoubiquitination. Monoubiquitination of the FANCD2/FANCI heteordimer leads to its recruitment to sites of DNA damage. The FANCD2/FANCI complex is monoubiquitinated constitutively during S-phase, and in response to DNA damage (Nakanishi *et al.,* 2002; Taniguchi *et al.,* 2002; Hussain *et al.,* 2004; Wang *et al.,* 2004a). The constitutive monoubiquitination of this complex may be in response to endogenous DNA damage or to replication intermediates that need processing. RPA is required for monoubiquitination of FANCD2 (Andreassen *et al.,* 2004).

The monoubiquitinated FANCD2/FANCI complex is required for incision or 'unhooking' of ICLs and for a subsequent translesion synthesis step in the repair of the ICLs (Knipscheer *et al.,* 2009). Monoubiquitinated FANCD2/FANCI may recruit nucleases required for the initial incision steps of ICL repair, which may include MUS81, XPF/ERCC1 and SLX4 (Fig. 1.5) (Bhagwat *et al.,* 2009; Rouse 2009; Wang *et al.,* 2010; Cybulski *et al.,* 2011; Yamamoto *et al.,* 2011). A newly identified protein which is thought to be a member of the FA pathway has recently been identified, FA-associated nuclease-1 (FAN1) (Smogorzewska *et al.,* 2010). FAN1 is a nuclease which is recruited to sites of ICLs by monoubiquitinated FANCD2/FANCI (Liu *et al.,* 2010b). FAN1 contains an ubiquitin binding domain (UBZ) which interacts with monoubiquitinated FANCD2 (Castella *et al.,* 2010; Kratz *et al.,* 2010; Liu *et al.,* 2010b; MacKay *et al.,* 2010; O'Donnell *et al.,* 2010; Smogorzewska *et al.,* 2010). Monoubiquitinated FANCD2/FANCI may also recruit TLS polymerases which are required for subsequent resynthesis following incision of the ICL (Fig. 1.5). TLS polymerases may interact with monoubiquitinated FANCD2/FANCI through the ubiquitin interacting domains of the TLS polymerases (Moldovan *et al.,* 2009a). FANCD2/FANCI may also recruit factors involved in HR, including BRCA1, BRCA2 and RAD51, required for the subsequent repair of DSBs formed during the processing of ICLs (Fig. 1.5) (Garcia-Higuera *et al.,* 2001; Taniguchi *et al.,* 2002; Wang *et al.,* 2004a; Wang *et al.,* 2004b).

The FA pathway is further regulated by deubiquitination of monoubiquitinated FANCD2/FANCI by the deubiquitinating enzyme USP1 (Nijman *et al.*, 2005; Smogorzewska *et al.*, 2007). USP1 also regulates TLS through the deubiquitination of PCNA (Huang *et al.*, 2006; Zhuang *et al.*, 2008). USP1 is found in a complex with UAF1, an interaction which is required for the deubiquitinating function of USP1 (Cohn *et al.*, 2007; Cohn *et al.*, 2009). Following DNA damage, the activity of USP1 is inhibited through rapid degradation, leading to a build up of monoubiquitinated FANCD2 and FANCI in the nucleus, facilitating ICL repair (Cohn *et al.*, 2007; Oestergaard *et al.*, 2007; Cohn *et al.*, 2009).

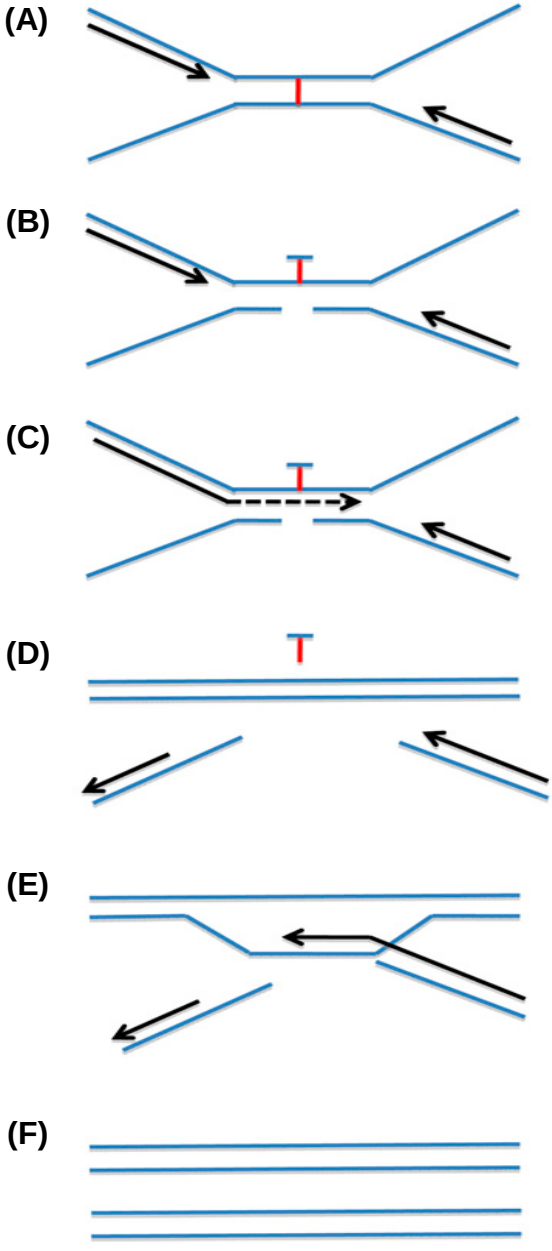

Figure 1.5: Model for repair of interstrand crosslinks (ICLs). (A) The replication fork stalls on encountering an ICL. (B) ICL is 'unhooked' from one strand through the action of nucleases which may include MUS81, XPFF/ERCC1, SLX4 and FAN1. (C) The unhooked ICL may then be bypassed by TLS and (D) the remaining adduct is repaired by NER. (E) The resulting double strand break can then be repaired by HR, resulting in two DNA strands (F). (Taken from *Kee et al.,* 2010).

1.7.3 Tolerence to DNA damage by translesion synthesis (TLS)

Replication in the presence of damage can result in arrest of replication fork progression, fork collapse, and potentially giving rise to DNA strand breaks. Cisplatin induced DNA intrastrand-crosslinks and ICLs which are not repaired before DNA replication can block the replicative polymerases α, δ, and ε which poses a significant danger to the cell. Human cells express specialised, low fidelity DNA polymerases which carry out DNA replication in the presence of damage (Johnson *et al.,* 1999; Masutani *et al.,* 1999; Masutani *et al.,* 2000; Lehmann *et al.,* 2007). TLS polymerases can directly bypass cisplatin-induced intrastrand crosslinks; however, TLS also plays a role in the repair of cisplatin induced ICLs as outlined in Section 1.7.2. TLS polymerases including DNA polymerases eta (η), iota (ι), kappa (κ) and Rev1 belong to the Y family of polymerases (Lehmann *et al.,* 2007). Other specialised polymerases including polymerase zeta (ζ) belong to the X family of polymerases (Burgers *et al.,* 2001).

On a structural level, TLS polymerases have a more open active site which is able to accommodate structurally altered DNA bases (Johnson *et al.,* 1999; Friedberg *et al.,* 2001; Trincao *et al.,* 2001; Alt *et al.,* 2007; Biertumpfel *et al.,* 2010). Human DNA pol η is encoded by the *POLH* gene (Johnson *et al.,* 1999; Masutani *et al.,* 1999). DNA pol η is involved in bypass of UV-induced CPDs and cisplatin-induced lesions in DNA (Kannouche *et al.,* 2001; Bassett *et al.,* 2003; Chaney *et al.,* 2005; Alt *et al.,* 2007). Mutations in this gene lead to the disorder xeroderma pigmentosum variant (XPV) which is characterised by high sensitivity to UV and increased skin cancer predisposition. Key cellular phenotypes of XPV cells included hypersensitivity to UV-irradiation, especially

when cells are co-treated with caffeine (Maher *et al.,* 1976) and generation of shorter nascent DNA fragments following UVC-irradiation (Lehman *et al.,* 1975).

On encountering lesions in the DNA, replicative polymerases are displaced by TLS polymerases in a process called the polymerase switch. The recruitment of TLS polymerases is regulated and is dependent on the monoubiquitination of the homotrimeric sliding clamp, proliferating cell nuclear antigen (PCNA) on K164 by the Rad6/Rad18 ubiquitin-conjugating enzyme complex (Hoege *et al.,* 2002; Haracska *et al.,* 2004; Zhuang *et al.,* 2008) . DNA pol η is recruited to DNA through its PCNA-interacting peptide (PIP) and ubiquitin-binding zinc finger (UBZ) domains (Haracska *et al.,* 2001; Kannouche *et al.,* 2004a; Kannouche *et al.,* 2004b; Bienko *et al.,* 2005; Acharya *et al.,* 2008). It was reported that RPA interacts directly with Rad18 in both yeast and mammalian cells, indicating that RPA-coated ssDNA may act as a signal for DNA damage-induced PCNA monoubiquitination (Kannouche *et al.,* 2004a; Davies *et al.,* 2008). Once TLS has taken place and the damage is bypassed, deubiquitination of PCNA by USP1 may lead to dissociation of DNA pol η, allowing the recruitment of Pol δ and resumption of processive DNA replication (Huang *et al.,* 2006; Zhuang *et al.,* 2008).

1.7.4 DNA double strand break repair.

A good example of the dependence of DDR on sequential post translational modification of key proteins is the repair of DSBs. DSBs formed either directly or as a result of damage encountered by the replication machinery during S-phase are potentially lethal lesions to a cell. Cisplatin-induced DNA damage encountered during S-phase can result in replication fork arrest and fork collapse leading to the formation of DSBs (Branzei *et al.*, 2007). DSBs are also formed as an intermediate in the repair of interstrand crosslinks (Fig. 1.5) (Deans *et al.*, 2011). Upon DSB formation, the MRN complex, consisting of Mre11, Rad50 and Nbs1, recognises and binds to either side of the break. ATM is recruited leading to the phosphorylation of the C-terminus of the histone variant H2AX on Ser139 (γH2AX) (Rogakou *et al.,* 1998; Burma *et al.,* 2001). Phosphorylation of

H2AX occurs rapidly following DNA damage and extends for megabases on the DNA flanking the DSB. γH2AX is recognised by the mediator of DNA damage checkpoint (MDC1) protein which is also required for the localisation of repair factors to sites of damage, including BRCA1 and 53BP1 (Lou *et al.,* 2003; Bekker-Jensen *et al.,* 2005; Stucki *et al.,* 2005; Lou *et al.,* 2006). MDC1 is phopsphorylated by ATM which then recruits the E3 ubiquitin ligase RNF8 to the site of the DSB. RNF8 interacts with the N-terminal forkhead associated (FHA) domain and ATM-phosphorylated TQXF motifs on MDC1 (Huen *et al.,* 2007; Mailand *et al.,* 2007). RNF8, together with the E2 conjugating enzyme UBC13 ubiquitinate γH2AX (Huen *et al.,* 2007; Mailand *et al.,* 2007). RNF8-mediated ubiquitination of γH2AX is necessary but not sufficient for the recruitment of repair factors (Doil *et al.,* 2009). Further ubiquitination is required by RNF168 to sustain the accumulation of repair proteins at sites of DSBs, including BRCA1 and 53BP1 which are required for DNA repair and cell cycle checkpoint activation (Doil *et al.,* 2009). Another E3 ubiquitin ligase, RNF168, acts downstream of MDC1 and RNF8. RNF168 recognises the polyubiquitinated chains on γH2AX (Doil *et al.,* 2009). RNF168 in conjunction with UBC13 mediates further ubiquitination of γH2AX, amplifying the signal to downstream proteins (Doil *et al.,* 2009). The presence of E3 ligase at the sites of DNA damage may function in the ubiquitination of further proteins substrates required for the cellular response to DNA damage. The treatment of the human melanoma cell line, Mel JuSo, with the proteasome inhibitor MG132 resulted in the loss of accumulation of BRCA1 and 53BP1 at sites of DSB (Dantuma *et al.,* 2006). Treatment of cells with MG132 resulted in the depletion of the cellular ubiquitin pool available for the ubiquitination of other proteins, preventing the ubiquitination of γH2AX and the subsequent accumulation of BRCA1 and 53BP1 (Dantuma *et al.,* 2006).

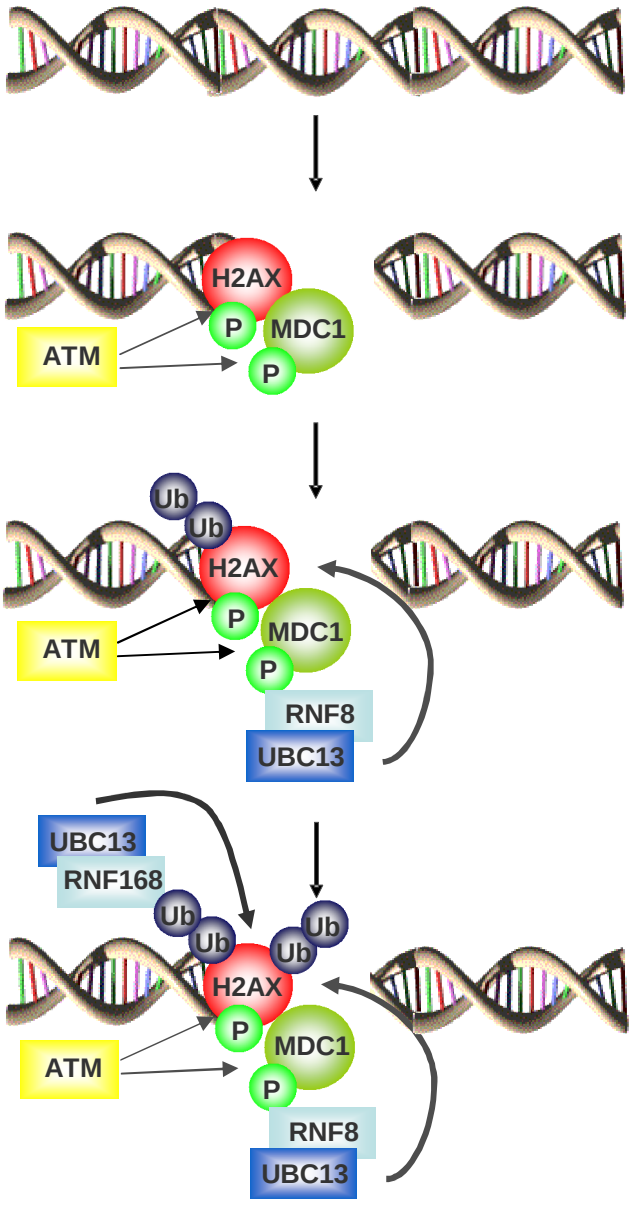

Figure 1.6 Schematic diagram showing signalling from a DNA double strand break (DSB). (Protien abbreviations are defined in text (adapted from Panier *et al.*, 2009 and Al-Hankim *et al.*, 2010)

1.7.4.1 Homologous Recombination (HR)

In cells in late S and in G2 phases, homologous recombination (HR) functions in the repair of DSBs. In HR sister chromatids serve as a template for the resynthesis of the break in the DNA sequence (San Filippo *et al.,* 2008).

The first step in HR involves the localisation of the MRN complex to the ends of the DSB. The endo- and exonuclease activites of Mre11 in the MRN complex resect the ends to leave a 3' ssDNA overhang which becomes coated and stabilised by RPA (Sugiyama *et al.,* 1997). RPA is then displaced from the ssDNA, when ssDNA becomes coated by Rad51, leading to the formation of a Rad51 nucleofilament. Formation of Rad51 filaments on RPA-coated ssDNA is facilitated by mediator proteins including the tumour suppressors BRCA1, BRCA2 and DSS1 (Gudmundsdottir *et al.,* 2004; Esashi *et al.,* 2007; Jensen *et al.,* 2010; Kristensen *et al.,* 2010; Liu *et al.,* 2010a). DSS1 associates with the C-terminal domain of BRCA2 and has been shown to be required for the normal function of BRCA2 in human cells (Kojic *et al.,* 2003). The recruitment of BRCA1 depends on the ubiquitination of γH2AX carried out by RNF168. BRCA1 associates with sites of damage through its interactions with the protein Abraxas and interacting partner RAP80 (receptor associated protein 80) (Kim *et al.,* 2007; Sobhian *et al.,* 2007; Wang *et al.,* 2007; Yan *et al.,* 2007).

The Rad51 nucleoprotein filament carries out a homology search and strand invasion on the undamaged sister chromatid (Sung 1994). Strand invasion results in disruption of base pairing, creation of a D-loop in the homologous strand (San Filippo *et al.,* 2008). A Holliday junction (HJ) then forms, mediated by the nucleofilament (San Filippo *et al.,* 2008). The homologous sister chromatid is then used as a template to extend the invading strand (Rothkamm *et al.,* 2003). DNA polymerases η, δ, and ε are involved in the extension of the 3' terminus of the invading DNA strand (Kawamoto *et al.,* 2005; McIlwraith *et al.,* 2005; Maloisel *et al.,* 2008) The ends are then ligated by DNA ligase I and the Holliday junctions is resolved by the endonucleases which may involve the activity of Gen1, MUS81/EME1 and SLX1/SLX4, resulting in the formation of two

undamaged DNA stands (Ip *et al.,* 2008; Fekairi *et al.,* 2009; Munoz *et al.,* 2009; Svendsen *et al.,* 2009; Svendsen *et al.,* 2010).

1.8 Replication Protein A (RPA).

In all of the above mentioned DNA repair pathways, replication protein A (RPA) is a common factor which plays a major role (Andreassen *et al.,* 2004; Davies *et al.,* 2008; Dou *et al.,* 2010; Lee *et al.,* 2010; Oakley *et al.,* 2010; Shi *et al.,* 2010). RPA is a stable heterotrimeric single-stranded DNA (ssDNA) binding protein, plays essential roles in DNA metabolic pathways including DNA replication (Wold *et al.,* 1988), DNA recombination (Sugiyama *et al.,* 1997; Lee *et al.,* 2010; Shi *et al.,* 2010) and DNA repair processes (Missura *et al.,* 2001; Andreassen *et al.,* 2004; Davies *et al.,* 2008; Dou *et al.,* 2010; Lee *et al.,* 2010; Oakley *et al.,* 2010; Shi *et al.,* 2010) . RPA homologues have been identified in all eukaryotes (Brill *et al.,* 1989; Nasheuer *et al.,* 1992; Ishiai *et al.,* 1996). RPA was first identified as a protein required for the initiation and elongation steps during replication of simian virus 40 (SV40)-origin containing plasmid DNA *in vitro* (Wold *et al.,* 1988). RPA is composed of three tightly associated subunits: RPA1 (p70), RPA2 (p32) and RPA3 (p14), with of molecular sizes of 68-, 29- and 14kDa (Fairman *et al.,* 1988; Wold *et al.,* 1988; Bochkarev *et al.,* 1997). RPA plays a major role in checkpoint activation and the DNA damage response as RPA is required for the recruitment of ATRIP-ATR to regions of ssDNA generated at stalled replication forks following DNA damage (Zou *et al.,* 2003; Dart *et al.,* 2004). The RPA protein contains six oligonucleotide binding (OB) folds (Fig, 1.8), named DNA binding domains (DBD), which give the protein its DNA binding ability (Bochkarev *et al.,* 1997; Pfuetzner *et al.,* 1997). The structure of the OB fold is made up of β-sheets that form β-barrels, which are able to wrap around ssDNA (Murzin 1993).

1.8.1 RPA1

The ssDNA-binding activity of RPA is primarily due to the RPA1 subunit. The RPA1 subunit structure contains four OB-folds, one in the N-terminal (DBD A) and C-terminal region (DBD F) and two in the central region of the subunit (DBD B and DBD C) (Fig. 1.8) (Bochkarev *et al.,* 1997; Bochkareva *et al.,* 2001;

Bochkareva *et al.,* 2002). DBD F in the N-terminal is important for the interaction of trimeric RPA with other proteins, and in the regulation of DNA metabolism. RPA1 is phosphorylated on Thr180 *in vivo* in response to HU, IR and UV treatment (Nuss *et al.,* 2005; Matsuoka *et al.,* 2007; Stokes *et al.,* 2007). RPA1 can also be sumoylated by SUMO 2/3 on K577 and K449 (Dou *et al.,* 2010). Sumoylation of RPA1 is proposed to promote HR, by facilitating the recruitment of RAD51 (Dou *et al.,* 2010).

1.8.2 RPA2

The RPA2 subunit contains one OB-fold named DBD D, in the centre of the protein which has weak DNA binding capacity (Bochkarev *et al.,* 1999). The N-terminal of RPA2 is serine and threonine-rich, and is phosphorylated on two sites, Ser23 and Ser29, during the normal cell cycle, and is hyperphosphorylated in response to DNA damage as a result of additional phosphorylation on Ser33, Thr21, Ser4 and Ser8. Phosphorylation of RPA2 changes the affinity of RPA for ssDNA and alters the interaction of RPA with other proteins. The C-terminal of RPA2 is involved in the interactions of trimeric RPA with other proteins.

A human homologue of RPA2 called RPA4 was originally identified in a screen for proteins that interact with RPA1 (Keshav *et al.,* 1995). RPA4 has 63% amino acid sequence homology to RPA2 (Keshav *et al.,* 1995). RPA4 can replace RPA2 and form a complex with RPA1 and RPA3 in normal tissues but not in tissues with a large fraction of proliferating cells (Keshav *et al.,* 1995; Haring *et al.,* 2010). RPA4 is not expressed in detectable levels in transformed cultured cell lines (Haring *et al.,* 2010). Formation of the alternative RPA trimer, consisting of RPA1, RPA4 and RPA3 does not support DNA replication in RPA2-depleted HeLa cells expressing RPA4 (Haring *et al.,* 2010). However the alternative RPA trimer is able to support DNA repair, *in vitro*, through NER and function during HR (Keshav *et al.,* 1995; Haring *et al.,* 2010; Kemp *et al.,* 2010)
.

1.8.3 RPA3

The RPA3 subunit is required for RPA heterotrimer formation and stabilisation (Weisshart *et al.*, 2004). In the absence of RPA3, SV40 DNA replication initiation and elongation is inhibited in cell free extracts (Weisshart *et al.*, 2004). The C-terminus of RPA3 functions in maintaining the stability of the structure of the heterotrimer (Bochkareva *et al.*, 2002). RPA3 has one OB, fold named DBD E. However to date other roles of RPA3 are not known (Bochkarev *et al.*, 1999; Weisshart *et al.*, 2004).

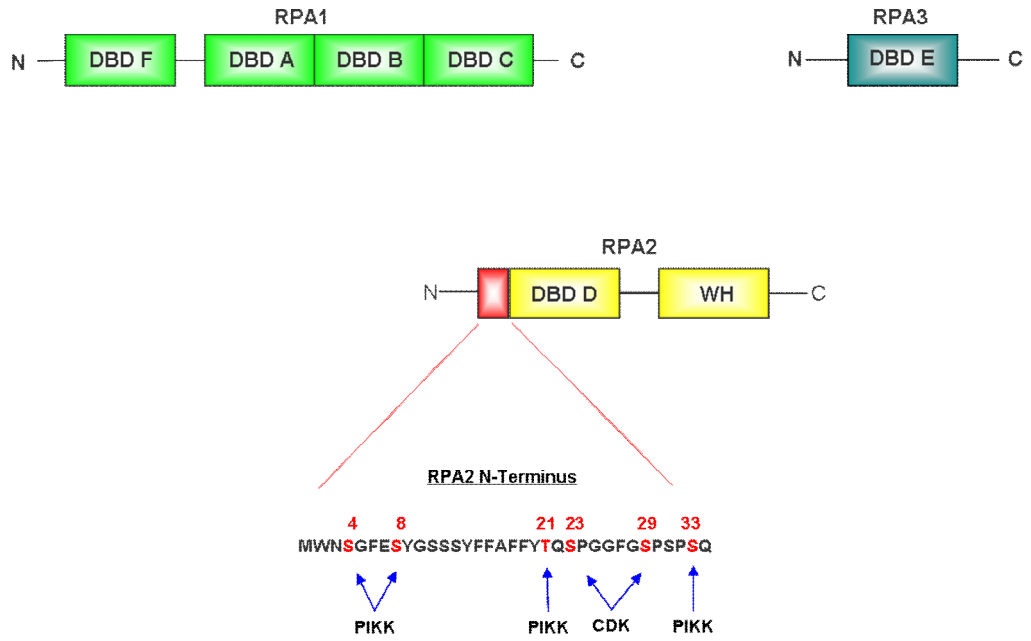

Figure 1.8: Human replication protein A (RPA). RPA is composed of the subunits RPA1, RPA2 and RPA3. The N-terminus of RPA2 contains a phosphorylation domain (shown at bottom of figure). Phosphorylation sites are highlighted in red. DBD, DNA binding domains, WH, winged helix domain, modified from Binz *et al,*. (2004); and Oakley *et al,*. 2010).

1.8.4 RPA DNA Binding and Role in DNA Replication.

RPA binds to ssDNA with a dissociation constant of 10^8 to 10^{11} M^{-1} (Kim *et al.*, 1992; Kim *et al.*, 1994; Kim *et al.*, 1995). RPA binds to double-stranded DNA (dsDNA) with approximately a thousand fold difference compared to its binding to ssDNA (Kim *et al.*, 1994; Lao *et al.*, 1999). However, RPA binds with enhanced affinity to dsDNA that has been damaged by cisplatin or UV (Turchi (Turchi *et al.*, 1999; Binz *et al.*, 2003; Oakley *et al.*, 2010). This is likely to be the result of the disruption of hydrogen bonds between complementary DNA bases leading to generation of a small region of ssDNA at the site of damage (Clugston *et al.*, 1992; Burns *et al.*, 1996; Patrick *et al.*, 1998; Missura *et al.*, 2001). Initial binding of RPA to ssDNA involves the interaction of DBD A and B to DNA 8-10 nucleotides in length (Bochkareva *et al.*, 2002). The nucleotide length is extended to 12-23 nucleotides through the interaction of DBD C. Finally the involvement of DBD D allows RPA to occlude a region of ssDNA of 30 nucleotides (Bochkareva *et al.*, 2002). The stepwise processes for RPA binding to 30 nucleotides occurs at a slower rate than RPA binding to smaller lengths ssDNA (Patrick *et al.*, 2001).

During DNA replication, RPA associates with origins of replication where it promotes the recruitment of DNA polymerase α (Iftode *et al.*, 1997; Tanaka *et al.*, 1998; Maga *et al.*, 2001). RPA interacts with pol α through the N-terminal of RPA1 (Dornreiter *et al.*, 1992; Braun *et al.*, 1997). DNA damage induced hyperphosphorylation of RPA2 on the N-terminal has been shown to inhibit DNA replication and to decrease the interaction of RPA with pol α (Carty *et al.*, 1994; Oakley *et al.*, 2003; Patrick *et al.*, 2005). This may play a vital role in DNA metabolism following DNA damage. DNA damage-induced phosphorylation of RPA may affect the DNA replication function of the protein allowing time for cells to repair the damage.

1.8.5 Phosphorylation of RPA2

The RPA2 subunit of RPA has a serine and threonine-rich N-terminal (Fig. 1.8). RPA2 is phosphorylated in a cell cycle-dependent manner by the cyclin-dependent kinases (CDK1 and CDK2) (Din *et al.,* 1990; Dutta *et al.,* 1992; Anantha *et al.,* 2007). Phosphorylation by the CDKs occurs during S-phase on S23, by cyclin A-CDK2, and during mitosis on Ser 29, by cyclin B-CDK2 (Din *et al.,* 1990; Dutta *et al.,* 1992; Fang *et al.,* 1993; Henricksen *et al.,* 1994; Anantha *et al.,* 2007). As cells progress into G1, RPA2 is dephosphorylated and relocates to the nucleus. Anantha *et al.,* (2007) demonstrated that CDK-dependent phosphorylation on Ser23 and Ser29 can prime RPA2 for phosphorylation on other damage-dependent sites. Mutation of Ser23 to alanine reduced damage-dependent phosphorylation of RPA2 on other sites (Anantha *et al.,* 2007). In addition, using the CDK inhibitor roscovitine to prevent phosphorylation on Ser23 and Ser29, it was found that the same decrease in phosphorylation occurred on other sites of RPA2 following DNA damage (Anantha *et al.,* 2007) consistent with the requirement for phosphorylation on Ser23 prior to phosphorylation of other sites in the N-terminal of RPA2 (Anantha *et al.,* 2007).

As noted, RPA2 is hyperphosphorylated following DNA damage in a PIKK-dependent process (Cruet-Hennequart *et al.,* 2006; Anantha *et al.,* 2007; Cruet-Hennequart *et al.,* 2008). A variety of DNA damaging agents including cisplatin, UV and IR have been shown to lead to phosphorylation of RPA2 on N-terminal sites by PIKKs (Liu *et al.,* 1993; Carty *et al.,* 1994; Zernik-Kobak *et al.,* 1997; Cruet-Hennequart *et al.,* 2006; Anantha *et al.,* 2007; Cruet-Hennequart *et al.,* 2008). DNA damage by cisplatin and UV induces phosphorylation of RPA2 on Ser4, Ser8, Thr21 and Ser33 (Cruet-Hennequart *et al.,* 2006; Cruet-Hennequart *et al.,* 2008). RPA2 is phosphorylated on Ser33 by ATR following UV and cisplatin treatment and on Ser4 and Ser8 in a DNA-PK-dependent manner (Cruet-Hennequart *et al.,* 2006; Anantha *et al.,* 2007; Cruet-Hennequart *et al.,* 2008). ATM is required for RPA2 phosphorylation following IR (Liu *et al.,* 1993; Cheng *et al.,* 1996). RPA is excluded from the chromatin during mitosis (Oakley *et al.,* 2003; Stephan *et al.,* 2009). However, damage induced during mitosis

causes RPA to relocate to DNA. RPA2 which is phosphorylated on Ser23 and Ser29 is further phosphorylated on Ser4, Ser8 and Thr21, but not on Ser33, in an ATM-dependent manner (Anantha *et al.,* 2008; Anantha *et al.,* 2009; Stephan *et al.,* 2009).

Phosphorylation of the RPA2 subunit of RPA induces a conformational change in the heterotrimer reducing its affinity for ssDNA (Binz *et al.,* 2003; Liu *et al.,* 2005). Evidence suggests that the phosphorylated N-terminal domain of RPA2 interacts with the DBD F of RPA1, competing with the binding of RPA1 of ssDNA, and allowing DNA damage response proteins to interact with the N-terminal of RPA1 (Oakley *et al.,* 2010). RPA binds with higher affinity to cisplatin-damaged dsDNA than to undamaged dsDNA (Turchi *et al.,* 1999; Binz *et al.,* 2003; Oakley *et al.,* 2010). Phosphorylation of RPA2 also inhibits DNA replication probably due to the decrease in interaction with the replicative DNA polymerase α (Oakley *et al.,* 2003; Patrick *et al.,* 2005). It has been demonstrated that RPA2 phosphorylation is required for HR to occur in MCF-7, breast cancer cells treated with hydroxyurea (HU) (Shi *et al.,* 2010). Lee *et al.,* (2010) demonstrated, also, that de-phosphorylation of RPA2 by PP4 is required for HR (Lee *et al.,* 2010). RPA2 phosphorylation reduces the affinity of RPA for DNA. RPA2 needs to be dephosphorylated in order for DNA synthesis following DNA repair (Lee *et al.,* 2010). RPA2 may undergo cycles of phosphorylation and dephosphorylation, both of which appear to be required for HR.

1.8.6 RPA-protein interactions

As RPA plays an important role in a variety of aspects of DNA metabolism it is essential that it interacts with proteins involved in these processes. RPA interacts with proteins involved in DNA replication, recombination and repair. RPA interacts with proteins through interactions with the N-terminus of RPA1 and the C-terminus of RPA2 (Lin *et al.,* 1996; Jacobs *et al.,* 1999; Oakley *et al.,* 2010). RPA-interacting proteins include ATRIP (Zou *et al.,* 2003), DNA-PKcs, BRCA2 (Wong, Ionescu *et al.,* 2003), p53 (Dutta *et al.,* 1993), Mre11 (Olson *et al.,* 2007), PCNA (Dianov *et al.,* 1999) and FANCD2 (Andreassen *et al.,* 2004).

Proteins interact with RPA2 through the winged helix-turn-helix domain within the C-terminus. DNA damage-induced phosphorylation of RPA2 does not affect the interaction of proteins through RPA2 (Mer *et al.,* 2000). Proteins that interact with RPA through the C-terminus of RPA2 include XPA, Rad52 and TIPIN. However, Rad52 contains two different sequences which allow it to interact with RPA1 and RPA2. The interaction of RPA with XPA is necessary for NER (Matsuda *et al.,* 1995).

Recently it has been shown that RPA2 interacts directly with the ubiquitin ligase RFWD3 (Gong *et al.,* 2011; Liu *et al.,* 2011). RFWD3 contains as SQ motif and is a substrate of ATM and ATR (Matsuoka *et al.,* 2007; Mu *et al.,* 2007). RFWD3 is recruited to stalled replication forks through its interaction with RPA2. RFWD3 also appears to play a role in Chk1 activation following DNA damage (Gong *et al.,* 2011).

1.9 Proteasome inhibition in the DNA damage response

Proteasome inhibitors are emerging as promising cancer therapies, with the development of bortezomib in the treatment of multiple myeloma (Kanagasabaphy *et al.,* 2007; Wu *et al.,* 2010). Proteasome inhibitors also sensitise cancer cell lines to DNA damaging agents used in cancer therapy including γ-irradiation, melphalan and cisplatin (Motegi *et al.,* 2009). A number of studies investigating the role of the proteasome in DNA repair pathways have been carried out. Studies utilised either small molecule proteasome inhibitors or the genetic disruption of the ubiquitin pathway to investigate the effect on cellular response to DNA damage. However, the molecular basis by which proteasome inhibitors sensitise cancer cells is not clear.

Proteasome inhibition has been shown to inhibit HR-mediated repair of IR-induced DSBs (Murakawa *et al.,* 2007). Proteasome inhibition by lactacystin or MG132 did not affect the activity of ATM and the MRN complex. However, accumulation of ATRIP-ATR and RPA2 phosphorylated at Thr21 at sites of damage was severely attenuated (Murakawa *et al.,* 2007). However, it is not known from this if unphosphorylated RPA2 was recruited. It was also observed

that proteasome inhibition suppressed the formation of Rad51 and BRCA1 foci (Murakawa *et al.,* 2007; Motegi *et al.,* 2009). From this evidence it appears that the proteasome functions in HR at a stage before the formation of the Rad51 nucleofilament.

One of the essential components of the HR pathway is the DSS1 protein (Li *et al.,* 2006; Kristensen *et al.,* 2010; Liu *et al.,* 2010a). Together with its binding partner BRCA2, it is required for Rad51 nucleofilament formation. DSS1 may function in recruiting the proteasome to sites of DNA damage repair as DSS1 is a component of the of the 19S regulatory subunit of the 26S proteasome degradation (Krogan *et al.,* 2004; Josse *et al.,* 2006). DSS1 interacts with RPN7 and RPN3 (components of the proteasome) and is required for proteasome dependent degradation of ubiquitinated proteins (Krogan *et al.,* 2004; Josse *et al.,* 2006) .

Robison *et al.,* (2007), showed that proteasome inhibition by MG132 resulted in a reduction in etoposide induced ATM activation and phospho-Nbs1 foci formation in Hela cells (Robison *et al.,* 2007). Etoposide is a topoisomerase II inhibitor which stabilises the interaction of topoisomerase II and DNA (Caldecott *et al.,* 1990). Etoposide prevents religation of DNA strands following DSBs formation (Hande 2003). The ends of DSBs are concealed by topoisomerase II which is removed through the proteasomal degradation of topoisomerase II proteins (Desai *et al.,* 2001; Zhang *et al.,* 2006). Proteasome inhibitors impair the removal of topoisomerase proteins from sites of DSB preventing cells from recognising the breaks resulting in a reduction in the activation of ATM and phospho-Nbs1 foci formation (Desai *et al.,* 2001; Zhang *et al.,* 2006).. Proteasome inhibition did not alter formation of etoposide induced RPA2 and RPA2-pS4S8 foci formation most likely as a result of the generation of ssDNA at stalled replication forks at sites of etoposide induced DNA damage (Robison *et al.,* 2007).

In a study by Jacquemont *et al.,* (2007) it was shown that proteasome function was required for the Fanconi anemai pathway (Jacquemont *et al.,* 2007). Treatment of Hela cells with proteasome inhibitors, MG132, lactacyctin or

bortezomib, before and after cisplatin treatment prevented cisplatin-induced FANCD2 monoubiquitination and subsequent foci formation (Jacquemont *et al.*, 2007). This evidence implies that proteasome function is required for FANCD2 monoubiquitination.

HR was impaired in chicken DT40 cells and human cells lacking the E2 conjugating enzyme UBC13 (Zhao *et al.*, 2007). In these cells RPA2-pT21 and BRCA1 foci formation was also disrupted, similar to the observations following proteasome inhibition, implying that UBC13 is required for the resection of DSBs forming ssDNA (Motegi *et al.*, 2009). UBC13 is required for K63-linked ubiquitination. This modification does not normally target proteins for proteasomal degradation; however, some cases of degradation of K63-ubiquitinated proteins have been reported (Duncan *et al.*, 2006). The role of UBC13 in HR has not yet been fully elucidated.

Proteasome inhibition has also been shown to inhibit NER as treatment of cells with proteasome inhibitors prevented the removal of UV-lesions and cisplatin-induced crosslinks (Mimnaugh *et al.*, 2000). The XPC-HR23A protein complex is responsible for the detection of damage in the NER pathway (Sugasawa *et al.*, 2001; Wittschieben *et al.*, 2005). HR23A and its yeast homologue, Rad23, contain an ubiquitin-like (UBL) domain which interacts with subunits of the 19S regulatory particle of the proteasome, including Rpt4 and Rpt6 (Watkins *et al.*, 1993; Schauber *et al.*, 1998; Hiyama *et al.*, 1999). In S. cerevisiae Rad23 facilitates NER through an interaction with the 19S proteasome. Mutation of *Rpt4* and *Rpt6* inhibited NER (Gillette *et al.*, 2001).

1.10 Research objectives:

The main objective of this project was to investigate the effect of proteasome inhibition on cisplatin-induced DNA damage responses in DNA polymerase η-deficient cells.

(i) Investigation of proteasome inhibition on the sensitivity of pol η-deficient cells to cisplatin.

(ii) Examination of the effect of proteasome inhibition on cisplatin-induced cell cycle arrest in pol η-deficient cells.

(iii) Characterisation of the effect of proteasome inhibition on cisplatin-induced phosphorylation of DNA damage response proteins.

Chapter 2:
Materials and Methods

2.1 Cell lines

The SV40-transformed normal human fibroblast cell line (GM00637) and the XP30RO cell line (GM0317A) were obtained from the National Institute for General Medical Sciences (NIGMS) Human Genetic Cell Repository (Coriell Institute for Medical Research, New Jersey). The TR30-2 cell line is derived from the XP30RO cell line in which polη is expressed from a *POLH* transgene. The PD20i and PD20:RV human fibroblast cell lines were obtained from the Oregon Health and Science University (OHSU) Fanconi anemia Cell Repository (Portland, OR, USA).

2.2 Cell culture

Unless otherwise stated all cell culture reagents were obtained from Sigma-Aldrich. XP30RO, GM00637 and TR30-2 cell lines were cultured in Minimal Essential Media (MEM) supplemented with 10% non-heat inactivated foetal bovine serum (FBS), 2X vitamins, (Gibco, Gaithersburg, MD, USA) 2X essential amino acids, 2X non-essential amino acids, 2mM L-glutamine and 1% penicillin-streptomycin. PD20i and PD20: RV cells were cultured in Minimal Essential Media (alpha modification) supplemented with 15% non-heat inactivated FBS, 2mM L-glutamine and 1% penicillin-streptomycin solution. Cells were routinely cultured in 75 cm^2 tissue culture flasks (Corning). When cells were approximately 80% confluent they were detached from the tissue culture flask using 3mls 2X trypsin-EDTA solution in Hanks balanced salt solution. When cells had detached, trypsin was neutralised by the addition of 5mls of fresh growth medium. Cells were collected by centrifugation at 1200rpm for 5minutes in a Rotanta 460 centrifuge (Hettich Zentrifugen, Tuttlingen, Germany). The cell pellet was resuspended in fresh growth medium and counted using Kova® Glasstic® Slide 10 combination coverslip-microscope slides (Hycor Biomedical Ltd., CA, USA), prior to reseeding at 4 x 10^5 cells in a 75 cm^2 tissue culture flask containing 15ml growth medium. Cells were maintained at 37°C with 5% CO_2 in a Nuaire™ US Autoflow CO_2 Water-Jacketed Incubator with Class 100 HEPA Filtration System. All tissue culture procedures were carried out in a Nuaire™ Biological Safety Cabinet (NU-437-400E, Nuaire, Plymouth, MN, USA).

Disposable sterile plasticware was used throughout and surfaces were sprayed with 70% industrial methylated spirits (IMS) during all cell culture procedures.

2.3 Cryopreservation

Cell lines were stored in liquid nitrogen at 1.5 x 10^6/ml in freezing medium consisting of culture medium containing 20% uninactivated FBS and 10% dimethlysulfoxide (DMSO, Sigma-Aldrich). Cells were removed from flasks by trypsinisation as described above. Cells were centrifuged at 1200rpm for five minutes, counted and resuspended at 1.5 x 10^6/ml in freezing medium. The cell suspension was transferred to 1.5ml cryovials (Nunc, Wiesbaden, Germany) in 1ml aliquots. The vials were placed in a Nalgene™ Cryo 1°C freezing container (Rochester, NY, USA) containing room temperature 100% isopropanol, and stored at -80°C overnight. The next day cells vials were transferred to a liquid nitrogen storage system (Jencons-PLS, Bedfordshire, UK) for long term storage.

2.4 Resuscitation

On removal from liquid nitrogen, cells were thawed out by placing the vial at 37°C. The thawed cell suspension was removed from the vial and added to 5mls of pre-warmed growth medium. Cells were collected by centrifugation at 1000 r.p.m for 5 minutes. The cell pellet was resuspended in fresh growth medium and transferred to a 25 cm^2 flask (Corning). Cells were incubated at 37˚C and 5% CO_2 and the growth medium was changed the following day.

2.5 Cell treatment

2.5.1 Cis-diammine platinum (II) dichloride (cisplatin) treatment

Cells were seeded in 60 mm or 100 mm dishes and grown to approximately 70% confluence. Cisplatin ('Ebewe'), 1 mg/ml stock solution, was added directly to the growth medium. The final concentration is indicated in individual experiments. Control cells were treated with the appropriate volume of sterile dH_20. Medium containing cisplatin was maintained on the cells until the time of harvest as indicated in different experiments.

2.5.2 MG132 treatment.

Cells were seeded in 60mm or 100mm dishes and grown to approximately 70% confluence. MG132 (Calbiochem) was dissolved in 100% ethanol (Sigma-Aldrich) to give a stock concentration of 2mM and was stored at -20°C. MG132 was added directly to the growth medium to give a final concentration of 2μM. Control cells were treated with the appropriate volume of ethanol. Where indicated, cells were co-treated with cisplatin and MG132 or with each of these agents seperately. Medium containing MG132 was maintained on the cells for the time indicated in individual experiments.

2.5.3 Phosphatidylinositide-3 kinase-like kinase (PIKK) inhibitor treatment

Inhibitors of DNA-PK (NU7741; KuDOS Pharmaceuticals, Cambridge, UK) and ATM (KU55933; KuDOS Pharmaceuticals) were dissolved in 100% DMSO (Sigma-Aldrich) and stored at -20C at a stock concentration of 10 mM. At the time of cisplatin treatment cells were co-treated with 10μM DNA-PK inhibitor, 10μM ATM inhibitor or mock treated with DMSO giving a final DMSO concentration of 0.1% (v/v). Medium containing inhibitors was maintained on the cells until the time of harvest.

2.6 XTT cell viability assay.

The XTT assay (Roche) is based on the cleavage of the yellow tetrazolium salt, XTT, which is carried out by metabolically active cells to yield an orange formazan dye. Therefore the amount of formazan dye formed directly correlates to the number of metabolically active cells. Cells were seeded in triplicate in 96-well tissue culture plates at 5×10^3 cells per well. Cells were treated as indicated in individual experiments. After treatment, cell viability was determined directly either after the treatment period, or the medium was removed, cells were rinsed with fresh media and were then allowed to recover for 4 days in new media. The labelling solution was prepared as follows immediately before use: 100μl of electron coupling reagent (PMS (N-methyl dibenzopyrazine methyl sulfates); 0.383 mg/ml [1.25mM] in PBS) and 5ml of labelling reagent (sodium 3´-[1-

(phenylaminocarbonyl)- 3,4 tetrazolium]-bis (4-methoxy-6-nitro) benzene sulfonicacid hydrate in RPMI 1640, without phenol red) was added to growth media. 150µl was pipetted into each well of the 96-well tissue culture plate. Cells were incubated for a further four hours after which the absorbance was measured at 490nm using a Victor^2 1420 plate reader (Wallac, MA, USA). Results were expressed as the percentage viability relative to the viability of untreated cells.

2.7 Flow cytometry, propidium iodine staining and BrdU incorporation

One hour prior to the time of harvesting, cells were pulse-labelled with 10µM bromodeoxyuridine (BrdU), a thymidine analogue which can be actively incorporated into DNA during replication. After labelling, cells were harvested by trypsinisation as outlined in Section 2. 2. Cells were washed in PBS by centrifugation at 12000 rpm for 5 minutes. The cell pellet was resuspended in 1ml of ice-cold PBS and cells were fixed by the slow, dropwise, addition of 3ml ice-cold 100% ethanol. Fixed cells were stored at -20°C. On the day of analysis, cells were allowed to thaw at room temperature and centrifuged at 2000 rpm for 10 minutes in a Rotanta 400 centrifuge. The supernatant was discarded. The cell pellet was disrupted and 1 ml 2N HCl-0.5% Triton X-100 was added in a dropwise manner to permeablise the cells. Cells were incubated at room temperature with gentle rocking for 30 minutes. Cells were centrifuged at 1000 rpm for 10 minutes and the supernatant was discarded. HCl was neutralised by the addition of 1ml 0.5ml Na_2B_407 pH 8.5, which was followed by centrifugation at 1000 rpm for 10 minutes. Cells were re-suspended in 750µl PBS, 1% w/v BSA, 0.5% v/v Tween-100 followed by the addition of 15 µl of FITC-labelled anti-BrdU antibody (BD Biosciences). Tubes were rotated at room temperature in the dark for 1 hour. Cells were centrifuged at 1000 rpm for 3 minutes. Cells were washed twice in PBS-1% w/v BSA-0.5% v/v Tween-100 by centrifugation. Cellular DNA was stained by resuspending the cell pellet in 500µl propidium iodide (PI/RNase) (BD Biosciences) for 15 minutes at room temperature in the dark. Samples were acquired using a FACSCalibur flow cytometer. Data was analysed using Cell Quest™ Software.

2.8 Analysis of RPA2-phosphoSer4/Ser8 by flow cytometry

Following treatment cells were harvested by trypsinisation as outlined in Section 2. 2. Cells were fixed in Fix & Perm® solution A (ADG, Bio Research GMBH), for 15 min at room temperature, then washed in PBS. Cells were permeablised in Perm® Solution B. They were then incubated with 100 µl of a 1/500 dilution of anti-phosphoSer4/Ser8-RPA2 antibody (Bethyl Laboratories) for 1 h at room temperature in Fix & Perm® Solution B. Cells were washed with PBS, and stained with secondary antibody, anti-rabbit-FITC at a 1/1,000 dilution for 45 min at room temperature in the dark. After washing in PBS, the cells were incubated in 500µl PI/RNase staining solution (BD Biosciences) for 45 min, before being analysed by flow cytometry using a FACSCalibur. Data analysis was carried out using Cell Quest^{TM} software.

2.9 Preparation of protein lysates.

All steps during the preparation of protein lysates were carried out on ice. Following cell treatment, cells were washed twice with ice-cold PBS. The appropriate volume of cell lysis buffer (PBS, pH 7.6, containing 0.1% SDS [Bio-Rad Laboratories, CA, USA], 0.5% deoxycholic acid (DOC, Sigma-Aldrich), 1% Triton X-100 (Sigma-Aldrich), containing protease and phosphatase inhibitors (Table 2.1), was added to the tissue culture dishes. Cells were scraped into the lysis buffer using cell scrapers (Sigma-Aldrich) and transferred to a 1.5ml tube (Eppendorf), vortexed and incubated on ice for 15 minutes. The tubes were then centrifuged at 14,000 rpm at 4^{o}C for 15 minutes in a Sigma 1-15K centrifuge (Sigma Laborzentrifugen, Osterode am Harz, Germany). The supernatant was transferred to a new 1.5 ml tube and stored at -20^{o}C.

Protease Inhibitors	**Stock concentration**	**Final concentration**
Aprotinin	2 mg/ml	2 µg/ml
Leupeptin	1 mg/ml	1 µg/ml
Phenylmethylsulfonyl fluoride (PMSF)	100 mM	1 mM
Phosphatase inhibitors		
Sodium orthovanadate (Na_3VO_4)	100 mM	1 mM
Sodium fluoride (NaF)	500 mM	5 mM

Table 2.1: Stock concentration and final concentrations of protease and phosphatase inhibitors in protein lysate buffer.

2.10 Preparation of protein lysates under denaturing conditions.

Following cell treatment, cells were harvested by trypsinisation (Section 2.2). Approx 10^7 cells were resuspended in 100µl of denaturing lysis buffer (50 mM Tris, pH 7.4, 1% (w/v) SDS, 5 mM EDTA) containing 10 mM dithiothreitol (DTT), 15 U/ml DNase 1 and protease and phosphatase inhibitors as shown in Table 2.1. The addition of DNase 1 may not be necessary, as it has been shown that DNAse 1 is not active under these conditions (Tullis *et al.*, 1974; Lacks *et al.*, 1979). Lysates were placed in boiling water for 5 minutes, after which 900µl of non-denaturing lysis buffer (50 mM Tris, pH 7.4 1 % (w/v) Triton X-100, 300 mM NaCl, 5 mM EDTA) containing protease and phosphatase inhibitors as in Table 2.1 was added and sample was incubated on ice for 10 minutes. The sample was centrifuged at 14000 rpm for 15 minutes. The resulting supernatant was collected and stored at -20°C.

2.11 Subcellular fractionation.

Differential salt fractionation was used to isolate chromatin-bound and soluble proteins. Following cell treatment, cells were trypsinised as described in Section 2.2, and the resulting cell pellet was washed in ice-cold PBS. Cells were lysed with subcellular lysis buffer (50mM Tris-HCl, pH 7.5, 150mM NaCl, 0.1% Nonidet P-40, 0.5% Triton X-100, 5µg/ml pepstatin, 5µg/ml leupeptin, 5µg/ml

aprotinin, 10mM NaF, 10mM β-glycerophosphate, 1mM Na_3VO_4, 1mM PMSF) on ice for 10 minutes. The insoluble fraction was isolated by centrifugation at 10,000rpm for 10 minutes at 4°C in a Sigma 1-15K centrifuge. The resulting supernatant was collected and stored at -20°C; this was designated the soluble fraction. The pellet was washed with PBS and resuspended in subcellular lysis buffer containing 100µg/ml DNase I (Sigma-Aldrich), and incubated at 37°C for 30 minutes. 1M ammonium sulphate was added to a final concentration of 250mM, and the lysate was further incubated for 10 minutes at room temperature. The insoluble fraction was precipitated by centrifugation at 10,000 rpm for 10 minutes at 4°C in a Sigma 1-15K centrifuge. The supernatant was collected and stored at -20°C. This was designated the chromatin-bound fraction (CBF).

2.12 Determination of protein concentration.

The protein concentration in cell lysates was determined using the DC Protein Assay (Bio-Rad Laboratories). BSA standards ranging from 0-1mg/ml were prepared in protein lysis buffer from a stock BSA solution (2mg/ml). 5 µl of each standard was transferred into duplicate wells of a 96-well plate (Sarstedt). Protein samples were briefly vortexed and 2µl of each sample was added into duplicated wells. Reagent A' was prepared immediately prior to use by addition of 20 µl of reagent S per millilitre of reagent A. 25 µl of reagent A' was added to each well, followed by 200µl of reagent B. 2 µl of reagent A' was added to each well, followed by 200µl of reagent B. The colour was allowed to develop for 15 minutes, after which the absorbance was read at 490 nm on a Victor^2 1420 Multilabel Counter (Wallac, MA, USA). Using Microsoft Excel software a standard curve of absorbance versus protein concentration was constructed from the absorbance of the BSA standards. The protein concentration in the unknown cell lysates was calculated using the equation of the standard curve.

2.13 Sodium Dodecyl Sulphate-Polyacrylamide Gel Electrophoresis (SDS-PAGE)

SDS-PAGE gels were prepared according to Table 2.2. Cell lysates were separated by SDS-PAGE using the Bio-Rad Mini-Protean® 3 Cell System. 15-30µg of protein lysate, prepared as described in Section 2.12, was mixed with 4X Laemmli buffer (250 mM Tris pH 6.8, 9.2% (w/v) SDS, 40% (v/v) Glycerol, 0.1% (w/v) bromophenol blue, 5% (v/v) β-mercaptoethanol; (Laemmli 1970)) and placed in boiling water for 5 minutes. The sample was loaded on the gel in 1X running buffer (19.2mM glycine, 2.5mM TrisBase, 0.01% (w/v) SDS). 5µl of pre-stained protein marker (either from Fermentas or ThermoScientific) was loaded in one well of each gel. Empty wells were filled with 1X Laemmli buffer. Gels were run in 1X running buffer. Electrophoresis was carried out at constant voltage of 130V for 2-3 hours depending on the molecular weight of the proteins being analysed.

Running Gel (2 x 1mm gels)	**7%**	**12%**
Acrylamide %	**(ml)**	**(ml)**
H_2O	5.3	3.3
30% (w/v) Acrylamide-Bis (BioRad)	2	4
1.5M Tris pH 8.8	2.5	2.5
10% (w/v) SDS	0.1	0.1
10% (w/v) APS	0.1	0.1
TEMED	0.008	0.004

Stacking Gel (2 x 1mm gels)	**(ml)**
H_2O	1.4
30% (w/v) Acrylamide-Bis	0.33
Tris 1M pH 6.8	0.25
10%(w/v) SDS	0.02
10% (w/v) APS	0.02
TEMED	0.002

Table 2.2: Components of SDS-PAGE running gel and stacking gel.

2.14 Coomassie blue staining.

Following the separation of protein samples by SDS-PAGE as described in Section 2.13, the gel was fixed and stained with coomassie blue stain (40% (v/v) methanol, 10% (v/v) acetic acid, 0.2% (w/v) Brilliant Blue R (Sigma)), for 1 hour on a rocker. The gel was then destained using 40% (v/v) methanol, 10% (v/v) acetic acid until the blue bands of the stained proteins were seen. Gels were stored in dH_2O at 4°C.

2.15 Silver staining.

Following the separation of protein samples by SDS-PAGE as described in Section 2.13 the gel was fixed in 50% (v/v) methanol/12% (v/v) acetic acid containing 0.02% (v/v) formaldehyde, for 1 hour at room temperature with gentle rocking. This was followed by incubation of the gel in 50% (v/v) ethanol for 30 minutes. The fixed gel was placed in 0.02% (w/v) sodium thiosulphate for 1 minute and washed five times for 20 seconds each time in dH_20. The gel was stained with 0.2% (w/v) silver nitrate containing 0.02% (v/v) formaldehyde for 45 minutes at room temperature with rocking, and then rinsed briefly in dH_2O twice for 30 seconds. The gel was developed in a solution containing 6% (w/v) sodium carbonate, 0.001% (w/v) sodium thiosulphate and 0.02% (v/v) formaldehyde until the protein bands appeared. To stop colour development, the developer was removed and the gel incubated with 1% (v/v) acetic acid. The gel was stored in dH_2O at 4^oC.

2.16 Western blotting.

Following the separation of protein samples by SDS-PAGE as described in Section 2.13, gels were soaked in 1X transfer buffer (19.2 mM glycine, 2.5 mM TrisBase). PVDF (Polyvinylidene fluoride) membrane (Immobilon™-P Transfer Membrane, 0.45µm pore size; Millipore, MA, USA) was pre-activated in 100% methanol for 3 minutes, followed by incubation in dH_20 for 3 minutes and then cold 1X transfer buffer until use. Sponge pads and filter paper (Whatman, UK) used in the transfer procedure were also pre-soaked in cold 1X transfer buffer. Protein samples separated by SDS-PAGE were transferred from the gel to PVDF

membrane using the Mini Trans-Blot® Cell System (Bio-Rad). The transfer cassette was assembled with the gel placed on the anode side, and the PVDF membrane on the cathode side of the cassette. Five filter papers were placed on either side of the PVDF membrane and gel, with a sponge on the outside. Any air bubbles between the gel and membrane were removed. Transfer was carried out at 100 V for 45 minutes, in a tank containing pre-chilled 1X transfer buffer and an ice pack. Following protein transfer, the protein binding sites on the membrane were blocked in 5% (w/v) non-fat milk (Marvel, Premier Foods) in TBS-T (10mM TrisBase, 68 mM NaCl, pH 7.6, containing 0.05% Tween-100) for 1 hour at room temperature with gentle rocking. Primary antibody (Table 2.3), diluted in 5% (w/v) milk/TBS-T was incubated with the membrane overnight at 4^{o}C with rocking. Membranes were washed with TBS-T three times for 7 minutes each time. Horseradish peroxidase (HRP)-conjugated secondary antibody (Jackson ImmunoResearch), was diluted 1/5000 in 3% (w/v) milk/TBS-T and was incubated with the membrane for 1 hour at room temperature with rocking. The membranes were then washed three times, for seven minutes, with TBS-T. Membranes to be blotted with GAPDH and RPA2 (anti-rat) were blocked with 5% (w/v) BSA, instead of non-fat milk, in TBS-T for 90 minutes. The anti-GAPDH antibody was diluted in 5% (w/v) BSA and incubated with the membrane overnight at 4^{o}C. Following washing steps, as outlined above, HRP-conjugated anti-rabbit antibody, diluted in 3% (w/v) milk/TBS-T, was incubated with the membrane for 1 hour.

HRP-conjugated secondary antibodies bound to the membrane following washing were detected using ECL+ Western Blotting Detection Reagent (Amersham Biosciences, Buckinghamshire, UK). ECL+ solution was prepared by addition 25µl of solution B per 1ml of solution A used. 1ml of ECL+ solution was applied to each membrane for 5 minutes at room temperature. ECL+ solution was then removed and membranes were transferred to a film cassette (Sigma-Aldrich). Light emitted by the chemoluminescent product of the HRP-catalysed reaction was detected by exposure to Konica Minolta Medical Film in the dark. The film was developed manually in Devalex® X-Ray Developer until bands appeared, rinsed in dH_2O and then fixed in Fixaplus® X-Ray Fixer (Champion Photochemistry, Essex, UK). The film was rinsed in dH_2O and

allowed to dry. Alternatively, the film was developed using a CP1000 Automatic Film Processor (Agfa, Mortsel, Belgium) using the same reagents. Where indicated, the intensity of protein signal detected by western blotting was quantified using the Fujifilm LAS-3000 imager and Imagegauge V4.21 software.

Antibody	Species	Dilution	Supplier
Anti-Chk1	Rabbit	1/1000	Cell Signaling Technology Inc.
Anti-phospho Chk1 Ser317	Rabbit	1/1000	Cell Signaling Technology Inc.
Anti- RPA2 (Ab-3)	Mouse	1/4000	Calbiochem
Anti-RPA2	Rat	1/5 (5% BSA)	Dr. Heinz-Peter Nasheuer, NUI, Galway
Anti-phospho RPA2 Ser4/Ser8	Rabbit	1/4000	Bethyl Laboratories
Anti-γH2AX	Mouse	1/1000	Millipore
Anti-Histone (H1)	Mouse	1/1000	Abcam Ltd.
Anti-GAPDH	Mouse	1/5000 (5% BSA)	Abcam Ltd.
Anti-RPA4	Mouse	1/1000	Abcam Ltd.
Anti-RPA1 (Ab-1)	Mouse	1/500	Calbiochem
Anti-FANCD2	Rabbit	1/10000	Novus Biologicals
Anti-Ubiquitin (P4D1)	Mouse	1/5000	Santa Cruz Biotechnology
Anti-Actin	Rabbit	1/5000	Sigma-Aldrich
Anti-SUMO-1	Sheep	1/1000	Prof. Ron Hay, University of Dundee
Anti-HA	Mouse	1/5000	Santa Cruz Biotechnology
Anti-SUMO-2/3	Sheep	1/1000	Prof. Ron Hay, University of Dundee

Table 2.3: Primary antibodies and dilutions used in western blotting.

Secondary antibodies	Dilution	Supplier
Horseradish peroxidase (HRP) –conjugated-Goat-anti-mouse, anti-rabbit, anti-rat, IgG,	1:5000	Jackson ImmunoResearch

Table 2.4: Secondary antibodies used in western blotting

2.17 Calculation of approximate protein molecular weight

The approximate molecular weight of proteins detected by western immunoblotting was relative front (Rf) value of the protein, calculated using the formula outlined below. The length of the gel was measured. The distance, in millimeters, from the top of the gel to each protein standard was measured. The Rf value for each standard was calculated. A graph was constructed plotting Rf values of each protein standard against log molecular weight.

$$\text{Rf value} = \frac{\text{Distance from top of membrane to protein band}}{\text{Total length of membrane}}$$

The distance from the top of the gel to the protein band of unknown molecular weight was measured. The Rf value for this band was calculated, and, the corresponding log molecular weight, was obtained from the standard curve. The approximate molecular weight of the protein was calculated.

2.18 Immunofluorescence

22x22mm glass coverslips (VWR) were first cleaned prior to use for immunofluorescence. Coverslips were immersed in concentrated HCl overnight. The next day coverslips were rinsed extensively in dH2O followed by boiling in dH_2O for 15 minutes. Coverslips were allowed to cool and were washed first with dH_20, then with 95% (v/v) ethanol and finally rinsed in 100% (v/v) ethanol. Coverslips were then placed in single layers on sterile Petri dishes and allowed to dry under UV light overnight, in a closed Laminar Flow Hood. Prior to seeding cells, one coverslip was placed into the cell culture dish. Cells were grown directly on coverslips.

Following treatment for time periods indicated in individual experiments, cells were washed gently twice with pre-warmed PBS and fixed with 3.7% (w/v) PFA for 10 minutes at room temperature. PFA was removed and cells were washed twice in PBS. Coverslips were stored in PBS at 4°C until immunostaining was carried out.

Prior to immunostaining coverslips were transferred cell side up to parafilm, in a light proof box. Cells were permeablised with PBS containing 0.1% (v/v) Triton X-100 for 10 minutes, and rinsed with PBS. Non-specific antibody binding sites were blocked with PBS/0.1% (v/v) Triton X-100 containing 1% (w/v) BSA for 30 minutes. The coverslips were then incubated with 200µl of primary antibody for one hour. All antibodies were diluted in PBS/ 0.1% (v/v) Triton X-100 containing 1% (w/v) BSA. After removal of the antibody the coverslips were washed extensively with 500 µl of PBS/0.1% (v/v) Triton X-100, three times for 5 minutes each. The appropriate fluorescently-labelled secondary antibody was diluted in PBS/0.1% (v/v) Triton X-100 containing 1% (w/v) BSA. 200µl of diluted antiody was applied to the coverslips. The coverslips were incubated in the dark for one hour. Coverslips were washed three times in 500µl PBS for five minutes. To stain DNA, the cells were incubated in 4',6-diamidino-2-phenylindole (DAPI, Sigma-Aldrich) solution diluted 1/30000 in dH_2O, for 5 minutes in the dark. The coverslips were washed with PBS-0.1% (v/v) Triton X-100, followed with one wash in PBS and a final wash with dH_20. The coverslips were then inverted and mounted on SuperFrost glass slides (BDH) using Slowfade (Invitrogen). The edges of the coverslips were secured onto the slides using nail varnish. Slides were stored in the dark at 4°C if required.

Primary Antibody	Working Dilution	Supplier
Anti-phospho Ser4/Ser8 RPA2	1/4000	Bethyl Laboratories
Anti-FANCD2	1/10000	Novus Biologicals
Anti-γ-tubulin	1/100	Santa Cruz Biotechnology
Anti-Coilin	1/1000	Sigma Aldrich
Anti-PML	1/1000	Jena Biosciences

Table 2.4: Primary antibodies and dilutions used in immunofluorescence.

Secondary Antibody	Working Dilution	Supplier
Alexa 488-conjugated-Goat anti- rabbit	1/1000	Invitrogen
Alexa 594-conjugated-Goat-anti-mouse	1/1000	Invitrogen

Table 2.5: Secondary antibodies and dilutions used in immunofluorescence.

2.19 Phosphoprotein purification

Phosphorylated proteins were isolated from whole cell lysates using a phosphoprotein purification kit (Qiagen Ltd., West Sussex, United Kingdom). Cells were cultured and treated in 75cm^2 tissue culture flasks. Approximately 10^7 cells, were incubated on ice for 30 minutes in 5 ml phosphoprotein lysis buffer (Qiagen) containing 0.25% (w/v) CHAPS {3-[(3-cholamidopropyl)dimethylammonio]-1-propanesulfonate}, 50 U/ml Benzonase® nuclease and a protease inhibitor tablet (Qiagen). Phosphoprotein lysis buffer was made up immediately prior to use and kept on ice. The cell lysate was centrifuged at 14000rpm for 15 minutes at 4C and the resulting supernatant was transferred to a new tube. The following steps were carried out at room temperature. The PhosphoProtein Purification Column was prepared by

detaching the top cap and allowing the storage buffer to flow out. The PhosphoProtein purification column was equilibrated by adding phopsphoprotein lysis buffer containing 0.25% CHAPS and allowing the buffer to flow out. 2.5mg of protein lysate was adjusted to a concentration of 0.1 mg/ml by adding PhosphoProtein Lysis Buffer containing 0.25% CHAPS. The cell lysate was added to the pre-equilibrated PhosphoProtein Purification Column and allowed to flow though allowing the phosphoproteins to bind to the column. The flow through was collected in a 50ml tube. The column was washed with 6ml of phopsphoprotein lysis buffer containing 0.25% CHAPS. Proteins bound to the column were eluted with 3ml of PhosphoProtein elution buffer containing 0.25% CHAPS. Elute proteins were concentrated using Nanosep® Ultrafiltration columns (10 kDa molecular weight cutoff) until the eluate was concentrated to approximately 50 µl. this was transferred to a 1.5ml tube and stored at -20C.

2.20 Affi-Gel Blue enrichment of RPA

XP30RO cells were cultured and treated in 75cm^2 tissue culture flasks and were harvested by trypsinisation as in Section 2.2. Approximately 1x10^8 cells were lysed with NETN lysis buffer (20mM Tris pH 8.0, 1mM EDTA, 0.5% (v/v) NP-40 containing 100mM NaCl) on ice for 15 minutes. The resulting lysate was centrifuged at 14000 rpm for 15 minutes at 4°C. Protein concentration of lysate was determined as in Section 2.12 and 2 mg of protein lysate was incubated with 80 µl of Affi-Gel Blue beads (Bio-Rad Laboratories) at 4^{o}C for 2 hours, with rotation. The Affi-Gel blue beads were centrifuged at 10,000 rpm for 5 minutes and supernatant was removed. Affi-Gel blue beads were washed twice by centrifugation at 10,000 rpm for 5 minutes with 250µl NETN buffer containing 2M NaCl. Beads were then washed twice by centrifugation with 250µl NETN containing 900 mM NaCl. Protein bound to the Affi-Gel Blue beads was eluted by boiling of the Affi-Gel Blue beads for 5 minutes in 10 µl of Laemmli buffer. Eluted protein was stored at -20^{o}C, for analysis for analysis by coomassie blue staining and western immunoblotting.

2.21 Transformation of competent cells.

One aliquot (100ul) of *E. coli* Top10 cells were thawed out on ice. 50ng of plasmid DNA was added to the cells. Cells were incubated on ice for 30 minutes after which cells were heat-shocked for 2 min at 42°C. 1 ml of LB was added and cultures incubated with shaking at 37°C for 45 min. Cells were collected by centrifugation at 1200 rpm The cell pellet was resuspended in 100 µl LB-medium and plated onto agar containing 100µg/ml ampicilin. Plates were incubated at 37°C overnight.

2.22 Plasmid DNA purification.

A 200ml overnight culture was prepared by inoculating 200ml of LB broth, containing 100µg/ml ampicilin, with one colony of transformed *E. coli* cells (Section 2.21) and incubated at 37°C with shaking. Plasmid DNA purification was carried out using the Maxi Prep kit from Qiagen according to manufacturers instructions. DNA quantification and purity was determined using a NanoDrop Spectrophotometer (Nanodrop). The OD at 260nm and 280nm was measured. A_{260}/A_{280} provides an estimate of the purity of DNA. A ratio between1.7-2.0 indicates an acceptable level of DNA purity.

2.23 Transient transfection

XP30RO cells were plated out and grown to approximately 80% confluency. FuGENE ® HD transfection reagent (Roche) was incubated for 15 minutes at room temperature with plasmid DNA at a ratio of 6µl per 2µg DNA in 100µl of serum-free MEM medium. The transfection mixture was added to cells in media containing 10% FBS. Cells were transfected for 24 hours after which transfection media was removed and cells were treated as indicated in specific experiments.

2.24 Immunoprecipitation

2.24.1 Immunoprecipitation using magnetic Dynabeads®

Immunoprecipitation was carried out using Dynabeads® M-270 Epoxy magnetic beads (Invitrogen). Beads are composed of cross-linked polystyrene with a magnetic material distributed throughout. The beads are coated with a layer of epoxy functional groups which both seals the magnetic material inside the beads, and allows antibodies to bind to the surface of the beads. Dynabeads can be coated via primary amino groups in the antibodies. Once coupled with the antibody the beads are used to isolate the target protein from whole cell lysates.

1mg of Dynabeads was weighed out into a 1.5 ml eppendorf tube. Beads were washed in 500µl of 0.1M sodium phosphate buffer, pH 7.4. The tube was placed on a magnet to allow the beads to accumulate at the side of the tube. The supernatant was removed leaving the beads undisturbed. The tube was removed from the magnet and the wash step was repeated a further two times. The beads were then washed in 500µl of PBS, pH 7.4. 1mg of washed beads were coated with 1µg of anti-RPA2 antibody. 1µg of antibody was made up to a volume of 250µl with PBS pH7.4 which was used to resuspend the washed beads. 250µl of 3M ammonium sulphate made up in 0.1M sodium phosphate buffer pH 7.4 was also added to the beads to give a final concentration of 1.5M ammonium sulphate. This was incubated overnight at 37°C with rotation. The next day the tube was placed on a magnet, and the antibody-coupled beads were collected at the side of the tube. The supernatant was removed and the beads were washed four times with PBS. The final wash was for 5 minutes at room temperature with rotation. Antibody-coupled beads were the washed once with 500µl of lysis buffer. The lysis buffer was removed and 1mg of antibody-coupled beads was incubated in 400µg of protein lysate at a concentration of 1µg/ml overnight at 4°C with rotation. Following overnight incubation, beads were washed three times with 200µl of lysis buffer. Bound protein was eluted by incubation of the beads with 60µl of 0.1M citrate (pH 3.1) at room temperature for 5 minutes with rotation. The tube was then placed on a magnet and beads were collected at the

side. The supernatant containing the isolated protein was transferred to a new tube and stored at -20°C.

2.24.2 Immunoprecipitation using protein A/G agarose beads

400µg of whole cell protein lysate was incubated at 4°C overnight with rotation with 1µg of primary antibody against the protein to be immunoprecipitated. Following overnight incubation, the sample was centrifuged at 10 000 rpm for 5 minutes and the supernatant transferred to a new tube. 30 µl of Protein A/G PLUS-Agarose Immunoprecipitation Reagent (Santa Cruz Biotechnology) was washed with 0.5 ml lysis buffer (Section 2.9) containing protease and phosphatase inhibitors as in Table 2.1. Following centrifugation at 10 000 rpm for 5 minutes, the supernatant was removed, and the Protein A/G beads were resuspended in lysis buffer to a final volume of 30 µl. The beads were then transferred to the tube containing cell lysate and primary antibody abd incubated for 1 hour with end-over-end mixing at 4^{o}C to bind to antibody-bound protein. The beads were pelleted by centrifugation at 10 000 rpm for 3 minutes, followed by removal and storage of the supernatant. Unbound protein was removed by washing the beads four times with 250 µl of lysis buffer containing phosphatase and protease inhibitors. After final centrifugation, the supernatant was removed completely. The protein of interest was eluted by incubation of the Protein A/G beads in 10 µl of Laemmli buffer in boiling water for 5 minutes. The sample was stored at -20^{o}C.

2.25 Isopeptidase-T treatment.

Following immunoprecipitation as outlined in Section 2.24.1, buffer exchange was carried out on the eluted protein to replace 0.1M citrate buffer (pH 3.1) with isopeptidase-T reaction buffer (25mM HEPES, pH 7.6). Eluted protein was applied to an Ultrafree 0.5 centrifugal filter device with a Biomax 5 kDa nominal molecular weight limit (NMWL) membrane (Millipore). 100µl of reaction buffer was also added and centrifuged at 10,000 rpm for 10 minutes or until approximately 60µl of lysate remained in the upper chamber. This process was repeated until the pH of the solution in the upper chamber was approximately pH 7.6. The approximate pH was measured using pH indicator paper (Sigma-

Aldrich). The final volume obtained was 40µl which was divided into two 0.5ml tubes. 1µg of isopeptidase T was added to one tube and incubated at 37°C for 2 hours. As a control, isopeptidase-T reaction buffer was placed in the second tube, which was also incubated at 37°C for 2 hours.

2.26 λ -phosphatase treatment.

15µl whole cell lysate with a concentration of 2µg/ml was placed in two separate 0.5ml tubes. 2 µl 10X λ-phosphatase reaction buffer and 2 µl 10X $MnCl_2$ (both from New England Biolabs) were added to both tubes to give a final concentration of 1X $MnCl_2$. 1 µg of λ phosphatase (New England Biolabs) was added to one aliquot and incubated at 37^{o}C for 1 hour. As a control the other aliquot was mock-treated with λ-phosphatase reaction buffer and incubated at 37^{o}C for 1 hour. The reaction was stopped by the addition of 5 µl of 4X Laemmli buffer and by placing the tubes in boiling water for 5 minutes. The samples were stored at -20^{o}C before analysis by SDS-PAGE and western blotting.

2.27 Preparation of samples for Mass Spectrometry

(i) Immunoprecipitation of RPA2 was carried out as outlined in Section 2.24.2. Eluted protein was divided into three equal volumes and separated by SDS-PAGE in different lanes on the same gel. The gel was cut into three sections. One section was stained with coomassie blue (Section 2.14), one was stained with silver stain (Section 2.15) and the third section was analysed using western blotting and anti-RPA2 antibody. Bands of interest were excised from the coomassie stained gel. Excised bands were placed in individual eppendorf tubes containing 0.1% acetic acid. Bands were sent at room temperature to the Mass Spectrometry Resource at the Conway Institute at UCD. In-gel tryptic digestion was carried out on excised bands. Proteins were analysed by liquid chromatography mass spectrometry (LC-MS/MS), using a Thermo Fisher LTQ mass spectrometer. The peaklist-generating software was Mascot Distiller v2.1 and the search engine used was Protein Prospector v4.25.4. The database searched was SwissProt.2007.04.19 (264492 entries). The

measure of confidence in the identification peptides was indicated by posterior error probability (PEP) values. The lower the PEP value the higher the confidence of protein identification. Data was analysed at UCD in collaboration by Dr. G. Cagney.

(ii) Immunoprecipitation of RPA2 was carried out as outlined in Section 2.25.1. Seven individual immunoprecipitations were carried out using 400µg of protein each. Eluted protein from each immuoprecipitation was pooled and concentrated using a 5kDa cut-off spin column. The elution buffer was exchanged for lysis buffer until the pH reached approximately pH 7 (Section 2.25), yielding a final volume of 40µl. 3µl of the final concentrated protein was analysed by SDS-PAGE and western blotting using an-anti RPA2 antibody. The remaining protein was sent on dry ice to the College of Life Sciences, University of Dundee to the laboratory of Professor Ron Hay, where the protein was separated by SDS-PAGE and analysed by coomassie staining. Two areas of the gel were excised and in-gel tryptic digestion was carried out. Peptides were analysed by Orbitrap MS (1 h HPLC gradient) to give two RAW data files. Data were processed by MaxQuant with the integral Andromeda search protocol (version 1.1.1.14). Searches were performed with parameters set at 1% false discovery rate (FDR) and was also repeated with no FDR filtering. The measure of confidence in the identification peptides was indicated by PEP values.

Chapter 3
Results

3. Effect of proteasome inhibition on cisplatin induced DNA damage responses.

The proteasome plays a major role in the regulation of cellular processes. Proteins are targeted to the proteasome through polyubiquitination, where proteins are degraded (Section 1.4). Inhibition of the proteasome has been used recently as a cancer treatment strategy, with the development of the proteasome inhibitor bortezomib or Velcade® as a treatment for patients with multiple myeloma (Adams 2004; Adams *et al.,* 2004; Kropff *et al.,* 2006; Adams *et al.,* 2009). In a screen of cancer cells lines, bortezomib has been shown to have wide range of anti cancer activity (Caravita *et al.,* 2006). In a clinical setting, proteasome inhibitors are either used as single agents or are also used in conjunction with other cancer treatment. Proteasome inhibitors sensitise cancer cell lines to routinely-used cancer treatments including cisplatin (Mimnaugh *et al.,* 2000).

As outlined in Section 1.6, cisplatin is a platinum-based chemotherapeutic drug which reacts with DNA to form inter- and intrastrand crosslinks (Perez 1998; Berndtsson *et al.,* 2007). Cisplatin is used successfully in the treatment of germ cell cancers, and is especially effective against testicular cancer, and to a lesser extent, against ovarian cancers, as well as being used regularly in the treatment of head, neck and non-small cell lung cancers. The cytotoxic effects of cisplatin are mainly due to the induction of intrastrand and interstrand crosslinks in DNA (Section 1.6) (Kartalou *et al.,* 2001; Chaney *et al.,* 2005).

In the present study, a DNA polη-deficient human cell line (XP30RO) was used as the model system in which to investigate the effect of proteasome inhibition on cisplatin-induced DNA damage responses. XP30RO cells lack functional DNA polymerase η due to a thirteen base-pair deletion in exon two of the *POLH* gene (Johnson *et al.,* 1999; Masutani *et al.,* 1999). DNA pol η is required for error-free translesion synthesis past UV-induced cyclobutane pyrimidine dimers (CPDs) (Masutani *et al.,* 2000; Yao *et al.,* 2001). Purified pol η can bypass purified cisplatin-induced guanine-guanine intrastrand crosslinks (Alt *et al.,*

2007; Biertumpfel *et al.*, 2010). DNA pol η also plays a role in the repair of cisplatin-induced interstrand crosslinks (Ho *et al.*, 2010). This model system was used as cells lacking DNA pol η are more sensitive to cisplatin than normal cells, display increased cell cycle arrest when compared to pol η-proficient, cells and a number of DNA damage responses are more strongly activated in polη-deficient cells following cisplatin treatment (Cruet-Hennequart *et al.*, 2008; Cruet-Hennequart *et al.*, 2009).

3.1 Effect of MG132 on protein ubiquitination.

MG132 is a synthetic peptide aldehyde proteasome inhibitor which has been widely used to study the effects of proteasome inhibition (Lee *et al.*, 1998). MG132 readily enters the cell and binds to the β-5 subunits of the 26S proteasome inhibiting the chymotryptic activity (Lee *et al.*, 1998). One consequence of proteasome inhibition is an increase in the level of polyubiquitinated proteins in the cell, as polyubiquitinated proteins are not degraded (Dantuma *et al.*, 2006). There is also evidence that inhibition of the proteasome by MG132 may lead to the depletion of the pool of freely-available ubiquitin, as polyubiquitinated proteins are not degraded and therefore free ubiquitin is not recycled from these proteins (Dantuma *et al.*, 2006; Takeshita *et al.*, 2009). Accumulation of polyubiquitinated proteins is consistent with inhibition of proteasome-mediated degradation (Dantuma *et al.*, 2006). To determine whether MG132 treatment led to accumulation of polyubiquitinated proteins in XP30RO cells, cells were treated with 2μM MG132 for up to 24 hours (Fig. 3.1) and the level of ubiquitinated proteins was analysed by western blotting using an anti-ubiquitin antibody.

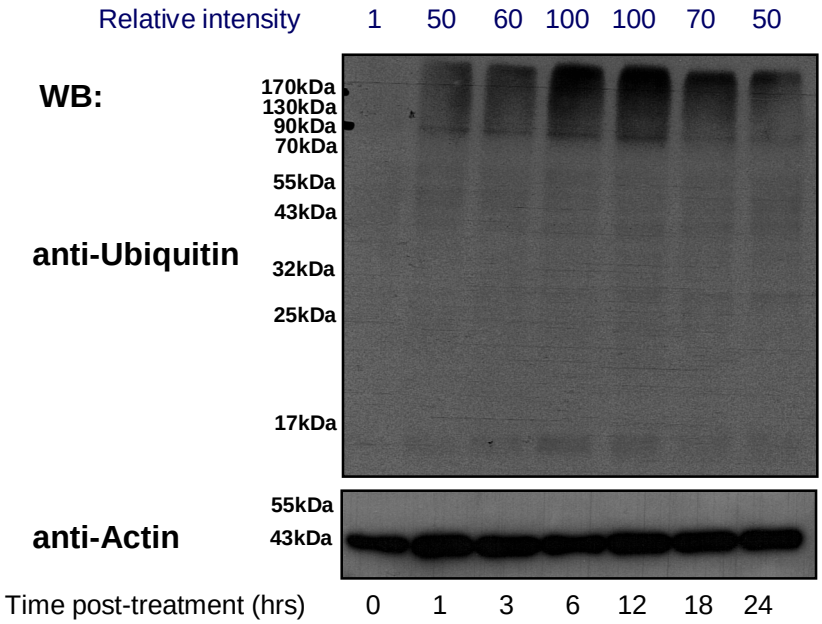

Figure 3.1: Effect of MG132 on the level of polyubiquitinated proteins. XP30RO cells were treated with 2μM MG132 for the indicated times. Cellular extracts were separated by SDS-PAGE, and analysed by western blotting using specific antibodies against ubiquitin or β-actin. The intensity of the ubiquitinated protein levels was determined by densitometry shown at the top of the image. The density at 12 hours was set at 100% and the intensities of the other time points were calculated relative to this value. Data is derived from one experiment.

The effects of proteasome inhibition on DNA damage responses were investigated using a dose of 2μM MG132 to inhibit the proteasome, based on previously published data (Jacquemont *et al.*, 2007). The level of ubiquitinated proteins in XP30RO cells was analysed by western blotting at the indicated times (Fig. 3.1) post-treatment with MG132. The level of ubiquitinated proteins in each lane were determined by densitometry, using Imagegauge V4.21 software. The level of ubiquitinated proteins increased 1 hour after exposure to MG132 and was highest at 6 and 12 hours (Fig. 3.1) indicating that there has been inhibition of the proteasome. However, levels of ubiquitinated proteins decreased at 18 and 24 hours, but remained above the level in cells that were not treated with MG132. The observed increase in polyubiquitinated proteins is consistent with inhibition of the proteasome.

3.2 Characterisation of the sensitivity of DNA polymerase η-deficient human fibroblasts (XP30RO).

Cells lacking functional DNA pol η are more sensitive to cisplatin compared to cells expressing DNA pol η (Bassett *et al.*, 2004; Albertella *et al.*, 2005; Cruet-Hennequart *et al.*, 2008). To characterise the sensitivity of the XP30RO (-pol η) cell line used in this present study, the sensitivity of XP30RO (- pol η) and TR30-2 (+ pol η) cell lines to cisplatin was determined. TR30-2 cells are derived from the XP30RO cell line in which pol η is expressed from a *POLH* transgene. Cells were incubated with increasing doses of cisplatin, up to 1µg/ml, for 24 hours. After 24 hours, cisplatin was removed by replacing the cell culture media. Cells were grown in drug-free media for a further four days, after which cell viability was measured (Fig. 3.2) using the XTT cell viability assay (Section 2.6).

(A)

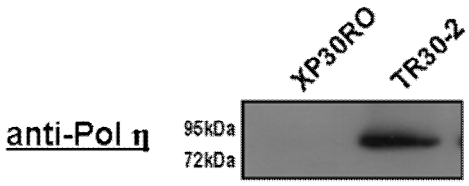

(B)

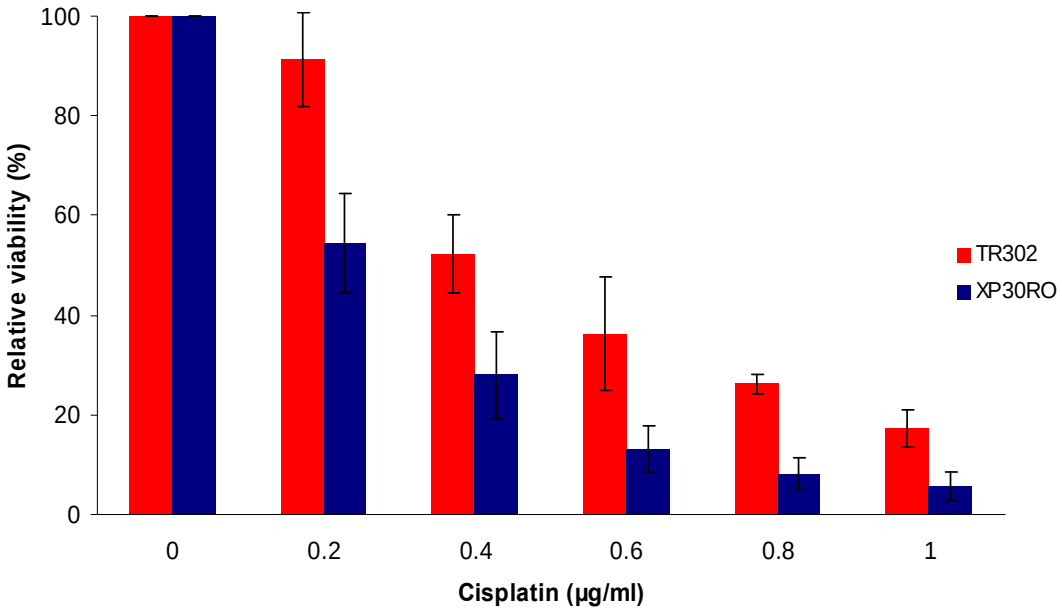

Figure 3.2: Cell viability of XP30RO (-pol η) and TR30-2 (+pol η) cell lines following cisplatin treatment. (A) XP30RO and TR30-2 cell extracts were separated on SDS-PAGE and analysed by western blotting using an anti-pol η antibody. (B) XP30RO and TR30-2 cell lines were treated with the indicated doses of cisplatin for 24 hours after which medium was replaced with drug-free media. Viability was determined using the XTT assay after 4 days. Data is the average of three experiments. Error bars represent one standard deviation.

There was a dose-dependent decrease in cell viability in both XP30RO and TR30-2 cell lines following treatment with 0.2-1 μg/ml cisplatin (Fig. 3.2). At all doses examined XP30RO cells lacking pol η were more sensitive to cisplatin compared to TR30-2 cells. This demonstrates that pol η-deficient cells are more sensitive to cisplatin compared to cells expressing pol η, consistent with previously reported data (Bassett *et al.,* 2004; Albertella *et al.,* 2005; Cruet-Hennequart *et al.,* 2008; Cruet-Hennequart *et al.,* 2009).

3.3 Effect of MG132 on the cisplatin sensitivity of DNA polymerase η-deficient human fibroblasts.

To determine the effect of MG132 on the cisplatin sensitivity of XP30RO cells, two co-treatment approaches were investigated (Fig. 3.3); (A) XP30RO cells were either mock-treated, treated with 0.5μg/ml cisplatin, with 2μM MG132 or co-treated with both drugs for 24 hours (Fig. 3.3A) (B) XP30RO cells were either mock-treated, treated with 0.5μg/ml cisplatin for 24 hours, treated with 2μM MG132 for 6 hours or treated with 0.5μg/ml cisplatin for 18 hours followed by the addition of 2μM MG132 to the medium, with incubation for a further 6 hours in cisplatin and MG132 (Fig. 3.3B) Cell viability was measured, without further incubation, using the XTT cell viability assay (Fig. 3.3).

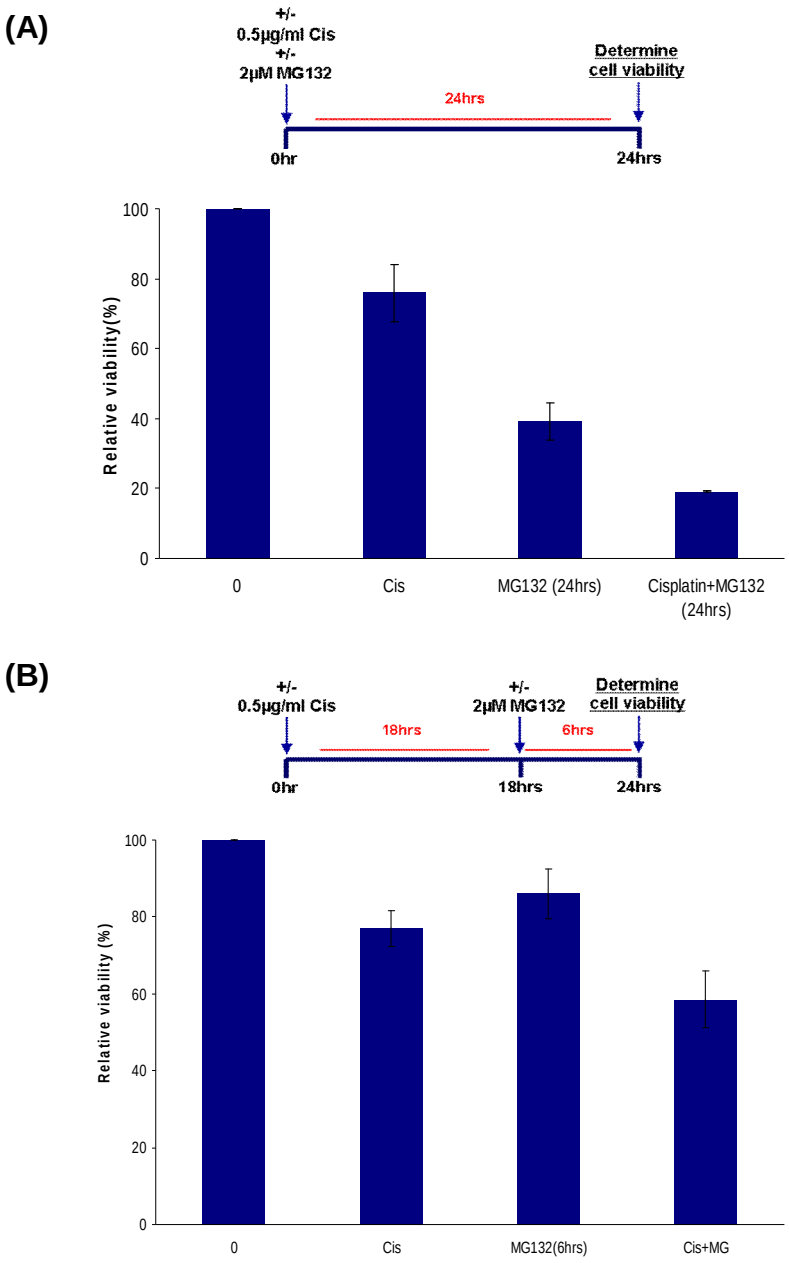

Figure 3.3: Viability of XP30R0 cells following cisplatin treatment and proteasome inhibition. (A) XP30RO cells were either mock-treated (0), treated with 0.5µg/ml cisplatin (Cis), with 2µM MG132 (MG132 (24hrs)), or co-treated with both 0.5µg/ml cisplatin and 2µM MG132 for 24 hours (Cis+MG132 (24hrs)). (B) XP30RO cells were either mock-treated (0), treated with 0.5µg/ml cisplatin for 24 hours (Cis), with 2µM MG132 for 6 hours (MG132 (6hrs)) or co-treated with 2µM MG132 18 hours following cisplatin treatment (Cis+MG). Cell viability was then measured using the XTT assay. Data represents an average of three independent experiments. Error bars represent one standard deviation.

Exposure of cells to 0.5µg/ml cisplatin for 24 hours reduced cell viability by approximately 20%. Treatment of XP30RO cells with 2µM MG132 alone for 24 hours decreased cell viability by approximately 60% (Fig. 3.3A). Co-treatment of cells with 2µM MG132 and 0.5µg/ml cisplatin decreased cells viability by a further 20% (Fig. 3.3A). The reduction in cell viability following co-treatment of cells with both agents for 24 hours was an additive affect (Fig. 3.3A).

XP30RO cells treated with 2µM MG132 for 6 hours showed a 15% decrease in viability (Fig. 3.3B) compared to an approximately 60% decrease when treated for 24 hours (Fig. 3.3A). Treatment of cells with 0.5µg/ml cisplatin for 18 hours followed by co-treatment of cells with 0.5µg/ml cisplatin and 2µM MG132 for a further 6 hours, decreased viability of cells by approximately 40% (Fig. 3.3B). The reduction in cell viability following co-treatment was again an additive affect (Fig. 3.3B). Treatment of cells with protocol outlined in Figure 3.3B resulted in a level of survival, which was compatible with further investigation of the effects of proteasome inhibition on cisplatin-induced DNA damage responses. The treatment of cells with 0.5µg/ml cisplatin for 18 hours followed by co-treatment of cells with 0.5µg/ml cisplatin and 2µM MG132 for a further 6 hours with 0.5 µg/ml cisplatin and 2µM MG132 will be referred to below as 'Cis+MG'.

3.4 Effect of proteasome inhibition on cisplatin-induced cell cycle arrest in pol eta-deficient XP30RO cells.

Regulated proteolysis plays an important role in cell cycle progression (Minshull *et al.,* 1989; King *et al.,* 1996a). The levels of individual cyclins are controlled by regulated proteolysis throughout the cell cycle (Minshull *et al.,* 1989; King *et al.,* 1996a). Other cell cycle regulators, including the CDK inhibitor p21, are regulated through proteasomal degradation; degradation of p21 is required for the resumption of the cell cycle (Wang *et al.,* 2005b).

As described in Section 1.5, following damage to genomic DNA, a period of time is required to allow DNA repair to take place (Hartwell *et al.,* 1989; Ishikawa *et al.,* 2006). Exposure of cells to cisplatin results in an accumulation of cells in S phase (Cruet-Hennequart *et al.,* 2008; Cruet-Hennequart *et al.,* 2009). S-phase progression is delayed in pol η-deficient cells exposed to cisplatin, compared to normal cells (Cruet-Hennequart *et al.,* 2008; Cruet-Hennequart *et al.,* 2009).

To investigate how proteasome inhibition affected cisplatin-induced cell cycle arrest, XP30RO cells were treated with either 2μM MG132 or with 0.5 μg/ml cisplatin alone, or co-treated with both agents for up to 18 hours. Cells were harvested for analysis of cell cycle distribution by flow cytometery using propidium iodide (PI) staining (Fig. 3.4). DNA replication was investigated by measuring BrdU incorporation. One hour before harvesting, cells were pulse labelled with 10μM BrdU, a thymidine analogue that can be incorporated into DNA in S-phase cells which are actively undergoing DNA replication. Using a FITC-conjugated antibody against BrdU, cells which have incorporated BrdU into DNA can be labelled and detected by flow cytometry (Fig. 3.5). The threshold used to define cells positive for BrdU staining was determined using a control in which the cells were stained only with the FITC-conjugated antibody against BrdU (Fig. 3.5). Any cells having a signal above the threshold in the 'FITC' (FL1H) channel were scored as positive as indicated in Figure 3.5A (negative control). The G1 and G2/M populations of cells are also indicated, which have low levels of fluorescence intensity on the 'FITC' channel (Fig. 3.5A)

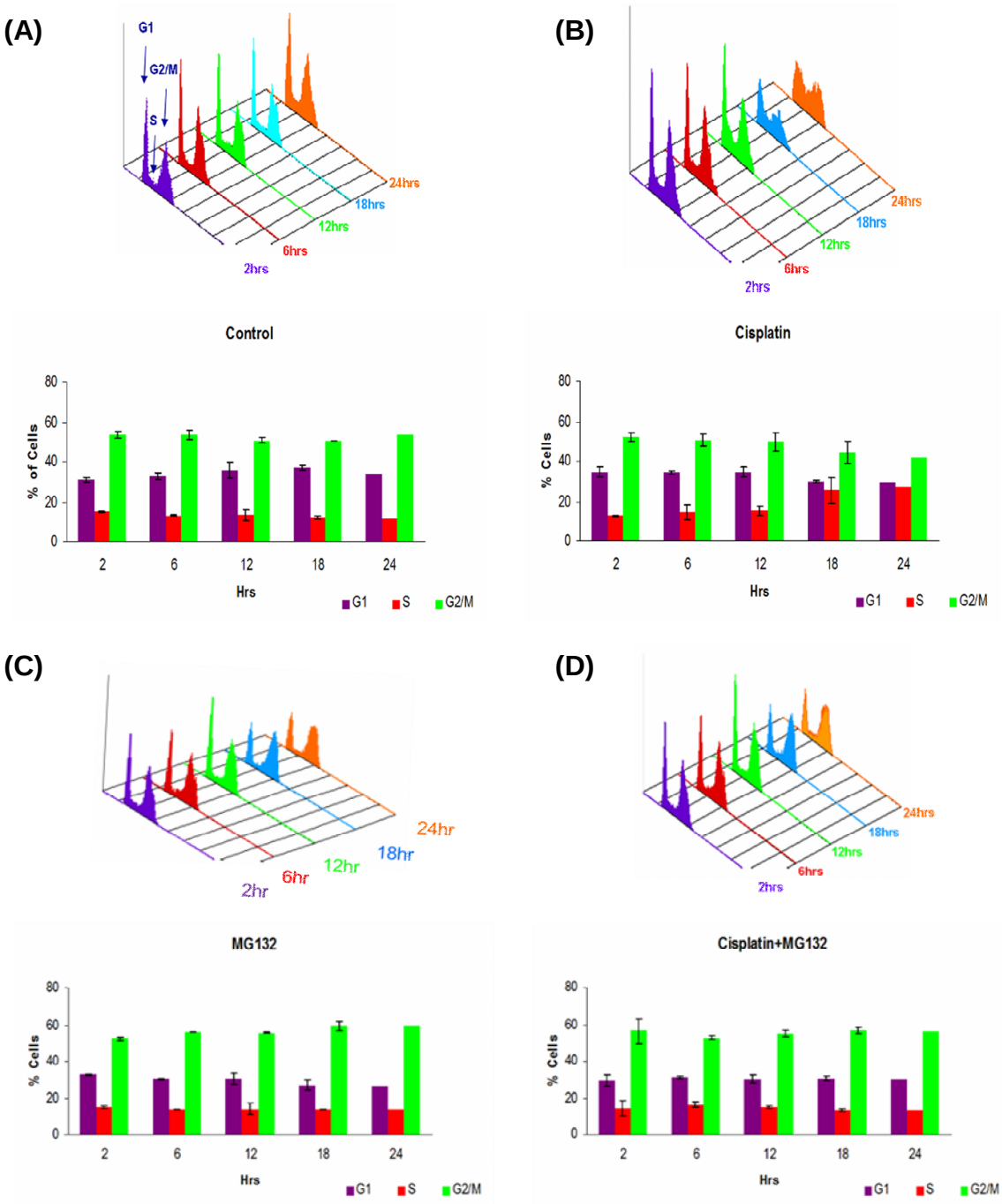

Figure 3.4: Effect of cisplatin and MG132 on cell cycle progression. XP30RO cells were either mock-treated (A), treated with 0.5µg/ml cisplatin (B), with 2µM MG132 (C), or co-treated with 0.5µg/ml cisplatin and 2µM MG132 (D). Cells were harvested and fixed at the indicated times and stained for DNA content using PI, and analysed using flow cytometry. Data represents an average of three experiments, except data for 24 hours, which is derived from a single experiment. Error bars represent one standard deviation

(A)

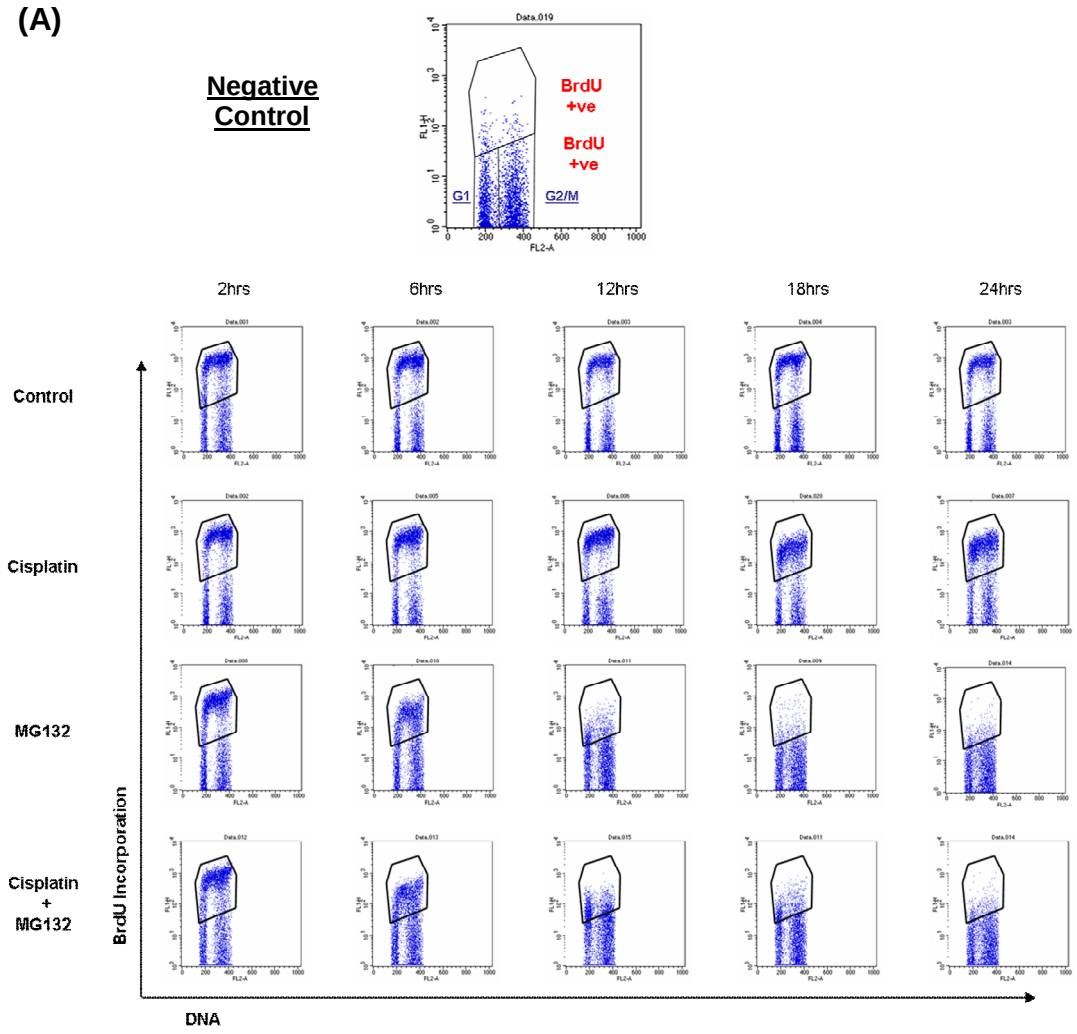
Negative Control
Data.019
BrdU +ve
BrdU +ve
G1
G2/M
FL1-H
FL2-A
2hrs
6hrs
12hrs
18hrs
24hrs
Control
Cisplatin
MG132
Cisplatin + MG132
BrdU Incorporation
DNA

(B)

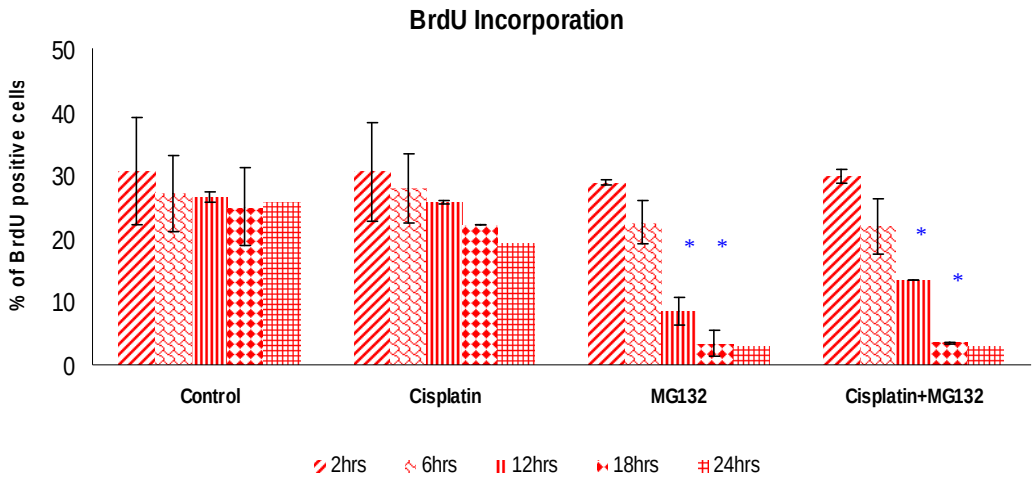
BrdU Incorporation
% of BrdU positive cells
50
40
30
20
10
0
Control
Cisplatin
MG132
Cisplatin+MG132
2hrs
6hrs
12hrs
18hrs
24hrs

Figure 3.5: Effect of cisplatin and MG132 on BrdU incorporation. (A) XP30RO cells were either mock-treated, treated with 0.5µg/ml cisplatin, treated with 2µM MG132 or co-treated with 0.5µg/ml cisplatin and 2µM MG132. Cells were pulse-labelled with 10µM BrdU for 1 hour prior to harvesting at the indicated time-points. BrdU incorporation was analysed using a FITC-labelled anti-BrdU antibody and flow cytometry. (B) Percentage of cells incorporating BrdU. Data represents the average of two independent experiments, except data for 24 hours, which is derived from a single experiment. Error bars represent one standard deviation. Statistical differences between control and treated cells were determined using Anova, where $p<0.05$, and are represented by *.

In control cells, the percentage of cells in G1, S and G2/M did not change between 2-24 hours (Fig. 3.4A). Treatment of cells with 0.5 µg/ml cisplatin resulted in an accumulation of cells in S-phase, which can be seen at 18 and 24 hours post-cisplatin treatment as a two-fold increase in the percentage of cells with S-phase DNA content (Fig. 3.4B). The percentage of cells incorporating BrdU was also decreased in cells treated with 0.5µg/ml cisplatin which is consistent with cisplatin-induced inhibition of ongoing replication (Fig 3.5). This demonstrates that even though cisplatin treatment leads to an increase in the percentage of cells in S-phase, there is a decrease in the percentage of cells actively incorporating BrdU, indicating a delay in progression through S-phase.This data is consistent with that previously reported by Cruet-Hennequart *et al*. (2008).

Treatment of XP30RO cells with 2µM MG132 did not have an effect on the distribution of cells in the different stages of the cell cycle, as determined using PI staining to measure DNA content (Fig. 3.4C). However the percentage of cells actively incorporating BrdU was dramatically reduced (Fig. 3.5). Treatment of cells with 2µM MG132 for 6 hours resulted in a decrease in the percentage of cells incorporating BrdU, while treatment of cells with MG132 for 12, 18 and 24 hours lead to a dramatic decrease in BrdU incorporation (Fig. 3.5) with approximately 3% of cells staining positive for BrdU at 18 and 24hours.

Co-treatment of cells with 0.5 µg/ml cisplatin and 2µM MG132 did not lead to the same accumulation of cells in S-phase as observed following cisplatin treatment alone (Fig. 3.4D). Rather, cell cycle distribution and BrdU incorporation were similar to that observed when cells were treated with MG132 alone. As shown in Figure 3.5, BrdU incorporation had already decreased 6 hours after treatment of XP30RO cells with MG132 alone; hence cells co-treated with MG132 and cisplatin did not show a delay in S phase compared to cells treated with cisplatin alone (Fig. 3.5). Thus, the main effect of MG132 was to prevent ongoing cell cycle progression and DNA replication, consistent with a role in preventing cyclin turnover, however, levels of individual cyclins was not examined here.

To further investigate the effect of MG132 on cisplatin-induced cell cycle arrest, the effect of (i) addition of MG132 to cells 18 hours after exposure to cisplatin (Cis+MG protocol outlined in Section 3.3); and (ii) removal of MG132 and cisplatin was examined. XP30RO cells were treated using the 'Cis+MG' protocol (Section 3.3) where cells are treated with 0.5µg/ml cisplatin for 18 hours, followed by the addition of 2µM MG132 to the medium and incubation of cells for a further 6 hours. The effects of proteasome inhibition induced by MG132 are reversible (Lee *et al.*, 1998); therefore cell cycle progression was also investigated following the removal of the cisplatin and MG132 treatment. Cells were harvested for analysis of cell cycle distribution by flow cytometery using propidium iodide (PI) staining. S-phase progression was investigated by measuring BrdU incorporation, as outlined above.

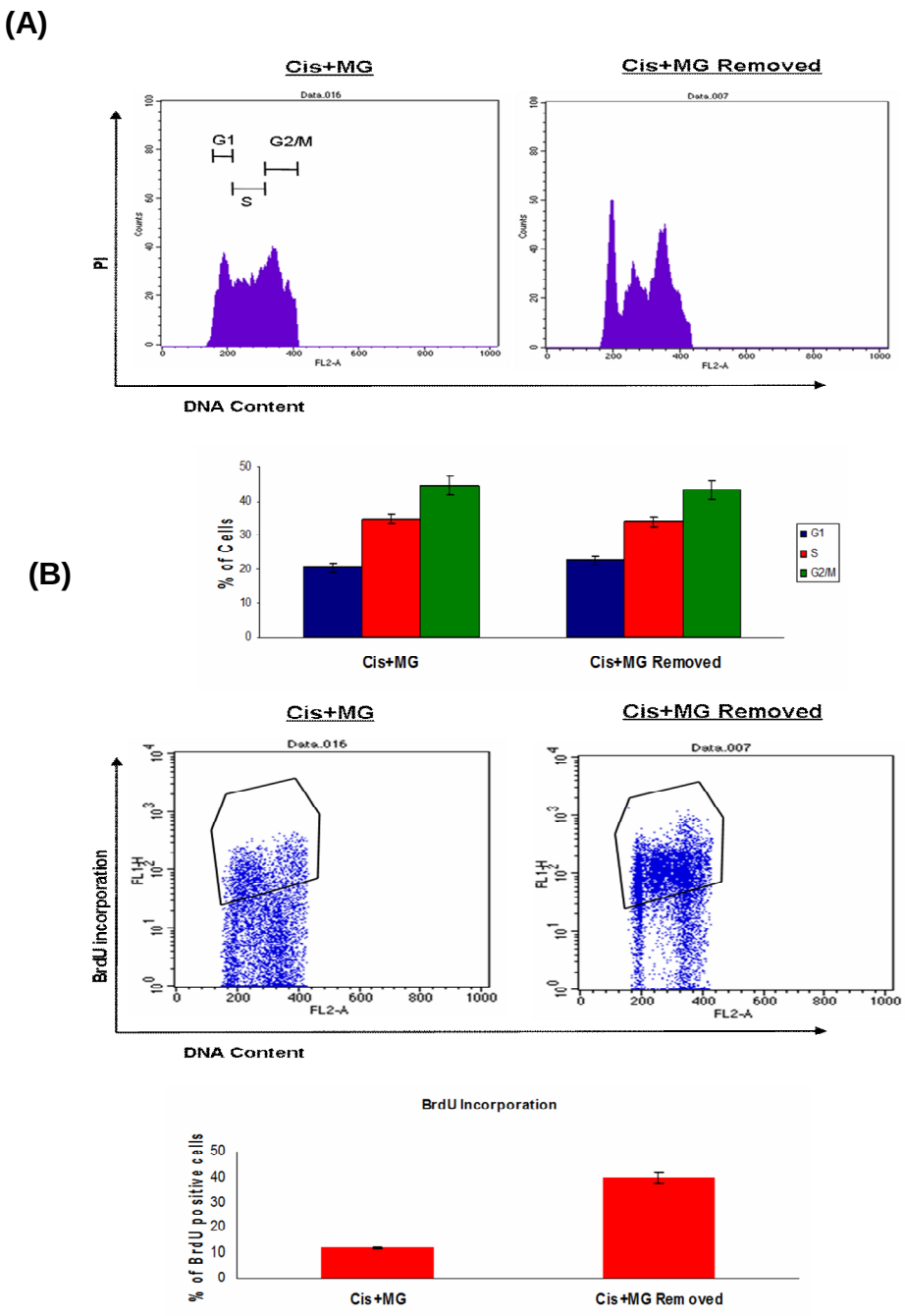

Figure 3.6: (A) XP30RO cells were treated using the 'Cis+MG' protocol (Section 3.3). Cells were either harvested (Cis+MG) or the cisplatin and MG132 treatment was removed and cells were grown in drug free media for 4 hours after which time cells were harvested. Cells were fixed and stained for DNA content using PI and flow cytometry. (B) Cells were treated as in (A) and were pulse-labelled with 10μM BrdU for 1 hour prior to harvesting. BrdU incorporation was analysed using an anti-BrdU antibody and flow cytometry. Data represents the

average of two independent experiments. Error bars represent one standard deviation.

Treatment of cells using the 'Cis+MG' protocol resulted in an accumulation of XP30RO cells in S phase (Fig. 3.6A) similar to that seen following the treatment of cells for 18 and 24 hours with cisplatin alone (Fig 3.4B). The percentage of cells incorporating BrdU following exposure of cells to 'Cis+MG' is approximately 10% (Fig. 3.6B). As shown in Figure 3.4, where cells were treated with cisplatin alone, there was a decrease in the percentage of cells incorporating BrdU indicating an inhibition of ongoing replication Therefore, cells treated with Cis+MG accumulate in S phase and subsequent treatment of cells with MG132 results in cell cycle arrest, shown by the absence of cells incorporating BrdU (Fig.3.6B). Upon the removal of both cisplatin and MG132, the distribution of cells in different cell cycle phases did not change (Fig. 3.6A). However, the percentage of cells incorporating BrdU increased to approximately 40% (Fig. 3.6B). This is consistent with the effects of the proteasome inhibitor MG132 on cell cycle progression being reversible. The approximate 4 fold increase in the percentage of cells incorporating BrdU is consistent with resumption of DNA synthesis.

3.5 Effect of proteasome inhibition on cisplatin-induced protein phosphorylation.

In the present study, the effect of MG132 on cisplatin-induced phosphorylation of H2AX, Chk1 and RPA2 was examined. XP30RO cells represent a TLS-defective cell line that is sensitive to cisplatin and related chemotherapeutic drugs (Bassett *et al.*, 2004; Albertella *et al.,* 2005; Cruet-Hennequart *et al.*, 2008; Cruet-Hennequart *et al.,* 2009). XP30RO cells lacking functional DNA pol η were used as the model system, in which to study cisplatin-induced phosphorylation of the DNA damage response proteins H2AX, Chk1 and RPA2 as cells lacking DNA pol η display increased phosphorylation of these proteins compared to cells expressing pol η (Cruet-Hennequart *et al.,* 2008).

Replication protein A (RPA), the major single stranded DNA binding protein in human cells, is involved in DNA replication, recombination and repair (Sugiyama *et al.,* 1997; Missura *et al.,* 2001; Lee *et al.,* 2010; Shi *et al.,* 2010). RPA also plays a major role in the DNA damage response. Human RPA2 is phosphorylated on Ser23 and S29 in a cell cycle-dependent manner by cyclin-dependent kinases, and following DNA damage by PIK kinases CDKs (Din *et al.,* 1990; Dutta *et al.,* 1992; Anantha *et al.,* 2007; Stephan *et al.,* 2009). RPA2 is phosphorylated on Ser4 and Ser8, Ser33 and Thr21 following exposure of cultured cells to chemotherapeutic drugs such as cisplatin, and to UV irradiation (Cruet-Hennequart *et al.,* 2006; Cruet-Hennequart *et al.,* 2008). H2AX is phosphorylated on serine 139 (γH2AX) in a PIK kinase-dependent manner in response to the formation of DSBs by DNA damaging agents including IR an cisplatin (Rogakou *et al.,* 1998; Burma *et al.,* 2001). γH2AX is an indirect marker of DSBs. As outlined in Section 1.7.4, phosphorylation of H2AX is an important event in the signalling the DDR from DSBs. DNA adducts induced by cisplatin can result in replication fork collapse resulting in the generation of DNA strand breaks. The checkpoint protein Chk1 is phosphorylated on Ser317 in an ATR-dependent manner in response to DNA damage.

In order to investigate the effect of proteasome inhibition on cisplatin-induced H2AX, Chk1 and RPA2 phosphorylation, XP30RO cells were treated as outlined

in Section 3.3. Cells were either mock-treated; treated with 0.5µg/ml cisplatin for 24 hours; with 2µM MG132 for 6 hours, or treated with 0.5µg/ml cisplatin for 18 hours followed by co-treatment with 0.5µg/ml cisplatin and 2µM MG132 for an additional 6 hours. Phosphorylation of H2AX, Chk1 and RPA2 was analysed by western blotting using phosphospecific antibodies against H2AX phosphorylated on Ser 319 (γH2AX), Chk1 phosphorylated on Ser317 (pChk1) and RPA2 phosphorylated on Ser4/Ser 8 (RPA2-pS4S8) and Ser33 (RPA2-pS33) (Fig 3.7).

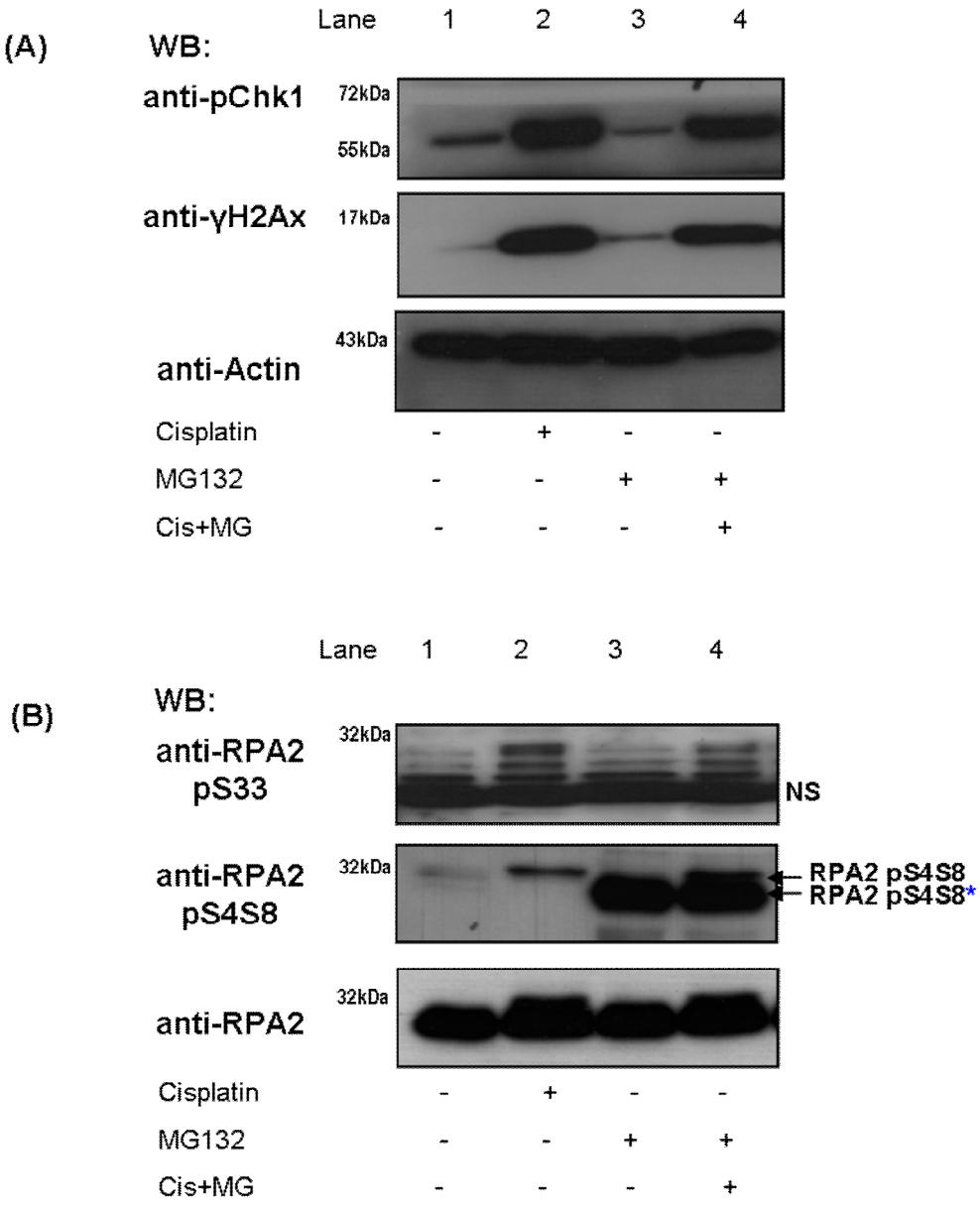

Figure 3.7 Effect of MG132 on cisplatin-induced protein phosphorylation. (A) XP30RO cells were either mock-treated (lane 1); treated with 0.5 μg/ml cisplatin for 24 hours (lane 2); with 2μM MG132 for 6 hours (lane 3) or treated with 0.5μg/ml cisplatin for 18 hours followed by co-treatment with 0.5μg/ml cisplatin and 2μM MG132 for a further 6 hours (Cis+MG, lane 4). Whole cell lysates were prepared, separated by SDS-PAGE and analysed by western blotting using phospho-specific antibodies against H2AX phosphorylated on Ser 319 (γH2AX),Chk1 phosphorylated on Ser317 (pChk1); β-Actin was used as a loading control. (B) XP30RO cells were treated as in (A) and extracts were analysed by western blotting using antibodies against RPA2 phosphorylated on Ser33 (pS33), against RPA2 phosphorylated on Ser4 and Ser8 (pS4S8), and against RPA2.NS-A non-specific band detected by anti-RPA2-pSer33 antibody.

An increase in pChk1 (Ser317) and γH2AX was detected in extracts of cells treated with 0.5 μg/ml cisplatin for 24 hours, compared to mock-treated cells (Fig. 3.7A, lane 2), consistent with reported data (Cruet-Hennequart *et al.*, 2008). MG132 did not induce pChk1 and γH2AX (Fig. 3.8A, lane 3). Co-treatment of cells with cisplatin and MG132 did not alter the level of cisplatin-induced pChk1 or γH2AX (Fig. 3.7A, lane 4).

Consistent with previous reports, cisplatin induced RPA2 phosphorylation on Ser33 and on Ser4/Ser8 was detectable in extracts from cells treated with 0.5 μg/ml cisplatin for 24 hours (Fig. 3.7B, lane2) (Cruet-Hennequart *et al.*, 2008). In extracts from cells treated with 2μM MG132 for 6 hours (Fig. 3.7B, lane 3), a novel band with faster gel mobility than the cisplatin-induced phospho-S4S8 RPA2 band was detected by immunoblotting using the anti-phospho-S4S8 RPA2 antibody (Fig. 3.7B). This novel band is shown as RPA2-pS4S8***** in Figure 3.7B, lane 3. This novel, faster mobility band is also detected in cells that had been treated with cisplatin alone for 18 hours and exposed to cisplatin and MG132 for an additional 6 hours (Fig 3.7B lane 4). The slow mobility form of cisplatin-induced RPA2-pS4S8 was also detectable in this sample (Fig. 3.7B, lane 4). The level of RPA2 phosphorylated on Ser33 did not change following treatment of cells with MG132 compared to mock-treated cells (Fig. 3.8B, lane 3) indicating that formation of RPA2-pS4S8* is independent of DNA damage. In contrast,

treatment of cells with cisplatin for 18 hours and exposure to cisplatin and MG132 for an additional 6 hours (Fig 3.8B, lane 4) did not alter the level of cisplatin-induced RPA2-pSer33 compared to treatment of cells with cisplatin alone (Fig. 3.7B).

From the proteins examined in the present study, proteasome inhibition did not affect cisplatin-induced H2AX or Chk1 phosphorylation. However because RPA2 phosphorylation on S4S8 was altered (Fig 3.7B), the effect of MG132 on RPA2 phosphorylation S4S8 was examined further.

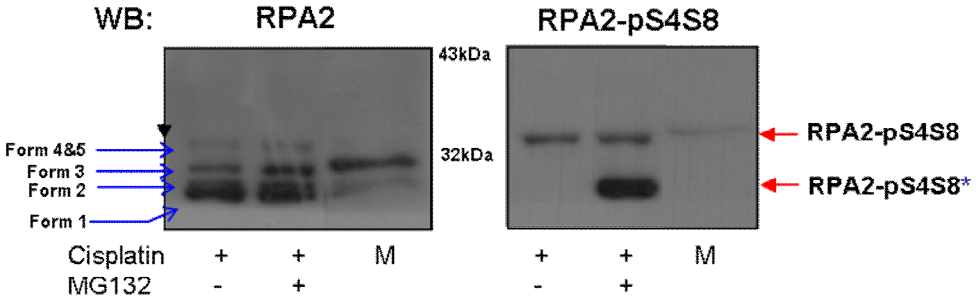

Figure 3.8: XP30RO cells were either treated with 0.5 µg/ml cisplatin for 24 hours, or with 0.5µg/ml cisplatin for 18 hours followed by co-treatment with 0.5µg/ml cisplatin and 2µM MG132 for a further 6 hours. XP30RO cells were arrested in mitosis (M) by treating cells with 0.1µM nocoodazole for 16 hours. Extracts were analysed by western blotting using anti-RPA2 and anti-RPA2-pS4S8 antibodies.

To determine whether the novel form of RPA2-pS4S8* corresponded in terms of gel mobility to any of the known forms of RPA2 (Din *et al.*, 1990; Dutta *et al.*, 1992; Nuss *et al.*, 2005). Extracts from XP30RO cells were analysed by western blotting using antibodies against RPA2 and RPA2-pS4S8 (Fig. 3.8). Five forms of RPA2, having different mobility on SDS-PAGE can be detected (Din *et al.*, 1990; Dutta *et al.*, 1992). Form 1 represents unphosphorylated RPA2. Phosphorylation during normal cell cycle results in form 2 (Dutta *et al.*, 1992; Niu *et al.*, 1997). Form 3 occurs from phosphorylation of RPA2 during mitosis (Oakley *et al.*, 2003; Anantha *et al.*, 2007). Damage induced phosphorylation of RPA2 results in forms 4 and 5 and is a result of hyperphosphorylation of the N-

terminal phosphorylation sites (Carty *et al.*, 1994; Nuss *et al.*, 2005). XP30RO cells were either treated with 0.5µg/ml cisplatin for 24 hours, or treated with 0.5µg/ml cisplatin for 18 hours and co-treated for a further 6 hours with 0.5µg/ml cisplatin and 2µM MG132. To generate the mitotic, phosphorylated form (form 3) of RPA2, XP30RO cells were arrested in mitosis by treating cells with the microtubule inhibitor nocodazole (0.1µM) for 16 hours. Extracts were first analysed by western blotting using an anti-RPA2 antibody, and the membrane was stripped and reprobed using the anti-RPA2-pS4S8 antibody (Fig. 3.8).

The different mobility forms of RPA2, outlined above, were detected in extracts from XP30RO cells, shown in Figure 3.8. The mobility of RPA2 form 3 was determined by analysing RPA2 from extracts of XP30RO cells arrested in mitosis (Fig. 3.8). Cisplatin-induced RPA2-pS4S8 corresponds in mobility to RPA2 forms 4 and 5 (Fig. 3.8). MG132 induced RPA2-pS4S8* corresponds most closely in mobility to form 2 of RPA2 which results from cell cycle dependent phosphorylation of RPA2 on Ser23.

To further investigate phosphorylation of RPA2 in MG132 treated cells, cell cycle dependent, RPA2 phosphorylation on Ser23 was examined. XP30RO cells were either mock-treated, treated with 0.5µg/ml cisplatin for 24 hours or treated with 2µM MG132 for 6 hours (Fig. 3.9).Cell extracts were analysed by western blotting and antibodies against RPA2-pS23 and RPA2.

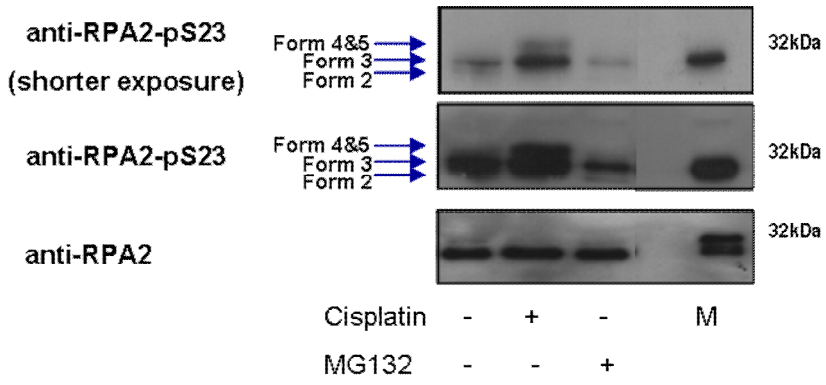

Figure 3.9: (A) XP30RO cells were either mock-treated, treated with 0.5 μg/ml cisplatin for 24 hours or with 2μM MG132 for 6 hours. XP30RO cells were arrested in mitosis by treating cells with 0.1μM nocodazole for 16 hours (M). Extracts were separated on SDS-PAGE and analysed by western blotting using anti-RPA2 and anti-RPA2-pSer23 antibodies.

In extracts from untreated cells, RPA2-pS23 is detected in form 2 and 3 of RPA2. The mobility of RPA2 form 3 was determined by analysing RPA2 from extracts of XP30RO cells arrested in mitosis (Fig. 3.9). Following cisplatin treatment RPA2-pS23 was detected in forms 2, 3, 4 and 5 of RPA2. Treatment of cells with 2μM MG132 led to a reduction in RPA2 phosphorylated on S23 compared to mock-treated cells (Fig. 3.9).

The effects of MG132 are reversible (Lee *et al.*, 1998). In order to further investigate whether formation of RPA2-pS4S8* was dependent on proteasome inhibition, the effect of removal of MG132 was examined. XP30RO cells were treated as outlined in the legend of Figure 3.8. XP30RO cells were either mock-treated; treated with 0.5μg/ml cisplatin for 24 hours; with 2μM MG132 for 6 hours, or treated with 2μM MG132 for 6 hours after which treatment was removed and cells were grown in drug free media for a further 4 hours. Extracts were examined by western blotting using anti-RPA2-pS4S8, anti-RPA2, anti-pChk1 (Ser317), anti-Chk1 and anti-γH2AX antibodies (Fig. 3.10).

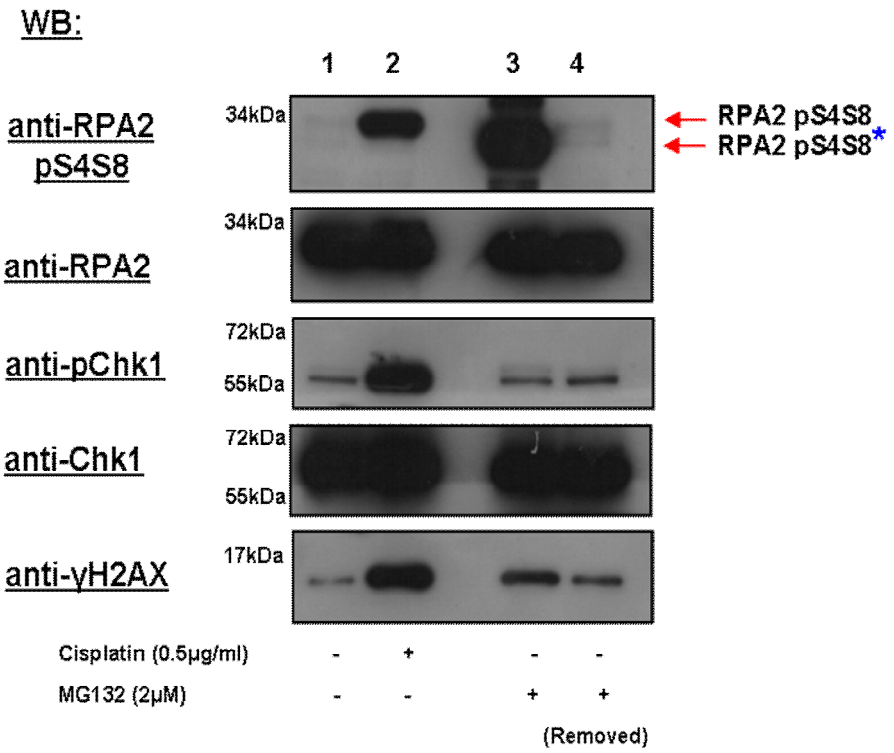

Figure 3.10: XP30RO cells were either mock-treated (lane 1), treated with 0.5 μg/ml cisplatin for 24 hours (lane 2), 2μM MG132 for 6 hours (lane 3). Lane 4 shows cells treated with 2μM MG132 for 6 hours, after which the chemical was removed and cells were allowed to grow in drug-free media for a further 4 hours. Protein extracts were analysed using phopsho-specific antibodies against the phosphorylated forms of Chk1 (Ser317), H2AX (Ser139), RPA2 (pS4S8), and against RPA2 and Chk1.

In extracts from cells treated with MG132 for 6 hours the novel RPA2-pS4S8* band was detected (Fig 3.10, lane 3). Levels of pChk1 and γH2AX in cells treated with MG132 for 6 hours were similar to those in mock-treated cells, consistent with the data presented in Figure 3.7. This indicates that induction of the faster mobility form of RPA2-pS4S8*is DNA damage independent but is MG132 dependent. Upon removal of MG132, RPA2-pS4S8* is barely detectable (Fig. 3.10, lane 4), consistent with this form of RPA2 being dependent on proteasome inhibition. Thus, an MG132-inducible, DNA damage-independent form of RPA2 phosphorylated on Ser4/Ser8 has been identified.

3.6 Characterisation of RPA2-pS4S8*

3.6.1 Analysis of RPA4

To further characterise RPA2-pS4S8*, the relationship between this band and the RPA2 homologue, RPA4, was investigated. RPA4 is a human homologue of RPA2, having 63% amino acid homology to RPA2 (Keshav *et al.*, 1995). RPA4 can replace RPA2 in trimeric RPA, and form a complex with RPA1 and RPA3 in certain cell type (Keshav *et al.*, 1995). This alternative RPA trimer does not support DNA replication and cell cycle progression but is active in DNA repair (Haring *et al.*, 2010; Kemp *et al.*, 2010). The molecular weight of RPA4 is 30kD, similar to that of RPA2 (Keshav *et al.*, 1995). The Ser4 and Ser8 residues are conserved between RPA2 and RPA4 (Keshav *et al.*, 1995), so it is possible that the anti RPA2-pS4S8 antibody could recognise RPA4 phosphorylated on these conserved residues. In order to investigate if the faster mobility band detected by the RPA2-pS4S8 antibody (RPA2-pS4S8*****) might correspond to RPA4, extracts from cells treated with MG132 for 6 hours, conditions under which RPA2-pS4S8* is readily detectable, were analysed by western blotting using an antibody against RPA4. Recombinant RPA4, run on the gel as a positive control, was readily detected under these conditions (Fig. 3.11). No RPA4 signal was detected in the extracts after western blotting (Fig. 3.11). This does not rule out however, that levels of RPA4 in these extracts are below the limits of detection of the anti-RPA4 antibody. These results suggest that the RPA2-pS4S8***** band is not likely to be RPA4, but rather represents a novel form of phosphorylated RPA2.

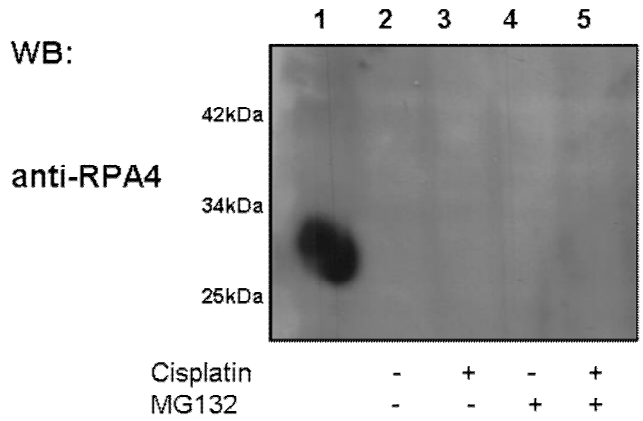

Figure 3.11 Analysis of RPA4 in XP30RO cells. Lane 1, 0.5 µg of recombinant RPA4. XP30RO cells were either mock-treated (lane 2), treated with 0.5 µg/ml cisplatin for 24 hours (lane 2), or with 2µM MG132 for 6 hours (lane 3). Lane 5 shows extracts of cells that were co-treated with 2µM MG132, 18 hours after treatment with 0.5 µg/ml cisplatin. Cells were harvested and extracts were analysed by SDS-PAGE followed by western blotting using an anti-RPA4 antibody.

3.6.2 Kinetics of RPA2-p-S4S8* formation

To determine whether formation of MG132-induced RPA2-pS4S8* was specific to XP30RO cells, XP30RO cells and the isogenic cell line TR30-2 were treated with 2µM MG132 and harvested at the indicated times (Fig.3.11). Cell extracts were analysed by western blotting (Fig 3.11).

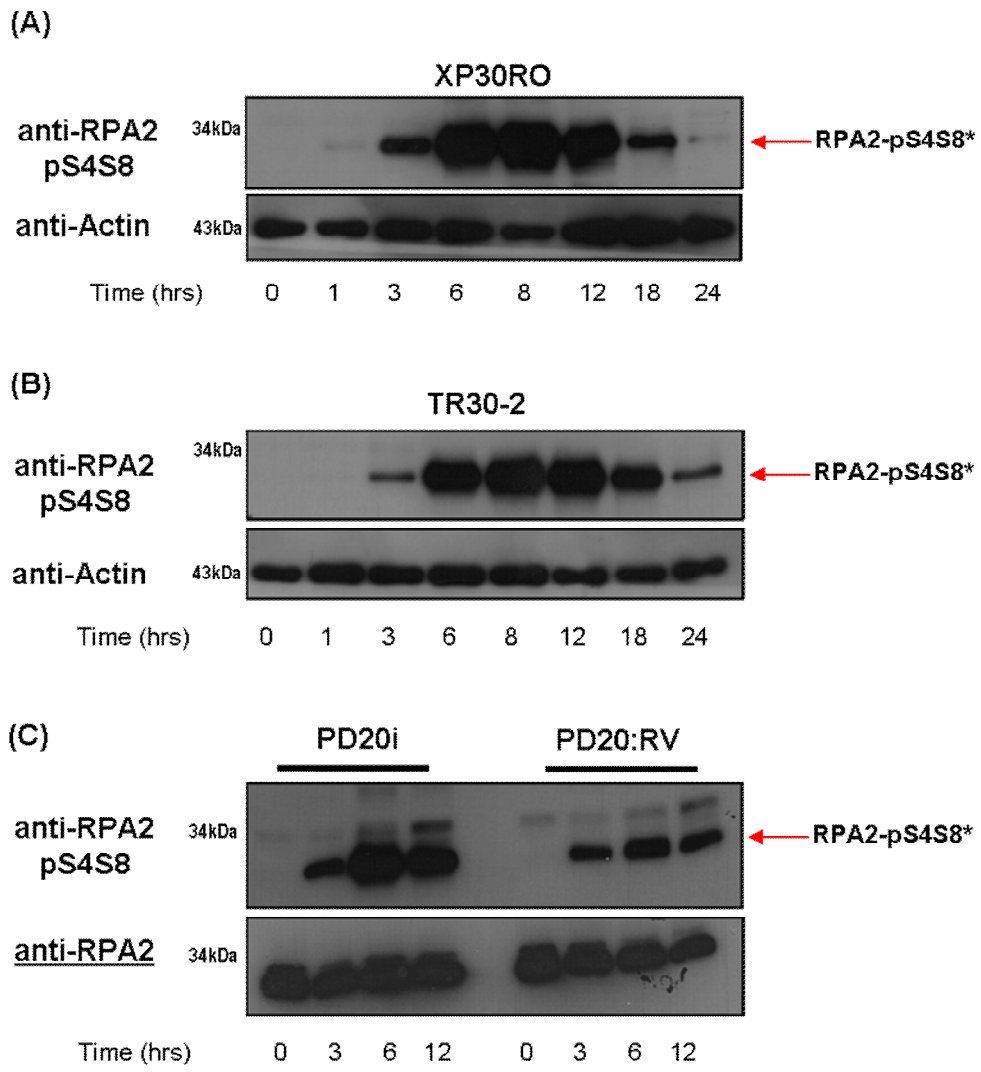

Figure 3.11: Kinetics of RPA2-pS4S8* formation. XP30RO (A) and TR30-2 (B) cells were treated with 2μM MG132 for the indicated times. Cells were harvested and extracts were analysed by SDS-PAGE and western blotting using a phospho-specific antibody against RPA2-pS4S8, and anti-actin antibody. (C) PD20i and PD20:RV cells were treated with 2μM MG132 for the indicated times. Cells were harvested and extracts were analysed by western blotting using the phospho-specific antibody against RPA2-pS4S8, and against RPA2.

The novel form RPA2-pS4S8***** was detected following treatment of cells with MG132 for 6 hours (Fig 3.48) This novel form was first readily detected after 3 hours exposure to MG132 in both XP30RO and TR302 cells. Levels of RPA2-pS4S8***** increased over time up to 6 hours, and were maintained up to 12 hours

and decreased at 18 and 24 hours (Fig 3.11). The kinetics are similar in the pol η– deficient (XP30RO) and -proficient (TR30-2) cell lines. Thus RPA2-pS4S8* formation is independent of pol η, consistent with the induction of RPA2 being DNA damage independent as outlined in Figure 3.10.

To investigate whether formation of RPA2-pS4S8* was unique to XP30RO and TR30-2 cells, the human Fanconi anemia cell line PD20i, which lacks functional FANCD2, and PD20:RV, which expresses FANCD2, were treated with MG132 (Fig 3.11C). Cell extracts were prepared at the times shown in Figure 3.12C, and analysed by SDS-PAGE and western blotting as outlined in Fig. 3.11 (legend). RPA-pS4S8* was detected in extracts of cells treated with 2μM MG132 for 3 hours. The levels of RPA2-pS4S8* increased at 6 hours and started to decrease by 12 hours. This demonstrates that the formation of RPA-pS4S8* is not cell line-specific as it is readily detectable in two human cell lines, other than the XP30RO and TR30-2 cell lines. While more RPA-pS4S8* was detected in PD20i cells (Fig. 3.11C) the levels of total RPA2 were also lower in these cells compared to PD20:RV cells.

3.6.3 λ- phosphatase treatment.

In order to investigate whether RPA2-pS4S8* is a phosphorylated protein, cell extracts prepared from MG132-treated cells were treated with λ-phosphatase. Extracts from XP30RO cells were treated with λ-phosphatase for 1 hour (Fig 3.12). Following SDS-PAGE and western blotting, the MG132-induced form of RPA2 detected using anti-RPA2-pS4S8 antibody was no longer detectable in extracts that had been treated with λ-phosphatase. This is consistent with RPA-pS4S8*being a phosphorylated form of RPA2 (Fig. 3.12).

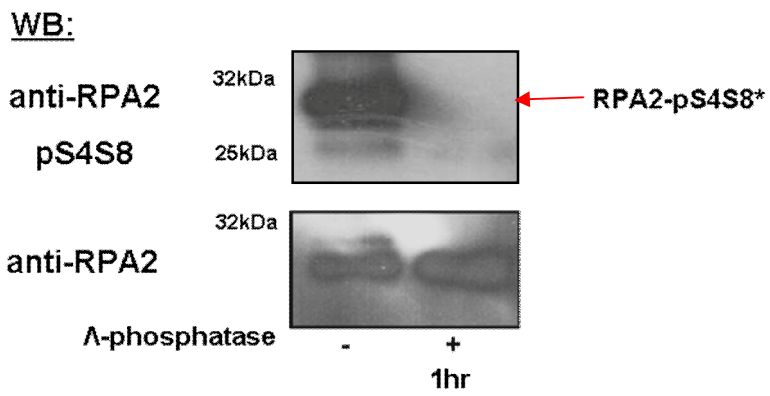

Figure 3.12: λ-phosphatase treatment. XP30RO cells were treated with 2μM MG132 for 6 hours. Cell extracts were treated (+) or not (-) with λ-phosphatase for 1 hour at 37°C. Extracts were then analysed by western blotting using anti RPA2-pS4S8 and anti-RPA2 antibodies.

The RPA2-pS4S8 antibody detects RPA2 that is phosphorylated on Ser4 and Ser8. However, it does not distinguish between phosphorylation of RPA2 on Ser4 or Ser8. To account for the faster mobility of RPA-pS4S8* on SDS-PAGE compared to the DNA-damage inducible RPA2-pS4S8 it is possible that the MG132-induced phosphorylated form of RPA2 may represent RPA2 that is phosphorylated on only one site, i.e. either on Ser4 or Ser8. However, further investigation of the specific sites that are phosphorylated on pS4S8* is required to definitively answer this question. From the present study, RPA2-pS4S8* does not appear to represent a large fraction of the total RPA2 protein in these cells making analysis of phosphorylation sites, by e.g. mass spectrometry, difficult. Generation and expression of RPA2 mutated at either Ser4 or Ser8, coupled with the knock-down of endogenous RPA2, would determine whether RPA2-pS4S8* represented RPA2 phosphorylated at either site. However, there is a possibility that the phospho-specific antibody against RPA2-pS4S8 may not recognise phosphorylation at either Ser4 or Ser8 if one of these serines is mutated to alanine.

3.6.4 PIKK dependence of RPA2-pS4S8*

Following treatment of XP30RO cells with cisplatin, RPA2 is phosphorylated on Ser4/Ser8 in a DNA-PK-dependent manner (Cruet-Hennequart *et al.*, 2008). Treatment of cells with a specific small molecule inhibitor of DNA-PK, NU7441, inhibits cisplatin-induced RPA2 phosphorylation on Ser4 and Ser8 (Cruet-Hennequart *et al.*, 2008).Use of a specific inhibitor of ATM, KU-55933, does not affect cisplatin-induced RPA2 phosphorylation (Cruet-Hennequart *et al.*, 2008). To determine the PIKK-dependence of the novel MG132-induced phosphorylated form of RPA2, RPA2-pS4S8*, MG132 exposed XP30RO cells were treated with the DNA-PK and ATM inhibitors, NU7441 and KU-55933.

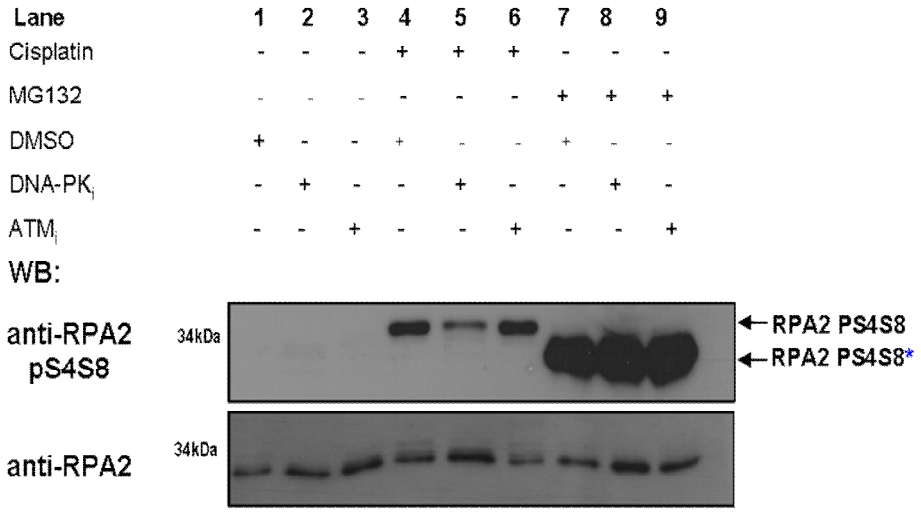

Figure 3.13 PIKK-dependence of RPA2-pS4S8*. XP30RO cells were either mock-treated (lanes1-3); treated with 0.5µg/ml cisplatin for 24 hours (lanes 4-6) or with 2µM MG132 for 6 hours (lane 7-9). Cells were also treated or not for 24 hours with either the DNA-PK inhibitor, NU7741 (10µM), or the ATM inhibitor, KU55933 (10µM). DMSO was used as a vehicle control. Proteins were separated on SDS-PAGE gels and were analysed using anti-phospho-RPA2-S4S8 antibody.

Consistent with previously reported data, the DNA-PK inhibitor NU7441 reduced cisplatin-induced phosphorylation of RPA2 on Ser4 and Ser8 (Fig 3.13, lane 5). The ATM inhibitor, KU-55933, did not affect RPA2 phosphorylation on Ser4/Ser8 (Fig 3.13, lane 6). However, co-treatment of cells with 2µM MG132

and inhibitors of DNA-PK or ATM did not appear to alter the levels of RPA2-pS4S8* (Fig 3.13 lane 8, 9). This indicates that RPA2-pS4S8* is not dependent on DNA-PK and ATM, providing further evidence that formation of this phosphorylated form of RPA2 is DNA damage-independent. However, the image in Fig 3.13 is over exposed and therefore any reduction in RPA2-pS4S8* would not be easily detectable (Fig 3.13 lanes 7-9). Therefore, it cannot be said conclusively that RPA2-pS4S8* is not dependent on DNA-PK and ATM.

3.6.5 Isolation of cellular phosphoproteins.

To further characterise MG132-induced RPA2-pS4S8***,** cellular phosphoproteins were isolated from XP30RO whole cell lysates, using a Phosphoprotein Purification kit (Qiagen). XP30RO cells were either left untreated or treated with 2μM MG132 for 6 hours under which conditions RPA2-pS4S8* is strongly detected in cell extracts (Fig.3.7B). Cells were lysed and extracts passed over a phosphoprotein purification column as described in Section 2.19. Proteins bound to the column were eluted, and analysed by SDS-PAGE followed by coomassie blue staining (Fig 3.14A) or western blotting (Fig. 3.14B). Isolated phosphoproteins accounted for approximately 7% of the total proteome in XP30RO cells, as determined by calculating the percentage of total protein that was recovered from the phosphoprotein purification column.

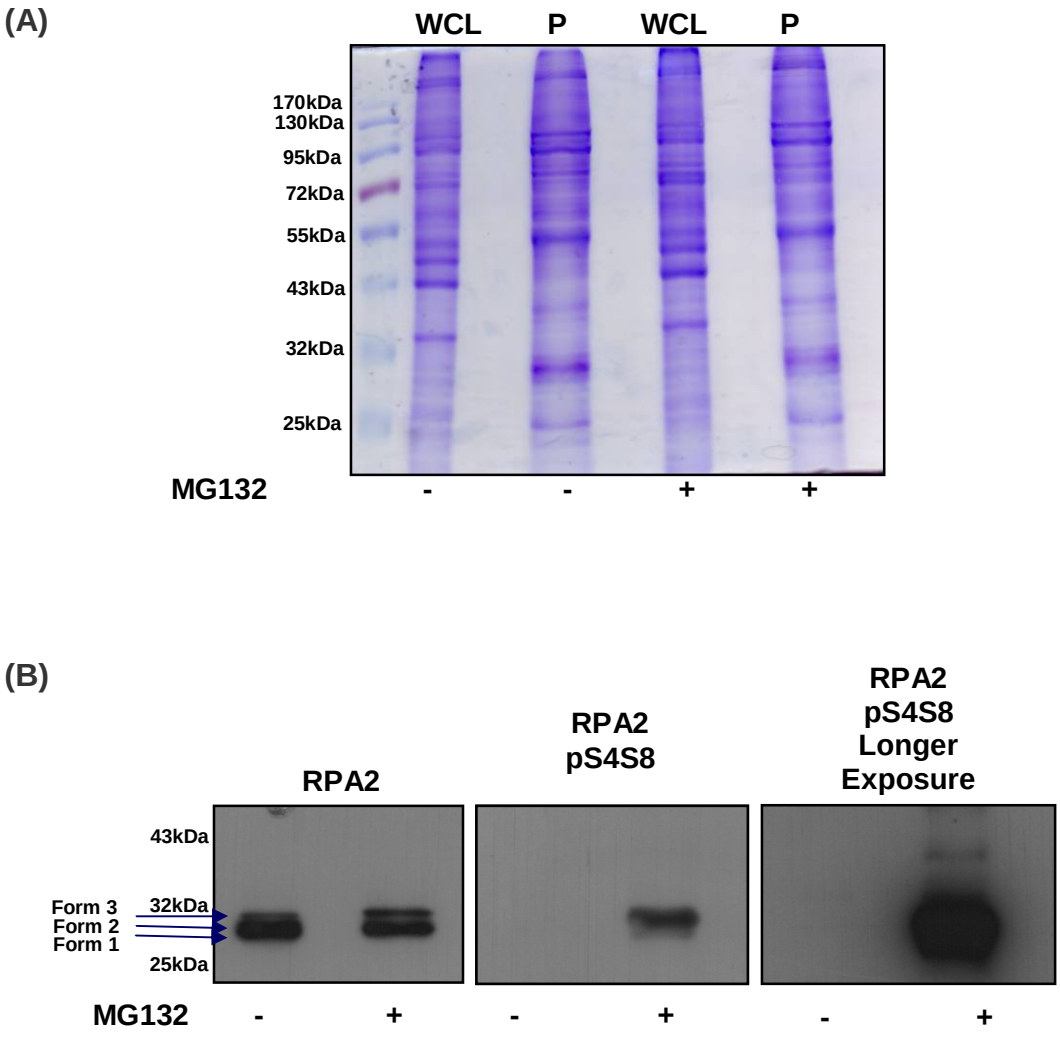

Figure 3.14: Isolation of phosphorylated proteins from XP30RO cells treated with MG132. (A) 15µg of whole cell lysate (WCL) and phospho-purified protein fractions (P) were analysed by SDS-PAGE and coomassie blue staining. (B) Isolated phospho-purified proteins from cell extracts of untreated cells or cells treated with 2µM MG132 for 6 hours, were analysed by western blotting using antibodies against RPA2 and against RPA-pS4S8

The protein composition of the phosphoprotein fraction, isolated from both untreated and MG132-treated XP30RO cells, differed when compared to that of whole cell lysates without prior phosphopurification, as demonstrated by the pattern of protein bands observed following SDS-PAGE and coomassie blue staining (Fig 3.14A) using equal amounts of protein as determined using the DC protein assay. However, these differences were not further investigated in the

present study. Bands corresponding in mobility to phosphorylated forms 2 and 3 of RPA2 (as outlined in Figure 3.8) were detected in eluted proteins following phosphopurification of extracts from untreated cells and from cells treated with MG132 (Fig. 3.14B). A band corresponding in mobility to unphosphorylated, form 1 of RPA2 was detected in untreated extracts which may result from non-specific binding of protein to the phosphopurification column or may result from RPA2 interacting with another phosphorylated protein. A direct comparison of the mobility of RPA2 in whole cell extracts to the eluted protein following phosphopurification on the same gel would confirm that the bands outlined in Figure 3.14B do represent the forms of RPA2 described above. Following phosphopurification, the MG132-induced RPA2-pS4S8***** form is present in the purified phosphoprotein fraction isolated from MG132 treated cellular extracts. This is consistent with RPA-pS4S8* being phosphorylated, and again is detected by the anti-RPA-pS4S8 antibody (Fig 3.14B).

3.6.6 Affi-Gel Blue RPA enrichment

RPA is characterised by very high affinity for single-stranded DNA. The protein binds tightly to ssDNA-cellulose, and to Affi-Gel Blue, an agarose-linked dye to which many DNA-binding proteins adsorb (Oakley *et al.,* 2003; Block *et al.,* 2004). Affi-Gel Blue was originally used to isolate and identify RPA as a factor necessary for *in vitro* replication of plasmids containing the SV40 origin of replication (Wold *et al.,* 1988). Affi-Gel Blue is now routinely utilised for purification of RPA (Oakley *et al.,* 2003; Block *et al.,* 2004), as RPA binds with high affinity to Affi-Gel Blue beads. If the RPA2-pS4S8* band observed by western blotting (Fig. 3.7) is a novel form of RPA2, RPA-pS4S8* should bind to Affi-Gel Blue and should only be eluted at high salt concentrations. Affi-Gel Blue RPA enrichment was carried out in extracts from mock-treated XP30RO cells, or in extracts of cells treated with 2μM MG132 for 6 hours, conditions under which RPA2-pS4S8* was strongly induced (Fig. 3.7). Following incubation of protein extracts with Affi-Gel Blue beads for 2 hours, to allow proteins to bind, beads were sequentially washed twice with 900mM NaCl, followed by two washes with 2M NaCl. Proteins bound to the Affi-Gel Blue

beads were then eluted by boiling the beads in Laemmli sample buffer, and analysed by SDS-PAGE and western blotting.

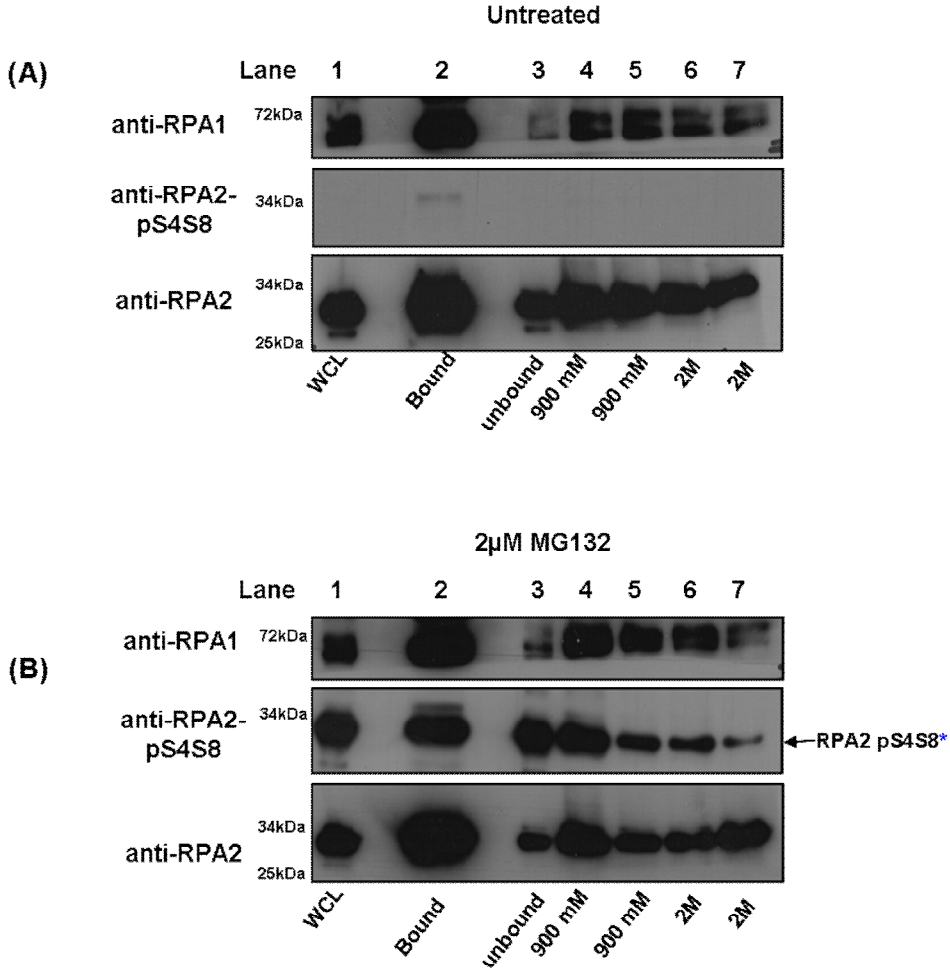

Figure 3.15: Affi-Gel Blue RPA enrichment from XP30RO cell extracts. XP30RO cells were either mock-treated (A) or treated with 2μM MG132 for 6 hours (B) Affi-Gel Blue enrichment was carried out on cell extracts. Bound protein was eluted, separated by SDS-PAGE and analysed by western blotting using antibodies against RPA1, RPA2 and RPA2-pS4S8. 20μg of WCL and unbound fraction and 25μl of each wash fraction was analysed.

The ssDNA-binding activity of RPA is primarily due to the RPA1 subunit. Following Affi-Gel Blue enrichment a large proportion of RPA1 was recovered in the bead-bound fraction compared to the unbound fraction, in both untreated and MG132-treated extracts (Fig. 3.15). Although RPA1 was eluted with washes containing increasing salt concentrations, a large proportion of RPA1 remained

bound to the Affi-Gel Blue beads (Fig. 3.15 A and B, lane 3). This is consistent with RPA1 binding with high affinity to Affi-Gel Blue (Oakley *et al.*, 2003; Block *et al.*, 2004). RPA2 was also found in the fraction bound to the Affi-Gel Blue beads, with the amount of RPA2 greater in the fraction bound to the Affi-Gel Blue beads (Fig. 3.15A and B, lane 2, lower panel) compared to the unbound fraction (Fig 3.15A and B, lane 3, lower panel). A proportion of RPA2 was eluted using 900mM and 2M NaCl washes (Fig. 3.15A and B lower panel). This is consistent with data presented above that the majority of RPA1 binds to Affi-Gel Blue.

The faster mobility band RPA2-pS4S8* was detected in the extract from cells treated with MG132 (Fig 3.15B, middle panel) and not in the mock-treated extracts (Fig 3.15A, middle panel) using the phospho-specific anti-RPA2-pS4S8 antibody. RPA2-pS4S8* was detected in the first 900mM NaCl wash, with decreasing amounts of RPA2-pS4S8* detected in subsequent washes (Fig. 3.15B). However, RPA2-pS4S8* was detected in proteins bound to the Affi-Gel Blue matrix following the 900mM and 2M NaCl washes. This provides evidence that RPA2-pS4S8* represents a form of RPA2.

3.6.7 Immunoprecipitation of RPA2-pS4S8.

To determine whether RPA2-pS4S8* could be isolated from cell extracts, immunoprecipitation using the anti-RPA2-pS4S8 antibody was carried out. XP30RO cells were either left untreated, treated with 0.5ug/ml cisplatin for 24 hours or treated with 2uM MG132 for 6 hours. Western blotting analysis of whole cell lysates (WCL) (Fig. 3.16, lower panel, lanes 1-3) using an anti-RPA2-pS4S8 antibody demonstrates that slow mobility hyperphosphorylated RPA2 is induced by cisplatin, while the faster mobility RPA2-pS4S8* band is only detected in MG132-treated cell extracts. Immunoprecipitation of RPA2-pS4S8 was carried out from extracts of XP30RO cells treated as described above. Both the slow-mobility cisplatin-induced hyperphosphorylated form of RPA2-pS4S8, and the MG132 induced RPA2-pS4S8* were detected by western blotting using anti-RPA2-pS4S8 antibody (Fig 3.16, lower panel, lanes 5-7). The pattern of bands detected using the anti-RPA2-pS4S8 antibody following

immunoprecipitation was consistent with the pattern observed using this antibody in western blotting of whole cell lysates (Fig.3.16, lower panel, lanes 1-3). A small amount of RPA2, not detected by the anti-RPA2-pS4S8 antibody was also present in eluted protein fraction following immunoprecipitation of RPA2-pS4S8 from all extracts (Fig. 3.16, upper panel, lane 5-7). This could be due to RPA2 interacting with another RPA2 protein phosphorylated on Ser4/Ser8, or to non-specific binding of the beads. Immunoprecipitation using a negative, IgG control would determine if this represents RPA2 or unspecific binding. The levels of RPA2 in MG132 treated cells does not change following immunoprecipitation using anti-RPA2-pS4S8 antibody indicating that RPA2-pS4S8* represents a small proportion of the total protein.

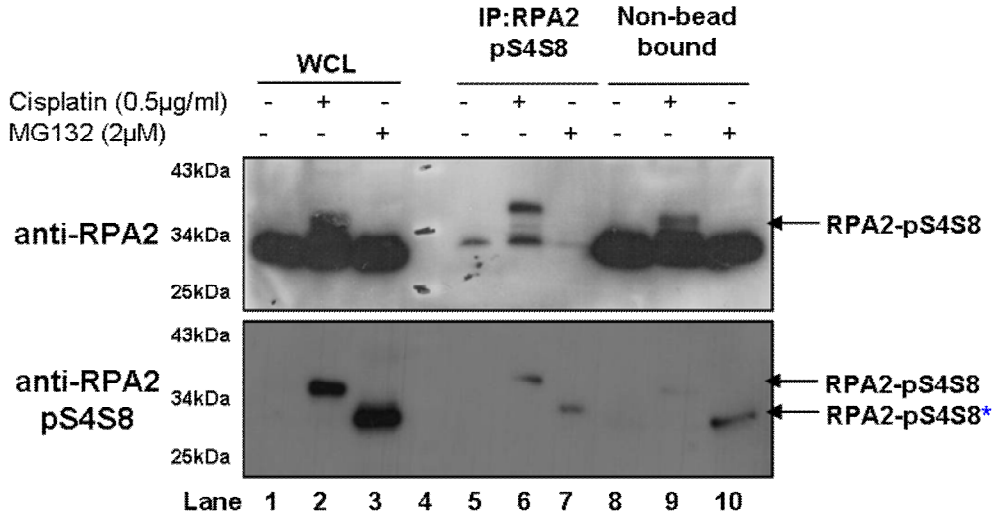

Figure 3.16 Immunoprecipitation of RPA2-pS4S8 from XP30RO cell extracts. XP30RO cells were either mock-treated, treated with 0.5µg/ml cisplatin for 24 hours or with 2µM MG132 for 6 hours. Extracts were prepared, and immunoprecipitation of RPA-pS4S8 was carried out. Eluted protein was analysed by SDS-PAGE and western blotting using antibodies against RPA2 (upper panel) and RPA2-pS4S8 (lower panel). 20µg of WCL and non-bead bound fraction was analysed. 20µg of WCL and the non-bead bound fraction was analysed. WCL: whole cell lysate; IP: immunoprecipitate.

3.6.8 Subcellular localisation of RPA2-pS4S8*

Using subcellular fractionation, it has been shown that the cisplatin-induced pS4S8 form of RPA2 accumulates in the chromatin-bound fraction (Cruet-Hennequart *et al.*, 2008). In order to investigate the subcellular localisation of RPA2-pS4S8***,** chromatin-bound and soluble protein fractions were prepared from XP30RO cells. Cells were either mock-treated or treated with 0.5µg/ml cisplatin for 18 hours followed by co-treatment of cells with 0.5µg/ml cisplatin and 2µM MG132 for a further 6 hours (Cis+MG). Following this treatment, treatment protocol, both the cisplatin-inducible and the MG132-inducible forms of RPA2 were detectable, as shown in Figure 3.7B (lane 4).

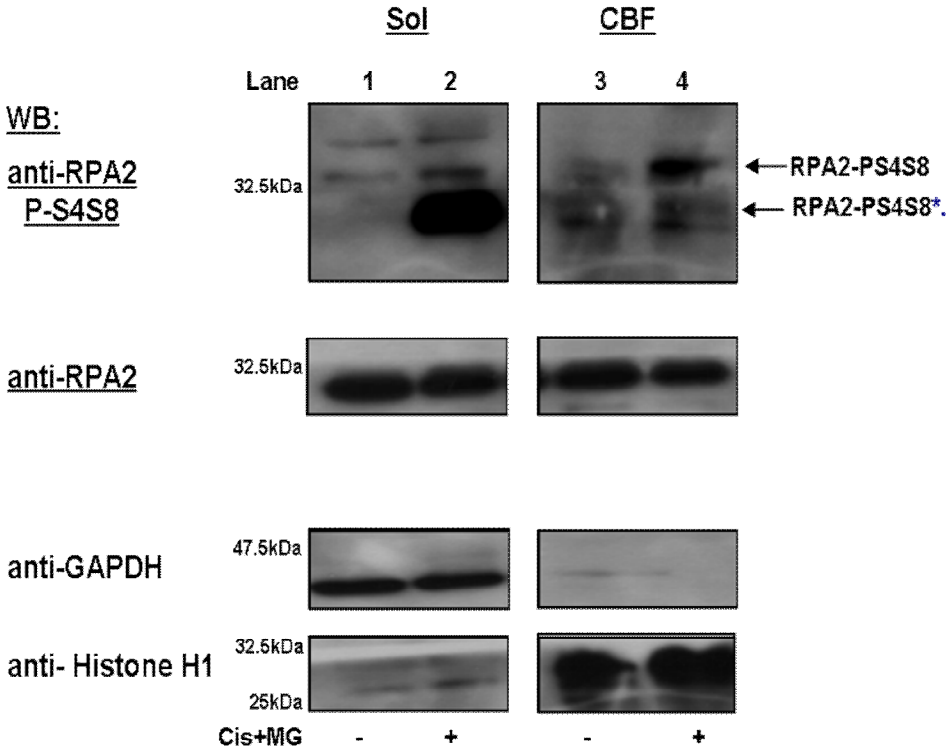

Figure 3.17: Subcellular localisation of RPA2-pS4S8*. XP30RO cells were either untreated, or treated with 0.5µg/ml cisplatin for 18 hours followed by co-treatment with 0.5µg/ml cisplatin and 2µM MG132 for a further 6 hours (Cis+MG). Extracts were fractionated into soluble (Sol) and chromatin-bound (CBF) fractions, as described in Section 2.11. Fractions were analysed by SDS-PAGE and western blotting using antibodies against RPA2 and RPA2-pS4S8. GAPDH and histone H1 were used as markers of the soluble and chromatin-bound fractions, respectively.

Consistent with previous reports, the majority of the cisplatin-induced phosphorylated form of RPA2 on S4S8 is detected in the chromatin-bound fraction (Fig. 3.17, lane 4) (Cruet-Hennequart *et al.*, 2008). However, following the treatment of cells with MG132, RPA2-pS4S8* was detected primarily in the soluble fraction (Fig. 3.17, Sol, lane 2). The level of RPA2 in both fractions did not change significantly. RPA-pS4S8* may represent a small fraction of the total RPA2, and any change is not detectable by western blotting. Levels of GAPDH and histone H1 did not change following treatment of cells (Fig. 3.17, lower panels). GAPDH was found in the soluble fraction, and histone H1 was in the chromatin-bound fraction, consistent with the specificity of the fractionation procedure. Thus, the novel phosphorylated form of RPA2 has a different subcellular localisation from cisplatin-induced phosphorylation of RPA2.

3.6.9 Cell cycle distribution of novel RPA2-pS4S8*

The relationship between cell cycle stage and the MG132-dependent phospho-form of RPA2 detected using the RPA2-pS4S8 antibody was investigated directly using dual-labelling flow cytometry as described in Cruet-Hennequart *et al.* 2009. Since RPA2-pS4S8* in extracts of MG132-treated cells had unique gel mobility (Fig 3.7 (lane 3) and no DNA damage-induced, slow-mobility RPA2-pS4S8 band was detectable by western blotting, any signal detected, using the anti-RPA2-pS4S8 antibody, in extracts of MG132-treated cells should represent RPA2-pS4S8*. MG132-treated cells were therefore dual-labelled for the novel intracellular phosphorylated form of RPA2, using the anti-RPA2-pS4S8 antibody and a FITC-labelled secondary antibody, and for DNA content using PI, and analysed using flow cytometry (Cruet-Hennequart *et al.* 2009).

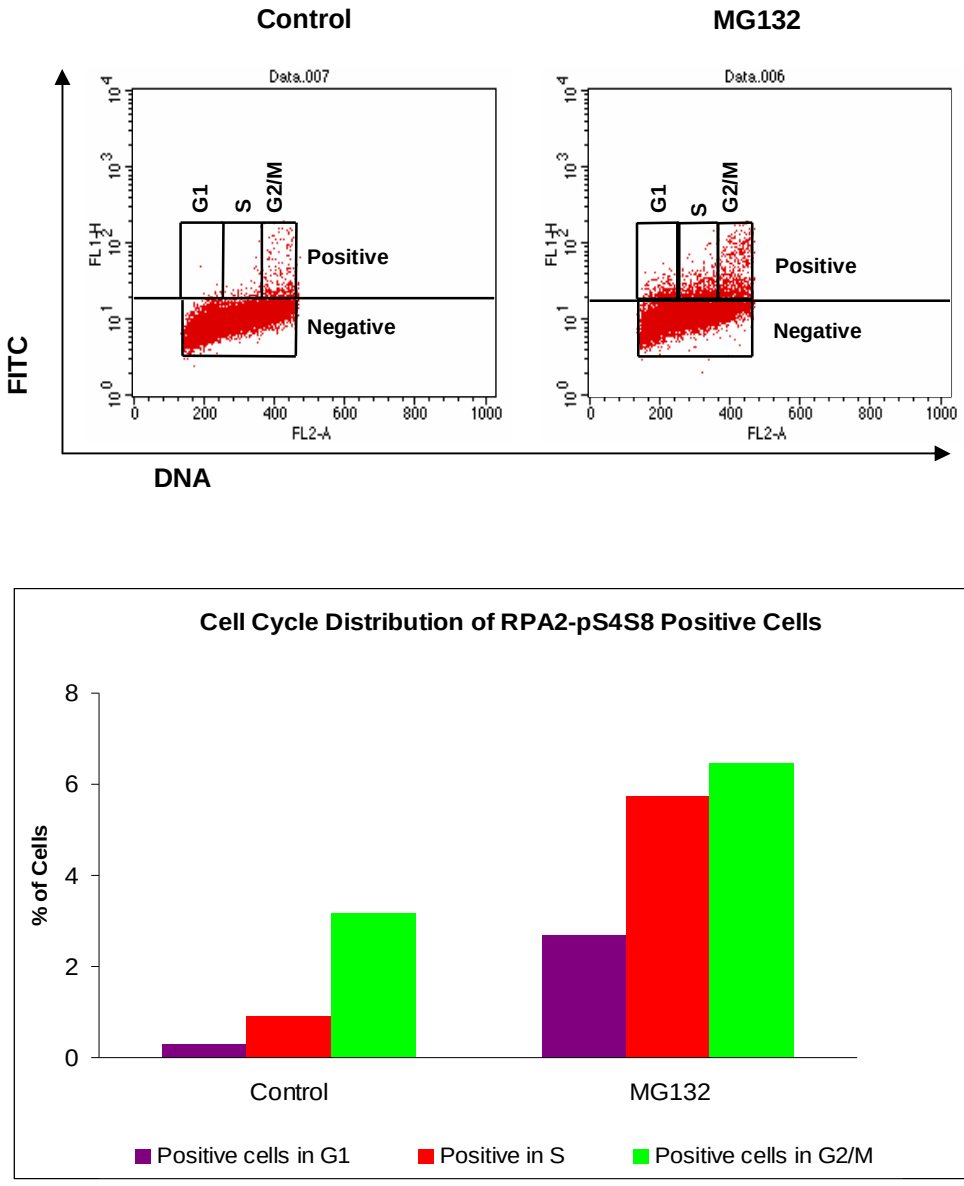

Figure 3.18: Cell cycle distribution of RPA2-pS4S8*. XP30RO cells were either mock-treated (control) or treated with 2µM MG132 for 6 hours. Cells were co-stained for DNA content using PI, and for RPA2-pS4S8 using the phospho-specific antibody against RPA-pS4S8, and a FITC-labelled secondary antibody. Flow cytometry, was carried out using a FACSCalibur and data analysed using Cell Quest™ software. Results are derived from a single experiment.

The threshold used to define cells positive for RPA2-pS4S8 staining was determined using a control in which the cells were stained only with the FITC-labelled secondary antibody (Fig. 3.18). Any cells having a signal above this threshold in the 'FITC' (FL1H) channel were scored as positive. In mock-treated cells, approximately 4% of cells stained positive using the phospho-specific

antibody against RPA2-pS4S8 (Fig. 3.18). Approximately 3% of cells were in the G2/M phase and the remaining 1% of cells was in the G1 and S phases. Following treatment of XP30RO cells with 2μM MG132 for 6 hours, there was approximately 4-fold increase in the percentage of total cells positive for RPA2-pS4S8 as determined by a shift of cells into the positive region of the dot plot. The majority of positive cells were in the S (5%) and G2/M (6%) phases. This analysis demonstrates that MG132-induced RPA2-pS4S8* occurs primarily in the S and G2/M phases XP30RO cells. Data presented here represents only one experiment, this would need to be repeated in order to confirm these results. On repeating this experiment the compensation could be altered at the time of acquisition of samples to account for the difference in fluorescent intensity of the G1 and G2/M phases (Fig 3.18).

3.6.10 Cellular localisation of RPA2-pS4S8

RPA2 phosphorylated on Ser4/Ser8 is localised to nuclear foci in cisplatin-treated XP30RO cells (Cruet-Hennequart *et al.*, 2008). The localisation of RPA2-pS4S8* in MG132-treated XP30RO cells was further investigated using immunofluorescence. XP30RO cells were grown on glass coverslips and either mock-treated, treated with 0.5μg/ml cisplatin for 24 hour or treated with 2μM MG132 for 6 or 24 hours. Cells were fixed and stained using anti-RPA-pS4S8 primary antibody and an Alexa 488-labelled secondary antibody.

Consistent with published data (Cruet-Hennequart *et al.*, 2008), following cisplatin treatment, RPA2 phosphorylated on Ser4/Ser8 was localised to nuclear foci (Fig. 3.19). In cells treated with MG132 alone, where RPA-pS4S8* was detected by western blotting, distinct foci were detected by immunofluorescence (indicated by arrow in Fig. 3.19). MG132-induced foci detected using the RPA2-pS4S8 antibody displayed a different pattern compared to RPA2-pS4S8 foci detected in cisplatin-treated cells. These distinct foci were detected following exposure of cells to 2μM MG132 for 6 and 24 hours (representative cell shown in Fig 3.19). After 24 hours MG132 treatment, the foci detected using the RPA2-pS4S8 antibody, were outside of the DAPI stained nucleus (Fig. 3.19). This indicates that RPA2-pS4S8 detected under these conditions, is not

associated with chromatin, consistent with the observation (Fig. 3.19) that MG132-induced RPA2-pS4S8* was located in the soluble fraction of cellular extracts. These number of cells positive for distinct RPA2-pS4S8* foci were not scored; however, the percentage of cells containing these foci appeared to be low. Representative cells showing altered localisation of RPA2-pS4S8* are shown in Figure 3.19.

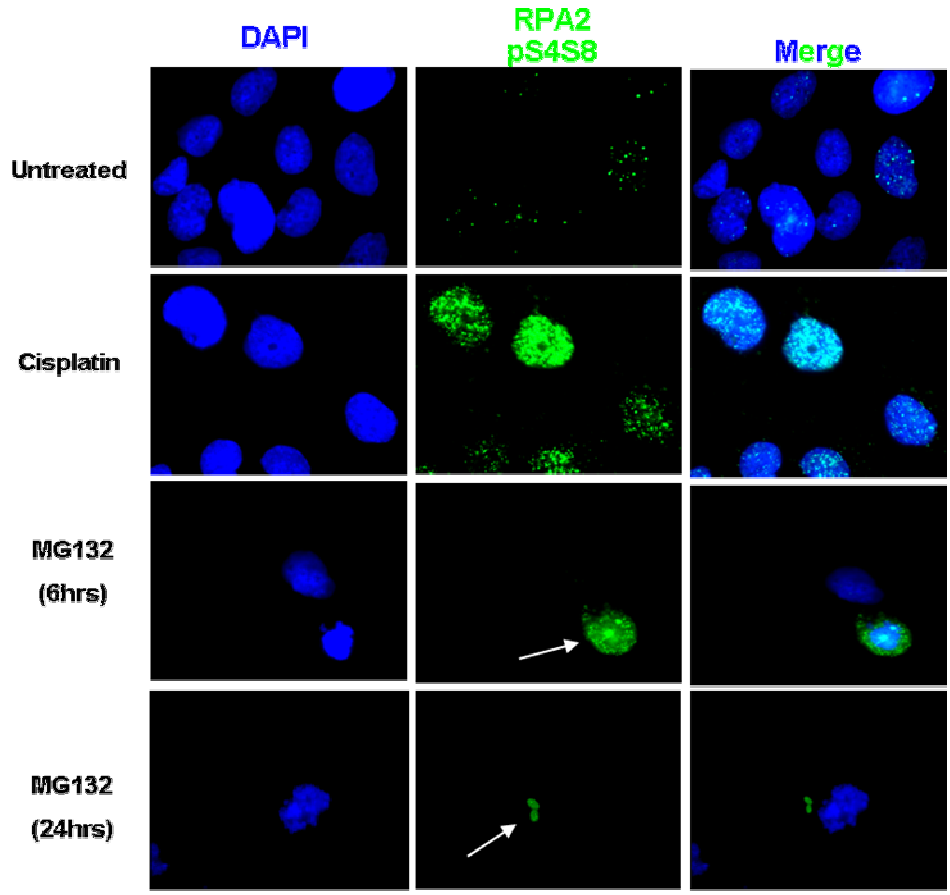

Figure 3.19: Cellular localisation of RPA2-pS4S8. XP30RO cells grown on glass coverslips were either mock-treated, treated with 0.5µg/ml cisplatin for 24 hours, or treated with 2µM MG132 for 6 or 24 hours. Cells were fixed, and stained using anti-RPA2-pS4S8 and an Alexa 594 fluorescently-labelled secondary antibody. Images were obtained using an Olympus 1X51 fluorescence microscope (Biochemistry, NUI Galway) at 100X magnification. Arrows indicate distinct MG132 induced RPA2-pS4S8 foci.

Nuclei contain a number of defined nuclear bodies, detectable by microscopy. In order to investigate if foci detected in MG132-treated cells using the RPA2-pS4S8 antibody were localised at a particular sub-nuclear body, the localisation

of three different nuclear bodies, promyelocytic leukaemia (PML) protein nuclear bodies, coiled bodies and centrosomes, were analysed.

In order to investigate if pattern of the above mentioned nuclear bodies, by immunofluorescence, resembles the pattern of the distinct MG132-induced RPA2-pS4S8 foci shown in Fig. 3.19, XP30RO cells were grown on glass coverslips and treated as outline in Figure 3.19. Cells were fixed and stained using markers of the individual classes of nuclear bodies. Antibodies against PML protein, coilin and γ-tubulin were used to stain for PML bodies, coiled bodies and centrosomes, respectively. Co-staining experiments of nuclear bodies and RPA-pS4S8 following proteasome inhibition were carried out; however, these were unsuccessful.

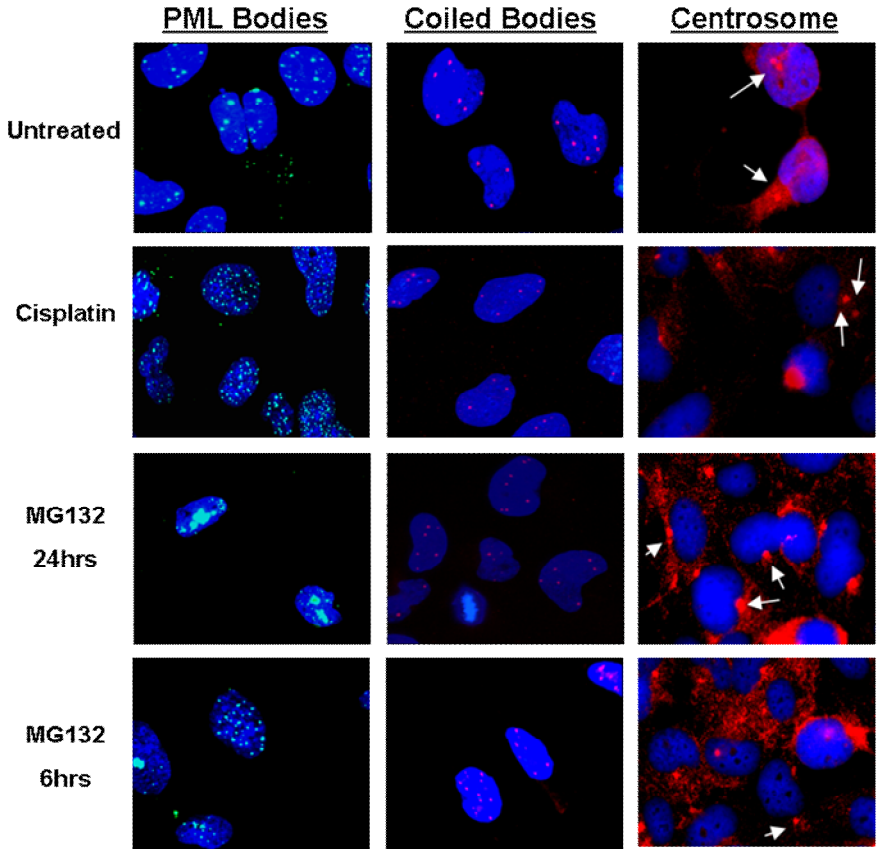

Figure 3.20 Pattern of distribution of sub-nuclear bodies. XP30RO grown on glass cover slips were mock-treated, treated with 0.5ug/ml cisplatin or treated with 2μM MG132 for 6 and 24 hours. Cells were fixed and stained for PML bodies using anti-PML, for coiled bodies using anti-coilin, and for centrosomes using anti-γ-tubulin (arrows). Images were obtained using an Olympus 1X51

fluorescence microscope Biochemistry, NUI Galway) at 100X magnification. Merged images are shown.

PML bodies are found in the nucleus of most cell types, and range in size from 0.1-1.0 μM in diameter (Lallemand-Breitenbach *et al.,* 2010). PML bodies contain the PML protein which can used as a marker in the analysis of PML bodies (Lallemand-Breitenbach *et al.,* 2010). The role of PML bodies in the cell is not known; however, many proteins involved in DNA replication, transcription and repair are located at PML bodies (Lallemand-Breitenbach *et al.,* 2010). Normal mammalian cells contain approximately 10-20 PML bodies (Lallemand-Breitenbach *et al.,* 2010). Mock-treated XP30RO cells contained approximately 16 PML bodies (Fig. 3.19).The number of PML bodies increased in cisplatin treated cells (Fig. 3.20). Following exposure of cells to MG132, PML bodies formed large clusters which began to appear at 6 hours but were more prominent at 24 hours of proteasome inhibition (Fig. 3.20), consistent with a previous reports (Lallemand-Breitenbach *et al.,* 2010). However, the appearance of PML bodies did not resemble the MG132-induced RPA2-pS4S8 foci shown in Figure 3.19.

Coiled or Cajal bodies are spherical bodies ranging in diameter from 0.3-1.0 μM. Normal cells contain approximately 1-5 Cajal bodies (Cioce *et al.,* 2005). The function of Cajal bodies is unknown; however, they may play a role in snRNP transport and maturation. Coiled bodies are highly enriched in the p80 coilin protein, which is used as a marker in the study of coiled bodies (Cioce *et al.,* 2005). The approximate number of coiled bodies in untreated cells was 5 (Fig 3.20). The number and distribution of coiled bodies per cell did not change following cisplatin treatment or proteasome inhibition (Fig. 3.20) and did not form foci similar to distinct RPA2-pS4S8 shown in Figure 3.17 following MG132 treatment.

The centrosome is as organelle in the cell which is the place of microtubule production (Azimzadeh *et al.,* 2007). Mammalian centrosomes are made up of a pair of centrioles, which are comprised of microtubules. The centrosome associates with the nuclear membrane; during cell division the centrosome

duplicates, each with its own pair of centrioles. The two centrosomes migrate to opposite ends of the nucleus, and interact with chromosomes through the production of mitotic spindle which is responsible for separating replicated chromatids into two daughter cells. γ-tubulin is used as a marker for centrosomes. The distribution of centrosomes did not change following cisplatin treatment or proteasome inhibition.

The distribution of the above nuclear bodies in cells did not resemble the distribution of RPA2-pS4S8 in MG132 treated cells (Fig 3.19). Optimisation of these co-staining experiments would determine whether MG132-induced RPA2-pS4S8 foci co-localised with any of the above mentioned nuclear bodies.

Summary.

A novel phosphorylated form of RPA2, RPA2-pS4S8* has been identified in MG132-treated human cells. This form of RPA2 is phosphorylation on Ser4/Ser8 but is not hyperphosphorylated, based on gel mobility and western blotting following SDS-PAGE. Induction of RPA2-pS4S8* is DNA damage independent but is dependent on proteasome inhibition. Affi-Gel Blue chromatography and immunoprecipitation were used to confirm that RPA2-pS4S8* is a form of RPA2. RPA2-pS4S8* is not associated with chromatin, but forms discrete foci detectable by immunofluorescence.

3.7 Effect of removal of MG132 on cisplatin-induced DNA damage responses.

Proteasome inhibition by MG132 is reversible (Lee *et al.*, 1998). The effect of the removal of MG132 on cisplatin-induced RPA2 phosphorylation was investigated. Co-treatment of cisplatin and MG132 for 24 hours was very toxic to cells (Fig. 3.3). In the present experiments, cells were treated using the protocol 'Cis+MG', where cells were treated with 0.5 µg/ml cisplatin for 18 hours after with cells were co-treated for a further 6 hours with cisplatin and 2µM MG132. After this time period, cisplatin and MG132 were removed and cells were grown in drug-free media for a further 2, 4 and 6 hours. Treatment protocol is outlined in Figure 3.21 below.

(A)

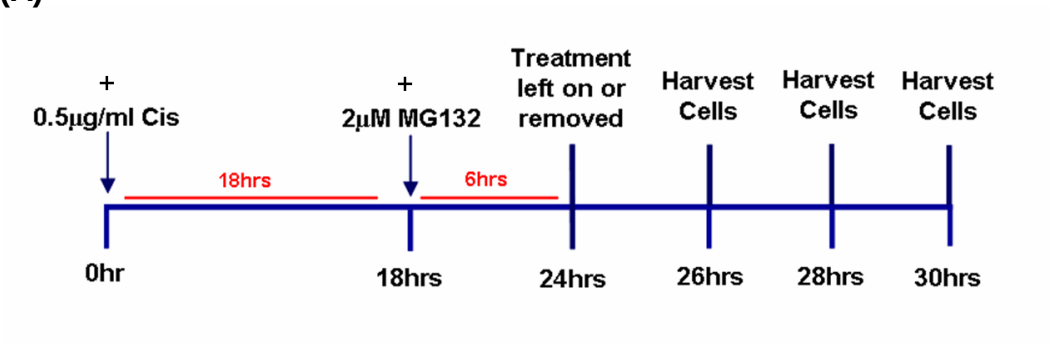

(B)

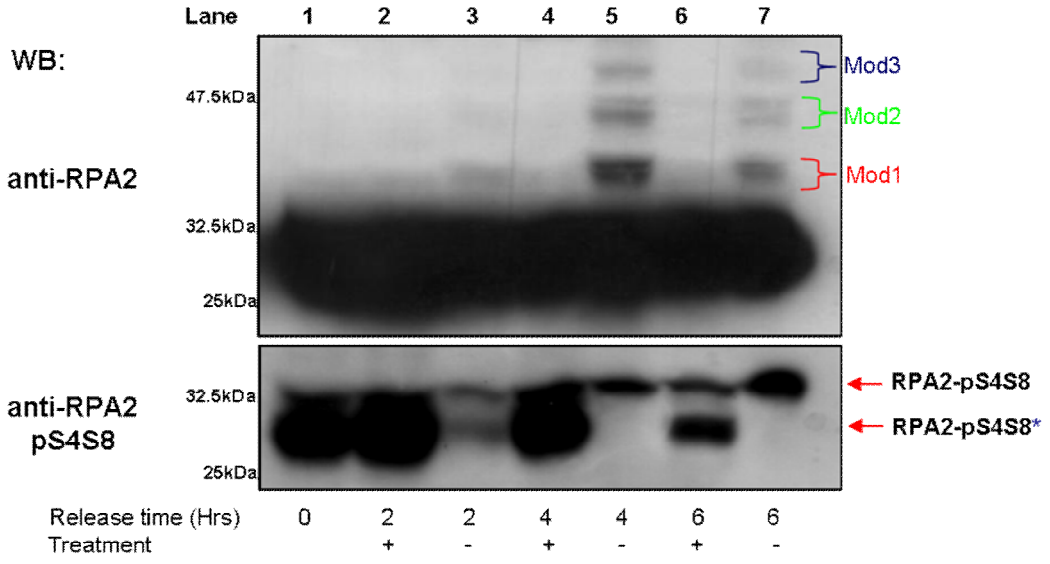

Figure 3.21: Effect of removal of MG132 on cisplatin-induced RPA2 **phosphorylation.** (A) Schematic diagram showing treatment protocol. XP30RO cells were either treated using the 'Cis+MG' protocol. Cells were either harvested (time 0), or the culture medium was either left on cells (+) or removed and replaced by drug-free medium (-) for a further 2, 4, and 6 hours. (B) XP30RO cells were treated as in (A). Extracts were prepared, separated on SDS-PAGE and analysed by western blotting using anti-RPA2 or anti-RPA2-pS4S8 antibodies.

Cisplatin induced RPA2 phosphorylation on S4S8 and MG132 induced RPA2-pS4S8* was detected in cells treated using the 'Cis+MG' protocol (Fig. 3.21, lower panel, lane 1), consistent with results shown in Figure 3.7B, lane 4. After removal of cisplatin and MG132, RPA2-pS4S8* was no longer detectable, consistent with this effect of MG132 being reversible. However, removal of cisplatin and MG132 did not have any effect on cisplatin induced RPA2-pS4S8 (Fig. 3.21, lane5).

Interestingly, after the removal of cisplatin and MG132 a series of slower mobility forms of RPA2 were detected following SDS-PAGE and western blotting using a specific antibody against RPA2 (Fig. 3.21B, upper panel). The slow mobility bands were detected 2 hours following the removal cisplatin and MG132 (Fig 3.21B, lane 3). The intensity of these bands peaked at 4 hours (Fig 3.21, lane 5) and decreased at 6 hours following drug removal (Fig 3.21, lane 7). The slower mobility forms of RPA2 are DNA damage dependent as they were only detected in cells that had been treated with cisplatin and MG132 and not in extracts from cells treated with MG132 alone as seen in Figure 3.10, lane4. Formation of the slow mobility bands was dependent on the removal of cisplatin and MG132, because when cells were continuously exposed to both cisplatin and MG132, the slow mobility bands were not detected (Fig. 3.21, lane 2, 4, 6).

For the purpose of this study, the series of bands detected using the RPA2 anti-body (Fig 3.21B) were named modification 1, 2, 3 (Mod 1, Mod 2 and Mod 3) as in Figure 3.21B. The treatment under which slow mobility bands were detected

will be referred to as 'Cis+MG Removed' where cells were harvested 4 hours following the removal of cisplatin and MG132.

The effect of the removal of MG132 treatment on cisplatin-induced phosphorylation of DDR proteins was analysed. XP30RO cells were either mock treated, treated with 0.5µg/ml cisplatin for 24 hours, treated with 2µM MG132 for 6 hours, treated using the 'Cis+MG' or 'Cis+MG132 Removed' protocol, as in the protocol outlined above. γH2AX and pChk1 were analysed using SDS-PAGE and western blotting.

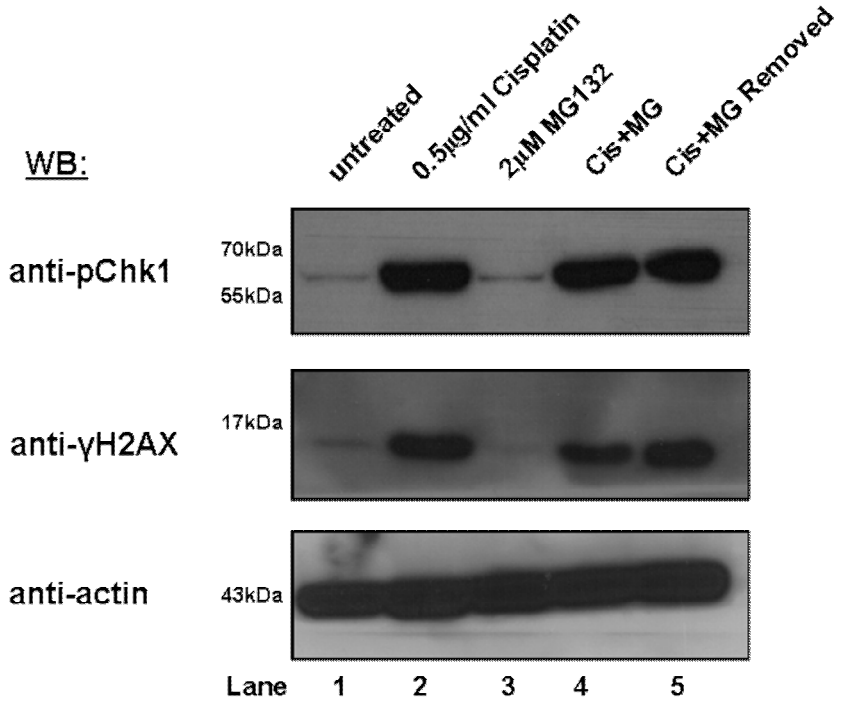

Figure 3.22: Effect of removal of MG132 on cisplatin induced DDR protein phosphorylation. XP30RO cells were either mock treated (lane 1), treated with 0.5µg/ml cisplatin for 24 hours (lane 2), with 2µM MG132 for 6 hours (lane 3), using the 'Cis+MG' (lane 4) or the 'Cis+MG132 Removed' protocols (lane 5). Cell extracts from cells were separated by SDS-PAGE and analysed by western blotting using anti-γH2AX, anti-pChk1 and anti-actin antibodies.

γH2AX is a marker of DNA strand breaks (Burma *et al.,* 2001), while Chk1 is phosphorylated in an ATR-dependent manner on Ser317 following replication arrest (Zhao *et al.,* 2001). Consistent with previous results (Cruet-Hennequart *et*

al., 2008), cisplatin induced γH2AX and Chk1 phosphorylated on Ser317 was detected in extracts from cells treated with cisplatin (Fig. 3.22, lane 2). In extracts from cells treated with MG132 there was no increase in levels of γH2AX or pChk1 compared to mock-treated cells (Fig. 3.22, lane 3), consistent with results presented in Figure 3.7A, lane 3. Treatment of cells using the 'Cis+MG132' protocol, where cells were treated with cisplatin for 18 hours and co-treated for a further 6 hours with cisplatin and MG132, did not alter the levels of cisplatin-induced γH2AX or pChk1 (Fig. 3.22, lane 4) when compared to cisplatin alone. Also, the levels of γH2AX or pChk1 did not change after removal of cisplatin and MG132 (Fig. 3.22, lane 5). The removal of MG132 did not alter the levels of cisplatin induced phosphorylation of γH2AX or pChk1. Detection of γH2AX and pChk1 following the removal of cisplatin and MG132 is consistent with the novel, slow mobility forms of RPA2 (Fig. 3.21) being dependent on DNA damage. The novel forms of RPA2 detected in Figure 3.21 were further characterised.

The initial detection of the slow mobility forms of RPA2 by western blotting was carried out using a mouse monoclonal antibody against RPA2 (Fig. 3.21B). However, the slow mobility bands were also detected using a separate rat monoclonal antibody against RPA2 (obtained from Dr. Heinz Peter Nasheuer, at NUI, Galway; Fig. 3.23, lane 4) demonstrating that these forms were unlikely to be due to non-specific cross reaction. However, an additional slow-mobility band was detected using this RPA2 (Fig. 3.23 lane 4, Mod*, indicated by arrow). For further investigation of these bands the mouse monoclonal antibody against RPA2 was used.

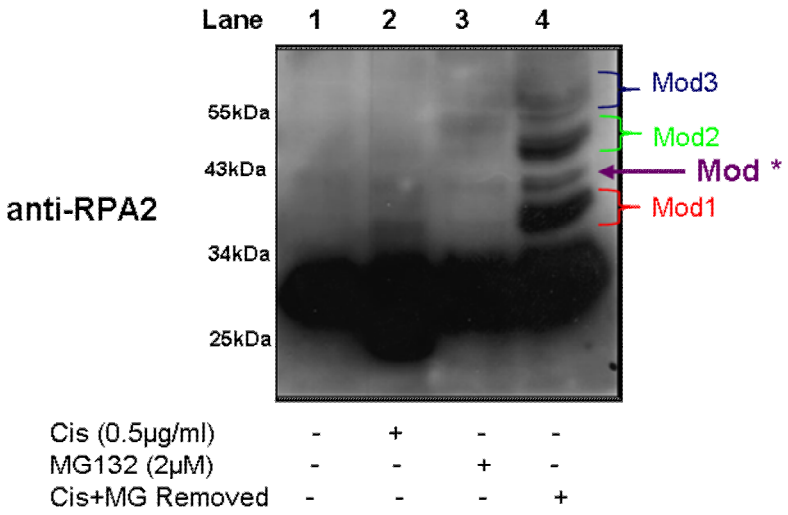

Figure 3.23: Detection of modified RPA2 using a rat anti-RPA2 monoclonal antibody. XP30RO cells were either mock-treated (lane 1), treated with 0.5µg/ml cisplatin for 24 hours (lane 2), treated with 2µM MG132 for 6 hours, or treated using the 'Cis+MG Removed' protocol (lane 4). Extracts were separated by SDS-PAGE and analysed by western blotting using a rat anti-RPA2 antibody.

3.7.1 λ-phosphatase treatment.

As described in Section 1.8, it is well-established that RPA2 can be post-translationally modified by phosphorylation a number of N-terminal sites in a cell cycle-dependent manner by CDKs, and in response DNA damaging agents by the PIKKs (Din et al. 1990; Dutta and Stillman 1992; Anantha et al. 2007(Cruet-Hennequart *et al.*, 2006; Anantha *et al.*, 2007; Cruet-Hennequart *et al.*, 2008). As RPA2 is phosphorylated following cisplatin treatment and the modified, slower mobility forms of RPA2 are also dependent on cisplatin treatment whole cell extracts from cells treated as described in the legend to Fig 3.24, were treated with λ-phosphatase in order to investigate whether the slower mobility forms of RPA2 were phosphorylated.

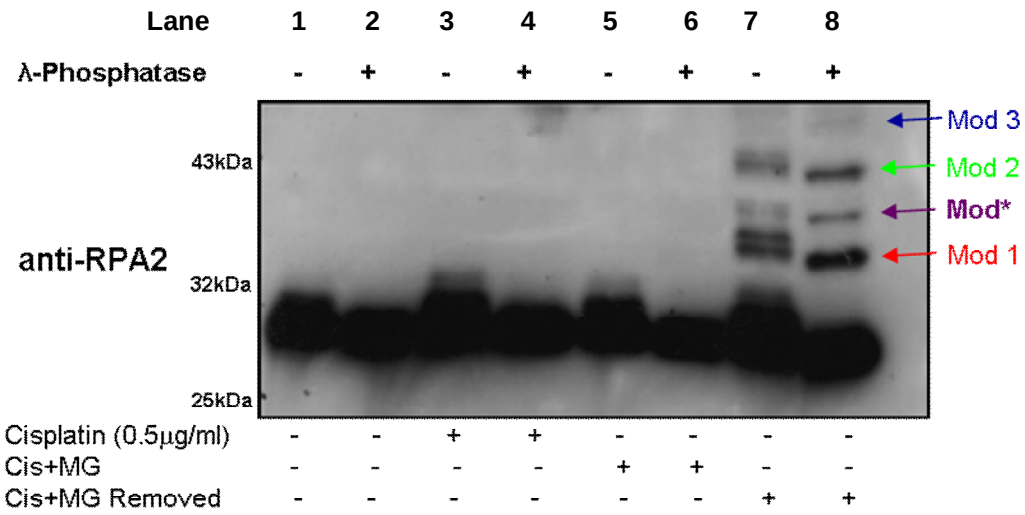

Figure 3.24 λ-phosphatase-treatment of XP30RO cell extracts. XP30RO cells were either mock-treated (lanes 1, 2), treated with 0.5µg/ml cisplatin (lanes 3, 4), treated with 'Cis+MG' (lanes 5, 6) or 'Cis+MG Removed' (lanes 7, 8). 30µg of protein was incubated at 37°C for 60 minutes in the presence (+) or absence (-) of λ-phosphatase. Cell extracts were analysed by SDS-PAGE and western blotting using anti-RPA2 antibody.

Each modified form of RPA2 appears as a pair of bands following western blotting (Fig. 3.21B). Treatment of whole cell lysates with λ-phosphatase eliminated the cell cycle-dependent phosphorylation (Fig. 3.24, compare lanes 1 and 2) and cisplatin-dependent phosphorylation of RPA2 (Fig. 3.24, compare lanes 3 and 4). Following λ-phosphatase treatment, the upper of each of the modified slow mobility forms defined in the previous section was eliminated (Fig 3.24 compare lanes 7 and 8). λ-phosphatase removed phosphorylation resulting in an increase in the intensity of the unphosphorylated form of the slower mobility forms of RPA2 (Fig. 3.24). This demonstrates that each of the slow mobility forms is a mixture of unphosphorylated and phosphorylated RPA2 protein.

3.7.2 PIKK-dependence of modified RPA2.

As outlined in Section 1.3, the PIKKs are activated in response to DNA damage and are, in part, responsible for the signal-transduction during the DNA damage response (Bakkenist *et al.*, 2004; Cimprich *et al.*, 2008). Previous work has shown that DNA-PK, but not ATM, is required for cisplatin induced RPA2 phosphorylation on Ser4/Ser8 (Cruet-Hennequart *et al.*, 2008). As the newly identified modified forms of RPA2 are cisplatin-dependent, the dependence of modified RPA2 on ATM and DNA-PK was investigated. In order to investigate the dependence of modified RPA2 on ATM and DNA-PK, XP30RO cells were treated using the 'Cis+MG Removed' protocol, in the presence or absence of the DNA-PK inhibitor, NU7741, or the ATM inhibitor KU55933. XP30RO cells were exposed to the inhibitors for 24 hours from the start of the experiment (Fig. 3.25).

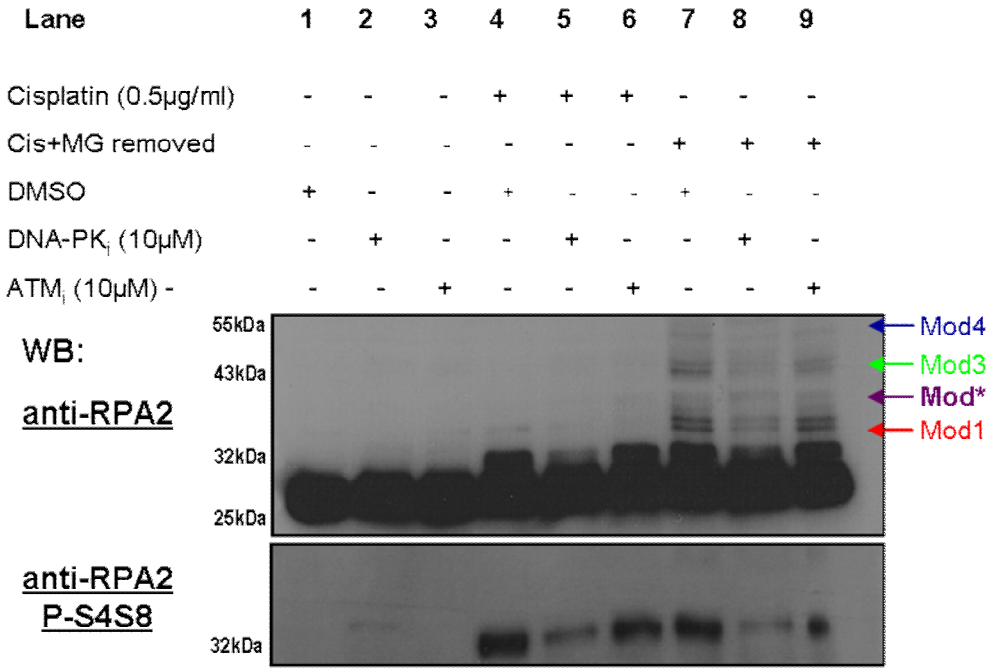

Figure 3.25: PIKK dependence of modified RPA2. XP30RO cells were either mock-treated, treated with 0.5µg/ml cisplatin for 24 hours, or treated using the 'Cis+MG Removed' protocol. Cells were co-treated for 24 hours with the DNA-PK inhibitor (DNAPKi: NU7741) or the ATM inhibitor (ATMi: KU55933) inhibitor. Cells were treated with DMSO as a solvent control. Proteins were

separated by SDS-PAGE gels and analysed using anti-RPA2 (upper panel), and anti-RPA2-pS4S8 (lower panel) antibodies.

Consistent with previously published data (Cruet-Hennequart *et al.*, 2008) treatment of XP30RO cells with the DNA-PK inhibitor NU7741 reduced cisplatin-induced phosphorylation of RPA2 on Ser4/Ser8 (Fig. 3.25, lane 5). Co-treatment of cells with ATM inhibitor did not have any affect on RPA-pS4S8 formation (Fig. 3.25, lane 6). DNA-PK inhibition reduced the signal of modified RPA2 (Fig. 3.25, lane 8) detected by western blotting, providing evidence for a role for DNA-PK in the formation of modified RPA2. This is consistent with evidence that modified RPA2 is phosphorylated (Fig. 3.24). It may be possible that a phosphorylation event mediated by DNA-PK is required for the formation of modified RPA2.

3.7.3 Affi-gel RPA enrichment

To further characterise the slow mobility forms of RPA2 detected using western blotting with anti-RPA2 antibodies, extracts from XP30RO cells treated using the 'Cis+MG Removed' protocol were fractionated using Affi-Gel Blue chromatography (Fig. 3.26).

As described in Section 3.5.6, RPA binds with high affinity to Affi-Gel Blue beads (Oakley *et al.*, 2003; Block *et al.*, 2004). If the slower mobility forms detected using anti-RPA2 antibodies represent modified forms of RPA2, then these should bind to Affi-Gel Blue beads and be eluted at increasing salt concentrations. Following incubation of Affi-Gel Blue beads with extracts of cells, treated using the 'Cis+MG Removed' protocol, beads were washed twice with 900mM NaCl, and then washed twice with 2M NaCl, after which bound eluted by boiling the beads in Laemmli sample buffer. Proteins were analysed by SDS-PAGE and western blotting.

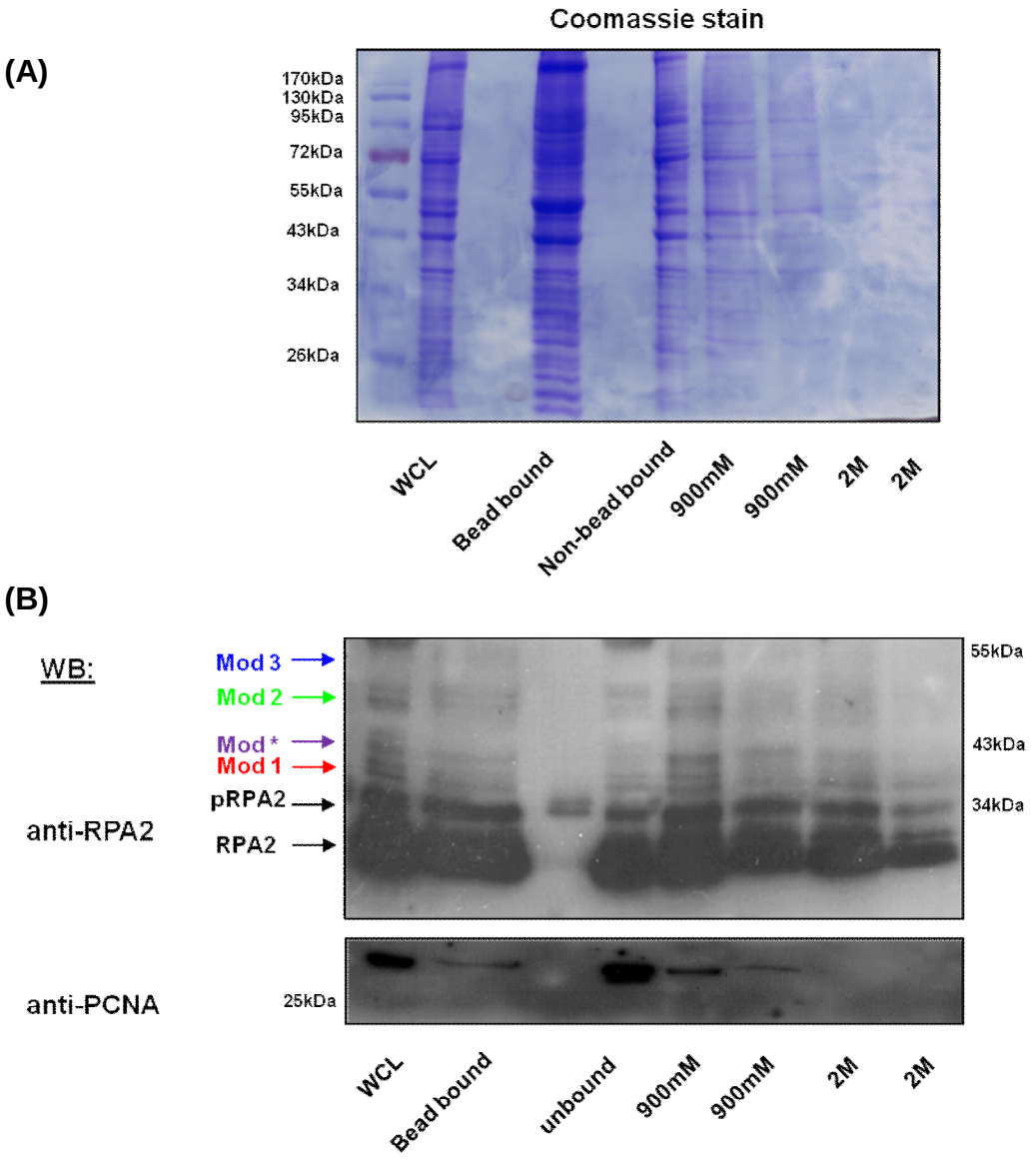

Figure 3.26: Affi-gel Blue RPA enrichment. XP30RO cells were treated using the protocol Cis+MG Removed'. Affi-Gel Blue enrichment was carried out on cellular extracts (Section 2.20). Bound protein was eluted, separated by SDS-PAGE and analysed by coomassie staining (A) and by western blotting using antibodies against RPA2 (upper panel) or PCNA (lower panel) (B). 20µg of WCL, 20µg unbound fraction and 25µl of each wash were analysed. All of the bound protein was also analysed.

Following Affi-Gel Blue enrichment a large proportion of the slow mobility forms of RPA2 was recovered following the first 900mM salt wash (Fig. 3.26B). To a lesser extent, the slow mobility forms of RPA2 were found in the subsequently 900mM and 2M salt washes (Fig. 3.26B). Modified forms of RPA2

were detected using the anti-RPA2 antibody the bead bound fraction following the 900mM and 2M washes , consistent with slow mobility forms representing forms of RPA2 (Fig.3.26B).

As a control for the specificity of protein binding to Affi-Gel Blue, the binding of PCNA to the matrix was analysed. The PCNA heterotrimer encircles ssDNA and is loaded onto DNA by replication factor C (Strzalka *et al.*, 2011). PCNA protein does not associate tightly with DNA and does not bind with high affinity to Affi-Gel Blue beads, as seen in Figure 3.26B. The residual PCNA detected using an anti-PCNA antibody maybe a result of the interaction of PCNA with a DNA binding protein (Dianov *et al.*, 1999). The majority of the PCNA protein is in the unbound fraction providing evidence that binding of RPA2 is specific (Fig. 3.26B).

3.7.3 Immunoprecipitation of RPA2 from cell extracts

To further examine the newly identified forms of RPA2, immunoprecipitation of RPA2 from cell extracts was carried out. Initially, in order to determine the amount of isolated RPA2 that is detectable by western blotting and silver staining following immunoprecipitation, different amounts of recombinant human RPA purified from *E. coli* (0-3μg) was analysed by SDS-PAGE followed by western blotting or by coomassie blue staining. Recombinant RPA was obtained from Dr. Heinz-Peter Nasheuer, CCB, NUI, Galway.

300pg of recombinant RPA2 was detectable by western blotting (Fig 3.27A). The level of detection using coomassie staining was approximately 10^3 times lower than that of western blotting. Thus 30ng of RPA2 was detectable by coomassie blue staining (Fig 3.27B). RPA2 was immunoprecipitated from 400μg of untreated cell extracts. Half of the eluted protein was analysed by SDS-PAGE and silver staining (Fig. 3.27C). The amount of RPA2 detected was compared to 30-300ng of recombinant RPA. From the comparison of the intensities of the protein bands detected, approximately 50ng of RPA protein was present in half of the eluted protein (Fig. 3.27C). Hence, approximately 100ng of RPA2 could potentially be isolated from

400µg of total cellular extract using immunoprecipitation under these experimental conditions.

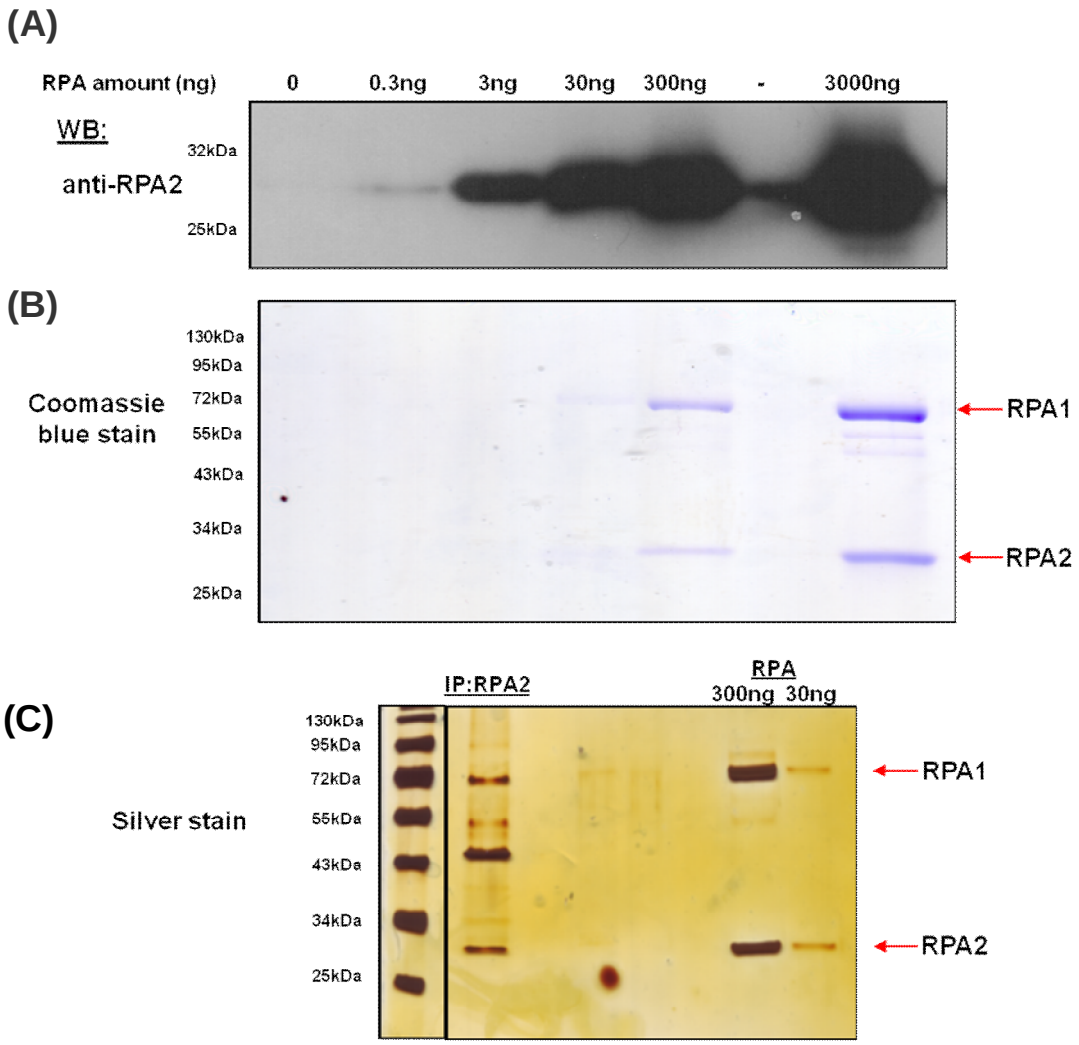

Figure 3.27: (A) Indicated amounts of recombinant human RPA2, purified from *E. coli* were analysed by SDS-PAGE, and western blotting using anti-RPA2 antibody. (B) A corresponding gel was stained with coomassie blue. (C) RPA2 was immunoprecipitated from untreated cellular extracts. Bound proteins were eluted and analysed by SDS-PAGE and sliver staining.

3.7.4 Characterisation of modified RPA2.

To further characterise slow mobility forms of RPA2 the approximate molecular weight of the novel slow mobility RPA2 bands shown in Figures 3.21 and 3.23 were calculated, using Rf values as outlined in Section 2.17. The approximate

molecular weights are outline below in Table 3.1. Molecular weights were calculated from two independent experiments.

Modification	Exp. 1	Exp. 2	Average
Mod 1	37kDa	38kDa	37.5kDa
Mod 2	43kDa	45kDa	44kDa
Mod 3	52kDa	55kDa	53.5kDa
Mod *	40kDa	42kDa	41kDa

Table 3.1: Approximate molecular weight of slow mobility forms of RPA2. Approximate molecular weights of modified RPA2 were determined by calculating RF values. Values above were the average of two independent western blots.

Generation of slow mobility forms of proteins detectable by SDS-PAGE and western blotting can result from the covalent attachment of modifier proteins such as SUMO and ubiquitin. Small Ubiquitin-like Modifier or SUMO proteins are a family of proteins, including Sumo 1, 2 and 3, with a molecular weight of 11kDa. (Hannoun *et al.*, 2010). Sumoylation involves the covalent attachment of a SUMO molecule to a target protein, modifying its function. As discussed in Section 1.4, proteins can be modified by the addition of one ubiquitin, 8kDa, resulting in monoubiquitination which modifies protein function, whereas the addition of multiple ubiquitin molecules leads to polyubiquitination of the protein and usually targets it for degradation by the proteasome. Modified RPA2 was examined further to determine whether sumoylation or ubiquitination accounted for the slow mobility forms of RPA2 on SDS-PAGE.

3.7.4.1 Sumoylation

It has been reported recently that the RPA1 subunit of the RPA trimer is sumoylated by SUMO 2/3 on K577 and K449 (Dou *et al.*, 2010). Sumoylation of RPA1 occurs in response to replication-mediated DSBs, and may facilitate the recruitment of Rad51 to initiate repair by HR (Dou *et al.*, 2010). In order to determine if the formation of the modified slow mobility forms of RPA2 were a result of sumoylation, RPA2 was immunoprecipitated from extracts of XP30RO cell that were either mock treated or treated using the 'Cis+MG Removed' protocol. Bound protein was eluted and analysed by SDS-PAGE and western blotting using anti-SUMO-1 and SUMO-2/3 antibodies (obtained from Professor Ron Hay, University of Dundee, Scotland).

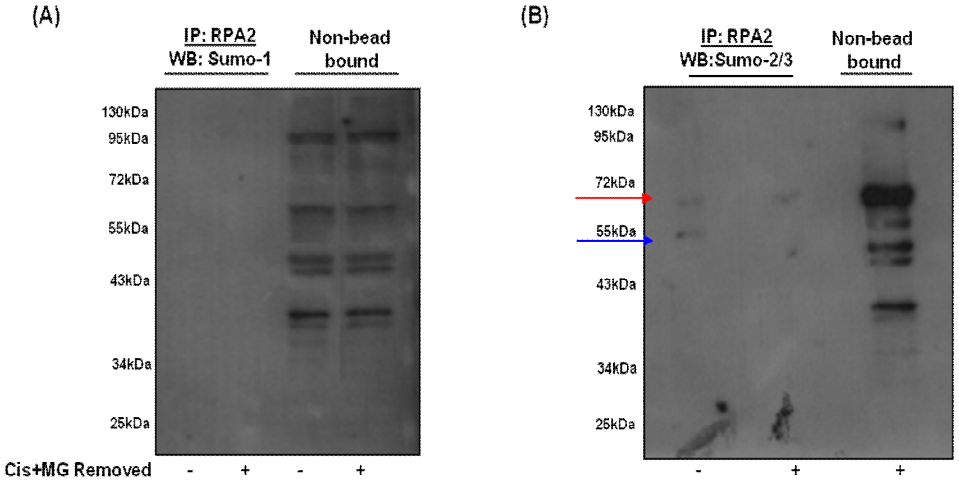

Figure 3.28: Sumoylation. RPA2 was immunoprecipitated from whole cell extracts from either mock-treated cells or from cells treated using the 'Cis+MG removed' protocol. Bound proteins were eluted and analysed by western blotting using anti-SUMO-1 (A), and anti-SUMO-2/3 (B) antibodies.

Immunoprecipitates analysed using anti-SUMO-1 antibody did not detect any bands corresponding to SUMO-1 either in the treated or mock-treated extracts (Fig. 3.28A). A number of bands were detected using the anti-SUMO-1 antibody in the non-bead bound fraction, showing that the antibody can detect proteins by western blotting. A band of approximately 70kDa in molecular weight was detected in both treated and untreated samples using the anti-SUMO-2/3

antibody (Fig. 3.28B) (indicated by red arrow). However, this band did not correspond in size to the slow mobility RPA2 bands. A band, 55kDa, detected in the untreated extracts corresponds to the size of the heavy chain of the antibody used in immunoprecipitation (Fig. 3.28B, indicated by blue arrow). The lack of SUMO-1 and SUMO 2/3 detection corresponding in mobility to modified forms of RPA2 suggests that these forms of RPA2 did not result from sumoylation. However, it may be possible that there was not enough isolated modified RPA2 for a signal for SUMO to be detected.

3.7.4.2 Ubiquitination.

As described in previous sections, cellular extracts in which the modified forms of RPA2 were detected were derived from cells that had been treated with the proteasome inhibitor, MG132. MG132 binds to and inactivates the enzymatic activity of the proteasome, leading to an increase in the level of ubiquitinated proteins. In order to investigate whether the slower mobility forms of RPA2 represented ubiquitinated RPA2 under these experimental conditions, a number of approaches were used (i) analysis of RPA2 immunoprecipitated from native and denatured whole cell extracts, using western blotting with an antibody specific for ubiquitin (Fig. 3.29 and 3.30); (ii) isopeptidase treatment of RPA2 immunoprecipitated from cell extracts (Fig. 3.31); (iii) analysis of RPA2 isolated from XP30RO cells expressing HA-tagged ubiquitin (Fig. 3.332), and (iv) mass spectrometry analysis of immunoprecipitated RPA2.

(i) Immunoprecipitation of RPA2 from native cell extracts.

RPA2 was isolated, using immunoprecipitation, from extracts from cells that were either mock-treated or treated using the 'Cis+MG removed' protocol. Bound proteins were eluted and analysed by SDS-PAGE and western blotting. The membrane was probed with an anti-ubiquitin antibody. The same membrane was then stripped and re-probed using anti-RPA2 antibody (Fig. 3.29).

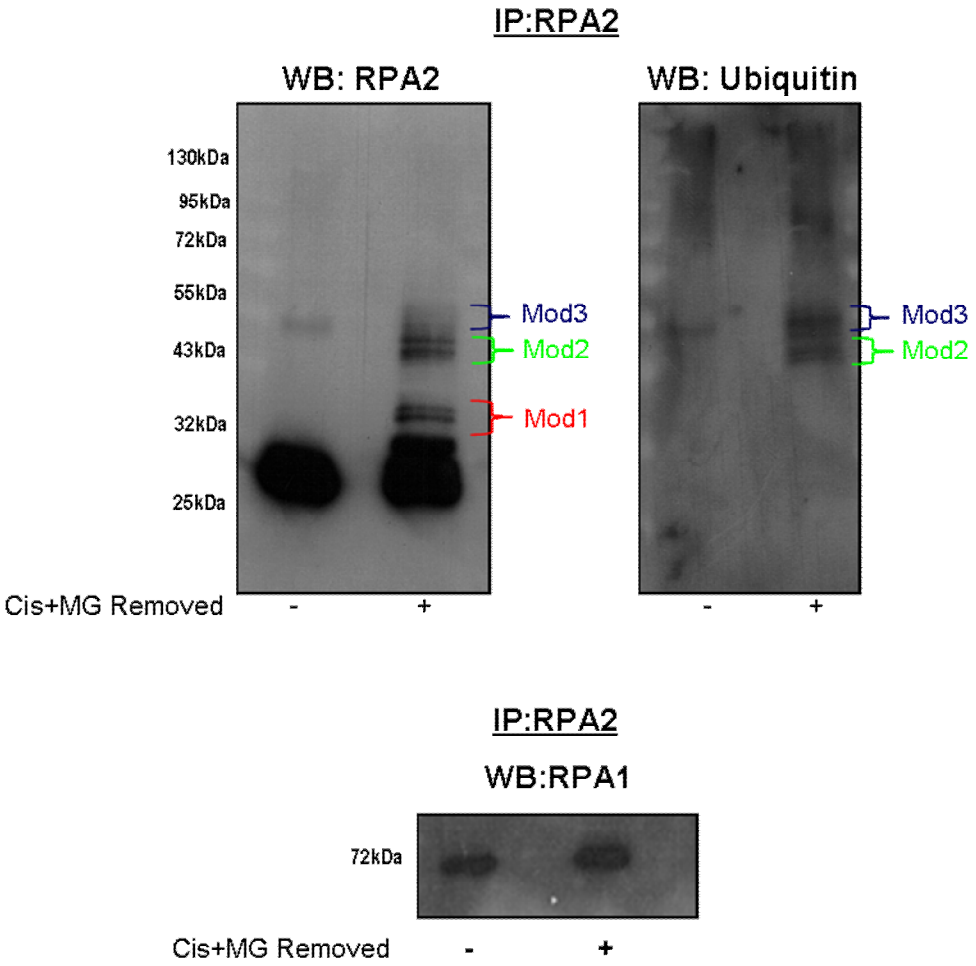

Figure 3.29: Immunoprecipitation of RPA2 from native cell extracts. RPA2 was immunoprecipitated from extracts from XP30RO cells either mock-treated or treated using the 'Cis+MG Removed' protocol. Eluted proteins were separated by SDS-, and analysed using western blotting and anti-RPA2, anti-ubiquitin and anti-RPA1 antibodies.

Immunoprecipitation of RPA2 from extracts of cells cellular extracts exposed to the treatment 'Cis+MG Removed' followed by western blotting showed that the novel forms of RPA2 were present in the immunoprecipitate, supporting the conclusion that these represent novel modified forms of RPA2 (Fig.3.29, left panel) Western blotting analysis of RPA2, isolated by immunoprecipitation, from native extracts, using a specific anti-ubiquitin antibody detected a series of bands. These bands detected using the anti-ubiquitin antibody migrated with the same mobility on SDS-PAGE as the modified forms 2 and 3 (Mod 2, Mod 3) of RPA2

detected using the anti-RPA2 antibody (Fig. 3.29, right panel), as determined by overlaying the films. The ubiquitin signal was only detected in the extracts of treated cells and is not in extracts of mock-treated cells. The band detected in the mock-treated extract, due to its mobility on the gel, is likely to be residual heavy chain of the antibody used in the immunoprecipitation which was eluted along with the bound proteins (Fig. 3.29).

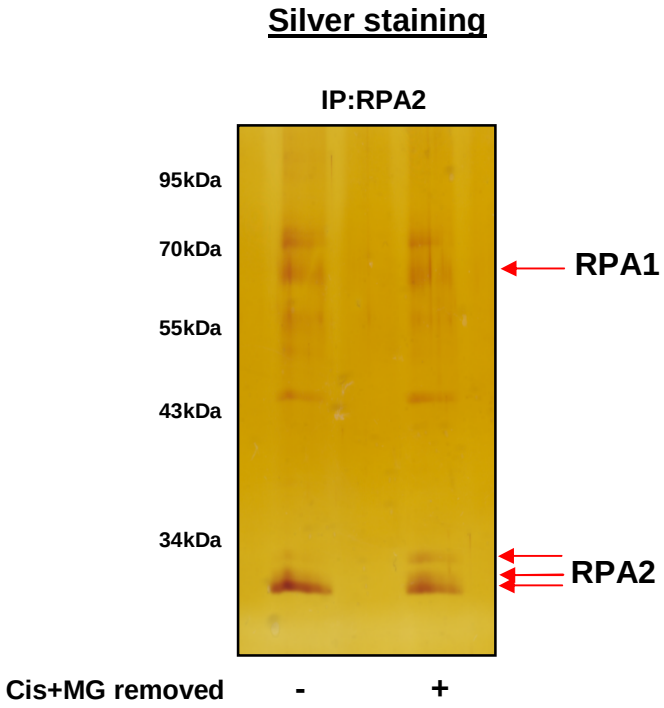

Figure 3.30: Immunoprecipitation of RPA2 from cellular extracts from cells that were either mock-treated or treated with treatment 'Cis+MG removed'. Bead-bound proteins were eluted and analysed by silver staining.

Isolated RPA2 was also analysed by silver staining (Fig. 3.30). Additional bands that correspond to the positions of phosphorylated forms of RPA2 (Fig. 3.30; indicated by arrows) was also detected. RPA1 (70kDa) was also readily detected by silver staining following the immunoprecipitation of RPA2 from these extracts (Fig. 3.30). This indicates that under these conditions, where modified RPA2 is detected, RPA2 is still associated with RPA1. However, the newly identified modified form of RPA2 is not detected by silver staining following

SDS-PAGE (Fig. 3.30). Thus, the modified forms of RPA2 appear to represent a small proportion of the total RPA2 protein, and as silver staining is less sensitive in detecting proteins than is western blotting using specific antibodies (Fig. 3.27), the novel modified forms could not be detected by silver staining.

(ii) Immunoprecipitation of RPA2 from denatured cell extracts.

RPA2 was also immunoprecipitated from extracts as outlined above; however at the time of harvesting extracts from cells were denatured as in described in Section 2.10. Denaturation of cellular extracts should destroy protein complex interactions prior to immunoprecipitation. Therefore, any resulting slow-mobility band detected using the anti-RPA2 antibody, or using an antibody specific for a particular modification, in subsequent analysis by western blotting should represent covalent modification of immunoprecipitated RPA2, rather than co-immunoprecipitation of RPA2 with an interacting protein. As a control for the efficiency of protein denaturation in destroying protein complexes, RPA1 was analysed following immunoprecipitation of RPA2 from denatured lysates. Given that the RPA trimer is extremely stable and that RPA1 binds very tightly to RPA2 under normal conditions, elimination of RPA1 protein from proteins immunoprecipitated using the anti-RPA2 antibody provides strong evidence that protein-protein interactions have been eliminated.

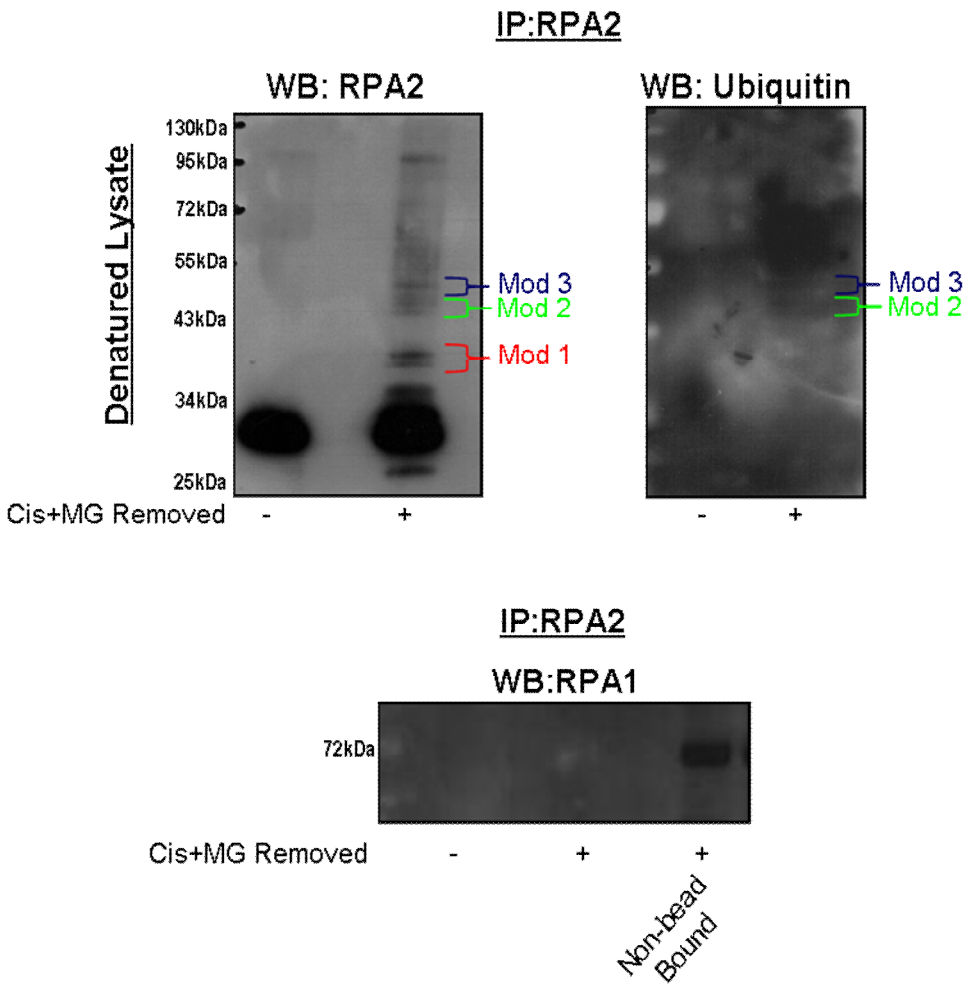

Figure 3.31: Immunoprecipitation of RPA2 from denatured cell extracts. RPA2 was immunoprecipitated from denatured lysates from XP30RO cells either mock treated or treated with the 'Cis+MG Removed' protocol. Eluted proteins were separated by SDS-PAGE and analysed using western blotting and anti-RPA2, anti- ubiquitin and anti-RPA1 antibodies.

The absence of a RPA1 signal in the immunoprecipitate from denatured lysate demonstrates that RPA2 is no longer in a complex in the RPA trimer. It is therefore unlikely that RPA2 is in a complex with any other proteins which could result in the modified signal (Fig. 3.31). Analysis of the immunoprecipitate from denatured lysates using the anti-ubiquitin antibody also detected bands of the same mobility as those in native lysates (Fig. 3.29). These bands corresponded to the modified forms 2 and 3 of RPA2 (Mod 2, Mod 3), by overlaying the films

(Fig. 3.31). As these forms were detected following immunoprecipitation of RPA2 from denatured lysates, this is consistent with the slow mobility bands detected using the RPA2 antibody representing a covalent modification on RPA2 and resulting from the addition of ubiquitin to the RPA2 protein. However, no ubiquitin signal was detected at the same mobility as the slower mobility form 1 (Mod 1) (Fig. 3.31) of RPA2. Reasons for this may be that according to its size this form of RPA2 is modified by only one ubiquitin, which may make this form less readily detectable by the anti-ubiquitin antibody. Another reason may be that this form results from the attachment of a different post-translational modification which has a similar size as ubiquitin.

(iii) Isopeptidase-T treatment.

Isopeptidase T is a member of the high molecular weight group of deubiquitinating enzymes which hydrolyse of isopeptide linkages of polyubiquitin chains. Isopeptidase T plays a role in the recycling of ubiquitin and in regulation of the activity of the 26S proteasome. In order to determine whether RPA2 is modified by ubiquitination, immunoprecipitated, modified RPA2 was treated with isopeptidase T. RPA2 was immunoprecipitated from whole cell lysates from XP30RO cells treated using the 'Cis+MG Removed' protocol. Bound protein was eluted using citric acid pH 3.1. Buffer exchange was carried, out as outlined in Section 2.25, to replace the elution buffer with the isopeptidase T reaction buffer (25 mM HEPES, 10 mM DTT pH 7.5). Protein was divided into three equal aliquots and was either incubated, or not, with isopeptidase T at 25°C for 1 or 2 hours. Protein was separated by SDS-PAGE and analysed by western blotting using anti-RPA2 antibody.

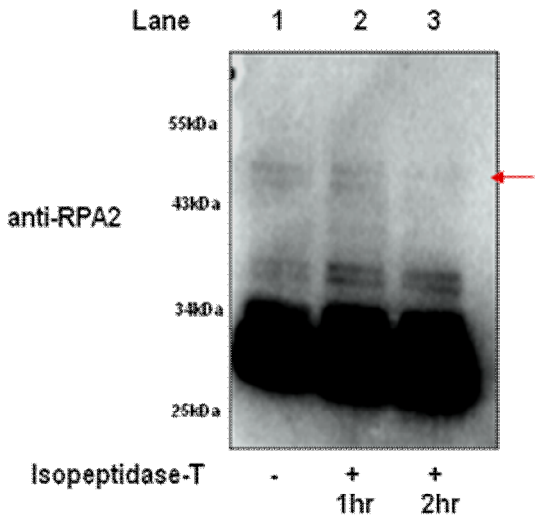

Figure 3.32: Isopeptidase T treatment. RPA2 was immunoprecipitated from extracts from XP30RO cells treated with 'Cis+MG Removed protocol' (Section 3.6). Protein was eluted and elution buffer was replaced with isopeptidase T reaction buffer. Eluted protein was incubated with isopeptidase T for 1 or 2 hours at 25°C. Eluted protein was untreated and incubated at 25 °C for 2 hours. Protein was separated by SDS-PAGE and analysed by western blotting using an anti-RPA2 antibody.

Treatment of immunoprecipitated RPA2 with isopeptidase T led to a reduction in the level of the modified forms of RPA2 detected by western blotting compared to a control which was not incubated with enzyme. However, isopeptidase-T treatment did not have an affect on modified form 1 (Fig.3.32 (mod1) which was not detected by the anti-ubiquitin antibody in Figure 3.29 and 3.31.

(iv) HA-Ubiquitin labelling

As shown in Figure 3.29 and 3.3,1 immunoprecipitation of RPA2 and subsequent western blotting analysis with a specific antibody against ubiquitin from extracts treated with the 'Cis+MG132 Removed' protocol detected bands corresponding to the slower mobility forms of RPA2. In order to further directly examine whether this represented ubiquitinated RPA2, XP30RO cells were transfected with a plasmid expressing ubiquitin tagged with hemagglutinin (HA) epitope tag.

If RPA2 is ubiquitinated under these conditions then RPA should bind HA-ubiquitin.

XP30RO cells were transiently transfected with HA-ubiquitin for 24 hours after which the transfection media was removed and cells were treated using the 'Cis+MG Removed' protocol. Cells were harvested and RPA2 was immunoprecipitated from extracts. Eluted protein was analysed by SDS-PAGE and western blotting using a specific antibody against HA and against RPA2.

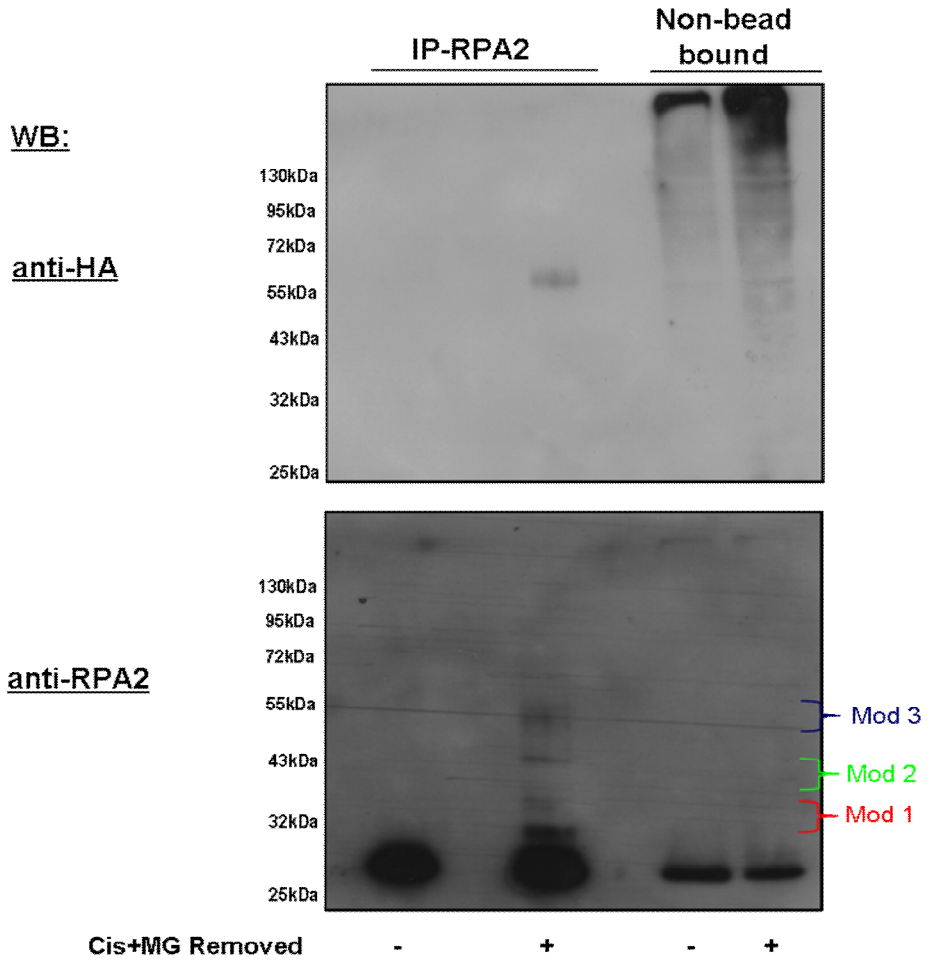

Figure 3.33: HA-ubiquitin labelling. XP30RO cells were transfected with a plasmid expressing HA-Ub for 24 hours. Transfection media was removed, and the cells were treated with the 'Cis+MG Removed' protocol. RPA2 was immunoprecipitated from cell extracts. Eluted proteins was separated by SDS-PAGE and analysed by western blotting using anti-HA and anti-RPA2 antibodies.

Following transfection of XP30RO cells with HA-Ub in XP30RO cells HA was detectable in cell extracts as seen in Fig 3.33 (upper panel). Modified RPA2 was detected in eluted protein following the immunoprecipitation of RPA2 (Fig 3.33, lower panel). A signal was detected using the anti-HA antibody in immunoprecipitate from treated cells at approximately 55kDa (Fig 3.35, upper panel) however due to the mobility of the band detected it is likely that this represents remaining IgG. No signal corresponding to the mobility of modified RPA2 was detected using anti-HA antibody. It is not known how much HA-Ub is incorporated into polyubiquitinated proteins versus endogenous ubiquitin. It may be possible the not enough HA-Ub was used in the ubiquitination of RPA2 to be detected by western blotting following immunoprecipitation.

(v) Analysis of modified RPA2 by mass spectrometry.

In order to directly investigate whether the modified form of RPA2 described in the previous sections results from ubiquitination. Mass spectrometry analysis of RPA2 isolated from cell extracts using immunoprecipitation, was carried out to (i) detect the presence of ubiquitinated RPA2 at the position of slow mobility forms on SDS-PAGE and (ii) to identify which of the 14 lysines in RPA2 was ubiquitinated. Ubiquitinated proteins, and the specific lysine of the protein that is modified by ubiquitin can be identified by mass spectrometry-based approaches (Denis *et al.*, 2007). This method relies on the identification of signature peptides from proteins containing an internal glycine/glycine (Gly/Gly) tag on the ubiquitinated lysine residue, remaining after tryptic digestion of ubiquitin within the –R-L-R-G-G- sequence. The Gly/Gly tag is a remnant derived from the presence of ubiquitin and gives the peptide a mass increase of 114.1Da following tryptic digestion (Denis *et al.*, 2007).

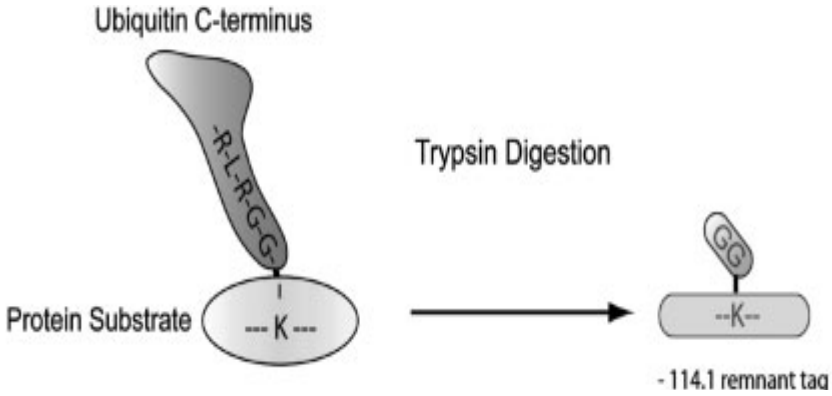

Figure: 3.34: Identification of ubiquitinated proteins by mass spectrometry. Detection of ubiquitinated proteins relies on the identification of a 114.1 Da tag on internal lysine residues, due to a -GG residue derived from ubiquitin following tryptic digestion (Taken from Denis *et al,* 2007).

Two separate approaches were used to investigate modified RPA2 by mass specrometry. In the first approach to determine whether RPA2 is ubiquitinated, modified RPA2 was isolated from whole cell lysates from XP30RO cells treated using the 'Cis+MG Removed' protocol. Modified RPA2 was isolated using the protein A/G-based immunoprecipitation method outlined in Section 2.24 of Materials and Methods. Eluted proteins were separated by SDS-PAGE and analysed using silver staining, coomassie blue staining and western blotting using an anti-RPA2 antibody. Protein bands from the coomassie blue stained gel were excised, shown in Figure 3.35A on the corresponding silver stained gel. Individual excised gel bands were sent, in 0.1% acetic acid, to the Mass Spectrometry Resource at the Conway Institute, University College Dublin. In-gel tryptic digestion and mass spectrometry analysis was performed at UCD in collaboration by Dr. G. Cagney.

(A)

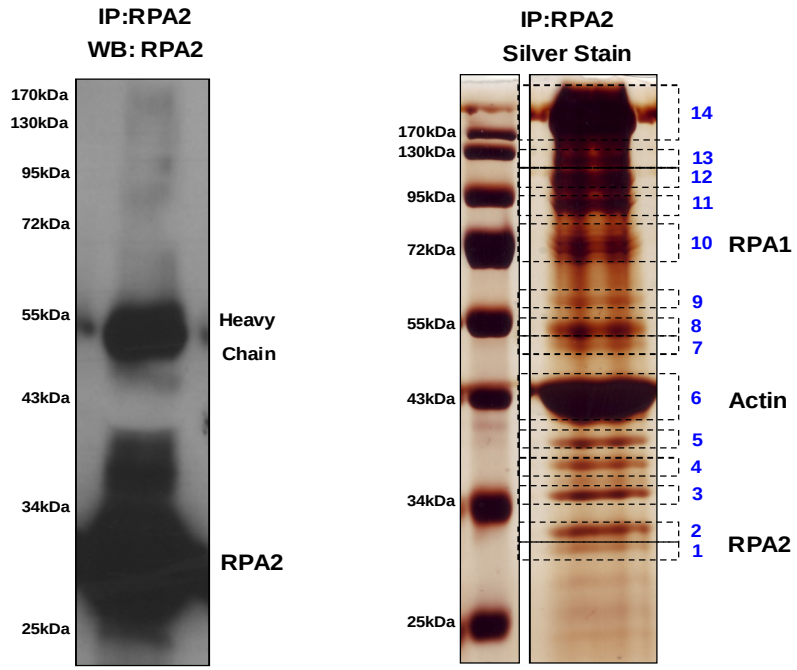

(B)

RPA2 Peptides	**PEP**
K.ACPRPEGLNFQDLK.N	1.32E-04
K.ACPRPEGLNFQDLKNQLK.H	1.14E-06
K.QAVDFLSNEGHIYSTVDDDHFK.S	7.01E-04
R.AQHIVPCTISQLLSATLVDEVFR.I	3.58E-07
R.HAEKAPTNIVYK.I	1.22E-14
R.IGNVEISQVTIVGIIR.H	9.79E-05
R.QWVDTDDTSSENTVVPPETYVK.V	1.01E-06
RPA1 Peptides	**PEP**
K.AAGPSLSHTSGGTQSK.V	6.15E-08
K.LFSLELVDESGEIR.A	1.10E-07
K.NEQAFEEVFQNANFR.S	1.23E-09
K.SENLGQGDKPDYFSSVATVVYLR.K	2.26E-04
K.SGGVGGSNTNWK.T	1.80E-05
K.VIDQQNGLYR.C	1.25E-04
K.VVTATLWGEDADKFDGSR.Q	3.54E-10
R.ATAFNEQVDKFFPLIEVNK.V	2.19E-05
R.GWFDAEGQALDGVSISDLK.S	8.90E-10
R.SLSVLSSSTIIANPDIPEAYK.L	1.52E-05
R.VKVETYNDESR.I	5.03E-08
Ubiquitin Peptides	**PEP**
K.TITLEVEPSDTIENVK.A	1.01E-06
K.ESTLHLVLR.L	3.76E-06
K.IQDKEGIPPDQQR.L	7.93E-07

(C)

1 mwnsgfesyg sssyggaggy tqspggfgsp apsqaekksr araqhivpct isqllsatlv
61 devfrignve isqvtivgii rhaekaptni vykiddmtaa pmdvrqwvdt ddtssentvv
121 ppetyvkvag hlrsfqnkks lvafkimple dmneftthil evinahmvls kansqpsagr
181apisnpgmse agnfggnsfm pangltvaqn qvlnlikacp rpeglnfqdl knqlkhmsvs
241 sikqavdfls neghiystvd ddhfkstdae

Figure 3.35: Mass spectrometry analysis of RPA2. (A) Immunoprecipitation of RPA2 from XP30RO cell extracts treated with the 'Cis+MG Removed'. Bound protein was eluted and analysed by SDS-PAGE and western blotting using anti- RPA2 antibody (left panel) and silver staining (right panel). Excised bands are indicated with boxes. (B) RPA2 and RPA1 and Ubiquitin peptides identified by mass spectrometry. (C) Highlighted in blue are the RPA2 peptides detected by mass spectrometry.

Seven distinct RPA2 peptides were identified in excised gel bands 1 and 2 as outlined in Figure 3.35. RPA2 was also identified in band 3 by the peptides 4 and 6 (Fig 3.35). The peptide R.AQHIVPCTISQLLSATLVDEVFR.I was detected in bands 4, 5, 8, 9, 10 and 11 which may represent a modified form of RPA2 due to the slower mobility of bands excised. Ubiquitin was detected in bands 1, 4, 5 and 9. However, no ubiquitinated RPA2 peptides were identified by mass spectrometry. Coverage of the RPA2 protein was low, with peptides corresponding to only 48% of the protein being detected. The modified forms of RPA2 appear to represent a small proportion of the total RPA2 protein in cells and may not be readily detectable by mass spectrometry. The amount of RPA2 isolated may not be enough to allow detection of the modified forms by mass spectrometry.

One problem with the above approach was the presence of the heavy chain of the IgG used in immunoprecipitation on the gel (Fig. 3.35). In a second approach to identify ubiquitinated RPA2 by mass spectrometry, RPA2 was immunoprecipitated from whole cell extracts from XP30RO cells treated using the 'Cis+MG Removed' protocol, using the (Invitrogen) (outlined in Section 2.24). Use of the Dynabead® system prevented the heavy chain of the antibody,

used during immunoprecipitation, from being eluted with proteins bound to beads. Seven individual immunoprecipitations were carried out, using 400 µg of total protein in each immunoprecipitation. Immunoprecipitation of RPA2 from 400 µg of whole cell lysate yields approximately 100ng of RPA2 protein, as shown in Section 3.7.3. Eluted protein, derived from all seven immunoprecipitations was pooled and concentrated using a 5kDa cut-off spin column. The immunoprecipitation buffer (0.1M citric acid pH 3.1) was exchanged for lysis buffer, until the pH was increased to approximately pH 7 (Section 2.25), yielding a final volume of 40µl predicted to contain approximately 700ng of RPA2 protein. 3 µl of the final concentrated protein, corresponding to approximately 50ng of protein, was analysed by SDS-PAGE and by western blotting, and using anti-RPA2 antibody (Fig 3.36A). The remaining eluted protein was sent on dry ice, to the College of Life Sciences, University of Dundee (to the laboratory of Prof. Ron Hay) where proteins were separated by SDS-PAGE and analysed using coomassie staining (Fig. 3.36A). Two areas of the gel (indicated in Fig 3.36, red boxes) were excised, and in-gel tryptic digestion was performed. Peptides were analysed using an Orbitrap MS. Data were processed by MaxQuant with the integral Andromeda search protocol.

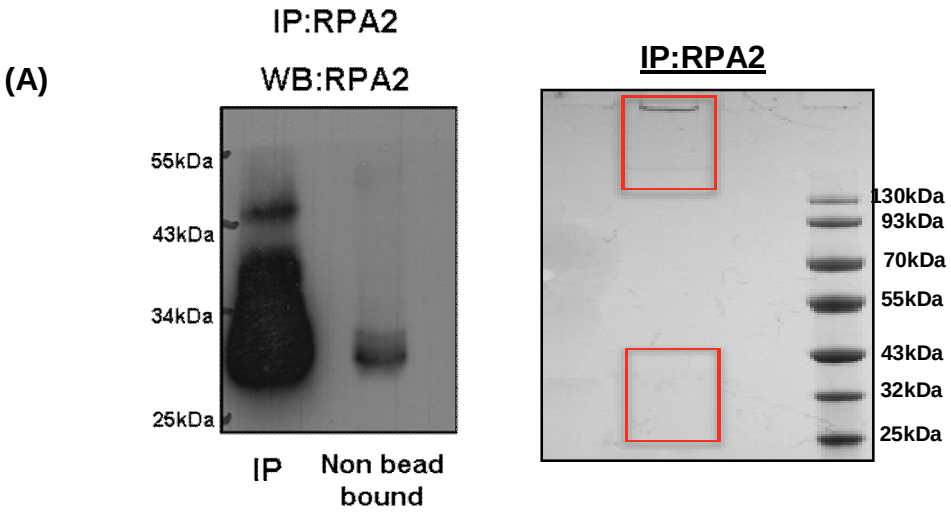

RPA2 Peptides	**PEP**
APTNIVYK	3.63E-03
APTNIVYKIDDMTAAPMDVR	2.67E-05
AQHIVPCTISQLLSATLVDEVFR	5.98E-06
HAEKAPTNIVYK	1.82E-02
HAEKAPTNIVYKIDDMTAAPMDVR	1.36E-01
IDDMTAAPMDVR	3.67E-05
IGNVEISQVTIVGIIR	1.09E-31
IMPLEDMNEFTTHILEVINAHMVLSK	1.30E-01
ACPRPEGLNFQDLK	1.93E-03
ACPRPEGLNFQDLKNQLK	3.03E-09
APISNPGMSEAGNFGGNSFMPANGLTVAQNQVLNLIK	3.96E-24
HMSVSSIK	3.17E-02
QAVDFLSNEGHIYSTVDDDHFK	5.45E-02
QAVDFLSNEGHIYSTVDDDHFKSTDAE	4.42E-06
RPA1 Peptides	**PEP**
AAGPSLSHTSGGTQSK	8.22E-04
DKNEQAFEEVFQNANFR	3.07E-02
DSLVDIIGICK	3.92E-05
GWFDAEGQALDGVSISDLK	1.90E-14
LFSLELVDESGEIR	1.57E-04
VIDQQNGLYR	8.71E-13
VKVETYNDESR	4.59E-03
VVTATLWGEDADKFDGSR	3.89E-02
LVMSIR	1.18E-01
RLVMSIR	6.92E-02
Ubiquitin Peptides	**PEP**
ESTLHLVLR	1.25E-04
AKIQDKEGIPPDQQR	8.32E-02
IQDKEGIPPDQQR	7.79E-04
TITLEVEPSDTIENVK	3.93E-22
TLSDYNIQK	1.32E-06

(C)

1 mwnsgfesyg sssyggaggy tqspggfgsp apsqaekksr araqhivpct isqllsatlv

61 devfrignve isqvtivgii rhaekaptni vykiddmtaa pmdvrq wvdt ddtssentvv

121 ppetyvkvag hlrsfqnkks lvafkimple dmneftthil evinahmvls kansqpsagr

181apisnpgmse agnfggnsfm pangltvaqn qvlnlikacp rpeglnfqdl knqlkhmsvs

241 sikqavdfls neghiystvd ddhfkstdae

Figure 3.36: Mass spectrometry analysis of RPA2. (A) Immunoprecipitation of RPA2 from XP30RO cell extracts treated with the 'Cis+MG Removed'. Bound protein was eluted and analysed by SDS-PAGE and western blotting using anti-RPA2 antibody (right panel) and coomassie staining (left panel). Excised bands are indicated with red boxes. (B) RPA2, RPA1 and ubiquitin peptides identified by mass spectrometry. (C) Highlighted in blue are the RPA2 peptides detected by mass spectrometry.

Seven RPA2 peptides were identified by mass spectrometry giving 51% coverage of the RPA2 protein. Ubiquitin was also detected however, no RPA2 peptides with the signature Gly/Gly were detected. RPA1 was also identified by 10 peptides which were primarily derived from the upper area that was excised from the gel. This may represent some protein which remained in the well following electrophoresis.

In both approaches RPA2 and ubiquitin were identified (Fig 3.35 and 3.26). However coverage of the RPA2 protein was low with 33% of the RPA2 protein not being detected (outlined below Fig 3.37) as determined by comparing RPA2 peptides identified in both experimental approaches. The undetected 33% of the RPA2 protein contains six lysines out of the total 14 lysines in the RPA2 amino acid sequence. In both cases the N-terminal of RPA2 which is phosphorylated was also not detected.

The isolation of increased amounts of modified RPA2 may improve the coverage of the protein detected by mass spectrometry and may also increase the possibility of detecting ubiquitinated RPA2 and the lysine at which the protein is ubiquitinated. The enzyme used to cleave proteins prior to mass spectrometry analysis in theses experiments was trypsin, the use of different enzymes which cleave proteins at different sites could also result in increased coverage of the RPA2 protein. Alternative enzymes used in mass spectrometry include chymotrypsin, LysC, GluC and AspN. Use of different enzymes can also increase the possibility of detecting ubiquitinated RPA2 e.g. the enzyme GluC digests proteins and generates a significantly longer signature peptide (STLHLVLRLRGG) at the site of ubiquitination compared to the signature

peptide generated by trypsin as outlined earlier in this section (Kirkpatrick *et al.*, 2005; Warren *et al.*, 2005).

1 mwnsgfesyg sssyggaggy tqspggfgsp apsqaekksr araqhivpct isqllsatlv
61 devfrignve isqvtivgii rhaekaptni vykiddmtaa pmdvrqwvdt ddtssentvv
121 ppetyvkvag hlrsfqnkks lvafkimple dmneftthil evinahmvls kansqpsagr
181apisnpgmse agnfggnsfm pangltvaqn qvlnlikacp rpeglnfqdl knqlkhmsvs
241 sikqavdfls neghiystvd ddhfkstdae

Figure 3.37: Amino acid sequence of RPA2. Amino acids highlighted in blue represent the portion of the RPA2 protein detected by mass spectrometry. The portion of the protein which was not detected is in black. Lysines not detected are highlighted in red.

Summary.

Evidence that RPA2 is modified in a cisplatin and MG132-dependent manner by ubiquitin, has been provided. The main evidence (i) is the identification of slow mobility forms of RPA2 by SDS-PAGE and western blotting, having relative molecular size consistent with ubiquitin modification; (ii) recovery of modified forms of RPA2 following immunoprecipitation of RPA2 from nature and denatured cell extracts (iii) western blotting of modified RPA2 using anti-ubiquitin, following immunoprecipitation from nature and denatured lysates (iv) binding of RPA containing modified RPA2 to Affi-Gel Blue. However, expression of HA-Ubiquitin did not result in labelling of RPA2 with HA. Mass spectrometry analysis of immunoprecipitated RPA2 did not detect ubiquitinated peptides of RPA2. Nonetheless, this provides the first evidence that RPA2 is modified by ubiquitin in response to DNA damage by cisplatin and proteasome inhibition, identifying a potential new avenue for regulation of RPA function.

Chapter 4
Results

4.1 Effect of pol η expression on cisplatin-induced monoubiquitination of FANCD2.

As outlined in Section 1.7.2, Fanconi anemia (FA) proteins play a key role in repair of ICLs in human cells (Moldovan *et al.,* 2009b; Moldovan *et al.,* 2009a). FA is a rare autosomal rescessive disorder, characteristed by bone marrow failure, developmental abnormalities and increased risk of cancer (Moldovan *et al.,* 2009b). Cells from FA patients have mutations in FA pathway genes. The absence of functional FA proteins leads to hypersensitivity to DNA crosslinking agents such as mitomycin C (MMC) and cisplatin and the formation of chromosome breaks and radial chromosomes (Poll *et al.,* 1985; German *et al.,* 1987; Ho *et al.,* 2006). Fourteen complementation groups of FA have been described to date: FANCA, -B, -C, -D1, -D2, -E, -F,-G, -I, -J, -L, -M, -N, -P as well as one FA-like complementation group (FA-O) (reviewed in Kee *et al.,* 2010; (Bagby 2003; Taniguchi *et al.,* 2006; Moldovan *et al.,* 2009b; Kee *et al.,* 2010; Somyajit *et al.,* 2010; Cybulski *et al.,* 2011) (Section 1.7.2).

FANCD2 is one of the key proteins in the FA pathway. FANCD2 is monoubiquitinated by the FA core complex on lysine 561 during the normal cell cycle and in response to DNA damaging agents (Nakanishi *et al.,* 2002; Taniguchi *et al.,* 2002; Hussain *et al.,* 2004; Wang *et al.,* 2004a; Kim *et al.,* 2008). Monoubiquitinated FANCD2 is recruited to nuclear foci, where it is required for the repair of ICLs. Monoubiquitination of FANCD2 is an essential step in the FA pathway (Knipscheer *et al.,* 2009; Moldovan *et al.,* 2009a).

While many cisplatin–induced DNA damage responses, including phosphorylation of RPA2, Chk1 and H2AX are enhanced in cells lacking DNA polymerase η compared to cells expressing pol η (Cruet-Hennequart *et al.,* 2008; Cruet-Hennequart *et al.,* 2009) the dependence of cisplatin-induced FANCD2 monoubiquitination on pol η expression has not been investigated. To determine whether pol η expression affected the level of FANCD2 ubiquitination in cisplatin treated cells, pol η-deficient cells (XP30RO) and pol η-proficient (normal and TR30-2) cells were treated with cisplatin. Monoubiquitination of

FANCD2 converts the protein into a form termed FANCD2-L, which can be detected on the basis of slower mobility on SDS-PAGE gel (Garcia-Higuera *et al.*, 2001). Normal, XP30RO and TR30-2 cells were treated with up to 5µg/ml cisplatin for 18 hours or for 40 hours. Whole cell lysates were analysed using SDS-PAGE and western blotting using an antibody specific for FANCD2. The extent of conversion of non-ubiquitinated FANCD2 (FANCD2-S) to the monoubiquitinated form (FANCD2-L) was determined by western blotting using a Fujifilm LAS-3000 imager, and Imagegauge V4.21 software.

(A)

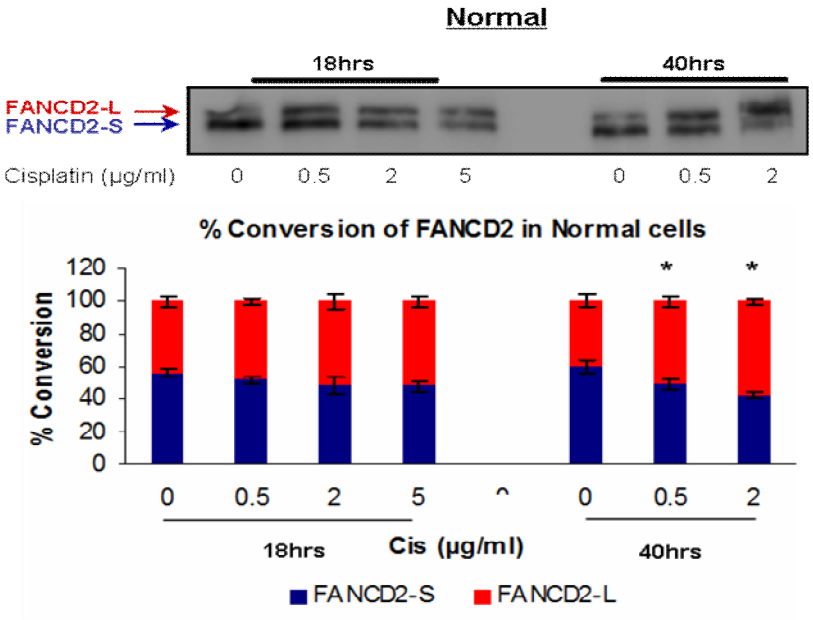

(B)

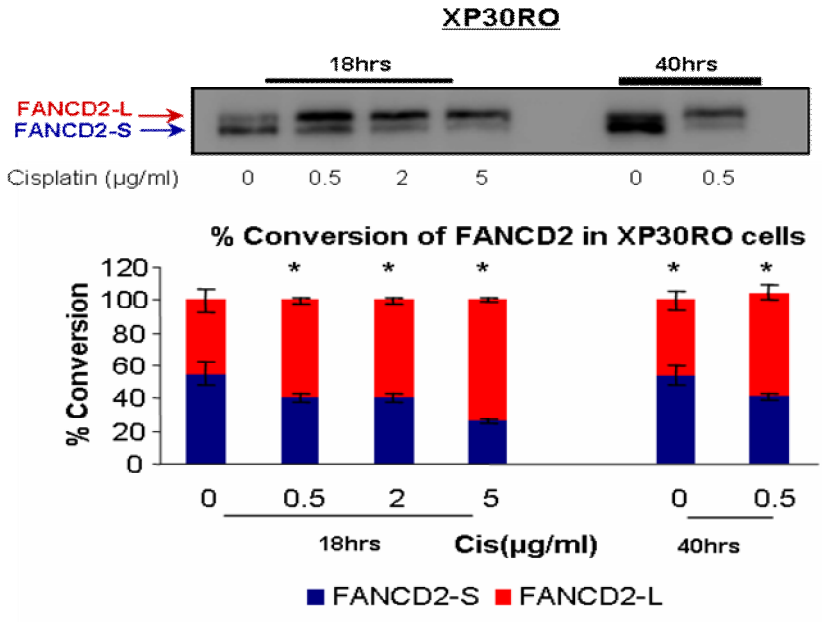

(C)

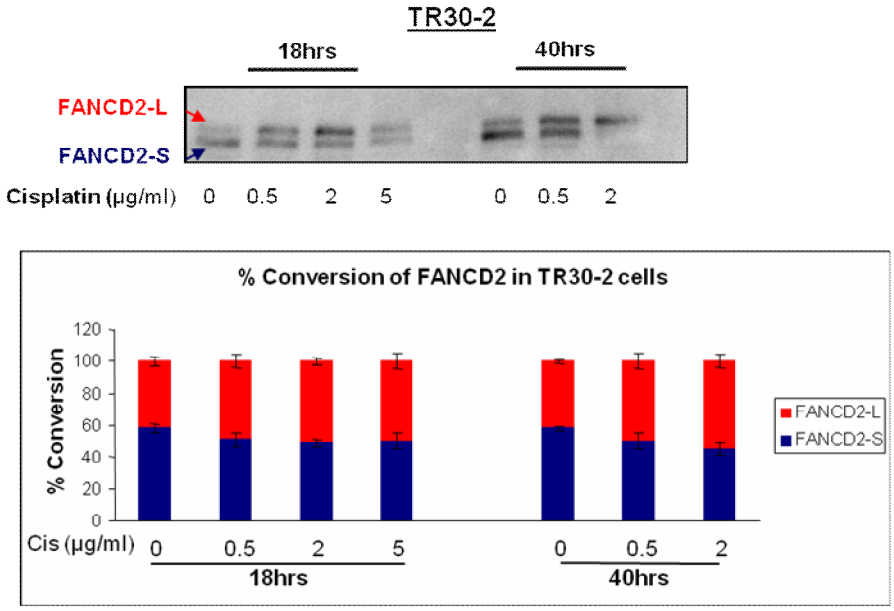

Figure 4.1: Cisplatin induced monoubiquitination of FANCD2. Normal, GM00637, (A) and XP30RO (B) and TR30-2 (C) cells were treated with 0, 0.5, 2 and 5µg/ml cisplatin for 18 hours or for 40 hours. Whole cell lysates were prepared, separated on a 7% SDS-PAGE gel and analysed by western blotting using an anti-FANCD2 antibody. The percentage conversion of FANCD2 (FANCD2-S) to monoubiquitinated form (FANCD2-L) was measured using a Fujifilm LAS-3000 imager, and Imagegauge V4.21 software. Data is derived from the average of three independent experiments. Error bars represent one standard deviation. Statistical differences between the extent of FANCD2 monoubiquitination in Normal and XP30RO cells were determined using Anova, where $p<0.05$ and represented by *.

Monoubiquitinated FANCD2 detected in untreated extracts from all cell lines represents constitutively ubiquitinated FANCD2. The proportion of FANCD2 protein in the monoubiquitinated form was greater in pol η-deficient, XP30RO cells following exposure to cisplatin compared to normal cells (Fig. 4.1). Following treatment of XP30RO cells with 5µg/ml cisplatin for 18 hour, approximately 70% of FANCD2 was in the monoubiqtuinated form compared to approximately 50% in normal cells, as determined using Imagegauge software (V4.21) (Fig. 4.1). Exposure of cells to 0.5µg/ml cisplatin, for 40 hours, resulted in a higher proportion of monoubiquitinated FANCD2 in pol η-deficient cells,

with 70% conversion in XP30RO cells compared to 50% in normal cells (Fig. 4.1). Treatment of XP30RO cells with 2μg/ml cisplatin for 40 hours was very toxic to the cells; therefore the protein concentration was too low to be analysed by western blotting.

To directly investigate the dependence of FANCD2 monoubiquitination on pol η expression, FANCD2 monoubiquitination was studied in an XP30RO-derived cell line (TR30-2) which stably expresses pol η from a *POLH* transgene. TR30-2 cells were treated with 0–5μg/ml cisplatin for 18 hours or 40 hours, Whole cell lysates were prepared, separated on a 7% SDS-PAGE gel and analysed by western blotting using an-anti FANCD2 antibody (Fig 4.1C).

The level of FANCD2 monoubiquitination did not change significantly following the treatment of TR30-2 cells with up to 5μg/ml cisplatin for 18 hours (Fig. 4.1C). There was a small increase of approximately 10% when cells were treated with 2μg/ml cisplatin for 40 hours compared to mock-treated cells (Fig 4.1C). Cisplatin induced monoubiquitination of FANCD2 was lower in TR30-2 cells compared to XP30RO cells, consistent with a role for replication arrest in FANCD2 monoubiquitination.

To further characterise the pol η-dependence of FANCD2 monoubiquitination, the timing of cisplatin-induced FANCD2-L formation was examined in XP30RO, normal and TR30-2 cells exposed to 0.5μg/ml cisplatin for up to 36 hours. Extracts were analysed using SDS-PAGE and western blotting using anti-FANCD2 antibody (Fig. 4.2).

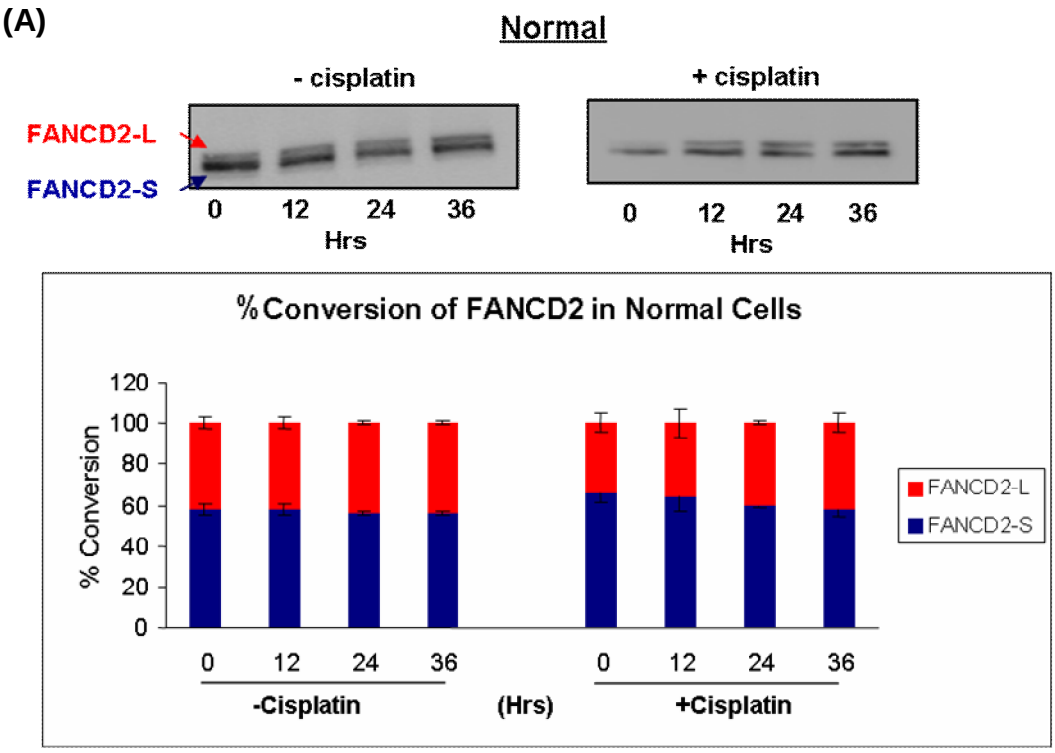
(A)
Normal
- cisplatin
+ cisplatin
FANCD2-L
FANCD2-S
0 12 24 36
Hrs
0 12 24 36
Hrs
% Conversion of FANCD2 in Normal Cells
% Conversion
120
100
80
60
40
20
0
0 12 24 36
-Cisplatin
(Hrs)
0 12 24 36
+Cisplatin
FANCD2-L
FANCD2-S

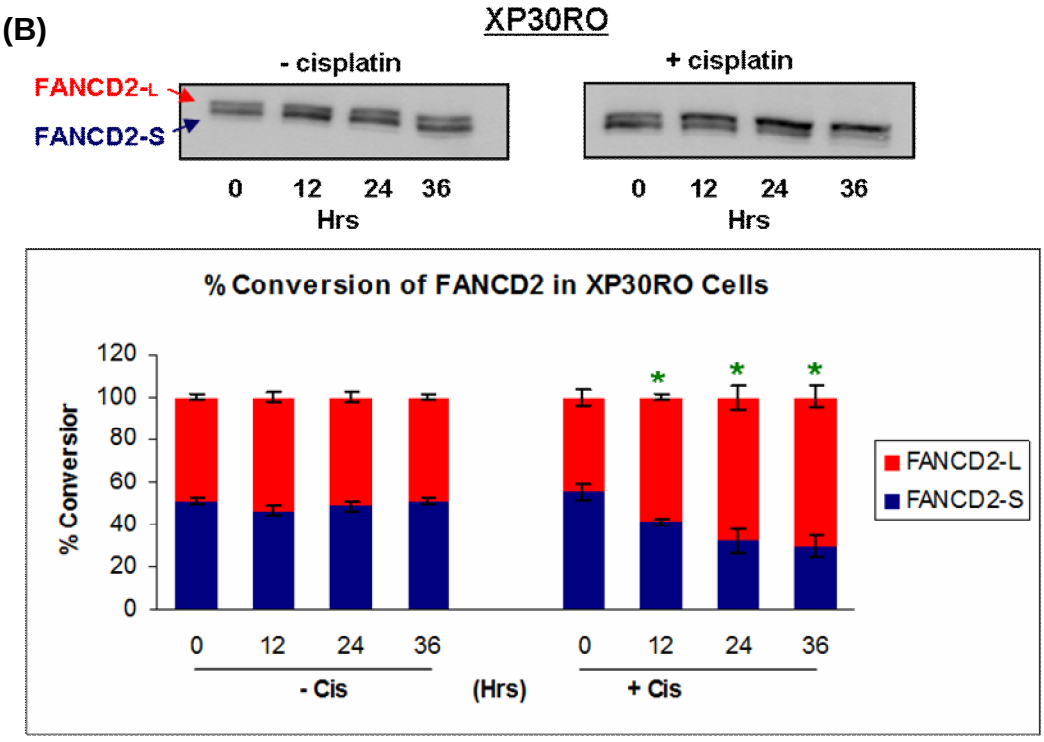
(B)
XP30RO
- cisplatin
+ cisplatin
FANCD2-L
FANCD2-S
0 12 24 36
Hrs
0 12 24 36
Hrs
% Conversion of FANCD2 in XP30RO Cells
% Conversior
120
100
80
60
40
20
0
*
*
*
0 12 24 36
- Cis
(Hrs)
0 12 24 36
+ Cis
FANCD2-L
FANCD2-S

(C)

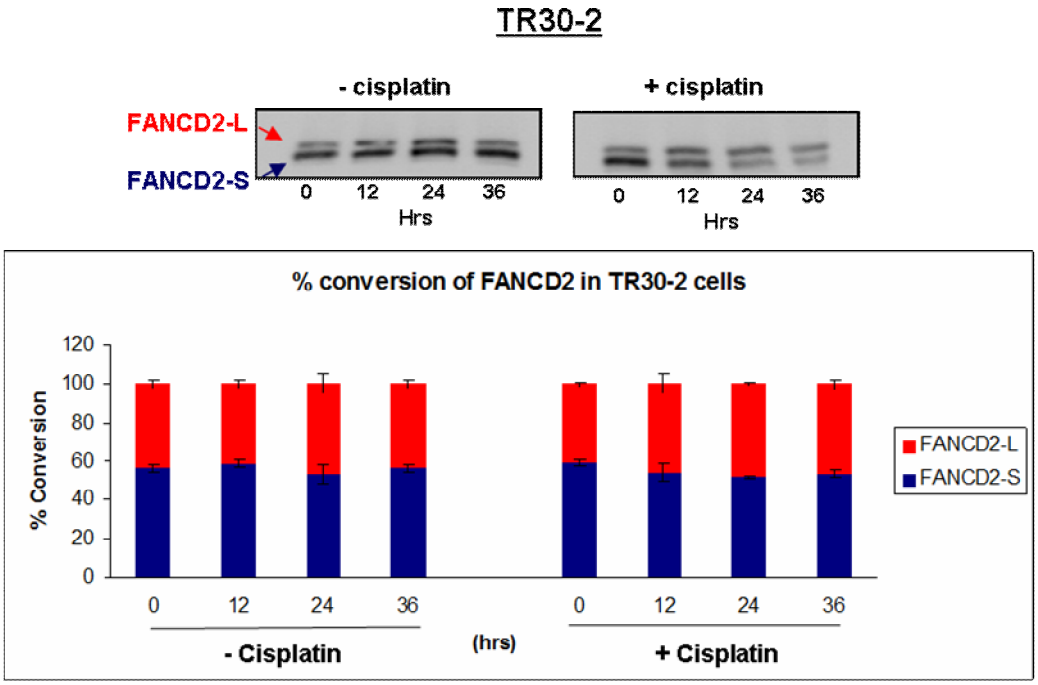

Figure 4.2: Time course of FANCD2 monoubiquitination. (A) Normal (GM00637), (B) XP30RO and (C) TR30-2 cells were either mock-treated or treated with 0.5µg/ml cisplatin. Extracts were prepared at the indicated times, separated by SDS-PAGE and analysed using western blotting using an anti-FANCD2 antibody. The percentage conversion of FANCD2-S to its monoubiquitinated FANCD2-L was measured using a Fujifilm LAS-3000 imager and Imagegauge V4.21 software. Data is derived from the average of three individual experiments. Error bars represent one standard deviation. Statistical differences in FANCD2 monoubiquitination between Normal and XP30RO cells treated with cisplatin were determined using Anova, where $p<0.05$ and represented by *.

In all cell lines the proportion, of FANCD2 that is monoubiquitinated did not change significantly in mock-treated cells over time (Fig 4.2). The proportion of FANCD2-L protein increased in response to cisplatin. There was more monoubiquitinated FANCD2-L in pol η-deficient cells, with approximately 70% of the FANCD2 protein is in this form after 24 hours, compared to 30% in normal cells and 40% in TR30-2 cells, as determined using Imagegauge software (V4.21) (Fig.4.2).

4.2 Cisplatin induced FANCD2 foci in pol η- deficient and –proficient cells

Following DNA damage, FANCD2 is monoubiquitinated and can be localised to nuclear foci where it interacts with proteins involved in DNA repair, including RPA. As shown in Figure 4.1 and 4.2, cisplatin-induced FANCD2 monoubiquitination is increased in polη-deficient cells compared to normal cells. In order to investigate the polη-dependence of the formation of cisplatin-induced FANCD2 foci, FANCD2 was analysed by immunofluorescence in normal, XP30RO and TR30-2 cell lines. Cell scored as positive for FANCD2 foci either contained more than ten foci, or were uniformly stained throughout the nucleus.

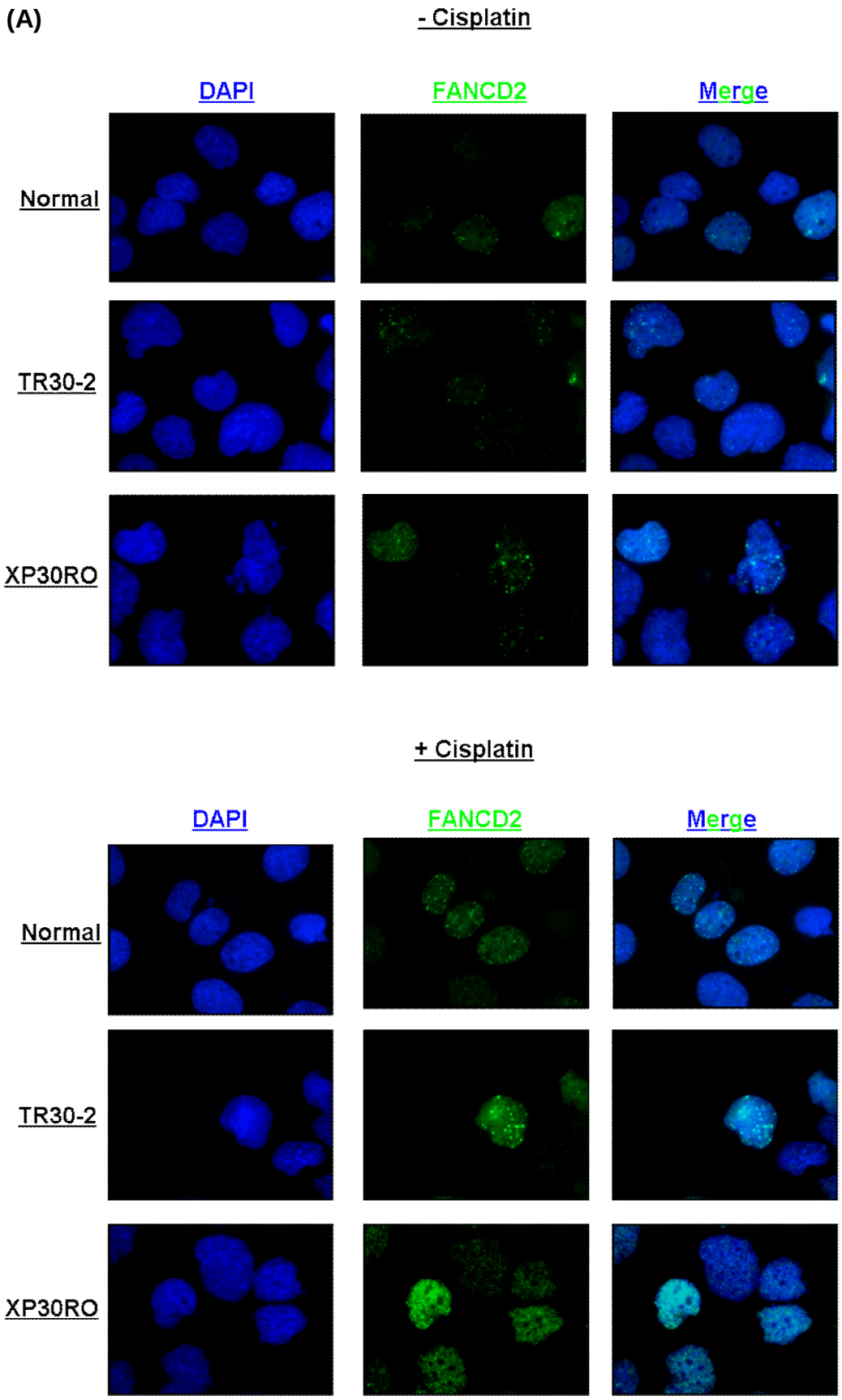
(A)
- Cisplatin
DAPI
FANCD2
Merge
Normal
TR30-2
XP30RO
+ Cisplatin
DAPI
FANCD2
Merge
Normal
TR30-2
XP30RO

(B)

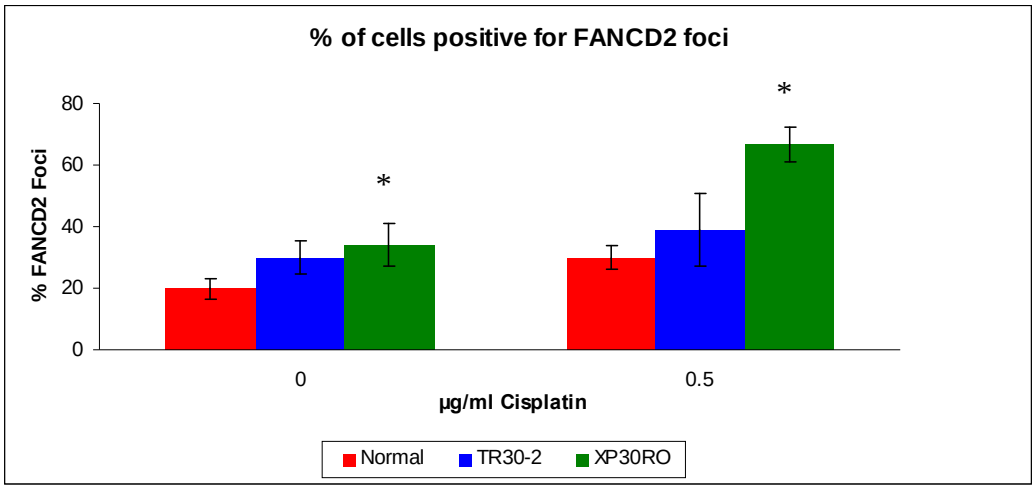

Figure 4.3: Cisplatin-induced FANCD2 foci. (A) Normal, XP30RO and TR30-2 cell lines were grown on glass cover-slips and either mock-treated or treated with 0.5µg/ml cisplatin for 24 hours. Cells were fixed and visualised as described in Section 2.18 (B) The number of cells staining positive for FANCD2 foci were counted and expressed as a percentage of the total number of cells counted. Approximately 200 cells were counted for each condition. Error bars represent one standard deviation. Statistical differences in the number of cells staining positive for FANCD2 between Normal and XP30RO cell lines that were either mock treated or treated with cisplatin were determined using Anova, where $p<0.05$ and represented by *.

Following treatment of cells with cisplatin, FANCD2 was localised into nuclear foci in all cells lines (Fig 4.3). The percentage of cells staining positive for FANCD2 was greater in DNA pol η-deficient cells compared to normal and TR30-2 cells which express pol η (Fig 4.3). There was an approximately two-fold increase in the percentage of cells positive for FANCD2 in XP30RO cells compared to normal cells (Fig 4.3B). However, it should also be noted that even in the absence of cisplatin treatment, the percentage of cells with FANCD2 foci is higher in XP30RO than normal or TR30-2 cells. The increase in the percentage of cells positive for FANCD2 foci in XP30RO is consistent with increased FANCD2 monoubiquitination seen by western blotting in Section 4.1.

4.3 DNA damage response protein phosphorylation in FANCD2-deficient human cells.

DNA polymerase η and FANCD2 are both involved in the processing of DNA damage induced by DNA interstrand crosslinking agents. As described in previous sections FANCD2 monoubiquitination was increased in pol η-deficient cells. However, the effect of FANCD2 deficiency on DDR protein phosphorylation has not been previously examined. Previously published data has demonstrated that cells lacking DNA polymerase η display increased phosphorylation of proteins involved in the DNA damage response including Chk1-pS317 and RPA-pS4S8 .

Cisplatin-induced phosphorylation of RPA2 on Ser4/Ser8 and Chk1 on Ser317 was analysed in cells lacking FANCD2. The PD20i cell line lacks FANCD2 due to a point mutation at amino acid 376 (Timmers *et al.,* 2001). PD20:RV cells are PD20i cells in which FANCD2 is re-expressed (Timmers *et al.,* 2001). PD20i and PD20:RV cells were treated with increasing doses of cisplain or MMC for 24 hours. Extracts were analysed by western blotting, using phosphospecific antibodies against RPA2 phosphorylated on Ser4/Ser8, and Chk1 phosphorylated on Ser317 (Fig. 4.4).

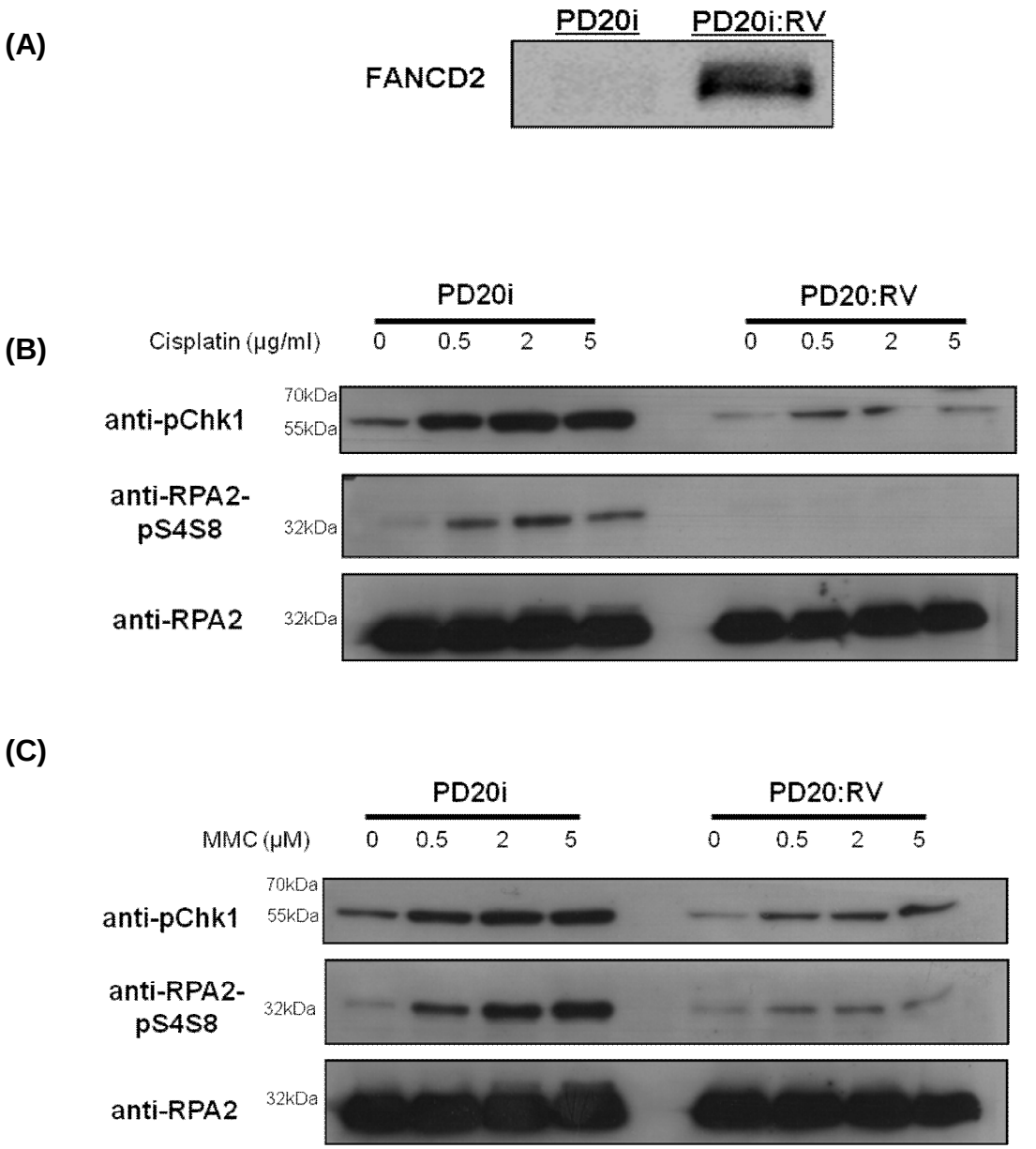

Figure 4.4: Cisplatin and MMC-induced DDR protein phosphorylation in PD20i and PD20:RV cells. (A) Extracts from PD20i and PD20:RV cells were analysed by SDS-PAGE and western blotting using an anti-FANCD2 antibody. (B) PD20i and PD20:RV cells were treated with 0-5 µg/ml cisplatin or (C) 0-5µM MMC for 24 hours. Extracts were separated by SDS-PAGE, and analysed by western blotting using phospho-specific antibodies against RPA2 phosphorylated on Ser4/Ser8 and anti-RPA2 antibody.

Western blotting analysis of extracts from PD20i and PD20:RV cells using an anti-FANCD2 antibody confirmed the absence of FANCD2 in PD20i and the expression of FANCD2 in PD20:RV cells (Fig. 4.4A). Chk1 phosphorylated on Ser317 (pChk1) was readily detectable in both PD20i and PD20:RV cell lines following cisplatin and MMC treatment (Fig. 4.4A and B) However, levels of pChk1 were higher in cells lacking FANCD2 compared to cells expressing FANCD2 at the concentrations tested.

Cisplatin-induced RPA2 phosphorylated on Ser4/Ser8 was readily detectable in cells lacking FANCD2 (Fig 4.4). RPA2 phosphorylated on Ser4/Ser8 was not detected in PD20:RV cells treated with the concentrations of cisplatin used in this experiment (Fig 4.4B). However, an extremely weak signal for RPA2 phosphorylated on Ser4/Ser8 could be detected following a longer exposure (data not shown). RPA2 phosphorylation was also detected following treatment of PD20i and PD20: RV cells with MMC (Fig 4.4C). Again, the level of MMC-induced RPA2 phosphorylation on Ser4/Ser8 was increased in cells lacking FANCD2, compared to PD20:RV cells (Fig 4.4C). This demonstrates that the DDR is more highly activated in cells lacking FANCD2 in response to cisplatin and MMC, compared to cells expressing FANCD2. This is consistent with the requirement for FANCD2 in the repair of cisplatin and MMC induced ICLs.

Summary.

FANCD2 was monoubiquitinated in a time- and dose-dependent manner following cisplatin treatment. Monoubiquitination of FANCD2 was detected on the basis of slower mobility form, FANCD2-L, following SDS-PAGE, There was an increase of FANCD2-L monoubiquitination in cells lacking pol η compared to cells expressing pol η. Cisplatin and MMC induced phosphorylation of the DNA damage response proteins, RPA2 and Chk1 was increased in cells lacking FANCD2, compared to cells expressing FANCD2 in response to cisplatin and MMC.

Chapter 5
Discussion

In the present study the effect of proteasome inhibition on cisplatin-induced DNA damage responses was investigated by examining cell viability, cell cycle progression and post-translational modification of DNA damage response proteins in human DNA pol η-deficient, XP30RO, treated with cisplatin and MG132. DNA pol η can carry out translesion synthesis facilitating bypass of cisplatin-induced intrastrand crosslinks during DNA replication, and also plays a role in the bypass step during repair of ICLs (Masutani *et al.*, 2000; Vaisman *et al.*, 2000; Biertumpfel *et al.*, 2010; Ho *et al.*, 2010). Damage induced by cisplatin activates the DNA damage response, resulting in the transduction of a signal from damaged DNA through a network of sensors, transducers and effectors mediated by the post-translational modification of key proteins. In response to cisplatin, a variety of DNA damage responses are more highly activated in XP30RO cells than in cells expressing polη (Cruet-Hennequart *et al.*, 2008).

The proteasome inhibitor MG132 binds to and inhibits the chymotryptic activity of the β-5 subunit of the 26S proteasome (Lee *et al.*, 1998). A consequence of proteasome inhibition is an increase in levels of polyubiquitinated proteins in the cell, as ubiquitinated proteins are unable to be degraded leading to their accumulation (Dantuma *et al.*, 2006). This was demonstrated in XP30RO cells where treatment of cells with MG132 resulted in an increase in the total level of polyubiquitinated proteins as detected by western blotting. As proteasome inhibition has been shown to sensitise cells to agents used in cancer treatment, including cisplatin and IR (Yunmbam *et al.*, 2001; Motegi *et al.*, 2009), the effect of MG132 on cisplatin-induced toxicity in XP30RO cells was determined. DNA pol η-deficient, XP30RO cells are more sensitive to cisplatin when compared to TR30-2 cells, an XP30RO-derived cell line expressing DNA pol η from a *POLH* transgene. This is consistent with previously reported data showing that pol η-deficient cells are more sensitive to cisplatin than normal fibroblasts and a cell line, TR30-9, expressing pol η from a tetracycline-inducible promoter (Bassett *et al.*, 2004; Albertella *et al.*, 2005; Cruet-Hennequart *et al.*, 2008).

Co-treatment of XP30RO cells with MG132 and cisplatin resulted in a greater reduction in cell viability compared to treatment of cells with either agent alone.

The reduction in cell viability following co-treatment was an additive affect rather than synergistic.

As cisplatin-induced ICLs are repaired by the co-ordinated action of several DNA repair pathways (Section 1.6), including NER, HR and the FA pathway (Hinz 2010; Ho *et al.,* 2010; Wood 2010), proteasome inhibition may prevent the repair of DNA damage resulting in the high sensitivity of cells to cisplatin and MG132. In studies investigating the role of the proteasome in DNA repair it has been shown that proteasome inhibition prevented DNA repair by different pathways (Jacquemont *et al.,* 2007; Murakawa *et al.,* 2007). The proteasome inhibitors MG132 or lactacystin prevented the removal of cisplatin-induced DNA adducts in human ovarian carcinoma, A2780, cells suggesting proteasome function is required for efficient repair by NER (Mimnaugh *et al.,* 2000; Wang *et al.,* 2005b). MG132 and lactacystin were also shown to suppress homologous recombination-mediated repair of IR-induced DSBs in Hela cells (Jacquemont *et al.,* 2007). The Fanconi anemia (FA) pathway which is required for the repair of DNA interstrand crosslinks (Section 1.7.1) was also impaired following inhibition of the proteasome (Jacquemont *et al.,* 2007). MG132 inhibited cisplatin- induced FANCD2 monoubiquitination and foci formation, a key event in the activation of the FA pathway (Jacquemont *et al.,* 2007). However, direct evidence that MG132 inhibits repair of intrastrand crosslinks or ICLs in the present system requires further investigation.

DNA adducts induced by cisplatin block the normal DNA replication machinery leading to cell cycle arrest (Kartalou *et al.,* 2001; Chaney *et al.,* 2005). Treatment of DNA pol η-deficient cells with cisplatin resulted in a prolonged accumulation of cells in S phase, compared to cells expressing pol η (Cruet-Hennequart *et al.,* 2008). The effect of proteasome inhibition on cisplatin- induced cell cycle arrest was examined. Consistent with published data, treatment of cells with cisplatin leads to an accumulation of cells in S-phase (Cruet-Hennequart *et al.,* 2008) and the percentage of cells actively incorporating BrdU is reduced. Co-treatment of cells with cisplatin and MG132 did not lead to an accumulation of cells in S-phase when compared to cells treated with cisplatin alone, and the percentage of cells incorporating BrdU was close to zero. The effect of co-treatment with both

agents was similar to that observed when cells were treated with MG132 alone. The lack of BrdU incorporation in cells treated with MG132 alone and in cells treated with both MG132 and cisplatin demonstrates that proteasome inhibition by MG132 results in cell cycle arrest independent of cisplatin-induced DNA damage. The lack of S-phase accumulation in cisplatin and MG132-treated cells is consistent with a failure to degrade key cyclins and a consequent failure of cells to progress through the cell cycle (Minshull *et al.,* 1989; King *et al.,* 1996a).

The proteasome regulates the levels of cyclins, which, in complex with specific CDKs, control cell cycle progression (Minshull *et al.,* 1989; Pines *et al.,* 1991; Pines 1993; King *et al.,* 1996a). Since proteasome inhibition would prevent degradation of cyclins (Minshull *et al.,* 1989; King *et al.,* 1996a), the resulting accumulation of cyclins would account for the strong cell cycle arrest observed following treatment of XP30RO cells with MG132. However, the levels of individual cyclins were not investigated in the present study. Proteasome inhibition of also prevents the degradation of other cell cycle regulators, including p53 and p21 which may also contribute to MG132-induced cell cycle arrest (Yu *et al.,* 2000; Wang *et al.,* 2005c).

The DNA damage response is mediated through the post-translational modification, including phosphorylation, of downstream effector proteins including the histone variant, H2AX, the checkpoint protein, Chk1 and the RPA2 subunit of the ssDNA binding protein replication protein A (RPA) (Cruet-Hennequart *et al.,* 2008; Huen *et al.,* 2008). The DDR is more highly activated in polη-deficient XP30RO cells resulting in increased phosphorylation of H2AX, Chk1 and RPA2 in response to cisplatin (Cruet-Hennequart *et al.,* 2008). H2AX is phosphorylated on serine 139 (generating γH2AX) in an ATM-dependent manner in response to a number of DNA damaging agents including cisplatin, UV and γ-irradiation (Rogakou *et al.,* 1998; Burma *et al.,* 2001). γH2AX is a marker of DNA strand breaks. In the present study, γH2AX was induced in XP30RO cells treated with cisplatin, consistent with previously reported data (Cruet-Hennequart *et al.,* 2008; Cruet-Hennequart *et al.,* 2009; Olive *et al.,* 2009). Proteasome inhibition by MG132 alone did not induce γH2AX formation as determined by western blotting, since the levels of γH2AX in MG132-treated

cells were similar to levels in untreated cells. In addition, treatment of cells with cisplatin for 18 hours followed by co-treatment with cisplatin and MG132 for a further six hours did not alter the amount of cisplatin-induced γH2AX. The effects of MG132 are reversible (Tsubuki *et al.,* 1993; de Bettignies *et al.,* 2010). However, there was no change in the levels of cisplatin-induced γH2AX upon removal of MG132 from XP30RO cells for up to six hours. Thus, proteasome inhibition does not induce γH2AX formation, and does not affect the level of cisplatin-induced γH2AX.

The present data are consistent with previous studies that MG132 and bortezomib did not alter the induction of γH2AX by cisplatin or IR in Hela cells (Jacquemont *et al.,* 2007; Murakawa *et al.,* 2007). From published reports it is clear that proteasome activity is not required in the formation of γH2AX following strand break formation, also indicating that ATM activity is not dependent on the proteasome. Murakawa *et al.,* (2007) demonstrated that, although induction of γH2AX was not altered in cells treated with proteasome inhibitors, there was a delay in the repair of DSBs, indicated by the persistence of γH2AX for longer periods compared to mock-treated cells. However, this was not examined in the present study. It has been shown that proteasome inhibitors prevented ubiquitination of γH2AX, which impaired the recruitment of other DNA repair factors (Dantuma *et al.,* 2006; Mailand *et al.,* 2007). Consistent with this, proteasome inhibitors delay the recruitment of 53BP1 and BRCA1, which is dependent on γH2AX ubiquitination (Jacquemont *et al.,* 2007). Proteasome inhibitors prevent the degradation of polyubiquitinated proteins reducing the amount of free ubiquitin (Dantuma *et al.,* 2006) which could prevent the availability of ubiquitin required for γH2AX ubiquitination. Thus, proteasome function is not required for the initial phosphorylation of H2AX or γH2AX foci formation; however, targeted degradation is required for subsequent recruitment of repair factors to sites of DSBs.

The checkpoint protein, Chk1, is phosphorylated in cells in response to cisplatin treatment (Cruet-Hennequart *et al.,* 2008). Chk1 is phosphorylated on Ser 317 in an ATR-dependent manner resulting in cell cycle arrest (Liu *et al.,* 2000). Proteasome inhibition by MG132 did not induce phosphorylation of Chk1 on

Ser317. Cisplatin-induced pChk1 formation was not altered in cells treated with cisplatin for 18 hours followed by co-treatment with cisplatin and MG132 for a further 6 hours. Zhang *et al.,* (2005) demonstrated that Chk1 is regulated through the ubiquitin-proteasome pathway in response to replicative stress (Zhang *et al.,* 2005). Degradation of Chk1 involves the cullin-based E3 ligases Cul1 and Cul4A, and has been proposed to function in the release of the S-phase checkpoint in A547 and MCF-7 cells following camptothecin treatment (Zhang *et al.,* 2005). However, under the experimental conditions analysed in the present study, no MG132-dependent alterations in Chk1 levels or phosphorylation were observed.

In contrast to the observation that H2AX and Chk1 phosphorylation was independent of MG132, phosphorylation of RPA2 was found to be altered in MG132-treated cells. Replication protein A (RPA) is a heterotrimeric single-stranded DNA binding protein composed of RPA1, RPA2 and RPA3. The RPA trimer plays a major role in DNA metabolism including DNA replication, repair and recombination (Wold *et al.,* 1988; Sugiyama *et al.,* 1997; Missura *et al.,* 2001; Lee *et al.,* 2010; Shi *et al.,* 2010) (Missura *et al.,* 2001). RPA also functions in the DNA damage response and checkpoint activation (Zou *et al.,* 2003; Dart *et al.,* 2004). The N-terminal of the RPA2 subunit is phosphorylated in a cell cycle-dependent manner on Ser 23 and Ser29 (Din *et al.,* 1990; Dutta *et al.,* 1992; Fang *et al.,* 1993; Henricksen *et al.,* 1994; Anantha *et al.,* 2007). RPA2 is also further phosphorylated on Ser4, Ser8, Thr21 and Ser33 in a PIKK-dependent manner following DNA damage (Cruet-Hennequart *et al.,* 2006; Anantha *et al.,* 2007; Cruet-Hennequart *et al.,* 2008). This hyperphosphorylated form of RPA2 is characterised by slow mobility on SDS-PAGE, and is readily identified by western blotting in extracts of cells exposed to DNA damaging agents (Carty *et al.,* 1994; Nuss *et al.,* 2005). As the proteasome functions in numerous cellular processes including the DNA damage response, the effect of proteasome inhibition on cisplatin-induced RPA2 phosphorylation is of interest.

RPA2 phosphorylated on Ser4/Ser8 and on Ser 33 was induced in cells following cisplatin treatment, consistent with previously reports (Cruet-Hennequart *et al.,* 2008). However, in extracts from XP30RO cells treated with MG132 alone, a

novel band was detected following western blotting using an anti-RPA2-pS4S8 antibody. On SDS-PAGE, this novel band, named RPA2-pS4S8*, migrates with faster mobility than cisplatin-induced RPA2 phosphorylated on Ser4/Ser8. Formation of MG132-induced RPA2-pS4S8* and cisplatin-induced RPA2-pS4S8 appears to be independent events, as both forms were detected in extracts of cells that were treated with cisplatin for 18 hours followed by co-treatment with cisplatin and MG132. Based on gel mobility and western blotting following SDS-PAGE, RPA2-pS4S8* is phosphorylated on Ser4/Ser8 but is not hyperphosphorylated. Identification of this novel form of RPA2 has not been reported previously (Oakley *et al.,* 2010). While RPA2 phosphorylated on Ser4/Ser8 is a DNA damage-dependent event, formation of RPA2-pS4S8* is DNA damage-independent. Thus the level of cisplatin-induced γH2AX and pChk1 (Ser317) in extracts where RPA2-pS4S8* was detected were similar to levels detected in mock-treated cells. Removal of MG132 resulted in loss of RPA2-pS4S8* consistent with novel RPA2-pS4S8* being dependent on ongoing proteasome inhibition. Identification of RPA2-pS4S8* points to a novel role for proteasome-mediated events in the regulation of RPA2 phosphorylation.

The induction of RPA2-pS4S8* is not cell line specific as it was detected in three different human cell lines examined in this study. Damage-induced phosphorylation of RPA2 on Ser4/Ser 8 is increased in cells lacking DNA pol η compared with cells expressing DNA pol η (Cruet-Hennequart *et al.,* 2006; Cruet-Hennequart *et al.,* 2008; Cruet-Hennequart *et al.,* 2009). However, the level of RPA2-pS4S8* in pol η-deficient XP30RO cells and pol η-proficient TR30-2 cells did not vary, adding to the evidence that RPA2-pS4S8* formation is a DNA damage -independent event.

The phospho-specific antibody against RPA2 phosphorylated on Ser4/Ser8 used in the analysis of RPA2 phosphorylation detects RPA2 phosphorylated on Ser4 and Ser 8. However, this antibody does not distinguish between phosphorylation of RPA2 on Ser4 or Ser8, or phosphorylation at both sites. One possibility is that the MG132-induced phosphorylated form of RPA2, RPA2-pS4S8* may represent RPA2 that is phosphorylated on only one site, that is on Ser4 or Ser8. Inhibition of the proteasome may prevent phosphorylation of RPA2 on other

sites by for example, inhibiting the degradation of factors required for the phosphorylation of RPA2, or preventing the activation a phosphatase needed for the dephosphorylation of RPA2 at this site.

Experiments using a specific small molecule inhibitor of DNA-PK have demonstrated that damage-induced phosphorylation of RPA2 on Ser4/Ser8 is a DNA-PK-dependent process (Cruet-Hennequart *et al.,* 2006; Cruet-Hennequart *et al.,* 2008). However, the levels of RPA2-pS4S8* in cells were not altered in the presence of the DNA-PK inhibitor NU7441. Treatment of cells with a specific inhibitor of ATM also did not affect the levels of MG132-induced RPA2-pS4S8*. Thus RPA2-pS4S8* formation is not dependent on DNA-PK or ATM activity. RPA2-pS4S8* is not likely to be phosphorylated by ATR as Ser4 and Ser8 are not S/T-Q sites and there is no evidence that ATR phosphorlyates these sites in RPA2; however, this was not investigated in the present study. Other kinases known to phosphorylate RPA2 are CDKs (Din *et al.,* 1990; Dutta *et al.,* 1992; Anantha *et al.,* 2007; Stephan *et al.,* 2009) which may be responsible for the formation of RPA2-pS4S8*. Treatment of cells with the CDK inhibitor, roscovitine, would determine whether RPA2-pS4S8* is dependent on CDK.

Damage-induced hyperphosphorylation of RPA2 has been proposed to play a role in directing RPA from DNA replication to DNA repair (Patrick *et al.*, 2005; Oakley *et al.,* 2010). Phosphorylation of the RPA2 subunit of RPA induces a conformational change in the trimer, reducing its affinity for ssDNA (Binz *et al.*, 2003; Liu *et al.,* 2005). The phosphorylated N-terminal domain of RPA2 interacts with the DBD F of RPA1, competing with the binding of RPA1 to ssDNA, thereby allowing DNA damage response proteins to interact with the N-terminal ,DBD F, of RPA1 (Oakley *et al.,* 2010). Hyperphosphorylation of RPA2 also inhibits DNA replication, probably due to the decrease in the interaction of RPA with the replicative DNA polymerase α (Oakley *et al.,* 2003; Patrick *et al.*, 2005). The functional role of RPA2-pS4S8* has not been determined in the present study. However, as generation of this form of RPA is independent of DNA-damage, results obtained in this study suggest that the formation of RPA2-pS4S8* may be associated with the localisation of RPA to distinct foci, as determined by immunofluorescence. Treatment of cells with MG132 alone

results in the detection of RPA-pS4S8* by western blotting, under which conditions damage-induced hyperphosphorylation of RPA2 on Ser4/Ser8 is not detected. Therefore, any signal detected by immunofluorescence in cells treated with MG132 alone is likely to represent RPA2-pS4S8*. Immunofluorescence analysis, using anti-RPA2-pS4S8 antibody, of cells treated with MG132 shows RPA2-pS4S8* in distinct foci that are located outside of the DAPI-stained nucleus. RPA2-pS4S8* was also located in the soluble fraction of cell extracts consistent with RPA2-pS4S8* not being localised to chromatin. Due to the size of the foci that stained positive for RPA-pS4S8* one possibility is that RPA2-pS4S8* localises to specific sub-nuclear bodies.

Proteins involved in DNA replication and checkpoint activation including the minichromosome maintenance (MCM) proteins and Chk1, have been shown to localise to the centrosome (Loffler *et al.,* 2006; Knockleby *et al.,* 2010). . Localisation at the centrosome suggests that these proteins may function in a role other than the normal function in DNA replication and checkpoint activation (Loffler *et al.,* 2006; Knockleby *et al.,* 2010). Chk1 localises to centrosomes in interphase cells during the unperturbed cell cycle, preventing the premature activation of CDK1-cyclin B and entry of cells into mitosis (Jackman *et al.,* 2003; Kramer *et al.,* 2004). In response to UV- and HU -induced DNA damage in U2OS cells, centrosomal Chk1 is phosphorylated in a PIKK-dependent manner (Loffler *et al.,* 2007). Phosphorylation of Chk1 is required for G2 checkpoint activation. While the subcellular localisation of RPA2-pS4S8* requires further investigation, evidence that RPA2-pS4S8* may be localised to specific sub-nuclear bodies may provide new insight into the regulation of RPA function in the cell.

To further investigate RPA2-pS4S8*, knock-down of endogenous RPA2 and the expression of RPA2 with serine-to-alanine mutations at Ser4 or Ser8 in cells, followed by western blotting using anti-RPA2-pS4S8 antibody, could be used to determine whether RPA2-pS4S8* represents RPA2 phosphorylated at either site. Expression of GFP-tagged RPA2 with serine-to-alanine mutations at Ser4 or Ser8 could also be an approach to determine whether RPA-pS4S8* functions in the localisation of RPA in human cells. Under normal conditions in cells, the

MG132-induced RPA2-pS4S8* observed by western blotting may be a transient event, and this form may be rapidly dephosphorylated or hyperphosphorylated on other sites *in vivo*. Inhibition of the proteasome may prevent events that would normally result either in dephosphorylation or hyperphosphorylation of RPA2-pS4S8*, leading to its accumulation, and allowing it to be observed by western blotting.

Since the effects of MG132 are reported to be reversible (Lee *et al.*, 1998) the effect of removal of MG132 on cisplatin-induced RPA2 phosphorylated on Ser4/Ser8 was examined. Cisplatin-induced phosphorylation of RPA2 on Ser4/Ser8 was not affected by the removal of MG132. However, MG132-induced RPA2-pS4S8* was no longer detected, consistent with accumulation of RPA2-pS4S8* being dependent on proteasome inhibition. Interestingly, upon removal of both cisplatin and MG132 from cells, a series of slow-mobility bands were observed by western blotting using a specific antibody against the RPA2 protein. The slow mobility bands were also detected following immunoprecipitation of RPA2, and following RPA enrichment using Affi-Gel Blue chromatography, consistent with the slow mobility bands representing forms of RPA2.

Slow mobility forms of RPA2 are DNA damage-dependent, unlike the MG132-induced RPA2-pS4S8* form discussed above. The modified, slow mobility forms of RPA2 were not observed in extracts from cells treated with either drug alone. As described earlier, γH2AX, pChk1 (Ser317) and RPA2 phosphorylated on Ser4/Ser8 were also induced under these experimental conditions, consistent with DNA damage induction under these conditions.

Each of the newly identified, modified, forms of RPA2 appears as a pair of closely-spaced bands following western blotting. It is well established that RPA2 is phosphorylated in response to DNA damage. Treatment of cell extracts with λ-phosphatase resulted in the disappearance of the upper band of the pair of bands in each modified form detected by western blotting. Thus, the upper bands of modified RPA2 resulted from phosphorylation, as well as from another modification which substantially alters the mobility of the RPA2 protein on SDS-

PAGE. The lower band in each case represents modified, unphosphorylated RPA2. By analogy with the post-translational modification of H2AX, which is phosphorylated and subsequently ubiquitinated in response to DSBs (Section 1.7.4) (Rogakou *et al.,* 1998; Burma *et al.,* 2001; Huen *et al.,* 2007; Mailand *et al.,* 2007), phosphorylation of RPA2 may be required for subsequent modification of the protein. The presence of unphosphorylated, modified RPA2, suggests that following the modification of RPA2, the protein is then dephosphorylated. Another possibility is that after modification of RPA2 the protein is phosphorylated.

A study by Shi *et al.*, (2010) demonstrated that phosphorylation of RPA2 is required for HR in response to HU in MCF-7 breast cancer cells (Shi *et al.,* 2010). Mutation of damage-induced phosphorylation sites in the N-terminal of RPA2 reduced HR as determined by a GFP-based HR assay, and also impaired the formation of Rad51 foci (Shi *et al.,* 2010). However, Lee *et al.*, (2010) demonstrated that dephosphorylation of RPA2, by a PP4 phosphatase complex, is also required to facilitate HR repair (Lee *et al.,* 2010). Hyperphosphorylated RPA2 impairs DNA replication; therefore dephosphorylation of RPA2 is required for the resumption of DNA synthesis following DNA repair (Lee *et al.*, 2010). In PP4-silenced cells, there was a reduction in HR and in the localisation of Rad51 to sites of damage. Dephosphorylation of modified RPA2 may also be required for efficient HR. However, while treatment of cell extracts with λ-phosphatase, as outlined above, demonstrated that modified RPA2 is phosphorylated, these bands were not detected using anti-RPA2-pS4S8 antibody. One reason for this may be that the modification on RPA2 did not allow the antibody to recognise the phosphorylation on Ser4/Ser8, or that modified RPA2 may not be phosphorylated on these sites. Analysis of cell extracts using phospho-specific antibodies against other phosphorylated N-terminal sites would determine which sites were phosphorylated on modified RPA2. Mutation of phosphorylation sites in the N-terminal of RPA2 and of other potential phosphorylation sites elsewhere in the protein (Nuss *et al.,* 2005)could also determine the dependence of the formation of modified RPA2 on specific phosphorylation sites of the protein.

As slow mobility, modified RPA2 was induced in extracts from cells treated with the proteasome inhibitor, and the gel mobility shift corresponded closely with the expected size change resulting from addition of ubiquitin molecules, the possibility that ubiquitination may account for the slow mobility form of RPA2 on SDS-PAGE under these conditions was explored. A number of approaches were utilised to determine whether RPA2 is ubiquitinated. RPA2 was immunoprecipitated from cell extracts and analysed using an anti-ubiquitin antibody, by western blotting. A signal for ubiquitin was detected corresponding in size to modifications 2 and 3 of RPA2. Immunoprecipitation of RPA2 was also carried out on denatured lysates, and analysed using the anti-ubiquitin antibody. A signal for ubiquitin was detected corresponding to the size of modifications 2 and 3. Denaturation of cell lysate at the time of harvest should destroy protein complexes, as demonstrated by the lack of RPA1 in the immunoprecipitate, following immunoprecipitation using anti-RPA2 antibody. These results are consistent with the hypothesis that the modified slow-mobility forms of RPA2 result from ubiquitination. However, further analysis of RPA2 by mass spectrometry did not identify ubiquitinated RPA2.

Ubiquitinated proteins, and the lysine of the protein that is modified by ubiquitin can be identified by mass spectrometry (Denis *et al.*, 2007). This method relies on the identification of proteins containing a glycine/glycine (Gly/Gly) tag on the ubiquitinated lysine following tryptic digestion of the target protein. The Gly/Gly tag is derived from the presence of ubiquitin, and results in an increase in the mass of the peptide of 114.1 Da, following tryptic digestion (Denis *et al.*, 2007). Mass spectrometry analysis was carried out on RPA2 immunoprecipitated from cell extracts in which modified RPA2 could be readily observed by western blotting. However, following mass spectrometry, no ubiquitinated RPA2 peptides were identified. Coverage of the protein was low, with no more that 55% of the protein being detected by mass spectrometry. RPA2 contains fourteen lysines, only eight which were detected in the RPA2 peptides identified using mass spectrometry. It is possible that RPA2 may be ubiquitinated on one of the six lysines that were not detected by mass spectrometry. While RPA2 peptides were detected by mass spectrometry, confirming that RPA2 was present, it may be that the amount of isolated modified RPA2 after immunoprecipitation was too

low, as modified RPA2 could only be detected by western blotting and was not detected by coommassie blue or silver staining for proteins on the gel. From the amount of modified RPA2 detected by western blotting, the proportion of modified RPA2 appears to represent a small fraction of the total RPA2 protein in the cell extract. Low amounts of RPA2 would reduced the chances of ubiquitinated RPA2 being detected by mass spectrometry. Isolation of an increased amount of modified RPA2 may result in the detection of ubiquitinated RPA2 and possibly identification of the lysine on which RPA2 is ubiquitinated.

Despite the failure to detect ubiquitinated RPA2 peptides by mass spectrometry, the evidence provided here that RPA2 is ubiquitinated suggests that RPA may be regulated through ubiquitination and possibly by proteasomal degradation following DNA damage. One consequence of protein ubiquitination is targeting of proteins to the proteasome for degradation (Thrower *et al.,* 2000). Proteasomal degradation of proteins involved in DNA damage response may function in the regulation of the timing of the recruitment and removal of repair factors at sites of DNA damage. Post-translational modification of the RPA complex is an integral component of the DDR (Zou *et al.,* 2003; Oakley *et al.,* 2010). Phosphorylation of RPA2 may redirect RPA from DNA replication to repair (Patrick *et al.,* 2005; Oakley *et al.,* 2010). Post-translational modifications of RPA, including sumoylation of RPA1 and phosphorylation of RPA2 have been shown to be required for the repair of replication-mediated DSB by HR (Dou *et al.,* 2010; Lee *et al.,* 2010; Shi *et al.,* 2010). It may be possible that ubiquitinated RPA2 may also play a role in facilitating efficient repair by HR.

Dou *et al.,* (2010) demonstrated that the RPA1 subunit of RPA is modified by the small ubiquitin like modifier SUMO 2/3 on lysines 449 and 577 (Dou *et al.,* 2010). Sumoylation of RPA1 was required for the recruitment of Rad51 to initiate HR (Dou *et al.,* 2010) . During S-phase, RPA1 is tightly associated with the SUMO-specific protease, SENP6, which maintains RPA1 in an unsumoylated state. Upon induction of replication-mediated DSBs, SENP6 dissociates from RPA1, resulting in RPA1 sumoylation (Dou *et al.,* 2010). Sumoylation of RPA1 enhances the binding affinity of RPA1 for Rad51, which contains a SUMO-binding motif, mediating the interaction of sumoylated RPA1

and Rad51 (Dou *et al.*, 2010). PIAS1 and PIAS4 may be the E3 SUMO ligases responsible for the sumoylation of RPA1, as depletion of PIAS1 and PIAS4 impaired RPA recruitment to sites of damage, and also reduced HR (Galanty *et al.*, 2009; Morris *et al.*, 2009).

Murakawa *et al.* (2007) investigated the effect of proteasome inhibition on HR-mediated repair of IR-induced DSBs showing that inhibition of the proteasome inhibited HR and prevented localisation of Rad51 and BRCA1 to sites of DNA repair. Murakawa *et al.* (2007) suggested a role for proteasome function, downstream of γH2AX and RPA foci formation, that is required for the recruitment of Rad51, and nucleofilament formation. Jacquemont *et al.* (2007) also showed that in Hela cells co-treated with either MG132 or bortezomib and cisplatin or IR did not alter damage induced γH2AX and RPA foci formation however, BRCA1 and Rad51 foci formation was impaired. As discussed in Section 1.7.4, RPA coats ssDNA generated during the resection of DSBs; this RPA must be displaced from DNA to allow Rad51 to bind and form Rad51 nucleofilaments. The ubiquitination and possible proteasomal degradation of RPA2 may be required for the recruitment of Rad51 onto DNA and subsequent DNA repair by HR. However, in the presence of the proteasome inhibitor, RPA2 would not be degraded, preventing Rad51 foci formation. This would account for the lack of Rad51 foci reported by Murakawa *et al.*, (2007) and by Jacquemont *et al.*, (2007). This model requires experimental testing.

Ubiquitination and degradation of RPA2 may normally be a rapid process, and the use of a proteasome inhibitor prevents RPA2 degradation, allowing the modification to be observed by western blotting. The proportion of RPA2 which is ubiquitinated appears to represent a small proportion of RPA2 protein; therefore degradation of RPA2 would not affect the amount of total RPA2 normally observed by western blotting of cell extracts. The small amount of modified RPA2 possibly indicates that only RPA involved in the repair of DNA by HR is ubiquitinated. The replacement of endogenous RPA2 with lysine-to-arginine mutations at the site of ubiquitination would directly address whether this putative form of ubiquitinated RPA2 played a role in HR. Analysis of Rad51 foci formation in cells expressing mutated RPA2 would determine

whether ubiquitination of RPA2 is required for Rad51 nucleofilament formation and for efficient HR. While further investigation is required, the identification of ubiquitinated RPA2 provides a new insight into the regulation of RPA by post-translational modifications following DNA damage.

The basis of the anti-cancer activity of proteasome inhibitors has not yet fully elucidated, and how these agents sensitise cells to other cancer treatments is not fully understood. One consequence of cancer treatment with proteasome inhibitors, including bortezomib, may be to prevent the removal by proteasomal degradation, of proteins at sites of DNA damage induced by, for example, cisplatin. This may impair the subsequent recruitment of other repair factors to sites of DNA damage (Wang *et al.,* 2005b). HR is one of the major DNA repair pathways involved in the repair of cisplatin-induced DNA damage. The identification of the ubiquitination of RPA2 may be a factor, targeted by proteasome inhibition in the prevention of the repair of cisplatin-induced DNA damage. Inhibition of DNA repair pathways by proteasome inhibition may be a significant factor in the efficacy of the anti-tumour effects displayed by proteasome inhibitors when used with other cancer treatments.

One way in which ubiquitination regulates protein function is through targeting proteins for proteasomal degradation; however, proteins can also be modified by addition of a single ubiquitin molecule. Monoubiquitination of proteins can regulate protein function and localisation in cells (Hicke 2001; Sigismund *et al.,* 2004). Monoubiquitination plays a major role in many cellular processes including in the context of the damage response, regulation of translesion synthesis and in ICL repair by the FA pathway. Cells from FA patients have mutations in genes encoding proteins of the FA pathway, that lead to the formation of chromosome breaks, radial chromosomes and hypersensitivity to DNA crosslinking agents such as mitomycin C (MMC) and cisplatin (Poll *et al.,* 1985; German *et al.,* 1987; Ho *et al.,* 2006). One of the vital steps in the repair of ICLs by the FA pathway is monoubiquitination of FANCD2 on lysine 561 by the FA core complex (Section 1.4.2). Monoubiquitination of FANCD2 is recruited to nuclear foci where it interacts with proteins involved in ICL repair (Nakanishi *et al.,* 2002; Andreassen *et al.,* 2004)

In the present study, it was demonstrated that FANCD2 is monoubiquitinated in a time- and dose-dependent manner in response to cisplatin. FANCD2 monoubiquitination was elevated in cells lacking pol η in response to cisplatin, compared to cells expressing pol η. FANCD2 foci formation was also increased in pol η-deficient cells following cisplatin treatment. Thus in addition to the previously reported increased cisplatin-induced phosphorylation of RPA2, Chk1 and H2AX in cells lacking DNA polymerase η compared to cells expressing pol η, ubiquitination of FANCD2 is also enhanced in these cells (Cruet-Hennequart *et al.,* 2008; Cruet-Hennequart *et al.,* 2009). The lack of DNA pol η may delay the translesion synthesis step during ICL repair (Ho *et al.,* 2010)leading to an increase of monoubiquitinated FANCD2 seen in pol η-deficient cells.

Although intrastrand crosslinks account for the majority of lesions induced by cisplatin, the small percentage of ICls formed are highly cytotoxic (Kartalou *et al.,* 2001; Chaney *et al.,* 2005). ICL covalently link the two strands of DNA preventing DNA replication. In S-phase, ICLs can lead to replication fork arrest and fork collapse resulting in the formation of DSBs. ICL repair in human cells is a complex process, the exact molecular mechanism of which remains to be elucidated (Raschle *et al.,* 2008). Proposed models for ICL repair describe 'unhooking' of the ICL from one DNA strand by endonucleases, translesion synthesis past the 'unhooked' ICL followed by completion of repair by HR (Figure 1.4) (Raschle *et al.,* 2008). The role of monoubiquitination of FANCD2 in the repair of ICL is proposed to be in the recruitment of repair factors involved in the many steps of ICL repair (Knipscheer *et al.,* 2009; Moldovan *et al.,* 2009b). Monoubiquitinated FANCD2 may recruit nucleases for the initial excision or 'unhooking' of the ICL (Bhagwat *et al.,* 2009; Rouse 2009; Wang *et al.,* 2010; Cybulski *et al.,* 2011; Yamamoto *et al.,* 2011) and may recruit DNA polymerases for the TLS step past the 'unhooked' ICL. The main polymerase implicated in the TLS step is DNA polymerase ζ, as DT40 cells lacking pol ζ were hypersensitive to ICL-inducing agents (Sonoda *et al.,* 2003; Niedzwiedz *et al.,* 2004; Auerbach *et al.,* 2010). In *Xenopus* cell free extracts it was also demonstrated that DNA pol ζ is necessary for the TLS step of ICL repair (Raschle *et al.,* 2008). However, cells from XPV patients, lacking pol η, were sensitive to ICL agents suggesting a role for pol η in ICL repair (Misra *et al.,*

1993; Chen *et al.,* 2006). In a recent study pol η was shown to be able to bypass 'unhooked' cisplatin-induced ICLS *in vitro* (Ho *et al.,* 2011). The authors suggested that the polymerase used in the TLS step of ICL repair may depend on the structure of ICL formed in the DNA (Ho *et al.,* 2011).

The main function of the FA pathway is the repair of ICL (Moldovan *et al.,* 2009b). However, the FA pathway may play a more general role in the co-ordination of DNA repair, as this pathway is also activated in response to non-ICL inducing agents including UV and IR (Garcia-Higuera *et al.,* 2001; Taniguchi *et al.,* 2002; Dunn *et al.,* 2006). Monoubiquitination of FANCD2 occurs almost exclusively during S phase, in an ATR-dependent manner, during the normal cell cycle and in response to damage in the DNA encountered by the replication machinery (Taniguchi *et al.,* 2002; Andreassen *et al.,* 2004). Constitutively monoubiquitinated FANCD2 may be the result of endogenous damage. DNA pol η is required for the bypass of cisplatin induced intrastrand cross links. In pol η-deficient cells, cisplatin treatment results in prolonged S phase arrest resulting from the inability to bypass these lesions (Cruet-Hennequart *et al.,* 2008). Increase delay of S phase progression in pol η-deficient cells may result in increased FANCD2 monoubiquitination compared to pol η-proficient cells. Monoubiquitinated FANCD2 may function in the recruitment of repair factors to sites of DNA damage. In cells lacking pol η, there is an increase in stalled replication forks and strand breaks. Increased FANCD2 monoubiquitination may result from the requirement of increased repair factors to sites of damage. Overall these results show a link between two key DDR pathways, TLS and the FA pathway.

Chapter 6
Bibliography

Abraham, R.T. 2004. PI 3-kinase related kinases: 'big' players in stress-induced signaling pathways. *DNA Repair (Amst)* **3**(8-9): 883-887.

Acharya, N., Yoon, J.H., Gali, H., Unk, I., Haracska, L., Johnson, R.E., Hurwitz, J., Prakash, L., and Prakash, S. 2008. Roles of PCNA-binding and ubiquitin-binding domains in human DNA polymerase eta in translesion DNA synthesis. *Proc Natl Acad Sci U S A* **105**(46): 17724-17729.

Adams, B.D., Claffey, K.P., and White, B.A. 2009. Argonaute-2 expression is regulated by epidermal growth factor receptor and mitogen-activated protein kinase signaling and correlates with a transformed phenotype in breast cancer cells. *Endocrinology* **150**(1): 14-23.

Adams, J. 2004. The development of proteasome inhibitors as anticancer drugs. *Cancer Cell* **5**(5): 417-421.

Adams, J. and Kauffman, M. 2004. Development of the proteasome inhibitor Velcade (Bortezomib). *Cancer Invest* **22**(2): 304-311.

Adams, J., Palombella, V.J., Sausville, E.A., Johnson, J., Destree, A., Lazarus, D.D., Maas, J., Pien, C.S., Prakash, S., and Elliott, P.J. 1999. Proteasome inhibitors: a novel class of potent and effective antitumor agents. *Cancer Res* **59**(11): 2615-2622.

Albertella, M.R., Green, C.M., Lehmann, A.R., and O'Connor, M.J. 2005. A role for polymerase eta in the cellular tolerance to cisplatin-induced damage. *Cancer Res* **65**(21): 9799-9806.

Alt, A., Lammens, K., Chiocchini, C., Lammens, A., Pieck, J.C., Kuch, D., Hopfner, K.P., and Carell, T. 2007. Bypass of DNA lesions generated during anticancer treatment with cisplatin by DNA polymerase eta. *Science* **318**(5852): 967-970.

Anantha, R.W. and Borowiec, J.A. 2009. Mitotic crisis: the unmasking of a novel role for RPA. *Cell Cycle* **8**(3): 357-361.

Anantha, R.W., Sokolova, E., and Borowiec, J.A. 2008. RPA phosphorylation facilitates mitotic exit in response to mitotic DNA damage. *Proc Natl Acad Sci U S A* **105**(35): 12903-12908.

Anantha, R.W., Vassin, V.M., and Borowiec, J.A. 2007. Sequential and synergistic modification of human RPA stimulates chromosomal DNA repair. *J Biol Chem* **282**(49): 35910-35923.

Andre, T., Boni, C., Mounedji-Boudiaf, L., Navarro, M., Tabernero, J., Hickish, T., Topham, C., Zaninelli, M., Clingan, P., Bridgewater, J. *et al.*,. 2004. Oxaliplatin, fluorouracil, and leucovorin as adjuvant treatment for colon cancer. *N Engl J Med* **350**(23): 2343-2351.

Andreassen, P.R., D'Andrea, A.D., and Taniguchi, T. 2004. ATR couples FANCD2 monoubiquitination to the DNA-damage response. *Genes Dev* **18**(16): 1958-1963.

Arata, Y., Fujita, M., Ohtani, K., Kijima, S., and Kato, J.Y. 2000. Cdk2-dependent and -independent pathways in E2F-mediated S phase induction. *J Biol Chem* **275**(9): 6337-6345.

Araujo, S.J., Nigg, E.A., and Wood, R.D. 2001. Strong functional interactions of TFIIH with XPC and XPG in human DNA nucleotide excision repair, without a preassembled repairosome. *Mol Cell Biol* **21**(7): 2281-2291.

Auerbach, P.A. and Demple, B. 2010. Roles of Rev1, Pol zeta, Pol32 and Pol eta in the bypass of chromosomal abasic sites in Saccharomyces cerevisiae. *Mutagenesis* **25**(1): 63-69.

Azimzadeh, J. and Bornens, M. 2007. Structure and duplication of the centrosome. *J Cell Sci* **120**(Pt 13): 2139-2142.

Bagby, G.C., Jr. 2003. Genetic basis of Fanconi anemia. *Curr Opin Hematol* **10**(1): 68-76.

Bakkenist, C.J. and Kastan, M.B. 2004. Initiating cellular stress responses. *Cell* **118**(1): 9-17.

Banin, S., Moyal, L., Shieh, S., Taya, Y., Anderson, C.W., Chessa, L., Smorodinsky, N.I., Prives, C., Reiss, Y., Shiloh, Y. *et al.*,. 1998. Enhanced phosphorylation of p53 by ATM in response to DNA damage. *Science* **281**(5383): 1674-1677.

Bartek, J., Lukas, C., and Lukas, J. 2004. Checking on DNA damage in S phase. *Nat Rev Mol Cell Biol* **5**(10): 792-804.

Bartek, J. and Lukas, J. 2003. Chk1 and Chk2 kinases in checkpoint control and cancer. *Cancer Cell* **3**(5): 421-429.

Bartek, J., Lukas, J., and Bartkova, J. 2007. DNA damage response as an anti-cancer barrier: damage threshold and the concept of 'conditional haploinsufficiency'. *Cell Cycle* **6**(19): 2344-2347.

Bartkova, J., Horejsi, Z., Koed, K., Kramer, A., Tort, F., Zieger, K., Guldberg, P., Sehested, M., Nesland, J.M., Lukas, C. *et al.*,. 2005. DNA damage response as a candidate anti-cancer barrier in early human tumorigenesis. *Nature* **434**(7035): 864-870.

Bassett, E., King, N.M., Bryant, M.F., Hector, S., Pendyala, L., Chaney, S.G., and Cordeiro-Stone, M. 2004. The role of DNA polymerase eta in translesion

synthesis past platinum-DNA adducts in human fibroblasts. *Cancer Res* **64**(18): 6469-6475.

Bassett, E., Vaisman, A., Havener, J.M., Masutani, C., Hanaoka, F., and Chaney, S.G. 2003. Efficiency of extension of mismatched primer termini across from cisplatin and oxaliplatin adducts by human DNA polymerases beta and eta in vitro. *Biochemistry* **42**(48): 14197-14206.

Bedford, L., Paine, S., Sheppard, P.W., Mayer, R.J., and Roelofs, J. 2010. Assembly, structure, and function of the 26S proteasome. *Trends Cell Biol* **20**(7): 391-401.

Bekker-Jensen, S., Lukas, C., Melander, F., Bartek, J., and Lukas, J. 2005. Dynamic assembly and sustained retention of 53BP1 at the sites of DNA damage are controlled by Mdc1/NFBD1. *J Cell Biol* **170**(2): 201-211.

Belani, C.P., Ramalingam, S., Perry, M.C., LaRocca, R.V., Rinaldi, D., Gable, P.S., and Tester, W.J. 2008. Randomized, phase III study of weekly paclitaxel in combination with carboplatin versus standard every-3-weeks administration of carboplatin and paclitaxel for patients with previously untreated advanced non-small-cell lung cancer. *J Clin Oncol* **26**(3): 468-473.

Bellon, S.F., Coleman, J.H., and Lippard, S.J. 1991. DNA unwinding produced by site-specific intrastrand cross-links of the antitumor drug cis-diamminedichloroplatinum(II). *Biochemistry* **30**(32): 8026-8035.

Berndtsson, M., Hagg, M., Panaretakis, T., Havelka, A.M., Shoshan, M.C., and Linder, S. 2007. Acute apoptosis by cisplatin requires induction of reactive oxygen species but is not associated with damage to nuclear DNA. *Int J Cancer* **120**(1): 175-180.

Bhagwat, N., Olsen, A.L., Wang, A.T., Hanada, K., Stuckert, P., Kanaar, R., D'Andrea, A., Niedernhofer, L.J., and McHugh, P.J. 2009. XPF-ERCC1 participates in the Fanconi anemia pathway of cross-link repair. *Mol Cell Biol* **29**(24): 6427-6437.

Bielas, J.H., Loeb, K.R., Rubin, B.P., True, L.D., and Loeb, L.A. 2006. Human cancers express a mutator phenotype. *Proc Natl Acad Sci U S A* **103**(48): 18238-18242.

Bienko, M., Green, C.M., Crosetto, N., Rudolf, F., Zapart, G., Coull, B., Kannouche, P., Wider, G., Peter, M., Lehmann, A.R. *et al.*,. 2005. Ubiquitin-binding domains in Y-family polymerases regulate translesion synthesis. *Science* **310**(5755): 1821-1824.

Biertumpfel, C., Zhao, Y., Kondo, Y., Ramon-Maiques, S., Gregory, M., Lee, J.Y., Masutani, C., Lehmann, A.R., Hanaoka, F., and Yang, W. 2010. Structure and mechanism of human DNA polymerase eta. *Nature* **465**(7301): 1044-1048.

Binks, S.P. and Dobrota, M. 1990. Kinetics and mechanism of uptake of platinum-based pharmaceuticals by the rat small intestine. *Biochem Pharmacol* **40**(6): 1329-1336.

Binz, S.K., Lao, Y., Lowry, D.F., and Wold, M.S. 2003. The phosphorylation domain of the 32-kDa subunit of replication protein A (RPA) modulates RPA-DNA interactions. Evidence for an intersubunit interaction. *J Biol Chem* **278**(37): 35584-35591.

Block, W.D., Yu, Y., and Lees-Miller, S.P. 2004. Phosphatidyl inositol 3-kinase-like serine/threonine protein kinases (PIKKs) are required for DNA damage-induced phosphorylation of the 32 kDa subunit of replication protein A at threonine 21. *Nucleic Acids Res* **32**(3): 997-1005.

Bochkarev, A., Bochkareva, E., Frappier, L., and Edwards, A.M. 1999. The crystal structure of the complex of replication protein A subunits RPA32 and RPA14 reveals a mechanism for single-stranded DNA binding. *EMBO J* **18**(16): 4498-4504.

Bochkarev, A., Pfuetzner, R.A., Edwards, A.M., and Frappier, L. 1997. Structure of the single-stranded-DNA-binding domain of replication protein A bound to DNA. *Nature* **385**(6612): 176-181.

Bochkareva, E., Belegu, V., Korolev, S., and Bochkarev, A. 2001. Structure of the major single-stranded DNA-binding domain of replication protein A suggests a dynamic mechanism for DNA binding. *EMBO J* **20**(3): 612-618.

Bochkareva, E., Korolev, S., Lees-Miller, S.P., and Bochkarev, A. 2002. Structure of the RPA trimerization core and its role in the multistep DNA-binding mechanism of RPA. *EMBO J* **21**(7): 1855-1863.

Boulikas, T. and Vougiouka, M. 2004. Recent clinical trials using cisplatin, carboplatin and their combination chemotherapy drugs (review). *Oncol Rep* **11**(3): 559-595.

Boutros, R., Dozier, C., and Ducommun, B. 2006. The when and wheres of CDC25 phosphatases. *Curr Opin Cell Biol* **18**(2): 185-191.

Branzei, D. and Foiani, M. 2007. Interplay of replication checkpoints and repair proteins at stalled replication forks. *DNA Repair (Amst)* **6**(7): 994-1003.

Braun, K.A., Lao, Y., He, Z., Ingles, C.J., and Wold, M.S. 1997. Role of protein-protein interactions in the function of replication protein A (RPA): RPA modulates the activity of DNA polymerase alpha by multiple mechanisms. *Biochemistry* **36**(28): 8443-8454.

Brill, S.J. and Stillman, B. 1989. Yeast replication factor-A functions in the unwinding of the SV40 origin of DNA replication. *Nature* **342**(6245): 92-95.

Burgers, P.M., Koonin, E.V., Bruford, E., Blanco, L., Burtis, K.C., Christman, M.F., Copeland, W.C., Friedberg, E.C., Hanaoka, F., Hinkle, D.C. *et al.*,. 2001. Eukaryotic DNA polymerases: proposal for a revised nomenclature. *J Biol Chem* **276**(47): 43487-43490.

Burma, S., Chen, B.P., Murphy, M., Kurimasa, A., and Chen, D.J. 2001. ATM phosphorylates histone H2AX in response to DNA double-strand breaks. *J Biol Chem* **276**(45): 42462-42467.

Burns, J.L., Guzder, S.N., Sung, P., Prakash, S., and Prakash, L. 1996. An affinity of human replication protein A for ultraviolet-damaged DNA. *J Biol Chem* **271**(20): 11607-11610.

Buscemi, G., Perego, P., Carenini, N., Nakanishi, M., Chessa, L., Chen, J., Khanna, K., and Delia, D. 2004. Activation of ATM and Chk2 kinases in relation to the amount of DNA strand breaks. *Oncogene* **23**(46): 7691-7700.

Cai, Z., Chehab, N.H., and Pavletich, N.P. 2009. Structure and activation mechanism of the CHK2 DNA damage checkpoint kinase. *Mol Cell* **35**(6): 818-829.

Caldecott, K., Banks, G., and Jeggo, P. 1990. DNA double-strand break repair pathways and cellular tolerance to inhibitors of topoisomerase II. *Cancer Res* **50**(18): 5778-5783.

Canman, C.E., Lim, D.S., Cimprich, K.A., Taya, Y., Tamai, K., Sakaguchi, K., Appella, E., Kastan, M.B., and Siliciano, J.D. 1998. Activation of the ATM kinase by ionizing radiation and phosphorylation of p53. *Science* **281**(5383): 1677-1679.

Caravita, T., de Fabritiis, P., Palumbo, A., Amadori, S., and Boccadoro, M. 2006. Bortezomib: efficacy comparisons in solid tumors and hematologic malignancies. *Nat Clin Pract Oncol* **3**(7): 374-387.

Carty, M.P., Zernik-Kobak, M., McGrath, S., and Dixon, K. 1994. UV light-induced DNA synthesis arrest in HeLa cells is associated with changes in phosphorylation of human single-stranded DNA-binding protein. *EMBO J* **13**(9): 2114-2123.

Castella, M. and Taniguchi, T. 2010. The role of FAN1 nuclease in the Fanconi anemia pathway. *Cell Cycle* **9**(21): 4259-4260.

Chan, D.W., Chen, B.P., Prithivirajsingh, S., Kurimasa, A., Story, M.D., Qin, J., and Chen, D.J. 2002. Autophosphorylation of the DNA-dependent protein kinase catalytic subunit is required for rejoining of DNA double-strand breaks. *Genes Dev* **16**(18): 2333-2338.

Chaney, S.G., Campbell, S.L., Bassett, E., and Wu, Y. 2005. Recognition and processing of cisplatin- and oxaliplatin-DNA adducts. *Crit Rev Oncol Hematol* **53**(1): 3-11.

Chen, Y.W., Cleaver, J.E., Hanaoka, F., Chang, C.F., and Chou, K.M. 2006. A novel role of DNA polymerase eta in modulating cellular sensitivity to chemotherapeutic agents. *Mol Cancer Res* **4**(4): 257-265.

Cheng, X., Cheong, N., Wang, Y., and Iliakis, G. 1996. Ionizing radiation-induced phosphorylation of RPA p34 is deficient in ataxia telangiectasia and reduced in aged normal fibroblasts. *Radiother Oncol* **39**(1): 43-52.

Chiu, Y.H., Sun, Q., and Chen, Z.J. 2007. E1-L2 activates both ubiquitin and FAT10. *Mol Cell* **27**(6): 1014-1023.

Chu, G. and Chang, E. 1988. Xeroderma pigmentosum group E cells lack a nuclear factor that binds to damaged DNA. *Science* **242**(4878): 564-567.

Chu, G. and Yang, W. 2008. Here comes the sun: recognition of UV-damaged DNA. *Cell* **135**(7): 1172-1174.

Ciccia, A., Ling, C., Coulthard, R., Yan, Z., Xue, Y., Meetei, A.R., Laghmani el, H., Joenje, H., McDonald, N., de Winter, J.P. *et al.*,. 2007. Identification of FAAP24, a Fanconi anemia core complex protein that interacts with FANCM. *Mol Cell* **25**(3): 331-343.

Ciechanover, A., Elias, S., Heller, H., and Hershko, A. 1982. "Covalent affinity" purification of ubiquitin-activating enzyme. *J Biol Chem* **257**(5): 2537-2542.

Cimprich, K.A. and Cortez, D. 2008. ATR: an essential regulator of genome integrity. *Nat Rev Mol Cell Biol* **9**(8): 616-627.

Cioce, M. and Lamond, A.I. 2005. Cajal bodies: a long history of discovery. *Annu Rev Cell Dev Biol* **21**: 105-131.

Cleaver, J.E. 1968. Defective repair replication of DNA in xeroderma pigmentosum. *Nature* **218**(5142): 652-656.

Cliby, W.A., Roberts, C.J., Cimprich, K.A., Stringer, C.M., Lamb, J.R., Schreiber, S.L., and Friend, S.H. 1998. Overexpression of a kinase-inactive ATR protein causes sensitivity to DNA-damaging agents and defects in cell cycle checkpoints. *EMBO J* **17**(1): 159-169.

Clugston, C.K., McLaughlin, K., Kenny, M.K., and Brown, R. 1992. Binding of human single-stranded DNA binding protein to DNA damaged by the anticancer drug cis-diamminedichloroplatinum (II). *Cancer Res* **52**(22): 6375-6379.

Cohn, M.A., Kee, Y., Haas, W., Gygi, S.P., and D'Andrea, A.D. 2009. UAF1 is a subunit of multiple deubiquitinating enzyme complexes. *J Biol Chem* **284**(8): 5343-5351.

Cohn, M.A., Kowal, P., Yang, K., Haas, W., Huang, T.T., Gygi, S.P., and D'Andrea, A.D. 2007. A UAF1-containing multisubunit protein complex regulates the Fanconi anemia pathway. *Mol Cell* **28**(5): 786-797.

Cole, A.R., Lewis, L.P., and Walden, H. 2010. The structure of the catalytic subunit FANCL of the Fanconi anemia core complex. *Nat Struct Mol Biol* **17**(3): 294-298.

Costanzo, V., Robertson, K., Ying, C.Y., Kim, E., Avvedimento, E., Gottesman, M., Grieco, D., and Gautier, J. 2000. Reconstitution of an ATM-dependent checkpoint that inhibits chromosomal DNA replication following DNA damage. *Mol Cell* **6**(3): 649-659.

Cruet-Hennequart, S., Coyne, S., Glynn, M.T., Oakley, G.G., and Carty, M.P. 2006. UV-induced RPA phosphorylation is increased in the absence of DNA polymerase eta and requires DNA-PK. *DNA Repair (Amst)* **5**(4): 491-504.

Cruet-Hennequart, S., Glynn, M.T., Murillo, L.S., Coyne, S., and Carty, M.P. 2008. Enhanced DNA-PK-mediated RPA2 hyperphosphorylation in DNA polymerase eta-deficient human cells treated with cisplatin and oxaliplatin. *DNA Repair (Amst)* **7**(4): 582-596.

Cruet-Hennequart, S., Villalan, S., Kaczmarczyk, A., O'Meara, E., Sokol, A.M., and Carty, M.P. 2009. Characterization of the effects of cisplatin and carboplatin on cell cycle progression and DNA damage response activation in DNA polymerase eta-deficient human cells. *Cell Cycle* **8**(18).

Cybulski, K.E. and Howlett, N.G. 2011. FANCP/SLX4: a Swiss army knife of DNA interstrand crosslink repair. *Cell Cycle* **10**(11): 1757-1763.

Dalle, S., Thieblemont, C., Thomas, L., and Dumontet, C. 2008. Monoclonal antibodies in clinical oncology. *Anticancer Agents Med Chem* **8**(5): 523-532.

Dantuma, N.P., Groothuis, T.A., Salomons, F.A., and Neefjes, J. 2006. A dynamic ubiquitin equilibrium couples proteasomal activity to chromatin remodeling. *J Cell Biol* **173**(1): 19-26.

Dart, D.A., Adams, K.E., Akerman, I., and Lakin, N.D. 2004. Recruitment of the cell cycle checkpoint kinase ATR to chromatin during S-phase. *J Biol Chem* **279**(16): 16433-16440.

Davies, A.A., Huttner, D., Daigaku, Y., Chen, S., and Ulrich, H.D. 2008. Activation of ubiquitin-dependent DNA damage bypass is mediated by replication protein a. *Mol Cell* **29**(5): 625-636.

de Bettignies, G. and Coux, O. 2010. Proteasome inhibitors: Dozens of molecules and still counting. *Biochimie* **92**(11): 1530-1545.

de Boer, J. and Hoeijmakers, J.H. 2000. Nucleotide excision repair and human syndromes. *Carcinogenesis* **21**(3): 453-460.

Deans, A.J. and West, S.C. 2011. DNA interstrand crosslink repair and cancer. *Nat Rev Cancer* **11**(7): 467-480.

Denis, N.J., Vasilescu, J., Lambert, J.P., Smith, J.C., and Figeys, D. 2007. Tryptic digestion of ubiquitin standards reveals an improved strategy for identifying ubiquitinated proteins by mass spectrometry. *Proteomics* **7**(6): 868-874.

Desai, S.D., Li, T.K., Rodriguez-Bauman, A., Rubin, E.H., and Liu, L.F. 2001. Ubiquitin/26S proteasome-mediated degradation of topoisomerase I as a resistance mechanism to camptothecin in tumor cells. *Cancer Res* **61**(15): 5926-5932.

Deveraux, Q., Ustrell, V., Pickart, C., and Rechsteiner, M. 1994. A 26 S protease subunit that binds ubiquitin conjugates. *J Biol Chem* **269**(10): 7059-7061.

Dianov, G.L., Jensen, B.R., Kenny, M.K., and Bohr, V.A. 1999. Replication protein A stimulates proliferating cell nuclear antigen-dependent repair of abasic sites in DNA by human cell extracts. *Biochemistry* **38**(34): 11021-11025.

Din, S., Brill, S.J., Fairman, M.P., and Stillman, B. 1990. Cell-cycle-regulated phosphorylation of DNA replication factor A from human and yeast cells. *Genes Dev* **4**(6): 968-977.

Doil, C., Mailand, N., Bekker-Jensen, S., Menard, P., Larsen, D.H., Pepperkok, R., Ellenberg, J., Panier, S., Durocher, D., Bartek, J. *et al.,*. 2009. RNF168 binds and amplifies ubiquitin conjugates on damaged chromosomes to allow accumulation of repair proteins. *Cell* **136**(3): 435-446.

Donzelli, M. and Draetta, G.F. 2003. Regulating mammalian checkpoints through Cdc25 inactivation. *EMBO Rep* **4**(7): 671-677.

Dornreiter, I., Erdile, L.F., Gilbert, I.U., von Winkler, D., Kelly, T.J., and Fanning, E. 1992. Interaction of DNA polymerase alpha-primase with cellular replication protein A and SV40 T antigen. *EMBO J* **11**(2): 769-776.

Dorsman, J.C., Levitus, M., Rockx, D., Rooimans, M.A., Oostra, A.B., Haitjema, A., Bakker, S.T., Steltenpool, J., Schuler, D., Mohan, S. *et al.,*. 2007. Identification of the Fanconi anemia complementation group I gene, FANCI. *Cell Oncol* **29**(3): 211-218.

Dou, H., Huang, C., Singh, M., Carpenter, P.B., and Yeh, E.T. 2010. Regulation of DNA repair through deSUMOylation and SUMOylation of replication protein A complex. *Mol Cell* **39**(3): 333-345.

Duncan, L.M., Piper, S., Dodd, R.B., Saville, M.K., Sanderson, C.M., Luzio, J.P., and Lehner, P.J. 2006. Lysine-63-linked ubiquitination is required for endolysosomal degradation of class I molecules. *EMBO J* **25**(8): 1635-1645.

Dunn, J., Potter, M., Rees, A., and Runger, T.M. 2006. Activation of the Fanconi anemia/BRCA pathway and recombination repair in the cellular response to solar ultraviolet light. *Cancer Res* **66**(23): 11140-11147.

Dutta, A., Ruppert, J.M., Aster, J.C., and Winchester, E. 1993. Inhibition of DNA replication factor RPA by p53. *Nature* **365**: 79-82.

Dutta, A. and Stillman, B. 1992. cdc2 family kinases phosphorylate a human cell DNA replication factor, RPA, and activate DNA replication. *EMBO J* **11**(6): 2189-2199.

Eastman, A. 1987. Cross-linking of glutathione to DNA by cancer chemotherapeutic platinum coordination complexes. *Chem Biol Interact* **61**(3): 241-248.

Ekholm, S.V. and Reed, S.I. 2000. Regulation of G(1) cyclin-dependent kinases in the mammalian cell cycle. *Curr Opin Cell Biol* **12**(6): 676-684.

El-Mahdy, M.A., Zhu, Q., Wang, Q.E., Wani, G., Praetorius-Ibba, M., and Wani, A.A. 2006. Cullin 4A-mediated proteolysis of DDB2 protein at DNA damage sites regulates in vivo lesion recognition by XPC. *J Biol Chem* **281**(19): 13404-13411.

Elsasser, S. and Finley, D. 2005. Delivery of ubiquitinated substrates to protein-unfolding machines. *Nat Cell Biol* **7**(8): 742-749.

Elsasser, S., Gali, R.R., Schwickart, M., Larsen, C.N., Leggett, D.S., Muller, B., Feng, M.T., Tubing, F., Dittmar, G.A., and Finley, D. 2002. Proteasome subunit Rpn1 binds ubiquitin-like protein domains. *Nat Cell Biol* **4**(9): 725-730.

Esashi, F., Galkin, V.E., Yu, X., Egelman, E.H., and West, S.C. 2007. Stabilization of RAD51 nucleoprotein filaments by the C-terminal region of BRCA2. *Nat Struct Mol Biol* **14**(6): 468-474.

Etlinger, J.D. and Goldberg, A.L. 1977. A soluble ATP-dependent proteolytic system responsible for the degradation of abnormal proteins in reticulocytes. *Proc Natl Acad Sci U S A* **74**(1): 54-58.

Evans, E., Moggs, J.G., Hwang, J.R., Egly, J.M., and Wood, R.D. 1997. Mechanism of open complex and dual incision formation by human nucleotide excision repair factors. *EMBO J* **16**(21): 6559-6573.

Fairman, M.P. and Stillman, B. 1988. Cellular factors required for multiple stages of SV40 DNA replication in vitro. *EMBO J* **7**(4): 1211-1218.

Falck, J., Coates, J., and Jackson, S.P. 2005. Conserved modes of recruitment of ATM, ATR and DNA-PKcs to sites of DNA damage. *Nature* **434**(7033): 605-611.

Falck, J., Mailand, N., Syljuasen, R.G., Bartek, J., and Lukas, J. 2001. The ATM-Chk2-Cdc25A checkpoint pathway guards against radioresistant DNA synthesis. *Nature* **410**(6830): 842-847.

Falck, J., Petrini, J.H., Williams, B.R., Lukas, J., and Bartek, J. 2002. The DNA damage-dependent intra-S phase checkpoint is regulated by parallel pathways. *Nat Genet* **30**(3): 290-294.

Fang, F. and Newport, J.W. 1993. Distinct roles of cdk2 and cdc2 in RP-A phosphorylation during the cell cycle. *J Cell Sci* **106 (Pt 3)**: 983-994.

Fang, S. and Weissman, A.M. 2004. A field guide to ubiquitylation. *Cell Mol Life Sci* **61**(13): 1546-1561.

Fekairi, S., Scaglione, S., Chahwan, C., Taylor, E.R., Tissier, A., Coulon, S., Dong, M.Q., Ruse, C., Yates, J.R., 3rd, Russell, P. *et al.*,. 2009. Human SLX4 is a Holliday junction resolvase subunit that binds multiple DNA repair/recombination endonucleases. *Cell* **138**(1): 78-89.

Ferguson, L.R., Liu, A.P., Denny, W.A., Cullinane, C., Talarico, T., and Phillips, D.R. 2000. Transcriptional blockages in a cell-free system by sequence-selective DNA alkylating agents. *Chem Biol Interact* **126**(1): 15-31.

Fichtinger-Schepman, A.M., Baan, R.A., Luiten-Schuite, A., van Dijk, M., and Lohman, P.H. 1985a. Immunochemical quantitation of adducts induced in DNA by cis-diamminedichloroplatinum (II) and analysis of adduct-related DNA-unwinding. *Chem Biol Interact* **55**(3): 275-288.

Fichtinger-Schepman, A.M., van der Veer, J.L., den Hartog, J.H., Lohman, P.H., and Reedijk, J. 1985b. Adducts of the antitumor drug cis-diamminedichloroplatinum(II) with DNA: formation, identification, and quantitation. *Biochemistry* **24**(3): 707-713.

Fousteri, M. and Mullenders, L.H. 2008. Transcription-coupled nucleotide excision repair in mammalian cells: molecular mechanisms and biological effects. *Cell Res* **18**(1): 73-84.

Frankenberg-Schwager, M., Kirchermeier, D., Greif, G., Baer, K., Becker, M., and Frankenberg, D. 2005. Cisplatin-mediated DNA double-strand breaks in replicating but not in quiescent cells of the yeast Saccharomyces cerevisiae. *Toxicology* **212**(2-3): 175-184.

Freemont, P.S. 2000. RING for destruction? *Curr Biol* **10**(2): R84-87.

Friedberg, E.C., Fischhaber, P.L., and Kisker, C. 2001. Error-prone DNA polymerases: novel structures and the benefits of infidelity. *Cell* **107**(1): 9-12.

Friedberg, E.C., McDaniel, L.D., and Schultz, R.A. 2004. The role of endogenous and exogenous DNA damage and mutagenesis. *Curr Opin Genet Dev* **14**(1): 5-10.

Furnari, B., Rhind, N., and Russell, P. 1997. Cdc25 mitotic inducer targeted by chk1 DNA damage checkpoint kinase. *Science* **277**(5331): 1495-1497.

Galanty, Y., Belotserkovskaya, R., Coates, J., Polo, S., Miller, K.M., and Jackson, S.P. 2009. Mammalian SUMO E3-ligases PIAS1 and PIAS4 promote responses to DNA double-strand breaks. *Nature* **462**(7275): 935-939.

Gallastegui, G., Munoz, R., Barona, A., Ibarra-Berastegi, G., Rojo, N., and Elias, A. Evaluating the impact of water supply strategies on p-xylene biodegradation performance in an organic media-based biofilter. *J Hazard Mater* **185**(2-3): 1019-1026.

Garcia-Higuera, I., Taniguchi, T., Ganesan, S., Meyn, M.S., Timmers, C., Hejna, J., Grompe, M., and D'Andrea, A.D. 2001. Interaction of the Fanconi anemia proteins and BRCA1 in a common pathway. *Molecular Cell* **7**(2): 249-262.

Gatei, M., Sloper, K., Sorensen, C., Syljuasen, R., Falck, J., Hobson, K., Savage, K., Lukas, J., Zhou, B.B., Bartek, J. *et al.*,. 2003. Ataxia-telangiectasia-mutated

(ATM) and NBS1-dependent phosphorylation of Chk1 on Ser-317 in response to ionizing radiation. *J Biol Chem* **278**(17): 14806-14811.

German, J., Schonberg, S., Caskie, S., Warburton, D., Falk, C., and Ray, J.H. 1987. A test for Fanconi's anemia. *Blood* **69**(6): 1637-1641.

Gillette, T.G., Huang, W., Russell, S.J., Reed, S.H., Johnston, S.A., and Friedberg, E.C. 2001. The 19S complex of the proteasome regulates nucleotide excision repair in yeast. *Genes Dev* **15**(12): 1528-1539.

Glickman, M.H., Rubin, D.M., Fried, V.A., and Finley, D. 1998. The regulatory particle of the Saccharomyces cerevisiae proteasome. *Mol Cell Biol* **18**(6): 3149-3162.

Glotzer, M., Murray, A.W., and Kirschner, M.W. 1991. Cyclin is degraded by the ubiquitin pathway. *Nature* **349**(6305): 132-138.

Gong, Z. and Chen, J. 2011. E3 ligase RFWD3 participates in replication checkpoint control. *J Biol Chem*.

Gottlieb, T.M. and Jackson, S.P. 1993. The DNA-dependent protein kinase: requirement for DNA ends and association with Ku antigen. *Cell* **72**(1): 131-142.

Gottlieb, T.M. and Jackson, S.P. 1994. Protein kinases and DNA damage. *Trends Biochem Sci* **19**(11): 500-503.

Groisman, R., Polanowska, J., Kuraoka, I., Sawada, J., Saijo, M., Drapkin, R., Kisselev, A.F., Tanaka, K., and Nakatani, Y. 2003. The ubiquitin ligase activity in the DDB2 and CSA complexes is differentially regulated by the COP9 signalosome in response to DNA damage. *Cell* **113**(3): 357-367.

Groll, M., Ditzel, L., Lowe, J., Stock, D., Bochtler, M., Bartunik, H.D., and Huber, R. 1997. Structure of 20S proteasome from yeast at 2.4 A resolution. *Nature* **386**(6624): 463-471.

Gudmundsdottir, K., Lord, C.J., Witt, E., Tutt, A.N., and Ashworth, A. 2004. DSS1 is required for RAD51 focus formation and genomic stability in mammalian cells. *EMBO Rep* **5**(10): 989-993.

Hanahan, D. and Weinberg, R.A. 2000. The hallmarks of cancer. *Cell* **100**(1): 57-70.

Hande, K.R. 2003. Topoisomerase II inhibitors. *Cancer Chemother Biol Response Modif* **21**: 103-125.

Hannoun, Z., Greenhough, S., Jaffray, E., Hay, R.T., and Hay, D.C. 2010. Post-translational modification by SUMO. *Toxicology* **278**(3): 288-293.

Haracska, L., Torres-Ramos, C.A., Johnson, R.E., Prakash, S., and Prakash, L. 2004. Opposing effects of ubiquitin conjugation and SUMO modification of PCNA on replicational bypass of DNA lesions in Saccharomyces cerevisiae. *Mol Cell Biol* **24**(10): 4267-4274.

Haracska, L., Unk, I., Johnson, R.E., Johansson, E., Burgers, P.M., Prakash, S., and Prakash, L. 2001. Roles of yeast DNA polymerases delta and zeta and of Rev1 in the bypass of abasic sites. *Genes Dev* **15**(8): 945-954.

Haring, S.J., Humphreys, T.D., and Wold, M.S. 2010. A naturally occurring human RPA subunit homolog does not support DNA replication or cell-cycle progression. *Nucleic Acids Res* **38**(3): 846-858.

Harper, J.W. and Elledge, S.J. 2007. The DNA damage response: ten years after. *Mol Cell* **28**(5): 739-745.

Hartwell, L.H. and Weinert, T.A. 1989. Checkpoints: controls that ensure the order of cell cycle events. *Science* **246**(4930): 629-634.

Henricksen, L.A. and Wold, M.S. 1994. Replication protein A mutants lacking phosphorylation sites for p34cdc2 kinase support DNA replication. *J Biol Chem* **269**(39): 24203-24208.

Hershko, A. 1999. Mechanisms and regulation of the degradation of cyclin B. *Philos Trans R Soc Lond B Biol Sci* **354**(1389): 1571-1575; discussion 1575-1576.

Hershko, A., Ciechanover, A., and Varshavsky, A. 2000. Basic Medical Research Award. The ubiquitin system. *Nat Med* **6**(10): 1073-1081.

Hicke, L. 2001. Protein regulation by monoubiquitin. *Nat Rev Mol Cell Biol* **2**(3): 195-201.

Hinz, J.M. 2010. Role of homologous recombination in DNA interstrand crosslink repair. *Environ Mol Mutagen* **51**(6): 582-603.

Hirao, A., Kong, Y.Y., Matsuoka, S., Wakeham, A., Ruland, J., Yoshida, H., Liu, D., Elledge, S.J., and Mak, T.W. 2000. DNA damage-induced activation of p53 by the checkpoint kinase Chk2. *Science* **287**(5459): 1824-1827.

Hiyama, H., Yokoi, M., Masutani, C., Sugasawa, K., Maekawa, T., Tanaka, K., Hoeijmakers, J.H., and Hanaoka, F. 1999. Interaction of hHR23 with S5a. The ubiquitin-like domain of hHR23 mediates interaction with S5a subunit of 26 S proteasome. *J Biol Chem* **274**(39): 28019-28025.

Ho, G.P., Margossian, S., Taniguchi, T., and D'Andrea, A.D. 2006. Phosphorylation of FANCD2 on two novel sites is required for mitomycin C resistance. *Mol Cell Biol* **26**(18): 7005-7015.

Ho, T.V., Guainazzi, A., Derkunt, S.B., Enoiu, M., and Scharer, O.D. 2011. Structure-dependent bypass of DNA interstrand crosslinks by translesion synthesis polymerases. *Nucleic Acids Res.*

Ho, T.V. and Scharer, O.D. 2010. Translesion DNA synthesis polymerases in DNA interstrand crosslink repair. *Environ Mol Mutagen* **51**(6): 552-566.

Hodson, C., Cole, A.R., Lewis, L.P., Miles, J.A., Purkiss-Trew, A., and Walden, H. 2011. Structural analysis of human FANCL, the E3 ligase in the fanconi anemia pathway. *J Biol Chem*.

Hoege, C., Pfander, B., Moldovan, G.L., Pyrowolakis, G., and Jentsch, S. 2002. RAD6-dependent DNA repair is linked to modification of PCNA by ubiquitin and SUMO. *Nature* **419**(6903): 135-141.

Hofmann, K. and Bucher, P. 1996. The UBA domain: a sequence motif present in multiple enzyme classes of the ubiquitination pathway. *Trends Biochem Sci* **21**(5): 172-173.

Holzer, A.K., Samimi, G., Katano, K., Naerdemann, W., Lin, X., Safaei, R., and Howell, S.B. 2004. The copper influx transporter human copper transport protein 1 regulates the uptake of cisplatin in human ovarian carcinoma cells. *Mol Pharmacol* **66**(4): 817-823.

Huang, H., Zhu, L., Reid, B.R., Drobny, G.P., and Hopkins, P.B. 1995. Solution structure of a cisplatin-induced DNA interstrand cross-link. *Science* **270**(5243): 1842-1845.

Huang, L., Turchi, J.J., Wahl, A.F., and Bambara, R.A. 1993. Activity of calf thymus DNA helicase E on cis-diamminedichloroplatinum (II)-damaged DNA. *J Biol Chem* **268**(35): 26731-26737.

Huang, T.T., Nijman, S.M., Mirchandani, K.D., Galardy, P.J., Cohn, M.A., Haas, W., Gygi, S.P., Ploegh, H.L., Bernards, R., and D'Andrea, A.D. 2006. Regulation of monoubiquitinated PCNA by DUB autocleavage. *Nat Cell Biol* **8**(4): 339-347.

Huen, M.S. and Chen, J. 2008. The DNA damage response pathways: at the crossroad of protein modifications. *Cell Res* **18**(1): 8-16.

Huen, M.S., Grant, R., Manke, I., Minn, K., Yu, X., Yaffe, M.B., and Chen, J. 2007. RNF8 transduces the DNA-damage signal via histone ubiquitylation and checkpoint protein assembly. *Cell* **131**(5): 901-914.

Huibregtse, J.M., Scheffner, M., Beaudenon, S., and Howley, P.M. 1995. A family of proteins structurally and functionally related to the E6-AP ubiquitin-protein ligase. *Proc Natl Acad Sci U S A* **92**(7): 2563-2567.

Hussain, S., Wilson, J.B., Medhurst, A.L., Hejna, J., Witt, E., Ananth, S., Davies, A., Masson, J.Y., Moses, R., West, S.C. *et al.*,. 2004. Direct interaction of FANCD2 with BRCA2 in DNA damage response pathways. *Hum Mol Genet* **13**(12): 1241-1248.

Iftode, C. and Borowiec, J.A. 1997. Denaturation of the simian virus 40 origin of replication mediated by human replication protein A. *Mol Cell Biol* **17**(7): 3876-3883.

Ip, S.C., Rass, U., Blanco, M.G., Flynn, H.R., Skehel, J.M., and West, S.C. 2008. Identification of Holliday junction resolvases from humans and yeast. *Nature* **456**(7220): 357-361.

Ishiai, M., Kitao, H., Smogorzewska, A., Tomida, J., Kinomura, A., Uchida, E., Saberi, A., Kinoshita, E., Kinoshita-Kikuta, E., Koike, T. *et al.*,. 2008. FANCI phosphorylation functions as a molecular switch to turn on the Fanconi anemia pathway. *Nat Struct Mol Biol* **15**(11): 1138-1146.

Ishiai, M., Sanchez, J.P., Amin, A.A., Murakami, Y., and Hurwitz, J. 1996. Purification, gene cloning, and reconstitution of the heterotrimeric single-stranded DNA-binding protein from Schizosaccharomyces pombe. *J Biol Chem* **271**(34): 20868-20878.

Ishida, S., Lee, J., Thiele, D.J., and Herskowitz, I. 2002. Uptake of the anticancer drug cisplatin mediated by the copper transporter Ctr1 in yeast and mammals. *Proc Natl Acad Sci U S A* **99**(22): 14298-14302.

Ishikawa, K., Ishii, H., and Saito, T. 2006. DNA damage-dependent cell cycle checkpoints and genomic stability. *DNA Cell Biol* **25**(7): 406-411.

Itakura, E., Takai, K.K., Umeda, K., Kimura, M., Ohsumi, M., Tamai, K., and Matsuura, A. 2004a. Amino-terminal domain of ATRIP contributes to intranuclear relocation of the ATR-ATRIP complex following DNA damage. *FEBS Lett* **577**(1-2): 289-293.

Itakura, E., Umeda, K., Sekoguchi, E., Takata, H., Ohsumi, M., and Matsuura, A. 2004b. ATR-dependent phosphorylation of ATRIP in response to genotoxic stress. *Biochem Biophys Res Commun* **323**(4): 1197-1202.

Jackman, M., Lindon, C., Nigg, E.A., and Pines, J. 2003. Active cyclin B1-Cdk1 first appears on centrosomes in prophase. *Nat Cell Biol* **5**(2): 143-148.

Jacobs, D.M., Lipton, A.S., Isern, N.G., Daughdrill, G.W., Lowry, D.F., Gomes, X., and Wold, M.S. 1999. Human replication protein A: global fold of the N-terminal RPA-70 domain reveals a basic cleft and flexible C-terminal linker. *J Biomol NMR* **14**(4): 321-331.

Jacquemont, C. and Taniguchi, T. 2007. Proteasome function is required for DNA damage response and fanconi anemia pathway activation. *Cancer Res* **67**(15): 7395-7405.

Jensen, R.B., Carreira, A., and Kowalczykowski, S.C. 2010. Purified human BRCA2 stimulates RAD51-mediated recombination. *Nature* **467**(7316): 678-683.

Jin, J., Li, X., Gygi, S.P., and Harper, J.W. 2007. Dual E1 activation systems for ubiquitin differentially regulate E2 enzyme charging. *Nature* **447**(7148): 1135-1138.

Joazeiro, C.A. and Weissman, A.M. 2000. RING finger proteins: mediators of ubiquitin ligase activity. *Cell* **102**(5): 549-552.

Johnson, R.E., Prakash, S., and Prakash, L. 1999. Efficient bypass of a thymine-thymine dimer by yeast DNA polymerase, Poleta. *Science* **283**(5404): 1001-1004.

Josse, L., Harley, M.E., Pires, I.M., and Hughes, D.A. 2006. Fission yeast Dss1 associates with the proteasome and is required for efficient ubiquitin-dependent proteolysis. *Biochem J* **393**(Pt 1): 303-309.

Kanagasabaphy, P., Morgan, G.J., and Davies, F.E. 2007. Proteasome inhibition and multiple myeloma. *Curr Opin Investig Drugs* **8**(6): 447-451.

Kannouche, P., Broughton, B.C., Volker, M., Hanaoka, F., Mullenders, L.H., and Lehmann, A.R. 2001. Domain structure, localization, and function of DNA polymerase eta, defective in xeroderma pigmentosum variant cells. *Genes Dev* **15**(2): 158-172.

Kannouche, P.L. and Lehmann, A.R. 2004a. Ubiquitination of PCNA and the polymerase switch in human cells. *Cell Cycle* **3**(8): 1011-1013.

Kannouche, P.L., Wing, J., and Lehmann, A.R. 2004b. Interaction of human DNA polymerase eta with monoubiquitinated PCNA: a possible mechanism for the polymerase switch in response to DNA damage. *Mol Cell* **14**(4): 491-500.

Kartalou, M. and Essigmann, J.M. 2001. Recognition of cisplatin adducts by cellular proteins. *Mutat Res* **478**(1-2): 1-21.

Kawamoto, T., Araki, K., Sonoda, E., Yamashita, Y.M., Harada, K., Kikuchi, K., Masutani, C., Hanaoka, F., Nozaki, K., Hashimoto, N. *et al.*,. 2005. Dual roles for DNA polymerase eta in homologous DNA recombination and translesion DNA synthesis. *Mol Cell* **20**(5): 793-799.

Kee, Y. and D'Andrea, A.D. 2010. Expanded roles of the Fanconi anemia pathway in preserving genomic stability. *Genes Dev* **24**(16): 1680-1694.

Keeney, S., Chang, G.J., and Linn, S. 1993. Characterization of a human DNA damage binding protein implicated in xeroderma pigmentosum E. *J Biol Chem* **268**(28): 21293-21300.

Kelland, L. 2007. The resurgence of platinum-based cancer chemotherapy. *Nat Rev Cancer* **7**(8): 573-584.

Kemp, M.G., Mason, A.C., Carreira, A., Reardon, J.T., Haring, S.J., Borgstahl, G.E., Kowalczykowski, S.C., Sancar, A., and Wold, M.S. 2010. An alternative form of replication protein a expressed in normal human tissues supports DNA repair. *J Biol Chem* **285**(7): 4788-4797.

Kerscher, O., Felberbaum, R., and Hochstrasser, M. 2006. Modification of proteins by ubiquitin and ubiquitin-like proteins. *Annu Rev Cell Dev Biol* **22**: 159-180.

Keshav, K.F., Chen, C., and Dutta, A. 1995. Rpa4, a homolog of the 34-kilodalton subunit of the replication protein A complex. *Mol Cell Biol* **15**(6): 3119-3128.

Kier, L.D., Yamasaki, E., and Ames, B.N. 1974. Detection of mutagenic activity in cigarette smoke condensates. *Proc Natl Acad Sci U S A* **71**(10): 4159-4163.

Kikugawa, K., Oikawa, N., Miyazawa, A., Shindo, K., and Kato, T. 2005. Interaction of nitric oxide with glutathione or cysteine generates reactive oxygen species causing DNA single strand breaks. *Biol Pharm Bull* **28**(6): 998-1003.

Kim, C., Paulus, B.F., and Wold, M.S. 1994. Interactions of human replication protein A with oligonucleotides. *Biochemistry* **33**(47): 14197-14206.

Kim, C., Snyder, R.O., and Wold, M.S. 1992. Binding properties of replication protein A from human and yeast cells. *Mol Cell Biol* **12**(7): 3050-3059.

Kim, C. and Wold, M.S. 1995. Recombinant human replication protein A binds to polynucleotides with low cooperativity. *Biochemistry* **34**(6): 2058-2064.

Kim, H., Chen, J., and Yu, X. 2007. Ubiquitin-binding protein RAP80 mediates BRCA1-dependent DNA damage response. *Science* **316**(5828): 1202-1205.

Kim, J.M., Kee, Y., Gurtan, A., and D'Andrea, A.D. 2008. Cell cycle-dependent chromatin loading of the Fanconi anemia core complex by FANCM/FAAP24. *Blood* **111**(10): 5215-5222.

Kim, S.T., Lim, D.S., Canman, C.E., and Kastan, M.B. 1999. Substrate specificities and identification of putative substrates of ATM kinase family members. *J Biol Chem* **274**(53): 37538-37543.

King, R.W., Deshaies, R.J., Peters, J.M., and Kirschner, M.W. 1996a. How proteolysis drives the cell cycle. *Science* **274**(5293): 1652-1659.

King, R.W., Glotzer, M., and Kirschner, M.W. 1996b. Mutagenic analysis of the destruction signal of mitotic cyclins and structural characterization of ubiquitinated intermediates. *Mol Biol Cell* **7**(9): 1343-1357.

Kirkpatrick, D.S., Denison, C., and Gygi, S.P. 2005. Weighing in on ubiquitin: the expanding role of mass-spectrometry-based proteomics. *Nat Cell Biol* **7**(8): 750-757.

Knipscheer, P., Raschle, M., Smogorzewska, A., Enoiu, M., Ho, T.V., Scharer, O.D., Elledge, S.J., and Walter, J.C. 2009. The Fanconi anemia pathway promotes replication-dependent DNA interstrand cross-link repair. *Science* **326**(5960): 1698-1701.

Knockleby, J. and Lee, H. 2010. Same partners, different dance: involvement of DNA replication proteins in centrosome regulation. *Cell Cycle* **9**(22): 4487-4491.

Kojic, M., Yang, H., Kostrub, C.F., Pavletich, N.P., and Holloman, W.K. 2003. The BRCA2-interacting protein DSS1 is vital for DNA repair, recombination, and genome stability in Ustilago maydis. *Mol Cell* **12**(4): 1043-1049.

Komatsu, M., Sumizawa, T., Mutoh, M., Chen, Z.S., Terada, K., Furukawa, T., Yang, X.L., Gao, H., Miura, N., Sugiyama, T. *et al.*,. 2000. Copper-transporting P-type adenosine triphosphatase (ATP7B) is associated with cisplatin resistance. *Cancer Res* **60**(5): 1312-1316.

Kozlov, S.V., Graham, M.E., Jakob, B., Tobias, F., Kijas, A.W., Tanuji, M., Chen, P., Robinson, P.J., Taucher-Scholz, G., Suzuki, K. *et al.*,. 2011. Autophosphorylation and ATM activation: additional sites add to the complexity. *J Biol Chem* **286**(11): 9107-9119.

Kraemer, K.H. 1997. Sunlight and skin cancer: another link revealed. *Proc Natl Acad Sci U S A* **94**(1): 11-14.

Kramer, A., Mailand, N., Lukas, C., Syljuasen, R.G., Wilkinson, C.J., Nigg, E.A., Bartek, J., and Lukas, J. 2004. Centrosome-associated Chk1 prevents premature activation of cyclin-B-Cdk1 kinase. *Nat Cell Biol* **6**(9): 884-891.

Kratz, K., Schopf, B., Kaden, S., Sendoel, A., Eberhard, R., Lademann, C., Cannavo, E., Sartori, A.A., Hengartner, M.O., and Jiricny, J. 2010. Deficiency of FANCD2-associated nuclease KIAA1018/FAN1 sensitizes cells to interstrand crosslinking agents. *Cell* **142**(1): 77-88.

Kristensen, C.N., Bystol, K.M., Li, B., Serrano, L., and Brenneman, M.A. 2010. Depletion of DSS1 protein disables homologous recombinational repair in human cells. *Mutat Res* **694**(1-2): 60-64.

Krogan, N.J., Lam, M.H., Fillingham, J., Keogh, M.C., Gebbia, M., Li, J., Datta, N., Cagney, G., Buratowski, S., Emili, A. *et al.*,. 2004. Proteasome involvement in the repair of DNA double-strand breaks. *Mol Cell* **16**(6): 1027-1034.

Kropff, M., Bisping, G., Wenning, D., Berdel, W.E., and Kienast, J. 2006. Proteasome inhibition in multiple myeloma. *Eur J Cancer* **42**(11): 1623-1639.

Kunkel, T.A. 2004. DNA Replication Fidelity. *J Biol Chem* **279**(17): 16895-16898.

Kurimasa, A., Kumano, S., Boubnov, N.V., Story, M.D., Tung, C.S., Peterson, S.R., and Chen, D.J. 1999. Requirement for the kinase activity of human DNA-dependent protein kinase catalytic subunit in DNA strand break rejoining. *Mol Cell Biol* **19**(5): 3877-3884.

Lacks, S.A., Springhorn, S.S., and Rosenthal, A.L. 1979. Effect of the composition of sodium dodecyl sulfate preparations on the renaturation of enzymes after polyacrylamide gel electrophoresis. *Anal Biochem* **100**(2): 357-363.

Laemmli, U.K. 1970. Cleavage of structural proteins during the assembly of the head of bacteriophage T4. *Nature* **227**(5259): 680-685.

Lallemand-Breitenbach, V. and de The, H. 2010. PML nuclear bodies. *Cold Spring Harb Perspect Biol* **2**(5): a000661.

Lao, Y., Lee, C.G., and Wold, M.S. 1999. Replication protein A interactions with DNA. 2. Characterization of double-stranded DNA-binding/helix-destabilization activities and the role of the zinc-finger domain in DNA interactions. *Biochemistry* **38**(13): 3974-3984.

Lee, D.H. and Goldberg, A.L. 1998. Proteasome inhibitors: valuable new tools for cell biologists. *Trends Cell Biol* **8**(10): 397-403.

Lee, D.H., Pan, Y., Kanner, S., Sung, P., Borowiec, J.A., and Chowdhury, D. 2010. A PP4 phosphatase complex dephosphorylates RPA2 to facilitate DNA repair via homologous recombination. *Nat Struct Mol Biol* **17**(3): 365-372.

Lehman, A.R., Kirk-Bell, S., Arlett, C.F., Paterson, M.C., Lohman, P.H., de Weerd-Kastelein, E.A., and Bootsma, D. 1975. Xeroderma pigmentosum cells with normal levels of excision repair have a defect in DNA synthesis after UV-irradiation. *Proc Natl Acad Sci U S A* **72**(1): 219-223.

Lehmann, A.R. 2003. DNA repair-deficient diseases, xeroderma pigmentosum, Cockayne syndrome and trichothiodystrophy. *Biochimie* **85**(11): 1101-1111.

Lehmann, A.R., Niimi, A., Ogi, T., Brown, S., Sabbioneda, S., Wing, J.F., Kannouche, P.L., and Green, C.M. 2007. Translesion synthesis: Y-family polymerases and the polymerase switch. *DNA Repair (Amst)* **6**(7): 891-899.

Li, J., Zou, C., Bai, Y., Wazer, D.E., Band, V., and Gao, Q. 2006. DSS1 is required for the stability of BRCA2. *Oncogene* **25**(8): 1186-1194.

Li, L. and Zou, L. 2005. Sensing, signaling, and responding to DNA damage: organization of the checkpoint pathways in mammalian cells. *J Cell Biochem* **94**(2): 298-306.

Lim, D.S., Kim, S.T., Xu, B., Maser, R.S., Lin, J., Petrini, J.H., and Kastan, M.B. 2000. ATM phosphorylates p95/nbs1 in an S-phase checkpoint pathway. *Nature* **404**(6778): 613-617.

Lin, Y.L., Chen, C., Keshav, K.F., Winchester, E., and Dutta, A. 1996. Dissection of functional domains of the human DNA replication protein complex replication protein A. *J Biol Chem* **271**(29): 17190-17198.

Liu, J., Doty, T., Gibson, B., and Heyer, W.D. 2010a. Human BRCA2 protein promotes RAD51 filament formation on RPA-covered single-stranded DNA. *Nat Struct Mol Biol* **17**(10): 1260-1262.

Liu, Q., Guntuku, S., Cui, X.S., Matsuoka, S., Cortez, D., Tamai, K., Luo, G., Carattini-Rivera, S., DeMayo, F., Bradley, A. *et al.*,. 2000. Chk1 is an essential kinase that is regulated by Atr and required for the G(2)/M DNA damage checkpoint. *Genes Dev* **14**(12): 1448-1459.

Liu, S., Chu, J., Yucer, N., Leng, M., Wang, S.Y., Chen, B.P., Hittelman, W.N., and Wang, Y. 2011. RFWD3 associates with replication protein A and facilitates RPA-mediated DNA damage response. *J Biol Chem*.

Liu, T., Ghosal, G., Yuan, J., Chen, J., and Huang, J. 2010b. FAN1 Acts with FANCI-FANCD2 to Promote DNA Interstrand Cross-Link Repair. *Science* **329**(5992): 693-696.

Liu, V.F. and Weaver, D.T. 1993. The ionizing radiation-induced replication protein A phosphorylation response differs between ataxia telangiectasia and normal human cells. *Mol Cell Biol* **13**(12): 7222-7231.

Liu, Y., Kvaratskhelia, M., Hess, S., Qu, Y., and Zou, Y. 2005. Modulation of replication protein A function by its hyperphosphorylation-induced conformational change involving DNA binding domain B. *J Biol Chem* **280**(38): 32775-32783.

Loeb, L.A. 1994. Microsatellite instability: marker of a mutator phenotype in cancer. *Cancer Res* **54**(19): 5059-5063.

Loeb, L.A., Loeb, K.R., and Anderson, J.P. 2003. Multiple mutations and cancer. *Proc Natl Acad Sci U S A* **100**(3): 776-781.

Loeb, L.A., Springgate, C.F., and Battula, N. 1974. Errors in DNA replication as a basis of malignant changes. *Cancer Res* **34**(9): 2311-2321.

Loffler, H., Bochtler, T., Fritz, B., Tews, B., Ho, A.D., Lukas, J., Bartek, J., and Kramer, A. 2007. DNA damage-induced accumulation of centrosomal Chk1 contributes to its checkpoint function. *Cell Cycle* **6**(20): 2541-2548.

Loffler, H., Lukas, J., Bartek, J., and Kramer, A. 2006. Structure meets function--centrosomes, genome maintenance and the DNA damage response. *Exp Cell Res* **312**(14): 2633-2640.

Lopes, M., Cotta-Ramusino, C., Pellicioli, A., Liberi, G., Plevani, P., Muzi-Falconi, M., Newlon, C.S., and Foiani, M. 2001. The DNA replication

checkpoint response stabilizes stalled replication forks. *Nature* **412**(6846): 557-561.

Lou, Z., Chini, C.C., Minter-Dykhouse, K., and Chen, J. 2003. Mediator of DNA damage checkpoint protein 1 regulates BRCA1 localization and phosphorylation in DNA damage checkpoint control. *J Biol Chem* **278**(16): 13599-13602.

Lou, Z., Minter-Dykhouse, K., Franco, S., Gostissa, M., Rivera, M.A., Celeste, A., Manis, J.P., van Deursen, J., Nussenzweig, A., Paull, T.T. *et al.*,. 2006. MDC1 maintains genomic stability by participating in the amplification of ATM-dependent DNA damage signals. *Mol Cell* **21**(2): 187-200.

Lowe, J., Stock, D., Jap, B., Zwickl, P., Baumeister, W., and Huber, R. 1995. Crystal structure of the 20S proteasome from the archaeon T. acidophilum at 3.4 A resolution. *Science* **268**(5210): 533-539.

Ma, Y., Pannicke, U., Lu, H., Niewolik, D., Schwarz, K., and Lieber, M.R. 2005. The DNA-dependent protein kinase catalytic subunit phosphorylation sites in human Artemis. *J Biol Chem* **280**(40): 33839-33846.

MacKay, C., Declais, A.C., Lundin, C., Agostinho, A., Deans, A.J., MacArtney, T.J., Hofmann, K., Gartner, A., West, S.C., Helleday, T. *et al.*,. 2010. Identification of KIAA1018/FAN1, a DNA repair nuclease recruited to DNA damage by monoubiquitinated FANCD2. *Cell* **142**(1): 65-76.

Maga, G., Frouin, I., Spadari, S., and Hubscher, U. 2001. Replication protein A as a "fidelity clamp" for DNA polymerase alpha. *J Biol Chem* **276**(21): 18235-18242.

Maher, V.M., Ouellette, L.M., Curren, R.D., and McCormick, J.J. 1976. Frequency of ultraviolet light-induced mutations is higher in xeroderma

pigmentosum variant cells than in normal human cells. *Nature* **261**(5561): 593-595.

Mailand, N., Bekker-Jensen, S., Faustrup, H., Melander, F., Bartek, J., Lukas, C., and Lukas, J. 2007. RNF8 ubiquitylates histones at DNA double-strand breaks and promotes assembly of repair proteins. *Cell* **131**(5): 887-900.

Mailand, N., Falck, J., Lukas, C., Syljuasen, R.G., Welcker, M., Bartek, J., and Lukas, J. 2000. Rapid destruction of human Cdc25A in response to DNA damage. *Science* **288**(5470): 1425-1429.

Maloisel, L., Fabre, F., and Gangloff, S. 2008. DNA polymerase delta is preferentially recruited during homologous recombination to promote heteroduplex DNA extension. *Mol Cell Biol* **28**(4): 1373-1382.

Marques, A.J., Palanimurugan, R., Matias, A.C., Ramos, P.C., and Dohmen, R.J. 2009. Catalytic mechanism and assembly of the proteasome. *Chem Rev* **109**(4): 1509-1536.

Masutani, C., Kusumoto, R., Iwai, S., and Hanaoka, F. 2000. Mechanisms of accurate translesion synthesis by human DNA polymerase eta. *EMBO J* **19**(12): 3100-3109.

Masutani, C., Kusumoto, R., Yamada, A., Dohmae, N., Yokoi, M., Yuasa, M., Araki, M., Iwai, S., Takio, K., and Hanaoka, F. 1999. The XPV (xeroderma pigmentosum variant) gene encodes human DNA polymerase eta. *Nature* **399**(6737): 700-704.

Matsuda, N., Azuma, K., Saijo, M., Iemura, S., Hioki, Y., Natsume, T., Chiba, T., and Tanaka, K. 2005. DDB2, the xeroderma pigmentosum group E gene product, is directly ubiquitylated by Cullin 4A-based ubiquitin ligase complex. *DNA Repair (Amst)* **4**(5): 537-545.

Matsuda, T., Saijo, M., Kuraoka, I., Kobayashi, T., Nakatsu, Y., Nagai, A., Enjoji, T., Masutani, C., Sugasawa, K., Hanaoka, F. *et al.,*. 1995. DNA repair protein XPA binds replication protein A (RPA). *J Biol Chem* **270**(8): 4152-4157.

Matsuoka, S., Ballif, B.A., Smogorzewska, A., McDonald, E.R., 3rd, Hurov, K.E., Luo, J., Bakalarski, C.E., Zhao, Z., Solimini, N., Lerenthal, Y. *et al.,*. 2007. ATM and ATR substrate analysis reveals extensive protein networks responsive to DNA damage. *Science* **316**(5828): 1160-1166.

Matsuoka, S., Rotman, G., Ogawa, A., Shiloh, Y., Tamai, K., and Elledge, S.J. 2000. Ataxia telangiectasia-mutated phosphorylates Chk2 in vivo and in vitro. *Proc Natl Acad Sci U S A* **97**(19): 10389-10394.

Mavrou, A., Tsangaris, G.T., Roma, E., and Kolialexi, A. 2008. The ATM gene and ataxia telangiectasia. *Anticancer Res* **28**(1B): 401-405.

McIlwraith, M.J., Vaisman, A., Liu, Y., Fanning, E., Woodgate, R., and West, S.C. 2005. Human DNA polymerase eta promotes DNA synthesis from strand invasion intermediates of homologous recombination. *Mol Cell* **20**(5): 783-792.

Meetei, A.R., de Winter, J.P., Medhurst, A.L., Wallisch, M., Waisfisz, Q., van de Vrugt, H.J., Oostra, A.B., Yan, Z., Ling, C., Bishop, C.E. *et al.,*. 2003. A novel ubiquitin ligase is deficient in Fanconi anemia. *Nat Genet* **35**(2): 165-170.

Meetei, A.R., Yan, Z., and Wang, W. 2004. FANCL replaces BRCA1 as the likely ubiquitin ligase responsible for FANCD2 monoubiquitination. *Cell Cycle* **3**(2): 179-181.

Mer, G., Bochkarev, A., Gupta, R., Bochkareva, E., Frappier, L., Ingles, C.J., Edwards, A.M., and Chazin, W.J. 2000. Structural basis for the recognition of DNA repair proteins UNG2, XPA, and RAD52 by replication factor RPA. *Cell* **103**(3): 449-456.

Merrick, C.J., Jackson, D., and Diffley, J.F. 2004. Visualization of altered replication dynamics after DNA damage in human cells. *J Biol Chem* **279**(19): 20067-20075.

Mimnaugh, E.G., Yunmbam, M.K., Li, Q., Bonvini, P., Hwang, S.G., Trepel, J., Reed, E., and Neckers, L. 2000. Prevention of cisplatin-DNA adduct repair and potentiation of cisplatin-induced apoptosis in ovarian carcinoma cells by proteasome inhibitors. *Biochem Pharmacol* **60**(9): 1343-1354.

Minshull, J., Pines, J., Golsteyn, R., Standart, N., Mackie, S., Colman, A., Blow, J., Ruderman, J.V., Wu, M., and Hunt, T. 1989. The role of cyclin synthesis, modification and destruction in the control of cell division. *J Cell Sci Suppl* **12**: 77-97.

Mirkin, E.V. and Mirkin, S.M. 2007. Replication fork stalling at natural impediments. *Microbiol Mol Biol Rev* **71**(1): 13-35.

Misra, R.R. and Vos, J.M. 1993. Defective replication of psoralen adducts detected at the gene-specific level in xeroderma pigmentosum variant cells. *Mol Cell Biol* **13**(2): 1002-1012.

Missura, M., Buterin, T., Hindges, R., Hubscher, U., Kasparkova, J., Brabec, V., and Naegeli, H. 2001. Double-check probing of DNA bending and unwinding by XPA-RPA: an architectural function in DNA repair. *EMBO J* **20**(13): 3554-3564.

Mitsiades, N., Mitsiades, C.S., Richardson, P.G., Poulaki, V., Tai, Y.T., Chauhan, D., Fanourakis, G., Gu, X., Bailey, C., Joseph, M. *et al.*,. 2003. The proteasome inhibitor PS-341 potentiates sensitivity of multiple myeloma cells to conventional chemotherapeutic agents: therapeutic applications. *Blood* **101**(6): 2377-2380.

Moldovan, G.L. and D'Andrea, A.D. 2009a. FANCD2 hurdles the DNA interstrand crosslink. *Cell* **139**(7): 1222-1224.

Moldovan, G.L. and D'Andrea, A.D. 2009b. How the fanconi anemia pathway guards the genome. *Annu Rev Genet* **43**: 223-249.

Morris, J.R., Boutell, C., Keppler, M., Densham, R., Weekes, D., Alamshah, A., Butler, L., Galanty, Y., Pangon, L., Kiuchi, T. *et al.*,. 2009. The SUMO modification pathway is involved in the BRCA1 response to genotoxic stress. *Nature* **462**(7275): 886-890.

Moser, J., Kool, H., Giakzidis, I., Caldecott, K., Mullenders, L.H., and Fousteri, M.I. 2007. Sealing of chromosomal DNA nicks during nucleotide excision repair requires XRCC1 and DNA ligase III alpha in a cell-cycle-specific manner. *Mol Cell* **27**(2): 311-323.

Motegi, A., Murakawa, Y., and Takeda, S. 2009. The vital link between the ubiquitin-proteasome pathway and DNA repair: impact on cancer therapy. *Cancer Lett* **283**(1): 1-9.

Mu, J.J., Wang, Y., Luo, H., Leng, M., Zhang, J., Yang, T., Besusso, D., Jung, S.Y., and Qin, J. 2007. A proteomic analysis of ataxia telangiectasia-mutated (ATM)/ATM-Rad3-related (ATR) substrates identifies the ubiquitin-proteasome system as a regulator for DNA damage checkpoints. *J Biol Chem* **282**(24): 17330-17334.

Munoz, I.M., Hain, K., Declais, A.C., Gardiner, M., Toh, G.W., Sanchez-Pulido, L., Heuckmann, J.M., Toth, R., Macartney, T., Eppink, B. *et al.*,. 2009. Coordination of structure-specific nucleases by human SLX4/BTBD12 is required for DNA repair. *Mol Cell* **35**(1): 116-127.

Murakawa, Y., Sonoda, E., Barber, L.J., Zeng, W., Yokomori, K., Kimura, H., Niimi, A., Lehmann, A., Zhao, G.Y., Hochegger, H. *et al.*,. 2007. Inhibitors of the proteasome suppress homologous DNA recombination in mammalian cells. *Cancer Res* **67**(18): 8536-8543.

Murata, S., Yashiroda, H., and Tanaka, K. 2009. Molecular mechanisms of proteasome assembly. *Nat Rev Mol Cell Biol* **10**(2): 104-115.

Murzin, A.G. 1993. OB(oligonucleotide/oligosaccharide binding)-fold: common structural and functional solution for non-homologous sequences. *EMBO J* **12**(3): 861-867.

Nakanishi, K., Taniguchi, T., Ranganathan, V., New, H.V., Moreau, L.A., Stotsky, M., Mathew, C.G., Kastan, M.B., Weaver, D.T., and D'Andrea, A.D. 2002. Interaction of FANCD2 and NBS1 in the DNA damage response. *Nat Cell Biol* **4**(12): 913-920.

Nasheuer, H.P., von Winkler, D., Schneider, C., Dornreiter, I., Gilbert, I., and Fanning, E. 1992. Purification and functional characterization of bovine RP-A in an in vitro SV40 DNA replication system. *Chromosoma* **102**(1 Suppl): S52-59.

Niedzwiedz, W., Mosedale, G., Johnson, M., Ong, C.Y., Pace, P., and Patel, K.J. 2004. The Fanconi anaemia gene FANCC promotes homologous recombination and error-prone DNA repair. *Mol Cell* **15**(4): 607-620.

Nigg, E.A. 1995. Cyclin-dependent protein kinases: key regulators of the eukaryotic cell cycle. *Bioessays* **17**(6): 471-480.

Niida, A., Wang, Z., Tomita, K., Oishi, S., Tamamura, H., Otaka, A., Navenot, J.M., Broach, J.R., Peiper, S.C., and Fujii, N. 2006. Design and synthesis of downsized metastin (45-54) analogs with maintenance of high GPR54 agonistic activity. *Bioorg Med Chem Lett* **16**(1): 134-137.

Niida, H., Tsuge, S., Katsuno, Y., Konishi, A., Takeda, N., and Nakanishi, M. 2005. Depletion of Chk1 leads to premature activation of Cdc2-cyclin B and mitotic catastrophe. *J Biol Chem* **280**(47): 39246-39252.

Nijman, S.M., Huang, T.T., Dirac, A.M., Brummelkamp, T.R., Kerkhoven, R.M., D'Andrea, A.D., and Bernards, R. 2005. The deubiquitinating enzyme USP1 regulates the Fanconi anemia pathway. *Mol Cell* **17**(3): 331-339.

Niu, H., Erdjument-Bromage, H., Pan, Z.Q., Lee, S.H., Tempst, P., and Hurwitz, J. 1997. Mapping of Amino Acid Residues in the p34 Subunit of Human Single-stranded DNA-binding Protein Phosphorylated by DNA-dependent Protein Kinase and Cdc2 Kinase in Vitro. *J Biol Chem* **272**(19): 12634-12641.

Nuss, J.E., Patrick, S.M., Oakley, G.G., Alter, G.M., Robison, J.G., Dixon, K., and Turchi, J.J. 2005. DNA damage induced hyperphosphorylation of replication protein A. 1. Identification of novel sites of phosphorylation in response to DNA damage. *Biochemistry* **44**(23): 8428-8437.

Nyberg, K.A., Michelson, R.J., Putnam, C.W., and Weinert, T.A. 2002. Toward maintaining the genome: DNA damage and replication checkpoints. *Annu Rev Genet* **36**: 617-656.

O'Donnell, L. and Durocher, D. 2010. DNA repair has a new FAN1 club. *Mol Cell* **39**(2): 167-169.

Oakley, G.G. and Patrick, S.M. 2010. Replication protein A: directing traffic at the intersection of replication and repair. *Front Biosci* **15**: 883-900.

Oakley, G.G., Patrick, S.M., Yao, J., Carty, M.P., Turchi, J.J., and Dixon, K. 2003. RPA phosphorylation in mitosis alters DNA binding and protein-protein interactions. *Biochemistry* **42**(11): 3255-3264.

Oestergaard, V.H., Langevin, F., Kuiken, H.J., Pace, P., Niedzwiedz, W., Simpson, L.J., Ohzeki, M., Takata, M., Sale, J.E., and Patel, K.J. 2007. Deubiquitination of FANCD2 is required for DNA crosslink repair. *Mol Cell* **28**(5): 798-809.

Olive, P.L. and Banath, J.P. 2009. Kinetics of H2AX phosphorylation after exposure to cisplatin. *Cytometry B Clin Cytom* **76**(2): 79-90.

Olson, E., Nievera, C.J., Klimovich, V., Fanning, E., and Wu, X. 2006. RPA2 is a direct downstream target for ATR to regulate the S-phase checkpoint. *J Biol Chem* **281**(51): 39517-39533.

Olson, E., Nievera, C.J., Liu, E., Lee, A.Y., Chen, L., and Wu, X. 2007. The Mre11 complex mediates the S-phase checkpoint through an interaction with replication protein A. *Mol Cell Biol* **27**(17): 6053-6067.

Orlowski, R.Z., Voorhees, P.M., Garcia, R.A., Hall, M.D., Kudrik, F.J., Allred, T., Johri, A.R., Jones, P.E., Ivanova, A., Van Deventer, H.W. *et al.*,. 2005. Phase 1 trial of the proteasome inhibitor bortezomib and pegylated liposomal doxorubicin in patients with advanced hematologic malignancies. *Blood* **105**(8): 3058-3065.

Pajonk, F., van Ophoven, A., Weissenberger, C., and McBride, W.H. 2005. The proteasome inhibitor MG-132 sensitizes PC-3 prostate cancer cells to ionizing radiation by a DNA-PK-independent mechanism. *BMC Cancer* **5**: 76.

Patrick, S.M., Oakley, G.G., Dixon, K., and Turchi, J.J. 2005. DNA damage induced hyperphosphorylation of replication protein A. 2. Characterization of DNA binding activity, protein interactions, and activity in DNA replication and repair. *Biochemistry* **44**(23): 8438-8448.

Patrick, S.M. and Turchi, J.J. 1998. Human replication protein A preferentially binds cisplatin-damaged duplex DNA in vitro. *Biochemistry* **37**(24): 8808-8815.

Patrick, S.M. and Turchi, J.J. 2001. Stopped-flow kinetic analysis of replication protein A-binding DNA: damage recognition and affinity for single-stranded DNA reveal differential contributions of k(on) and k(off) rate constants. *J Biol Chem* **276**(25): 22630-22637.

Paul, M.K. and Mukhopadhyay, A.K. 2004. Tyrosine kinase - Role and significance in Cancer. *Int J Med Sci* **1**(2): 101-115.

Pelzer, C., Kassner, I., Matentzoglu, K., Singh, R.K., Wollscheid, H.P., Scheffner, M., Schmidtke, G., and Groettrup, M. 2007. UBE1L2, a novel E1 enzyme specific for ubiquitin. *J Biol Chem* **282**(32): 23010-23014.

Perez, R.P. 1998. Cellular and molecular determinants of cisplatin resistance. *Eur J Cancer* **34**(10): 1535-1542.

Pfuetzner, R.A., Bochkarev, A., Frappier, L., and Edwards, A.M. 1997. Replication protein A. Characterization and crystallization of the DNA binding domain. *J Biol Chem* **272**(1): 430-434.

Pickart, C.M. 2001. Mechanisms underlying ubiquitination. *Annu Rev Biochem* **70**: 503-533.

Pines, J. 1993. Cyclins and their associated cyclin-dependent kinases in the human cell cycle. *Biochem Soc Trans* **21**(4): 921-925.

Pines, J. and Hunter, T. 1991. Cyclin-dependent kinases: a new cell cycle motif? *Trends Cell Biol* **1**(5): 117-121.

Poll, E.H., Arwert, F., Joenje, H., and Wanamarta, A.H. 1985. Differential sensitivity of Fanconi anaemia lymphocytes to the clastogenic action of cis-diamminedichloroplatinum (II) and trans-diamminedichloroplatinum (II). *Hum Genet* **71**(3): 206-210.

Rapic-Otrin, V., Navazza, V., Nardo, T., Botta, E., McLenigan, M., Bisi, D.C., Levine, A.S., and Stefanini, M. 2003. True XP group E patients have a defective UV-damaged DNA binding protein complex and mutations in DDB2 which reveal the functional domains of its p48 product. *Hum Mol Genet* **12**(13): 1507-1522.

Raschle, M., Knipscheer, P., Enoiu, M., Angelov, T., Sun, J., Griffith, J.D., Ellenberger, T.E., Scharer, O.D., and Walter, J.C. 2008. Mechanism of replication-coupled DNA interstrand crosslink repair. *Cell* **134**(6): 969-980.

Robinson, P.A. and Ardley, H.C. 2004. Ubiquitin-protein ligases. *J Cell Sci* **117**(Pt 22): 5191-5194.

Robison, J.G., Dixon, K., and Bissler, J.J. 2007. Cell cycle-and proteasome-dependent formation of etoposide-induced replication protein A (RPA) or Mre11/Rad50/Nbs1 (MRN) complex repair foci. *Cell Cycle* **6**(19): 2399-2407.

Rogakou, E.P., Pilch, D.R., Orr, A.H., Ivanova, V.S., and Bonner, W.M. 1998. DNA double-stranded breaks induce histone H2AX phosphorylation on serine 139. *J Biol Chem* **273**(10): 5858-5868.

Rosenberg, B. 1975. Possible mechanisms for the antitumor activity of platinum coordination complexes. *Cancer Chemother Rep* **59**(3): 589-598.

Rosenberg, B., L. VanCamp, et al. 1965. Inhibition of cell division in escherichia coli by electrolysis products from a platinum electrode. *Nature* **205**: 698-699.

Rosenberg, B., L. VanCamp, et al. 1969. Platinum compounds: a new class of potent antitumor agents. *Nature* **222**: 385-386.

Rothkamm, K., Kruger, I., Thompson, L.H., and Lobrich, M. 2003. Pathways of DNA double-strand break repair during the mammalian cell cycle. *Mol Cell Biol* **23**(16): 5706-5715.

Rouse, J. 2009. Control of genome stability by SLX protein complexes. *Biochem Soc Trans* **37**(Pt 3): 495-510.

Rubin, D.M., Glickman, M.H., Larsen, C.N., Dhruvakumar, S., and Finley, D. 1998. Active site mutants in the six regulatory particle ATPases reveal multiple roles for ATP in the proteasome. *EMBO J* **17**(17): 4909-4919.

San Filippo, J., Sung, P., and Klein, H. 2008. Mechanism of eukaryotic homologous recombination. *Annu Rev Biochem* **77**: 229-257.

Sancar, A., Lindsey-Boltz, L.A., Unsal-Kacmaz, K., and Linn, S. 2004a. Molecular mechanisms of mammalian DNA repair and the DNA damage checkpoints. *Annu Rev Biochem* **73**: 39-85.

Sancar, A. and Reardon, J.T. 2004b. Nucleotide excision repair in E. coli and man. *Adv Protein Chem* **69**: 43-71.

Savitsky, K., Bar-Shira, A., Gilad, S., Rotman, G., Ziv, Y., Vanagaite, L., Tagle, D.A., Smith, S., Uziel, T., Sfez, S. *et al.*,. 1995. A single ataxia telangiectasia gene with a product similar to PI-3 kinase. *Science* **268**(5218): 1749-1753.

Schauber, C., Chen, L., Tongaonkar, P., Vega, I., Lambertson, D., Potts, W., and Madura, K. 1998. Rad23 links DNA repair to the ubiquitin/proteasome pathway. *Nature* **391**(6668): 715-718.

Schmidt, M., Hanna, J., Elsasser, S., and Finley, D. 2005. Proteasome-associated proteins: regulation of a proteolytic machine. *Biol Chem* **386**(8): 725-737.

Scrima, A., Konickova, R., Czyzewski, B.K., Kawasaki, Y., Jeffrey, P.D., Groisman, R., Nakatani, Y., Iwai, S., Pavletich, N.P., and Thoma, N.H. 2008. Structural basis of UV DNA-damage recognition by the DDB1-DDB2 complex. *Cell* **135**(7): 1213-1223.

Seki, S., Ohzeki, M., Uchida, A., Hirano, S., Matsushita, N., Kitao, H., Oda, T., Yamashita, T., Kashihara, N., Tsubahara, A. *et al.*,. 2007. A requirement of FancL and FancD2 monoubiquitination in DNA repair. *Genes Cells* **12**(3): 299-310.

Sherr, C.J. and Roberts, J.M. 1999. CDK inhibitors: positive and negative regulators of G1-phase progression. *Genes Dev* **13**(12): 1501-1512.

Shi, W., Feng, Z., Zhang, J., Gonzalez-Suarez, I., Vanderwaal, R.P., Wu, X., Powell, S.N., Roti Roti, J.L., and Gonzalo, S. 2010. The role of RPA2 phosphorylation in homologous recombination in response to replication arrest. *Carcinogenesis* **31**(6): 994-1002.

Shieh, S.Y., Ahn, J., Tamai, K., Taya, Y., and Prives, C. 2000. The human homologs of checkpoint kinases Chk1 and Cds1 (Chk2) phosphorylate p53 at multiple DNA damage-inducible sites. *Genes Dev* **14**(3): 289-300.

Shivji, M.K., Podust, V.N., Hubscher, U., and Wood, R.D. 1995. Nucleotide excision repair DNA synthesis by DNA polymerase epsilon in the presence of PCNA, RFC, and RPA. *Biochemistry* **34**(15): 5011-5017.

Shuck, S.C., Short, E.A., and Turchi, J.J. 2008. Eukaryotic nucleotide excision repair: from understanding mechanisms to influencing biology. *Cell Res* **18**(1): 64-72.

Sigismund, S., Polo, S., and Di Fiore, P.P. 2004. Signaling through monoubiquitination. *Curr Top Microbiol Immunol* **286**: 149-185.

Sims, A.E., Spiteri, E., Sims, R.J., 3rd, Arita, A.G., Lach, F.P., Landers, T., Wurm, M., Freund, M., Neveling, K., Hanenberg, H. *et al.*,. 2007. FANCI is a second monoubiquitinated member of the Fanconi anemia pathway. *Nat Struct Mol Biol* **14**(6): 564-567.

Smogorzewska, A., Desetty, R., Saito, T.T., Schlabach, M., Lach, F.P., Sowa, M.E., Clark, A.B., Kunkel, T.A., Harper, J.W., Colaiacovo, M.P. *et al.*,. 2010. A genetic screen identifies FAN1, a Fanconi anemia-associated nuclease necessary for DNA interstrand crosslink repair. *Mol Cell* **39**(1): 36-47.

Smogorzewska, A., Matsuoka, S., Vinciguerra, P., McDonald, E.R., 3rd, Hurov, K.E., Luo, J., Ballif, B.A., Gygi, S.P., Hofmann, K., D'Andrea, A.D. *et al.*,. 2007. Identification of the FANCI protein, a monoubiquitinated FANCD2 paralog required for DNA repair. *Cell* **129**(2): 289-301.

So, S., Davis, A.J., and Chen, D.J. 2009. Autophosphorylation at serine 1981 stabilizes ATM at DNA damage sites. *J Cell Biol* **187**(7): 977-990.

Sobhian, B., Shao, G., Lilli, D.R., Culhane, A.C., Moreau, L.A., Xia, B., Livingston, D.M., and Greenberg, R.A. 2007. RAP80 targets BRCA1 to specific ubiquitin structures at DNA damage sites. *Science* **316**(5828): 1198-1202.

Somyajit, K., Subramanya, S., and Nagaraju, G. 2010. RAD51C: a novel cancer susceptibility gene is linked to Fanconi anemia and breast cancer. *Carcinogenesis* **31**(12): 2031-2038.

Sonoda, E., Okada, T., Zhao, G.Y., Tateishi, S., Araki, K., Yamaizumi, M., Yagi, T., Verkaik, N.S., van Gent, D.C., Takata, M. *et al.*,. 2003. Multiple roles of

Rev3, the catalytic subunit of polzeta in maintaining genome stability in vertebrates. *EMBO J* **22**(12): 3188-3197.

Sorensen, C.S., Syljuasen, R.G., Falck, J., Schroeder, T., Ronnstrand, L., Khanna, K.K., Zhou, B.B., Bartek, J., and Lukas, J. 2003. Chk1 regulates the S phase checkpoint by coupling the physiological turnover and ionizing radiation-induced accelerated proteolysis of Cdc25A. *Cancer Cell* **3**(3): 247-258.

Stein, J.J. 1967. The carcinogenic hazards of ionizing radiation in diagnostic and therapeutic radiology. *CA Cancer J Clin* **17**(6): 278-287.

Stephan, H., Concannon, C., Kremmer, E., Carty, M.P., and Nasheuer, H.P. 2009. Ionizing radiation-dependent and independent phosphorylation of the 32-kDa subunit of replication protein A during mitosis. *Nucleic Acids Res* **37**(18): 6028-6041.

Stokes, M.P., Rush, J., Macneill, J., Ren, J.M., Sprott, K., Nardone, J., Yang, V., Beausoleil, S.A., Gygi, S.P., Livingstone, M. *et al.*,. 2007. Profiling of UV-induced ATM/ATR signaling pathways. *Proc Natl Acad Sci U S A* **104**(50): 19855-19860.

Strzalka, W. and Ziemienowicz, A. 2011. Proliferating cell nuclear antigen (PCNA): a key factor in DNA replication and cell cycle regulation. *Ann Bot* **107**(7): 1127-1140.

Stucki, M., Clapperton, J.A., Mohammad, D., Yaffe, M.B., Smerdon, S.J., and Jackson, S.P. 2005. MDC1 directly binds phosphorylated histone H2AX to regulate cellular responses to DNA double-strand breaks. *Cell* **123**(7): 1213-1226.

Sudakin, V., Ganoth, D., Dahan, A., Heller, H., Hershko, J., Luca, F.C., Ruderman, J.V., and Hershko, A. 1995. The cyclosome, a large complex

containing cyclin-selective ubiquitin ligase activity, targets cyclins for destruction at the end of mitosis. *Mol Biol Cell* **6**(2): 185-197.

Sugasawa, K. 2006. UV-induced ubiquitylation of XPC complex, the UV-DDB-ubiquitin ligase complex, and DNA repair. *J Mol Histol* **37**(5-7): 189-202.

Sugasawa, K., Okamoto, T., Shimizu, Y., Masutani, C., Iwai, S., and Hanaoka, F. 2001. A multistep damage recognition mechanism for global genomic nucleotide excision repair. *Genes Dev* **15**(5): 507-521.

Sugasawa, K., Okuda, Y., Saijo, M., Nishi, R., Matsuda, N., Chu, G., Mori, T., Iwai, S., Tanaka, K., and Hanaoka, F. 2005. UV-induced ubiquitylation of XPC protein mediated by UV-DDB-ubiquitin ligase complex. *Cell* **121**(3): 387-400.

Sugiyama, T., Zaitseva, E.M., and Kowalczykowski, S.C. 1997. A single-stranded DNA-binding protein is needed for efficient presynaptic complex formation by the Saccharomyces cerevisiae Rad51 protein. *J Biol Chem* **272**(12): 7940-7945.

Sung, P. 1994. Catalysis of ATP-dependent homologous DNA pairing and strand exchange by yeast RAD51 protein. *Science* **265**(5176): 1241-1243.

Svendsen, J.M. and Harper, J.W. 2010. GEN1/Yen1 and the SLX4 complex: Solutions to the problem of Holliday junction resolution. *Genes Dev* **24**(6): 521-536.

Svendsen, J.M., Smogorzewska, A., Sowa, M.E., O'Connell, B.C., Gygi, S.P., Elledge, S.J., and Harper, J.W. 2009. Mammalian BTBD12/SLX4 assembles a Holliday junction resolvase and is required for DNA repair. *Cell* **138**(1): 63-77.

Takeshita, T., Wu, W., Koike, A., Fukuda, M., and Ohta, T. 2009. Perturbation of DNA repair pathways by proteasome inhibitors corresponds to enhanced

chemosensitivity of cells to DNA damage-inducing agents. *Cancer Chemother Pharmacol* **64**(5): 1039-1046.

Tanaka, T. and Nasmyth, K. 1998. Association of RPA with chromosomal replication origins requires an Mcm protein, and is regulated by Rad53, and cyclin- and Dbf4-dependent kinases. *EMBO J* **17**(17): 5182-5191.

Taniguchi, T. and D'Andrea, A.D. 2006. Molecular pathogenesis of Fanconi anemia: recent progress. *Blood* **107**(11): 4223-4233.

Taniguchi, T., Garcia-Higuera, I., Andreassen, P.R., Gregory, R.C., Grompe, M., and D'Andrea, A.D. 2002. S-phase-specific interaction of the Fanconi anemia protein, FANCD2, with BRCA1 and RAD51. *Blood* **100**(7): 2414-2420.

Taylor, W.R. and Stark, G.R. 2001. Regulation of the G2/M transition by p53. *Oncogene* **20**(15): 1803-1815.

Thoma, B.S. and Vasquez, K.M. 2003. Critical DNA damage recognition functions of XPC-hHR23B and XPA-RPA in nucleotide excision repair. *Mol Carcinog* **38**(1): 1-13.

Thrower, J.S., Hoffman, L., Rechsteiner, M., and Pickart, C.M. 2000. Recognition of the polyubiquitin proteolytic signal. *EMBO J* **19**(1): 94-102.

Tibbetts, R.S., Brumbaugh, K.M., Williams, J.M., Sarkaria, J.N., Cliby, W.A., Shieh, S.Y., Taya, Y., Prives, C., and Abraham, R.T. 1999. A role for ATR in the DNA damage-induced phosphorylation of p53. *Genes Dev* **13**(2): 152-157.

Tibbetts, R.S., Cortez, D., Brumbaugh, K.M., Scully, R., Livingston, D., Elledge, S.J., and Abraham, R.T. 2000. Functional interactions between BRCA1 and the checkpoint kinase ATR during genotoxic stress. *Genes Dev* **14**(23): 2989-3002.

Timmers, C., Taniguchi, T., Hejna, J., Reifsteck, C., Lucas, L., Bruun, D., Thayer, M., Cox, B., Olson, S., D'Andrea, A.D. *et al.*,. 2001. Positional cloning of a novel Fanconi anemia gene, FANCD2. *Mol Cell* **7**(2): 241-248.

Trincao, J., Johnson, R.E., Escalante, C.R., Prakash, S., Prakash, L., and Aggarwal, A.K. 2001. Structure of the catalytic core of S. cerevisiae DNA polymerase eta: implications for translesion DNA synthesis. *Mol Cell* **8**(2): 417-426.

Tsubuki, S., Kawasaki, H., Saito, Y., Miyashita, N., Inomata, M., and Kawashima, S. 1993. Purification and characterization of a Z-Leu-Leu-Leu-MCA degrading protease expected to regulate neurite formation: a novel catalytic activity in proteasome. *Biochem Biophys Res Commun* **196**(3): 1195-1201.

Tullis, R. and Price, P.A. 1974. The effect of calcium and magnesium on the ultraviolet spectrum of bovine pancreatic deoxyribonuclease A. *J Biol Chem* **249**(16): 5033-5037.

Turchi, J.J., Henkels, K.M., Hermanson, I.L., and Patrick, S.M. 1999. Interactions of mammalian proteins with cisplatin-damaged DNA. *J Inorg Biochem* **77**(1-2): 83-87.

Uziel, T., Lerenthal, Y., Moyal, L., Andegeko, Y., Mittelman, L., and Shiloh, Y. 2003. Requirement of the MRN complex for ATM activation by DNA damage. *EMBO J* **22**(20): 5612-5621.

Vaisman, A., Masutani, C., Hanaoka, F., and Chaney, S.G. 2000. Efficient translesion replication past oxaliplatin and cisplatin GpG adducts by human DNA polymerase eta. *Biochemistry* **39**(16): 4575-4580.

Varadan, R., Assfalg, M., Haririnia, A., Raasi, S., Pickart, C., and Fushman, D. 2004. Solution conformation of Lys63-linked di-ubiquitin chain provides clues to functional diversity of polyubiquitin signaling. *J Biol Chem* **279**(8): 7055-7063.

Varadan, R., Walker, O., Pickart, C., and Fushman, D. 2002. Structural properties of polyubiquitin chains in solution. *J Mol Biol* **324**(4): 637-647.

Voges, D., Zwickl, P., and Baumeister, W. 1999. The 26S proteasome: a molecular machine designed for controlled proteolysis. *Annu Rev Biochem* **68**: 1015-1068.

Voorhees, P.M. and Orlowski, R.Z. 2006. The proteasome and proteasome inhibitors in cancer therapy. *Annu Rev Pharmacol Toxicol* **46**: 189-213.

Wang, B., Matsuoka, S., Ballif, B.A., Zhang, D., Smogorzewska, A., Gygi, S.P., and Elledge, S.J. 2007. Abraxas and RAP80 form a BRCA1 protein complex required for the DNA damage response. *Science* **316**(5828): 1194-1198.

Wang, C. and Lambert, M.W. 2010. The Fanconi anemia protein, FANCG, binds to the ERCC1-XPF endonuclease via its tetratricopeptide repeats and the central domain of ERCC1. *Biochemistry* **49**(26): 5560-5569.

Wang, D. and Lippard, S.J. 2005a. Cellular processing of platinum anticancer drugs. *Nat Rev Drug Discov* **4**(4): 307-320.

Wang, H., Zhai, L., Xu, J., Joo, H.Y., Jackson, S., Erdjument-Bromage, H., Tempst, P., Xiong, Y., and Zhang, Y. 2006. Histone H3 and H4 ubiquitylation by the CUL4-DDB-ROC1 ubiquitin ligase facilitates cellular response to DNA damage. *Mol Cell* **22**(3): 383-394.

Wang, Q.E., Wani, M.A., Chen, J., Zhu, Q., Wani, G., El-Mahdy, M.A., and Wani, A.A. 2005b. Cellular ubiquitination and proteasomal functions positively modulate mammalian nucleotide excision repair. *Mol Carcinog* **42**(1): 53-64.

Wang, W., Nacusi, L., Sheaff, R.J., and Liu, X. 2005c. Ubiquitination of p21Cip1/WAF1 by SCFSkp2: substrate requirement and ubiquitination site selection. *Biochemistry* **44**(44): 14553-14564.

Wang, X., Andreassen, P.R., and D'Andrea, A.D. 2004a. Functional interaction of monoubiquitinated FANCD2 and BRCA2/FANCD1 in chromatin. *Mol Cell Biol* **24**(13): 5850-5862.

Wang, X. and D'Andrea, A.D. 2004b. The interplay of Fanconi anemia proteins in the DNA damage response. *DNA Repair (Amst)* **3**(8-9): 1063-1069.

Warren, M.R., Parker, C.E., Mocanu, V., Klapper, D., and Borchers, C.H. 2005. Electrospray ionization tandem mass spectrometry of model peptides reveals diagnostic fragment ions for protein ubiquitination. *Rapid Commun Mass Spectrom* **19**(4): 429-437.

Watkins, J.F., Sung, P., Prakash, L., and Prakash, S. 1993. The Saccharomyces cerevisiae DNA repair gene RAD23 encodes a nuclear protein containing a ubiquitin-like domain required for biological function. *Mol Cell Biol* **13**(12): 7757-7765.

Weisshart, K., Pestryakov, P., Smith, R.W., Hartmann, H., Kremmer, E., Lavrik, O., and Nasheuer, H.P. 2004. Coordinated regulation of replication protein A activities by its subunits p14 and p32. *J Biol Chem* **279**(34): 35368-35376.

Wilkinson, K.D. 2000. Ubiquitination and deubiquitination: targeting of proteins for degradation by the proteasome. *Semin Cell Dev Biol* **11**(3): 141-148.

Wittschieben, B.O., Iwai, S., and Wood, R.D. 2005. DDB1-DDB2 (xeroderma pigmentosum group E) protein complex recognizes a cyclobutane pyrimidine dimer, mismatches, apurinic/apyrimidinic sites, and compound lesions in DNA. *J Biol Chem* **280**(48): 39982-39989.

Wold, M.S. and Kelly, T. 1988. Purification and characterization of replication protein A, a cellular protein required for in vitro replication of simian virus 40 DNA. *Proc Natl Acad Sci U S A* **85**(8): 2523-2527.

Wood, R.D. 2010. Mammalian nucleotide excision repair proteins and interstrand crosslink repair. *Environ Mol Mutagen* **51**(6): 520-526.

Wright, J.A., Keegan, K.S., Herendeen, D.R., Bentley, N.J., Carr, A.M., Hoekstra, M.F., and Concannon, P. 1998. Protein kinase mutants of human ATR increase sensitivity to UV and ionizing radiation and abrogate cell cycle checkpoint control. *Proc Natl Acad Sci U S A* **95**(13): 7445-7450.

Wu, W.K., Cho, C.H., Lee, C.W., Wu, K., Fan, D., Yu, J., and Sung, J.J. 2010. Proteasome inhibition: a new therapeutic strategy to cancer treatment. *Cancer Lett* **293**(1): 15-22.

Xiao, Z., Chen, Z., Gunasekera, A.H., Sowin, T.J., Rosenberg, S.H., Fesik, S., and Zhang, H. 2003. Chk1 mediates S and G2 arrests through Cdc25A degradation in response to DNA-damaging agents. *J Biol Chem* **278**(24): 21767-21773.

Yamamoto, K.N., Kobayashi, S., Tsuda, M., Kurumizaka, H., Takata, M., Kono, K., Jiricny, J., Takeda, S., and Hirota, K. 2011. Involvement of SLX4 in interstrand cross-link repair is regulated by the Fanconi anemia pathway. *Proc Natl Acad Sci U S A* **108**(16): 6492-6496.

Yan, J., Kim, Y.S., Yang, X.P., Li, L.P., Liao, G., Xia, F., and Jetten, A.M. 2007. The ubiquitin-interacting motif containing protein RAP80 interacts with BRCA1 and functions in DNA damage repair response. *Cancer Res* **67**(14): 6647-6656.

Yaneva, M., Kowalewski, T., and Lieber, M.R. 1997. Interaction of DNA-dependent protein kinase with DNA and with Ku: biochemical and atomic-force microscopy studies. *EMBO J* **16**(16): 5098-5112.

Yang, Y., Kitagaki, J., Wang, H., Hou, D.X., and Perantoni, A.O. 2009. Targeting the ubiquitin-proteasome system for cancer therapy. *Cancer Sci* **100**(1): 24-28.

Yao, J., Dixon, K., and Carty, M.P. 2001. A single (6-4) photoproduct inhibits plasmid DNA replication in xeroderma pigmentosum variant cell extracts. *Environ Mol Mutagen* **38**(1): 19-29.

Yazdi, P.T., Wang, Y., Zhao, S., Patel, N., Lee, E.Y., and Qin, J. 2002. SMC1 is a downstream effector in the ATM/NBS1 branch of the human S-phase checkpoint. *Genes Dev* **16**(5): 571-582.

Ye, Y. and Rape, M. 2009. Building ubiquitin chains: E2 enzymes at work. *Nat Rev Mol Cell Biol* **10**(11): 755-764.

Yu, H., King, R.W., Peters, J.M., and Kirschner, M.W. 1996. Identification of a novel ubiquitin-conjugating enzyme involved in mitotic cyclin degradation. *Curr Biol* **6**(4): 455-466.

Yu, Y., Wang, W., Ding, Q., Ye, R., Chen, D., Merkle, D., Schriemer, D., Meek, K., and Lees-Miller, S.P. 2003. DNA-PK phosphorylation sites in XRCC4 are not required for survival after radiation or for V(D)J recombination. *DNA Repair (Amst)* **2**(11): 1239-1252.

Yu, Z.K., Geyer, R.K., and Maki, C.G. 2000. MDM2-dependent ubiquitination of nuclear and cytoplasmic P53. *Oncogene* **19**(51): 5892-5897.

Yunmbam, M.K., Li, Q.Q., Mimnaugh, E.G., Kayastha, G.L., Yu, J.J., Jones, L.N., Neckers, L., and Reed, E. 2001. Effect of the proteasome inhibitor ALLnL on cisplatin sensitivity in human ovarian tumor cells. *Int J Oncol* **19**(4): 741-748.

Zernik-Kobak, M., Vasunia, K., Connelly, M., Anderson, C.W., and Dixon, K. 1997. Sites of UV-induced phosphorylation of the p34 subunit of replication protein A from HeLa cells. *J Biol Chem* **272**(38): 23896-23904.

Zhang, A., Lyu, Y.L., Lin, C.P., Zhou, N., Azarova, A.M., Wood, L.M., and Liu, L.F. 2006. A protease pathway for the repair of topoisomerase II-DNA covalent complexes. *J Biol Chem* **281**(47): 35997-36003.

Zhang, Y. and Xiong, Y. 2001. A p53 amino-terminal nuclear export signal inhibited by DNA damage-induced phosphorylation. *Science* **292**(5523): 1910-1915.

Zhang, Y.W., Otterness, D.M., Chiang, G.G., Xie, W., Liu, Y.C., Mercurio, F., and Abraham, R.T. 2005. Genotoxic stress targets human Chk1 for degradation by the ubiquitin-proteasome pathway. *Mol Cell* **19**(5): 607-618.

Zhao, G.Y., Sonoda, E., Barber, L.J., Oka, H., Murakawa, Y., Yamada, K., Ikura, T., Wang, X., Kobayashi, M., Yamamoto, K. *et al.*,. 2007. A critical role for the ubiquitin-conjugating enzyme Ubc13 in initiating homologous recombination. *Mol Cell* **25**(5): 663-675.

Zhao, H. and Piwnica-Worms, H. 2001. ATR-mediated checkpoint pathways regulate phosphorylation and activation of human Chk1. *Mol Cell Biol* **21**(13): 4129-4139.

Zhao, S., Weng, Y.C., Yuan, S.S., Lin, Y.T., Hsu, H.C., Lin, S.C., Gerbino, E., Song, M.H., Zdzienicka, M.Z., Gatti, R.A. *et al.*,. 2000. Functional link between ataxia-telangiectasia and Nijmegen breakage syndrome gene products. *Nature* **405**(6785): 473-477.

Zhou, B.B. and Elledge, S.J. 2000. The DNA damage response: putting checkpoints in perspective. *Nature* **408**(6811): 433-439.

Zhuang, Z., Johnson, R.E., Haracska, L., Prakash, L., Prakash, S., and Benkovic, S.J. 2008. Regulation of polymerase exchange between Poleta and Poldelta by monoubiquitination of PCNA and the movement of DNA polymerase holoenzyme. *Proc Natl Acad Sci U S A* **105**(14): 5361-5366.

Zou, L. and Elledge, S.J. 2003. Sensing DNA damage through ATRIP recognition of RPA-ssDNA complexes. *Science* **300**(5625): 1542-1548.

Chapter 7
Publications

DNA Polymerase η, a Key Protein in Translesion Synthesis in Human Cells

Séverine Cruet-Hennequart, Kathleen Gallagher, Anna M. Sokòl, Sangamitra Villalan, Áine M. Prendergast, and Michael P. Carty

Abstract Genomic DNA is constantly damaged by exposure to exogenous and endogenous agents. Bulky adducts such as UV-induced cyclobutane pyrimidine dimers (CPDs) in the template DNA present a barrier to DNA synthesis by the major eukaryotic replicative polymerases including DNA polymerase δ. Translesion synthesis (TLS) carried out by specialized DNA polymerases is an evolutionarily conserved mechanism of DNA damage tolerance. The Y family of DNA polymerases, including DNA polymerase η (Pol η), the subject of this chapter, play a key role in TLS. Mutations in the human *POLH* gene encoding Pol η underlie the genetic disease xeroderma pigmentosum variant (XPV), characterized by sun sensitivity, elevated incidence of skin cancer, and at the cellular level, by delayed replication and hypermutability after UV-irradiation. Pol η is a low fidelity enzyme when copying undamaged DNA, but can carry out error-free TLS at sites of UV-induced dithymine CPDs. The active site of Pol η has an open conformation that can accommodate CPDs, as well as cisplatin-induced intrastrand DNA crosslinks. Pol η is recruited to sites of replication arrest in a tightly regulated process through interaction with PCNA. Pol η-deficient cells show strong activation of downstream DNA damage responses including ATR signaling, and accumulate strand breaks as a result of replication fork collapse. Thus, Pol η plays an important role in preventing genome instability after UV- and cisplatin-induced DNA damage. Inhibition of DNA damage tolerance pathways in tumors might also represent an approach to potentiate the effects of DNA damaging agents such as cisplatin.

Keywords DNA polymerase eta · Translesion synthesis · XPV · UV · Cisplatin · DDR

M.P. Carty (✉)
Centre for Chromosome Biology, School of Natural Sciences, National University of Ireland, Galway, University Rd, Galway, Ireland
e-mail: michael.carty@nuigalway.ie

H.P. Nasheuer (ed.), *Genome Stability and Human Diseases*, Subcellular Biochemistry 50, DOI 10.1007/978-90-481-3471-7_10,

Abbreviations

ATM	ataxia-telangiectasia mutated
ATR	ATM and Rad3-related
ATRIP	ATR-interacting protein
CPD	cyclobutane pyrimidine dimer
DDR	DNA damage response
DNA-PK	DNA-dependent protein kinase
Pol η	DNA polymerase eta
RPA	replication protein A
XPV	xeroderma pigmentosum variant

Introduction

Environmental and metabolic insults such as radiation, chemical agents and oxidative stress can generate DNA lesions, leading to mutation fixation, DNA strand breaks and genomic instability. DNA damage from exposure to UV radiation can lead to cancer, while DNA damaging agents such as platinum-based drugs are routinely used to kill tumor cells in chemotherapy. Cells that are actively carrying out DNA replication are particularly vulnerable to DNA damage, as endogenous and exogenous events challenge genome integrity by interfering with the progression, stability and restart of the replication fork. A number of DNA repair and DNA damage tolerance pathways counteract the deleterious consequences of DNA damage (Branzei and Foiani, 2008; Chang and Cimprich, 2009; Branzei and Foiani, 2007, see review "DNA Polymerases and Mutagenesis in Human Cancers" by Crespan et al., this book). Despite the presence of dedicated DNA repair pathways, not all damage is removed from the genome before DNA synthesis proceeds. A better understanding of the proteins involved in replication of damaged DNA is of relevance both to cancer initiation, and to cancer treatment using DNA damaging agents to induce replication-blocking lesions (Bartek et al., 2007).

Many DNA damaging agents induce lesions that block DNA synthesis by the replicative DNA polymerases α, δ and ε that normally carry out replication of genomic DNA (see review "DNA Polymerases and Mutagenesis in Human Cancers" by Crespan et al., this book). However, the fact that cells can complete replication in the presence of unrepaired damage indicates the existence of pathways that facilitate replication of damaged DNA without prior lesion removal. These are often referred to as post-replication repair (PRR) pathways, and in recent years have been more clearly defined at the molecular level. The main PRR pathways are translesion synthesis (TLS) involving low fidelity DNA polymerases such as DNA polymerase η (Pol η) (the subject of this review), and error-free PRR, a process that involves fork reversal and template strand switching (Chang and Cimprich, 2009; Hishida et al., 2009).

TLS has been extensively studied over the past decade, and involves the recruitment of specialized DNA polymerases to carry out replication past the lesion site

in the template strand (Branzei and Foiani, 2007; Branzei and Foiani, 2008; Chang and Cimprich, 2009). TLS represents a major mechanism for DNA damage tolerance in all species, being conserved through evolution from bacteria to humans. In *E. coli*, DNA polymerase V, the *umuC* gene product is required for TLS, and the main TLS polymerases, from yeast to humans, show homology to *E. coli* umuC gene. The *RAD30* gene encoding DNA polymerase η was first identified in *S. cerevisiae* (McDonald et al., 1997). The cloning of the human *RAD30* gene in 1999, and the demonstration that mutations in this gene leading to elimination of the full length active Pol η protein were found in all patients with the skin cancer-prone, sun sensitive genetic disease xeroderma pigmentosum variant (XPV) (Cleaver, 1972), provided a major impetus for further research into the process of TLS (Johnson et al., 1999a; Masutani et al., 1999b).

The human *RAD30* (*POLH*) gene is located on chromosome 6p21.1-6p12, and consists of 11 exons, of which exon 1 is untranslated (Yuasa et al., 2000). It was shown that purified Pol η, a 713 amino acid, 78 kDa protein could restore the ability of cell extracts from XPV cell lines to carry out complete replication of plasmid DNA containing a thymine-thymine cyclobutane pyrimidine dimer (CPD) in vitro (Masutani et al., 1999a). DNA polymerase ι (Pol ι), the product of the human *RAD30B* gene (McDonald et al., 1999), is highly homologous to Pol η, but can not substitute for it in TLS at sites of UV-induced damage. Most human TLS DNA polymerases, including Pol η, Pol ι, and Pol κ (Gerlach et al., 1999; Ogi et al., 1999), belong to the Y-family of DNA polymerases (Burgers et al., 2001; Lehmann et al., 2007; McCulloch and Kunkel, 2008). The dCMP transferase Rev1 (Nelson et al., 1996) also belongs to the Y family. However, the Rev3/Rev7 gene product, Pol ζ, which plays an important role in TLS for a number of lesions, belongs to the B family of DNA polymerases (Burgers et al., 2001; Lawrence and Maher, 2001). While TLS is often considered error-prone, several TLS polymerases can carry out error-free bypass of specific lesions (McCulloch and Kunkel, 2008; Prakash et al., 2005). This chapter will focus on Pol η, one of the Y family of DNA polymerases.

DNA Polymerase η, a Member of the Y Family of Polymerases

Unlike the replicative polymerases δ and ε, TLS polymerases, including Pol η, lack a 3′-5′ proofreading exonuclease activity and have high error rates, on the order 10^{-2}–10^{-4}, for base substitutions during DNA synthesis on undamaged DNA (McCulloch and Kunkel, 2008). However, compared to other DNA polymerases, TLS polymerases generally contain a more open active site which can accommodate bulky damaged bases (Friedberg, 2001; Ling et al., 2001; Trincao et al., 2001). This structural feature facilitates nucleotide incorporation opposite lesions in the DNA template; incorporation may be error-free or error-prone depending on the specific lesion to be bypassed.

Sequence alignment of the N-termini of Pol η proteins from lower to higher eukaryotes, revealed five conserved motifs, motifs I–V, and nine highly conserved

acidic residues (Kondratick et al., 2001). Three highly conserved acidic amino acids, present within the motifs I and III, are essential for polymerase activity, by coordinating the two metal ions in the active site necessary for catalytic activity (Kondratick et al., 2001). In human Pol η, an invariant tyrosine (Y52) and arginine (R55) in motif II, and an invariant lysine (K231) residue in motif IV, contribute to nucleotide binding and incorporation during DNA synthesis (Glick et al., 2003; Glick et al., 2001; Johnson et al., 2003). Motif V is a structural feature unique to Y family polymerases, termed the little finger (LF) domain or the polymerase-associated (PAD) domain (Yang and Woodgate, 2007). While all five motifs are essential for DNA synthesis, motif V is much less conserved between the Y-family polymerases than are the other motifs (Prakash et al., 2005). The C-terminus of Pol η contains the nuclear localization signal, as well as a number of structural features that play key roles in the recruitment of the DNA polymerase to sites of DNA damage. These include the PCNA-interacting peptide (PIP) domain (Haracska et al., 2001a), the ubiquitin-binding zinc finger (UBZ) domain (Bienko et al., 2005), and the Rev1-interacting region (Yang and Woodgate, 2007).

Y-family DNA polymerases, including Pol η, differ strikingly from high-fidelity DNA polymerases in that the active site is much more open. Crystallization of the catalytic core of yeast Pol η (Trincao et al., 2001), and of the related Dpo4 DNA polymerase from *Sulfolobus solfataricus* (Ling et al., 2001), with an oligonucleotide containing a thymine-thymine CPD demonstrated that the active site can accommodate both residues of the CPD. Human Pol η is specialized to preferentially insert two adenines opposite thymine-thymine CPDs, to carry out largely error-free bypass of this lesion (Carty et al., 2003; Cleaver et al., 2002a; Cordeiro-Stone and Nikolaishvili-Feinberg, 2002; Johnson et al., 1999a; Masutani et al., 2000; Stary et al., 2003; Thakur et al., 2001; Yao et al., 2001). The importance of Pol η in preventing UV-induced mutations and skin carcinogenesis is underlined by the demonstration that the human genetic disease xeroderma pigmentosum variant (XPV) results from loss of functional Pol η due to mutations in *POLH* (Johnson et al., 1999a; Masutani et al., 1999b). XPV patients account for almost 20% of XP cases and show UV-sensitivity, and strong predisposition to skin cancer (Cleaver, 1972). XPV cells have normal rates of nucleotide excision repair, but have a defect in DNA synthesis, and are hypermutable, after UV-irradiation (Lehmann, 1975; Tung et al., 1996). In the absence of Pol η, mutations in XPV cells accumulate at CPD sites, as a result of error-prone bypass by another TLS polymerase, possibly Pol ι (Gueranger et al., 2008; Stary et al., 2003; Wang et al., 2007). Thus, error-free TLS by Pol η plays a key role in preventing mutation fixation at CPD sites, the most common UV-induced lesion, and reduces the incidence of UV-induced skin cancer in the population (McCulloch et al., 2004; Johnson et al., 1999b). Knockout of the *POLH* gene in mice recapitulates the skin cancer susceptibility observed in Pol η-deficient XPV patients (Lin et al., 2006).

However, while Pol η carries out efficient and accurate replication at sites of thymine-thymine CPDs, for other lesions, Pol η has reduced affinity, poor incorporation rates or low fidelity (Vaisman et al., 2004; Shachar et al., 2009; McCulloch and Kunkel, 2008). UV light induces both CPDs and [6-4] pyrimidine-pyrimidone

photoproducts ([6-4PP]). CPDs are more abundant than [6-4]PPs in UV-irradiated DNA; however [6-4]PPs induce greater structural distortion in the DNA double helix, and probably for this reason are more mutagenic than CPDs, and are repaired faster by the nucleotide excision repair pathway (Vreeswijk et al., 1994). Purified Pol η can not bypass a thymine-thymine [6-4]PP in an oligonucleotide template in vitro (Masutani et al., 2000), but can insert a nucleotide opposite the 3′ base of the [6-4]PP. Combination of Pol η with purified Pol ζ allowed efficient bypass of a [6-4]PP in vitro (Johnson et al., 2001), leading to the proposal that bypass of certain lesions, such as the [6-4]PP, could be accomplished by a two-polymerase mechanism, wherein Pol η (or a related Y family DNA polymerase) inserts a nucleotide opposite the 3′ base of the lesion, with subsequent insertion of a nucleotide opposite the 5′ base, and extension of the primer terminus being carried out by Pol ζ, the *REV3L* gene product (Johnson et al., 2001; Shachar et al., 2009). Consistent with such a role for Pol η, it was found that, compared to extracts of normal cells, Pol η-deficient lymphoblast cell extracts were defective in replication of plasmid DNA containing a single thymine-thymine [6-4]PP in vitro (Yao et al., 2001). Other studies indicate that Pol η plays a role in bypass of [6-4]PP in some, but not all human cell lines, examined (Hendel et al., 2008). An important role for Pol ζ in bypass of [6-4]PPs was reported in the recent study of Shachar et al. (2009) in which gapped templates containing a unique [6-4]PP were transfected into U2OS cells and the level of individual DNA polymerases was down-regulated using siRNA. An investigation of the requirements for replication of modified plasmids containing a site-specific [6-4]PP in chicken DT40 cells also found a key role for Pol ζ in TLS at this lesion (Szuts et al., 2008). The relative contribution of TLS DNA polymerases to bypass of the [6-4]PP in different cell types requires further investigation.

Role of Pol η in Bypass of Lesions Induced by Platinum-Based Chemotherapeutic Drugs

In addition to its main biological role in bypass of UV-induced CPDs, recent interest has focused on the role of Pol η in bypass of lesions induced by platinum-based chemotherapeutic drugs, since damage tolerance by TLS may contribute to the resistance of tumor cells to chemotherapy. Since its accidental discovery 40 years ago, cisplatin (cis-diamminedichloroplatinum (II)) has been successfully used in the treatment of a number of human cancers, including testicular cancer, small cell lung cancer and lymphoma (Kelland, 2007b). Studies on cancer resistance and improvement of drug selectivity towards cancer cells led the development of cisplatin analogues, including carboplatin [*cis*-diammine(1,1-cyclobutanedicarboxylate)-platinum(II)], and oxaliplatin [(*trans*-*R*,*R*)1,2 diaminocyclohexaneoxalatoplatinum(II) (Aabo et al., 1998; Kelland, 2007a). Platinum-based chemotherapeutic agents damage DNA by covalent binding primarily to guanine residues, leading to the formation of monoadducts, intrastrand

and interstrand cross-links (Chaney et al., 2005; Kartalou and Essigmann, 2001). Intrastrand adducts between two adjacent guanines are the most common lesion. Pt-DNA adducts are removed by a combination of DNA repair pathways, including nucleotide excision repair (Chaney et al., 2005; Kelland, 2007b). However, not all platinum lesions are repaired prior to DNA replication, and the role of TLS in preventing DNA replication arrest at unrepaired lesions has received considerable attention in recent years.

Two lines of evidence support a role for Pol η in the response of human cells to replication-blocking platinum-DNA lesions. Firstly, in vitro experiments using purified Pol η and oligonucleotide templates containing a single guanine-guanine cisPt-DNA intrastrand adduct demonstrated that Pol η can bypass the platinum-guanine-guanine adduct more efficiently than other eukaryotic DNA polymerases (Masutani et al., 2000; Vaisman et al., 2000). The accuracy of lesion bypass is influenced by the sequence context of the lesion, but appears to be relatively error-free (Shachar et al., 2009). Secondly, cell lines lacking Pol η are more sensitive to cell killing by platinum-based drugs (Yamada et al., 2003; Bassett et al., 2004; Chaney et al., 2005; Chen et al., 2006; Albertella et al., 2005a). The demonstration that Pol η-deficient cell lines are sensitive to platinum-based chemotherapeutic agents has led to increased interest in the role of this enzyme in determining the outcome of exposure to these agents.

Structural and biochemical analysis of cisplatin-DNA lesion bypass by Pol η has revealed the set of structural features that enable Pol η to carry out replication across these strongly distorting DNA lesions (Alt et al., 2007). The large fragment of yeast Pol η was co-crystallized in a complex with incoming dNTPs and a template containing a site-specific Pt-GG adduct. When Pol η encounters a Pt-DNA lesion, the adduct is situated outside the active site. Two steps are required for lesion bypass. First, there is an efficient and error-free elongation step at the 3′dG, in which the incoming dCTP forms a Watson-Crick base pair with the 3′dG of the Pt-GG adduct in the enzyme active site. Second, there is a slower, less-efficient step which involves incorporation of either dCTP or dATP opposite the 5′dG of the adduct (Alt et al., 2007). This allows for incorporation of either dATP and dCTP at the lesion site, consistent with in vitro studies using purified Pol η in primer extension assays on oligomeric templates containing Pt-GG lesions (Masutani et al., 2000). Site-directed mutagenesis of yeast Pol η demonstrated that arginine 73, located in the enzyme active site plays a key role in bypass of the Pt-GG lesion (Alt et al., 2007). Understanding the structural requirements for lesion bypass by Pol η could aid in the development of modified platinum-based drugs which generate DNA adducts that are bypassed less efficiently in vivo (Alt et al., 2007).

The efficiency of bypass of Pt-GG adducts by purified Pol η in vitro is comparable to the bypass of CPDs; bypass of oxaliplatin lesions is more efficient than bypass of cisplatin lesions (Chaney et al., 2005; Vaisman et al., 2000; Bassett et al., 2003). The greater efficiency of Pol η in bypass of oxaliplatin adducts could account for the lower mutagenicity of oxaliplatin when compared to cisplatin (Chaney et al., 2005). Pol ζ may also play a role in bypass of Pt-GG adducts in vivo, as part of a two-polymerase mechanism for TLS, by extending the primer terminus following

insertion of nucleotides opposite the lesion by Y-family DNA polymerases (Shachar et al., 2009).

Role of Pol η in Bypass of Other Lesions in DNA

As described above, it is clear that Pol η is proficient in bypassing both UV and cisplatin-induced lesions in DNA. In addition to these lesions, Pol η can carry out efficient and accurate replication past an 8-oxoguanine (8-oxoG) lesion in vitro (Haracska et al., 2000b). 8-oxoG results from exposure of mammalian cells to oxidative stress; by promoting error-free replication through the 8-oxoG lesion, Pol η may contribute to reducing mutagenesis and carcinogenesis that could result from mutagenic bypass of this lesion by replicative DNA polymerases (Haracska et al., 2000b). Pol η has also been shown to bypass O^6-methylguanine (me^6G) (Haracska et al., 2000a) in vitro as well as lesions induced by the chemotherapeutic nucleoside analogues AraC and gemcitabine (Chen et al., 2006).

Purified Pol η bypasses N^2-deoxyguanosine DNA adducts formed by benzo[a]pyrene 7,8-diol 9,10-epoxide (BPDE) (Haracska et al., 2001d), butadiene epoxide (Minko et al., 2001), and the acrolein-derived adduct γ-hydroxy-1,N^2-propano-deoxyguanosine (γ-HOPdG) (Minko et al., 2003), but with a lower efficiency at both the nucleotide incorporation and extension steps. In the case of lesions induced by BPDE, DNA polymerase kappa (Pol κ) may play a more important role in TLS (Avkin et al., 2004; Shachar et al., 2009; Zhang et al., 2002).

In addition to its role in TLS during replication of DNA damaged by exogenous agents such as UV light, Pol η has also been implicated in other DNA transactions, including somatic hypermutation (Masuda et al., 2007; Diaz and Lawrence, 2005; Casali et al., 2006), strand invasion during homologous recombination (McIlwraith et al., 2005; Kawamoto et al., 2005), and DNA replication under conditions of nucleotide depletion (de Feraudy et al., 2007). A recent report indicates that naturally occurring DNA structures (such as G4-DNA, H-DNA, or Z-DNA) are also physiological substrates of Pol η, suggesting that Pol η may play a role in preventing genomic instability at certain DNA sequences that are capable of forming unusual secondary structures in human cells (Bétous et al., 2009).

Regulation of Pol η Recruitment

TLS DNA polymerases carry out DNA synthesis on undamaged templates with low fidelity. Thus, access of Y family DNA polymerases to primer termini during replication of genomic DNA in human cells must be tightly regulated, to prevent accumulation of mutations in the genome. Because the active sites of replicative DNA polymerases, including Pol α and Pol δ are unable to accommodate bulky lesions caused by UV or cisplatin, following replication arrest at sites of DNA damage, processive DNA polymerases are temporarily replaced by TLS DNA

polymerases to allow TLS to be carried out at the lesion site. During replication on undamaged DNA, Pol δ forms a stable holoenzyme with proliferating cell nuclear antigen (PCNA), and carries out processive and error-free DNA replication (Garg and Burgers, 2005; Nasheuer et al., 2002, 2007). PCNA plays an important role in DNA replication by modifying the function of the replicative Pols δ and ε, as well as by interaction with a number of proteins involved in cell cycle progression and DNA repair. PCNA is loaded onto DNA by the clamp loader, replication factor C (RFC), forming a homotrimeric ring on the DNA strand. Following loading of PCNA, RFC remains bound to DNA through its interaction with the single-stranded DNA binding protein, replication protein A (RPA) (Bambara et al., 1997; Kelman and Hurwitz, 1998). When Pol δ encounters a damaged base in the template, and is unable to continue replication, a switch to a specialized TLS DNA polymerase such as Pol η is required to allow lesion bypass to occur. The mechanism of the switch between the replicative DNA polymerase and the TLS DNA polymerase at the damage site has been the subject of much investigation. In *E. coli*, the β clamp can bind to both the replicative DNA polymerase III and the TLS Pol IV at the same time, and this interaction is necessary for the polymerase switch (Indiani et al., 2005). In eukaryotic cells, post-translational modification of accessory proteins regulates the recruitment and activity of Pol η. In *S. cerevisiae,* the major modification is ubiquitination of the trimeric sliding clamp, PCNA on lysine 164 by the ubiquitin-conjugating enzyme complex, Rad6/Rad18 (Hoege et al., 2002). Rad6, an E2 ubiquitin-conjugating enzyme acts in concert with Rad18, an E3 ubiquitin ligase, to monoubiquitinate PCNA. Rad6/Rad18-dependent monoubiquitination of PCNA on lysine 164 promotes translesion DNA synthesis involving Pol η (Stelter and Ulrich, 2003; Haracska et al., 2004). Davies et al. (2008) reported that RPA interacts directly with Rad18 in both yeast and mammalian cells, indicating that RPA is also required for DNA damage-induced PCNA ubiquitination (Davies et al., 2008). Both yeast and human Pol η, as well as the other TLS DNA polymerases, Pol ι and Pol κ, interact with PCNA physically and functionally (Haracska et al., 2001a; Haracska et al., 2001b; Haracska et al., 2002). In human cells, Pol η is associated with replication forks during S phase, and forms nuclear foci following damage induced by UV or cisplatin, but not after induction of double-strand breaks by IR (Kannouche et al., 2001). Pol ι colocalises and interacts with Pol η in damage-induced nuclear foci. However, in Pol η-deficient XPV cells the percentage of cells with Pol ι foci is reduced suggesting that Pol η plays a role in the localization of Pol ι to foci (Kannouche et al., 2003).

Human DNA Pol η interacts with both unmodified and monoubiquitinated PCNA (Kannouche et al., 2004; Hoege et al., 2002). Pol η can bind to the interdomain connector loop of unmodified PCNA, through the PCNA-interacting peptide (PIP) located in the extreme C-terminal of Pol η. Pol η binds with greater affinity to monoubiquitinated PCNA (Kannouche et al., 2004). In *S. cerevisiae*, inactivation of the PIP domain of Pol η inhibits TLS (Haracska et al., 2001c). A second PIP domain, located just C-terminal to the polymerase-associated domain (PAD), has also been identified in human Pol η (Acharya et al., 2008). Mutational analysis, performed in XPV cells complemented with Pol η having mutations in the PIP domains, indicated

that both PIP domains are necessary for TLS (Acharya et al., 2008). Inactivation of one domain slightly impairs, but does not completely abolish, the function of Pol η. Mutation of both PIP domains eliminates the ability of Pol η to form nuclear foci, and to carry out TLS in vivo, and confers the same UV sensitivity as that seen in Pol η-deficient XPV cells (Acharya et al., 2008).

Human Pol η also contains a C_2H_2 ubiquitin-binding zinc finger (UBZ) domain, located between the catalytic domain of the DNA polymerase and the PIP domain (Bienko et al., 2005; Plosky et al., 2006). The solution structure of the UBZ domain of Pol η has been determined using nuclear magnetic resonance (Bomar et al., 2007). The UBZ domain consists of two short anti-parallel β-strands and a carboxy-terminal α-helix, with a zinc ion located between the α-helix and β-strands. The UBZ domain binds ubiquitin through its C-terminal α-helix, and together with the PIP domain, enhances the binding of Pol η to monoubiquitinated PCNA (Bomar et al., 2007). The role of this binding domain in the polymerase switch and in TLS is still under investigation. Bienko et al. (2005) demonstrated that expression of Pol η, carrying a C638A mutation in the UBZ domain, in XPV cells resulted in UV sensitivity, while a D652A mutant of Pol η failed to form foci in UV-treated cells (Bienko et al., 2005). An extensive mutational analysis of the UBZ domain of Pol η, in which five different residues in the domain were altered (Acharya et al., 2008) indicates that not all mutations in the UBZ affect the function of Pol η in TLS. The UBZ mutant proteins were able to form replication foci following UV-irradiation to the same extent in the presence of Ub-PCNA or unmodified PCNA (Acharya et al., 2008). This indicates that the binding of Pol η to PCNA only requires the PIP domains of Pol η, and that mono-ubiqiuitination of PCNA on lysine 164 is not strictly required for Pol η binding. The role of ubiquitination of PCNA may result from the fact that ubiquitin alters the conformation of PCNA, making it more accessible to the PIP domain of Pol η when replication is stalled at sites of damage (Acharya et al., 2008). Support for this hypothesis comes from a study in yeast, demonstrating that Pol η can only replace Pol δ at DNA replication forks in the presence of Ub-PCNA but not unmodified PCNA (Zhuang et al., 2008). The PIP domain of Pol η was required for this switch (Zhuang et al., 2008).

Deubiquitination of PCNA may cause dissociation of Pol η once TLS has taken place, and allow the recruitment of Pol δ and resumption of processive replication. PCNA is de-ubiquitinated by the de-ubiquinating enzyme USP1. The importance of USP1 in regulating the level of Ub-PCNA is supported by the observation that in UV-irradiated human cell lines, UPS1 undergoes autocleavage, allowing PCNA to be monoubiquitinated (Huang et al., 2006). It has also been shown that PCNA can be polyubiquitinated on lysine 164, as well being SUMOylated at two sites, K127 and K164 (Hoege et al., 2002). These modifications may offer an additional level of regulation of translesion synthesis by Pol η.

An important question with regard to the regulation of TLS is whether lesion bypass occurs directly at the arrested replication fork, or alternatively, whether the replication fork proceeds, leaving gaps in the nascent strand that are subsequently filled by TLS after fork passage. Whether this is related to different requirements for TLS on the leading and lagging strands (Yao et al., 2001) requires further

investigation. A recent study in chicken DT40 cells investigated the requirements for these two processes (Edmunds et al., 2008). PCNA mono-ubiquitiation was found be essential for filling of post-replicative gaps (Edmunds et al., 2008). In contrast, both the TLS DNA polymerase-interaction domain and the ubiquitin-binding domain of Rev1 were required to maintain fork progression at sites of damage (Edmunds et al., 2008). Rev1 interacts with a number of other Y family DNA polymerases, and may play a role in loading TLS DNA polymerases at the lesion site (Edmunds et al., 2008). Pol η itself is ubiquitinated (Bienko et al., 2005), which may also modulate its interaction with Rev1.

Activation of DNA Damage Responses in Pol η-Deficient Cells

It is now recognized that TLS is an integral component of the network of DNA damage responses in the cell. Both replication arrest which generates single-stranded DNA, and DNA strand break formation resulting from replication fork collapse, activate downstream DNA damage response (DDR) pathways mediated by the phosphoinositide 3-kinase (PI-3 K)-related protein kinases (PIKKs) (Cimprich and Cortez, 2008). The PIKK family consists of five serine-threonine kinases, including ataxia-telangiectasia mutated (ATM), ATM and RAD3-related (ATR), DNA-protein kinase catalytic subunit (DNA-PKcs), mammalian target of rapamycin (mTOR; also known as FRAP) and hSMG1 (Abraham, 2004; Bakkenist and Kastan, 2004; Branzei and Foiani, 2008; Cimprich and Cortez, 2008; Durocher and Jackson, 2001; Harper and Elledge, 2007). ATM, ATR, and DNA-PK, high molecular weight protein kinases with significant sequence homology, act as primary transducers of the DDR, by phosphorylation of a large number of downstream protein substrates to initiate signaling cascades that ultimately result in cell cycle arrest or in apoptosis (Abraham, 2004; Zhou and Elledge, 2000; Matsuoka et al., 2007). ATR is activated following replication fork arrest, while ATM and DNA-PK are activated by DNA strand breaks (Harper and Elledge, 2007).

Compared to normal cells, Pol η-deficient XPV cells show extended replication fork arrest after UV-irradiation, characterized by the formation of shorter nascent DNA strands, and the generation of extensive regions of single-stranded DNA (Cordeiro-Stone et al., 1999; Cordeiro-Stone et al., 1997). In addition, replication forks arrested at sites of UV-induced damage in Pol η-deficient XPV cells may collapse, generating DNA double-strand breaks (Limoli et al., 2002a) or more correctly, DNA double-strand ends (Shrivastav et al., 2008). XPV cells, but not normal cells, are hypersensitive to both UV radiation and cisplatin when grown in the presence of caffeine, a non-specific inhibitor ATM and ATR (Sarkaria et al., 1999), indicating that PIKK signaling may be altered in Pol η-deficient cells (Thakur et al., 2001; Arlett et al., 1975; Yamada et al., 2000; Yamada et al., 2003; Cleaver et al., 1999). The response of XPV cells to wortmannin, an inhibitor of DNA-PK and ATM (Sarkaria et al., 1998), is also altered (Limoli et al., 2002b).

To minimize the detrimental effects of DNA damage on genome stability, replication arrest at lesion sites activates S-phase checkpoints (Zhou and Elledge, 2000).

In Pol η-deficient XPV cells, extensive regions of single-stranded DNA (ssDNA) are generated as a result of fork arrest at sites of UV damage (Boyer et al., 1990; Cordeiro-Stone et al., 1997). S-phase progression is delayed in Pol η-deficient XP30RO cells following treatment with UV or cisplatin, and this effect can be reversed by expression of Pol η from an inducible promoter (Cruet-Hennequart et al., 2006; Cruet-Hennequart et al., 2008). ssDNA generated at stalled replication forks activates ATR in an ATR-interacting protein (ATRIP)- and RPA-dependent process (Binz et al., 2004; Zou and Elledge, 2003); for more details see "Function of TopBP1 in Genome Instability" by Miiko et al. and "Eukaryotic Single-Stranded DNA Binding Proteins and Genomic Stability" by Broderick et al., this book). RPA, the major ssDNA binding protein in eukaryotic cells, binds to ssDNA generated after replication stress (Binz et al., 2004). Following DNA damage the RPA2 subunit of the heterotrimeric RPA complex is phosphorylated on a number of N-terminal sites by PIKKs (Carty et al., 1994; Oakley et al., 2001; Oakley et al., 2003; Zernik-Kobak et al., 1997; Liu and Weaver, 1993; Olson et al., 2006; Patrick et al., 2005). ATR signaling is increased in UV- and cisplatin-treated Pol η-deficient human cells lines, as shown by increased phosphorylation of serine 33 in the RPA2 subunit of trimeric RPA, a known ATR phosphorylation site (Bomgarden et al., 2006; Cruet-Hennequart et al., 2006). ATR mediated phosphorylation of the cell cycle checkpoint kinase Chk1 is enhanced in Pol η-deficient cells (Bomgarden et al., 2006; Cruet-Hennequart et al., 2006). ATR-mediated phosphorylation of Chk1 leads to inhibition of both replication fork progression and the firing of new replication origins (Paulsen and Cimprich, 2007), and inhibition of cell cycle progression by phosphorylation and inactivation of the Cdk activator Cdc25A (Xiao et al., 2003).

In the absence of Pol η in XPV cell lines, replication arrest following UV radiation or cisplatin not only leads to activation of the ATR-mediated checkpoint, but also to the generation of DNA strand breaks and activation of ATM and DNA-PK, as evidenced by enhanced phosphorylation of key substrates including RPA2, H2AX and Nbs1 in Pol η-deficient cells (Cruet-Hennequart et al., 2006; Cruet-Hennequart et al., 2008). Using specific inhibitors of ATM and DNA-PK, UV- and cisplatin-induced phosphorylation of RPA2 on serines 4 and 8 in Pol η-deficient cells was found to be dependent on DNA-PK rather than ATM (Cruet-Hennequart et al., 2006, 2008). DNA-PK-dependent RPA2 hyperphosphorylation, by reducing the affinity of RPA for cisplatin-damaged DNA, and altering its interaction with key protein partners (Patrick et al., 2005; Wu et al., 2005), may be important in the processing of strand breaks generated by collapse of replication forks arrested for a prolonged period in the absence of Pol η (Cruet-Hennequart et al., 2006, 2008).

Extended replication arrest in Pol η-deficient cells following UV exposure leads to DNA strand breaks as measured by formation of γ-H2AX foci (Limoli et al., 2002a, 2000; Cruet-Hennequart et al., 2006). Homologous recombination is also activated in XPV cells after DNA damage (Limoli et al., 2005, 2000, 2002b). Induction of sister chromatid exchanges following UV irradiation is greatly enhanced in SV40-transformed XPV cells (Cleaver et al., 1999). The p53-status of Pol η-deficient cells may also influence the response to replication arrest (Cleaver

et al., 2002b; Limoli et al., 2002a, 2000, 2002b; Thakur et al., 2001; Limoli et al., 2005). Consistent with this, knockdown of Pol η using siRNA in cell lines with different p53 backgrounds showed that Pol η participates in p53 activation after camptothecin and IR-induced damage (Liu and Chen, 2006), while expression of p53 and the cell cycle inhibitor p21 regulates the extent of TLS in lung cancer cell lines (Avkin et al., 2006). The relationship between p53 status, Pol η expression and TLS in response to replication-blocking lesions requires further investigation.

Regulation of Pol η Expression

Given that Pol η is a low fidelity DNA polymerase during replication of undamaged DNA, but is required to allow TLS and replication fork progression at sites of DNA damage, the in vivo activity of Pol η needs to be tightly regulated. In general, *POLH* mRNA appears to be constitutively expressed in mammalian cells (Thakur et al., 2001). Yamada et al. (2000) showed that mouse *POLH* mRNA was not induced by UV irradiation, but increased at the onset of DNA synthesis, suggesting that expression of *POLH* is dependent on cell proliferation. *POLH* mRNA levels were elevated in more highly proliferating mouse tissues, including testis, thymus, liver and skin consistent with a requirement for Pol η in cells undergoing DNA replication (Yamada et al., 2000). Human *POLH* mRNA expression was detected in most tissues examined, except for very low or undetectable levels in peripheral lymphocytes, fetal spleen, and adult muscle (Thakur et al., 2001). An alternatively spliced form of the *POLH* transcript lacking exon 2, has also been identified, and comprises almost half of the *POLH* mRNA expressed in the testis and fetal liver (Thakur et al., 2001). The alternatively spliced form is also detectable in human skin tumors (Flanagan et al., 2007); however, the biological significance of the alternatively spliced form is not understood. Pol η protein is also expressed in skin tumor tissue (Flanagan et al., 2007). There is some evidence that human *POLH* gene expression is inducible following DNA damage. *POLH* mRNA expression was induced by cisplatin in three of five human non-small cell lung cancer lines examined, and the level of expression was associated with the sensitivity of the cell lines to cisplatin (Ceppi et al., 2009). A p53-binding site has been identified in the promoter of human *POLH*, and *POLH* mRNA expression can be up-regulated in a p53-dependent manner following ionizing radiation or camptothecin treatment (Liu and Chen, 2006).

In *S. cerevisiae*, the level of Pol η protein is regulated by proteolysis, through poly-ubiquitination of the protein and proteasomal degradation (Skoneczna et al., 2007). Following UV-irradiation, Pol η protein is stabilized and levels increase (Skoneczna et al., 2007). In *C. elegans* embryos, which are very resistant to DNA damage, Pol η protein is degraded following damage through CRL4-Cdt2-mediated proteolysis (Kim and Michael, 2008). This process may be important in removal of Pol η protein from sites of DNA damage once it has carried out TLS (Kim and Michael, 2008). While human Pol η is ubiquitinated (Bienko et al., 2005), the role

of regulated proteolysis in controlling the level of Pol η protein in human cells remains to be determined. Phosphorylation of human Pol η in an ATR- and protein kinase C (PKC)-dependent manner may also play a role in regulating Pol η activity in human cells (Chen et al., 2008). Clearly, further research is required in order to better understand how Pol η protein abundance and activity is regulated both in unstressed human cells and following DNA damage.

Overexpression of specialized DNA polymerases is a feature of many cancers (Albertella et al., 2005b). Given the role of Pol η in TLS at sites of DNA damage, and the skin cancer susceptibility of XPV patients lacking functional Pol η, the sequence of the coding exons of the *POLH* gene, and expression of *POLH* mRNA has been characterized in a series of normal skin samples and skin tumor tissues (Flanagan et al., 2007; Glick et al., 2006). No sequence changes specifically associated with skin tumors were detected in *POLH* DNA in any of the samples analyzed (Flanagan et al., 2007; Glick et al., 2006). However, individual tumors varied in the level of *POLH* mRNA expression when compared to the paired normal skin tissue, as determined by real-time PCR analysis, suggesting that differences in gene expression, rather than sequence changes may be the main mechanism by which *POLH* status varies between normal and skin tumors (Flanagan et al., 2007; Glick et al., 2006). *POLH* expression was found to be significantly down-regulated in human lung, and stomach cancers, but not in colorectal cancers, compared to the paired normal tissue (Pan et al., 2005). In contrast, a more recent study using real-time PCR found that *POLH* expression is down-regulated in a cohort of colorectal cancers compared to paired normal adjacent tissues (Bétous et al., 2009). A recent analysis of *POLH* mRNA levels in a series of tissues from normal individuals and from non-small cell lung cancer (NSCLC) patients, found that *POLH* expression did not differ significantly between the normal tissue and lung tumor samples (Ceppi et al., 2009). However, *POLH* expression in advanced NSCLC patients treated with platinum-based chemotherapy was found to be an independent factor associated with survival, with high *POLH* expression levels strongly associated with shorter survival (Ceppi et al., 2009). Thus, it may be of interest to further characterise the relationship between *POLH* gene expression, Pol η protein levels and the response of other tumors to platinum-based DNA damage, to determine whether higher Pol η expression is associated with increased tolerance of DNA damage induced by chemotherapeutic agents.

Concluding Remarks

DNA polymerase η plays a key role in translesion synthesis at UV-induced DNA damage. Since the original characterization of the protein in human cells, and the identification of *POLH* gene mutations as the cause of the skin cancer-prone disease xeroderma pigmentosum variant, considerable progress has been made in elucidating the structure and function of Pol η. The demonstration that Pol η plays a role in bypass of platinum-induced DNA adducts has increased interest in the role of the

protein in DNA damage tolerance in tumor cells. Further research is required into the regulation of Pol η expression, the role of Pol η in normal cells, for example in DNA replication at altered DNA structures in the genome, and its role in recombination. Further insights into the coordination of multiple TLS DNA polymerases and accessory proteins during TLS on the leading and lagging strand, and the integration of TLS with the DDR in human cells, are also required. Finally, inhibition of TLS mediated by Pol η or other Y-family DNA polymerases might provide a mechanism to potentiate the effects of certain DNA damaging agents used in cancer treatment.

References

Aabo, K., Adams, M., Adnitt, P., Alberts, D. S., Athanazziou, A., Barley, V., Bell, D. R., Bianchi, U., Bolis, G., Brady, M. F., Brodovsky, H. S., Bruckner, H., Buyse, M., Canetta, R., Chylak, V., Cohen, C. J., Colombo, N., Conte, P. F., Crowther, D., Edmonson, J. H., Gennatas, C., Gilbey, E., Gore, M., Guthrie, D., and Yeap, B. Y. (1998) Chemotherapy in advanced ovarian cancer: four systematic meta-analyses of individual patient data from 37 randomized trials. Advanced Ovarian Cancer Trialists' Group. *Br J Cancer*, 78, 1479–1487.

Abraham, R. T. (2004) PI 3-kinase related kinases: 'big' players in stress-induced signaling pathways. *DNA Repair (Amst)*, 3, 883–887.

Acharya, N., Yoon, J. H., Gali, H., Unk, I., Haracska, L., Johnson, R. E., Hurwitz, J., Prakash, L., and Prakash, S. (2008) Roles of PCNA-binding and ubiquitin-binding domains in human DNA polymerase eta in translesion DNA synthesis. *Proc Natl Acad Sci USA*, 105, 17724–17729.

Albertella, M. R., Green, C. M., Lehmann, A. R., and O'Connor, M. J. (2005a) A role for polymerase eta in the cellular tolerance to cisplatin-induced damage. *Cancer Res*, 65, 9799–9806.

Albertella, M. R., Lau, A., and O'Connor, M. J. (2005b) The overexpression of specialized DNA polymerases in cancer. *DNA Repair (Amst)*, 4, 583–593.

Alt, A., Lammens, K., Chiocchini, C., Lammens, A., Pieck, J. C., Kuch, D., Hopfner, K. P., and Carell, T. (2007) Bypass of DNA lesions generated during anticancer treatment with cisplatin by DNA polymerase eta. *Science*, 318, 967–970.

Arlett, C. F., Harcourt, S. A., and Broughton, B. C. (1975) The influence of caffeine on cell survival in excision-proficient and excision-deficient xeroderma pigmentosum and normal human cell strains following ultraviolet-light irradiation. *Mutat Res*, 33, 341–346.

Avkin, S., Goldsmith, M., Velasco-Miguel, S., Geacintov, N., Friedberg, E. C., and Livneh, Z. (2004) Quantitative analysis of translesion DNA synthesis across a Benzo[a]pyrene-Guanine adduct in mammalian cells: the role of DNA polymerase kappa. *J Biol Chem*, 279, 53298–53305.

Avkin, S., Sevilya, Z., Toube, L., Geacintov, N., Chaney, S. G., Oren, M., and Livneh, Z. (2006) p53 and p21 regulate error-prone DNA repair to yield a lower mutation load. *Mol Cell*, 22, 407–413.

Bakkenist, C. J. and Kastan, M. B. (2004) Initiating cellular stress responses. *Cell*, 118, 9–17.

Bambara, R. A., Murante, R. S., and Henricksen, L. A. (1997) Enzymes and reactions at the eukaryotic DNA replication fork. *J Biol Chem*, 272, 4647–4650.

Bartek, J., Lukas, J., and Bartkova, J. (2007) DNA damage response as an anti-cancer barrier: damage threshold and the concept of 'conditional haploinsufficiency'. *Cell Cycle*, 6, 2344–2347.

Bassett, E., King, N. M., Bryant, M. F., Hector, S., Pendyala, L., Chaney, S. G., and Cordeiro-Stone, M. (2004) The role of DNA polymerase eta in translesion synthesis past platinum-DNA adducts in human fibroblasts. *Cancer Res*, 64, 6469–6475.

Bassett, E., Vaisman, A., Havener, J. M., Masutani, C., Hanaoka, F., and Chaney, S. G. (2003) Efficiency of extension of mismatched primer termini across from cisplatin and oxaliplatin adducts by human DNA polymerases beta and eta in vitro. *Biochemistry*, 42, 14197–14206.

Bétous, R., Rey, L., Wang, G., Pillaire, M.-J., Puget, N., Selves, J., Biard, D., Shin-Ya, K., Vasquez, K., Cazaux, C., and Hoffmann, J.-S. (2009) Role of TLS DNA polymerases eta and kappa in processing naturally occurring structured DNA in human cells. *Mol Carcinog*, 48, 369–378.

Bienko, M., Green, C. M., Crosetto, N., Rudolf, F., Zapart, G., Coull, B., Kannouche, P., Wider, G., Peter, M., Lehmann, A. R., Hofmann, K., and Dikic, I. (2005) Ubiquitin-binding domains in Y-family polymerases regulate translesion synthesis. *Science*, 310, 1821–1824.

Binz, S. K., Sheehan, A. M., and Wold, M. S. (2004) Replication protein A phosphorylation and the cellular response to DNA damage. *DNA Repair (Amst)*, 3, 1015–1024.

Bomar, M. G., Pai, M. T., Tzeng, S. R., Li, S. S., and Zhou, P. (2007) Structure of the ubiquitin-binding zinc finger domain of human DNA Y-polymerase eta. *EMBO Rep*, 8, 247–251.

Bomgarden, R. D., Lupardus, P. J., Soni, D. V., Yee, M. C., Ford, J. M., and Cimprich, K. A. (2006) Opposing effects of the UV lesion repair protein XPA and UV bypass polymerase eta on ATR checkpoint signaling. *EMBO J*, 25, 2605–2614.

Boyer, J. C., Kaufmann, W. K., Brylawski, B. P., and Cordeiro-Stone, M. (1990) Defective postreplication repair in xeroderma pigmentosum variant fibroblasts. *Cancer Res*, 50, 2593–2598.

Branzei, D. and Foiani, M. (2007) Interplay of replication checkpoints and repair proteins at stalled replication forks. *DNA Repair (Amst)*, 6, 994–1003.

Branzei, D. and Foiani, M. (2008) Regulation of DNA repair throughout the cell cycle. *Nat Rev Mol Cell Biol*, 9, 297–308.

Burgers, P. M., Koonin, E. V., Bruford, E., Blanco, L., Burtis, K. C., Christman, M. F., Copeland, W. C., Friedberg, E. C., Hanaoka, F., Hinkle, D. C., Lawrence, C. W., Nakanishi, M., Ohmori, H., Prakash, L., Prakash, S., Reynaud, C. A., Sugino, A., Todo, T., Wang, Z., Weill, J. C., and Woodgate, R. (2001) Eukaryotic DNA polymerases: proposal for a revised nomenclature. *J Biol Chem*, 276, 43487–43490.

Carty, M. P., Glynn, M., Maher, M., Smith, T., Yao, J., Dixon, K., McCann, J., Rynn, L., and Flanagan, A. (2003) The RAD30 cancer susceptibility gene. *Biochem Soc Trans*, 31, 252–256.

Carty, M. P., Zernik-Kobak, M., McGrath, S., and Dixon, K. (1994) UV light-induced DNA synthesis arrest in HeLa cells is associated with changes in phosphorylation of human single-stranded DNA-binding protein. *EMBO J*, 13, 2114–2123.

Casali, P., Pal, Z., Xu, Z., and Zan, H. (2006) DNA repair in antibody somatic hypermutation. *Trends Immunol*, 27, 313–321.

Ceppi, P., Novello, S., Cambieri, A., Longo, M., Monica, V., Lo Iacono, M., Giaj-Levra, M., Saviozzi, S., Volante, M., Papotti, M., and Scagliotti, G. (2009) Polymerase eta mRNA expression predicts survival of non-small cell lung cancer patients treated with platinum-based chemotherapy. *Clin Cancer Res*, 15, 1039–1045.

Chaney, S. G., Campbell, S. L., Bassett, E., and Wu, Y. (2005) Recognition and processing of cisplatin- and oxaliplatin-DNA adducts. *Crit Rev Oncol Hematol*, 53, 3–11.

Chang, D. J. and Cimprich, K. A. (2009) DNA damage tolerance: when it's OK to make mistakes. *Nat Chem Biol*, 5, 82–90.

Chen, Y. W., Cleaver, J. E., Hanaoka, F., Chang, C. F., and Chou, K. M. (2006) A novel role of DNA polymerase eta in modulating cellular sensitivity to chemotherapeutic agents. *Mol Cancer Res*, 4, 257–265.

Chen, Y. W., Cleaver, J. E., Hatahet, Z., Honkanen, R. E., Chang, J. Y., Yen, Y., and Chou, K. M. (2008) Human DNA polymerase eta activity and translocation is regulated by phosphorylation. *Proc Natl Acad Sci USA*, 105, 16578–16583.

Cimprich, K. A. and Cortez, D. (2008) ATR: an essential regulator of genome integrity. *Nat Rev Mol Cell Biol*, 9, 616–627.

Cleaver, J. (1972) Xeroderma pigmentosum: variants with normal DNA repair and normal sensitivity to ultraviolet light. *J Invest Dermatol*, 58, 124–128.

Cleaver, J. E., Afzal, V., Feeney, L., McDowell, M., Sadinski, W., Volpe, J. P., Busch, D. B., Coleman, D. M., Ziffer, D. W., Yu, Y., Nagasawa, H., and Little, J. B. (1999) Increased ultraviolet sensitivity and chromosomal instability related to P53 function in the xeroderma pigmentosum variant. *Cancer Res*, 59, 1102–1108.

Cleaver, J. E., Bartholomew, J., Char, D., Crowley, E., Feeney, L., and Limoli, C. L. (2002a) Polymerase eta and p53 jointly regulate cell survival, apoptosis and Mre11 recombination during S phase checkpoint arrest after UV irradiation. *DNA Repair*, 1, 41–57.

Cleaver, J. E., Bartholomew, J., Char, D., Crowley, E., Feeney, L., and Limoli, C. L. (2002b) Polymerase eta and p53 jointly regulate cell survival, apoptosis and Mre11 recombination during S phase checkpoint arrest after UV irradiation. *DNA Repair (Amst)*, 1, 41–57.

Cordeiro-Stone, M., Makhov, A. M., Zaritskaya, L. S., and Griffith, J. D. (1999) Analysis of DNA replication forks encountering a pyrimidine dimer in the template to the leading strand. *J Mol Biol*, 289, 1207–1218.

Cordeiro-Stone, M. and Nikolaishvili-Feinberg, N. (2002) Asymmetry of DNA replication and translesion synthesis of UV-induced thymine dimers. *Mutat Res*, 510, 91–106.

Cordeiro-Stone, M., Zaritskaya, L. S., Price, L. K., and Kaufmann, W. K. (1997) Replication fork bypass of a pyrimidine dimer blocking leading strand DNA synthesis. *J Biol Chem*, 272, 13945–13954.

Cruet-Hennequart, S., Coyne, S., Glynn, M. T., Oakley, G. G., and Carty, M. P. (2006) UV-induced RPA phosphorylation is increased in the absence of DNA polymerase eta and requires DNA-PK. *DNA Repair (Amst)*, 5, 491–504.

Cruet-Hennequart, S., Glynn, M. T., Murillo, L. S., Coyne, S., and Carty, M. P. (2008) Enhanced DNA-PK-mediated RPA2 hyperphosphorylation in DNA polymerase eta-deficient human cells treated with cisplatin and oxaliplatin. *DNA Repair (Amst)*, 7, 582–596.

Davies, A. A., Huttner, D., Daigaku, Y., Chen, S., and Ulrich, H. D. (2008) Activation of ubiquitin-dependent DNA damage bypass is mediated by replication protein A. *Mol Cell*, 29, 625–636.

de Feraudy, S., Limoli, C. L., Giedzinski, E., Karentz, D., Marti, T. M., Feeney, L., and Cleaver, J. E. (2007) Pol eta is required for DNA replication during nucleotide deprivation by hydroxyurea. *Oncogene*, 26, 5713–5721.

Diaz, M. and Lawrence, C. (2005) An update on the role of translesion synthesis DNA polymerases in Ig hypermutation. *Trends Immunol*, 26, 215–220.

Durocher, D. and Jackson, S. P. (2001) DNA-PK, ATM and ATR as sensors of DNA damage: variations on a theme? *Curr Opin Cell Biol*, 13, 225–231.

Edmunds, C. E., Simpson, L. J., and Sale, J. E. (2008) PCNA ubiquitination and REV1 define temporally distinct mechanisms for controlling translesion synthesis in the Avian cell line DT40. *Mol Cell*, 30, 519–529.

Flanagan, A. M., Rafferty, G., O'Neill, A., Rynne, L., Kelly, J., McCann, J., and Carty, M. P. (2007) The human POLH gene is not mutated, and is expressed in a cohort of patients with basal or squamous cell carcinoma of the skin. *Int J Mol Med*, 19, 589–596.

Friedberg, E. C. (2001) Why do cells have multiple error-prone DNA polymerases? *Environ Mol Mutagen*, 38, 105–110.

Garg, P. and Burgers, P. M. (2005) DNA polymerases that propagate the eukaryotic DNA replication fork. *Crit Rev Biochem Mol Biol*, 40, 115–128.

Gerlach, V. L., Aravind, L., Gotway, G., Schultz, R. A., Koonin, E. V., and Friedberg, E. C. (1999) Human and mouse homologs of *Escherichia coli* DinB (DNA polymerase IV), members of the UmuC/DinB superfamily. *Proc Natl Acad Sci USA*, 96, 11922–11927.

Glick, E., Chau, J. S., Vigna, K. L., McCulloch, S. D., Adman, E. T., Kunkel, T. A., and Loeb, L. A. (2003) Amino acid substitutions at conserved Tyrosine 52 alter fidelity and bypass efficiency of human DNA polymerase eta. *J Biol Chem*, 278, 19341–19346.

Glick, E., Vigna, K. L., and Loeb, L. A. (2001) Mutations in human DNA polymerase eta motif II alter bypass of DNA lesions. *EMBO J*, 20, 7303–7312.

Glick, E., White, L. M., Elliott, N. A., Berg, D., Kiviat, N. B., and Loeb, L. A. (2006) Mutations in DNA polymerase eta are not detected in squamous cell carcinoma of the skin. *Int J Cancer*, 119, 2225–2227.

Gueranger, Q., Stary, A., Aoufouchi, S., Faili, A., Sarasin, A., Reynaud, C.-A., and Weill, J.-C. (2008) Role of DNA polymerases eta, iota and zeta in UV resistance and UV-induced mutagenesis in a human cell line. *DNA Repair (Amst)*, 7, 1551–1562.

Haracska, L., Johnson, R. E., Unk, I., Phillips, B., Hurwitz, J., Prakash, L., and Prakash, S. (2001a) Physical and functional interactions of human DNA polymerase eta with PCNA. *Mol Cell Biol*, 21, 7199–7206.

Haracska, L., Johnson, R. E., Unk, I., Phillips, B. B., Hurwitz, J., Prakash, L., and Prakash, S. (2001b) Targeting of human DNA polymerase iota to the replication machinery via interaction with PCNA. *Proc Natl Acad Sci USA*, 98, 14256–14261.

Haracska, L., Kondratick, C. M., Unk, I., Prakash, S., and Prakash, L. (2001c) Interaction with PCNA is essential for yeast DNA polymerase eta function. *Mol Cell*, 8, 407–415.

Haracska, L., Prakash, S., and Prakash, L. (2000a) Replication past O(6)-methylguanine by yeast and human DNA polymerase eta. *Mol Cell Biol*, 20, 8001–8007.

Haracska, L., Torres-Ramos, C. A., Johnson, R. E., Prakash, S., and Prakash, L. (2004) Opposing effects of ubiquitin conjugation and SUMO modification of PCNA on replicational bypass of DNA lesions in *Saccharomyces cerevisiae*. *Mol Cell Biol*, 24, 4267–4274.

Haracska, L., Unk, I., Johnson, R. E., Phillips, B. B., Hurwitz, J., Prakash, L., and Prakash, S. (2002) Stimulation of DNA synthesis activity of human DNA polymerase kappa by PCNA. *Mol Cell Biol*, 22, 784–791.

Haracska, L., Washington, M. T., Prakash, S., and Prakash, L. (2001d) Inefficient bypass of an abasic site by DNA polymerase eta. *J Biol Chem*, 276, 6861–6866.

Haracska, L., Yu, S. L., Johnson, R. E., Prakash, L., and Prakash, S. (2000b) Efficient and accurate replication in the presence of 7,8-dihydro-8-oxoguanine by DNA polymerase eta. *Nat Genet*, 25, 458–461.

Harper, J. W. and Elledge, S. J. (2007) The DNA damage response: ten years after. *Mol Cell*, 28, 739–745.

Hendel, A., Ziv, O., Gueranger, Q., Geacintov, N., and Livneh, Z. (2008) Reduced efficiency and increased mutagenicity of translesion DNA synthesis across a TT cyclobutane pyrimidine dimer, but not a TT 6-4 photoproduct, in human cells lacking DNA polymerase eta. *DNA Repair*, 7, 1636–1646.

Hishida, T., Kubota, Y., Carr, A. M., and Iwasaki, H. (2009) RAD6-RAD18-RAD5-pathway-dependent tolerance to chronic low-dose ultraviolet light. *Nature*, 457, 612–615.

Hoege, C., Pfander, B., Moldovan, G. L., Pyrowolakis, G., and Jentsch, S. (2002) RAD6-dependent DNA repair is linked to modification of PCNA by ubiquitin and SUMO. *Nature*, 419, 135–141.

Huang, T. T., Nijman, S. M. B., Mirchandani, K. D., Galardy, P. J., Cohn, M. A., Haas, W., Gygi, S. P., Ploegh, H. L., Bernards, R., and D'Andrea, A. D. (2006) Regulation of monoubiquitinated PCNA by DUB autocleavage. *Nat Cell Biol*, 8, 341–347.

Indiani, C., McInerney, P., Georgescu, R., Goodman, M. F., and O'Donnell, M. (2005) A sliding-clamp toolbelt binds high- and low-fidelity DNA polymerases simultaneously. *Mol Cell*, 19, 805–815.

Johnson, R. E., Haracska, L., Prakash, S., and Prakash, L. (2001) Role of DNA polymerase zeta in the bypass of a (6-4) TT photoproduct. *Mol Cell Biol*, 21, 3558–3563.

Johnson, R. E., Kondratick, C. M., Prakash, S., and Prakash, L. (1999a) hRAD30 mutations in the variant form of xeroderma pigmentosum. *Science*, 285, 263–265.

Johnson, R. E., Prakash, S., and Prakash, L. (1999b) Efficient bypass of a thymine-thymine dimer by yeast DNA polymerase, Pol-eta. *Science*, 283, 1001–1004.

Johnson, R. E., Trincao, J., Aggarwal, A. K., Prakash, S., and Prakash, L. (2003) Deoxynucleotide triphosphate binding mode conserved in Y family DNA polymerases. *Mol Cell Biol*, 23, 3008–3012.

Kannouche, P., Broughton, B. C., Volker, M., Hanaoka, F., Mullenders, L. H., and Lehmann, A. R. (2001) Domain structure, localization, and function of DNA polymerase eta, defective in xeroderma pigmentosum variant cells. *Genes Dev*, 15, 158–172.

Kannouche, P., Fernandez de Henestrosa, A. R., Coull, B., Vidal, A. E., Gray, C., Zicha, D., Woodgate, R., and Lehmann, A. R. (2003) Localization of DNA polymerases eta and iota to the replication machinery is tightly co-ordinated in human cells. *EMBO J*, 22, 1223–1233.

Kannouche, P. L., Wing, J., and Lehmann, A. R. (2004) Interaction of human DNA polymerase eta with monoubiquitinated PCNA: a possible mechanism for the polymerase switch in response to DNA damage. *Mol Cell*, 14, 491–500.

Kartalou, M. and Essigmann, J. M. (2001) Recognition of cisplatin adducts by cellular proteins. *Mutat Res*, 478, 1–21.

Kawamoto, T., Araki, K., Sonoda, E., Yamashita, Y. M., Harada, K., Kikuchi, K., Masutani, C., Hanaoka, F., Nozaki, K., Hashimoto, N., and Takeda, S. (2005) Dual roles for DNA polymerase eta in homologous DNA recombination and translesion DNA synthesis. *Mol Cell*, 20, 793–799.

Kelland, L. (2007a) Broadening the clinical use of platinum drug-based chemotherapy with new analogues. Satraplatin and picoplatin. *Expert Opin Investig Drugs*, 16, 1009–1021.

Kelland, L. (2007b) The resurgence of platinum-based cancer chemotherapy. *Nat Rev Cancer*, 7, 573–584.

Kelman, Z. and Hurwitz, J. (1998) Protein-PCNA interactions: A DNA-scanning mechanism? *Trends Biochem Sci*, 23, 236–238.

Kim, S.-H. and Michael, W. M. (2008) Regulated proteolysis of DNA polymerase eta during the DNA-damage response in *C. elegans*. *Mol Cell*, 32, 757–766.

Kondratick, C. M., Washington, M. T., Prakash, S., and Prakash, L. (2001) Acidic residues critical for the activity and biological function of yeast DNA polymerase eta. *Mol Cell Biol*, 21, 2018–2025.

Lawrence, C. W. and Maher, V. M. (2001) Eukaryotic mutagenesis and translesion replication dependent on DNA polymerase zeta and Rev1 protein. *Biochem Soc Trans*, 29, 187–191.

Lehmann, A. R., Kirk-Bell, C. F., Arlett, C. F., Paterson, M. C., Lohman, P. H. M., de Weerd-Kastelein, E. A., and Bootsma, D. (1975) Xeroderma pigmentosum cells with normal levels of excision repair have a defect in DNA synthesis after UV-irradiation. *Proc Natl Acad Sci USA*, 72, 219–223.

Lehmann, A. R., Niimi, A., Ogi, T., Brown, S., Sabbioneda, S., Wing, J. F., Kannouche, P. L., and Green, C. M. (2007) Translesion synthesis: Y-family polymerases and the polymerase switch. *DNA Repair (Amst)*, 6, 891–899.

Limoli, C. L., Giedzinski, E., Bonner, W. M., and Cleaver, J. E. (2002a) UV-induced replication arrest in the xeroderma pigmentosum variant leads to DNA double-strand breaks, gamma-H2AX formation, and Mre11 relocalization. *Proc Natl Acad Sci USA*, 99, 233–238.

Limoli, C. L., Giedzinski, E., and Cleaver, J. E. (2005) Alternative recombination pathways in UV-irradiated XP variant cells. *Oncogene*, 24, 3708–3714.

Limoli, C. L., Giedzinski, E., Morgan, W. F., and Cleaver, J. E. (2000) Inaugural article: polymerase eta deficiency in the xeroderma pigmentosum variant uncovers an overlap between the S phase checkpoint and double-strand break repair. *Proc Natl Acad Sci USA*, 97, 7939–7946.

Limoli, C. L., Laposa, R., and Cleaver, J. E. (2002b) DNA replication arrest in XP variant cells after UV exposure is diverted into an Mre11-dependent recombination pathway by the kinase inhibitor wortmannin. *Mutat Res*, 510, 121–129.

Lin, Q., Clark, A. B., McCulloch, S. D., Yuan, T., Bronson, R. T., Kunkel, T. A., and Kucherlapati, R. (2006) Increased susceptibility to UV-induced skin carcinogenesis in polymerase eta-deficient mice. *Cancer Res*, 66, 87–94.

Ling, H., Boudsocq, F., Woodgate, R., and Yang, W. (2001) Crystal structure of a Y-family DNA polymerase in action: a mechanism for error-prone and lesion-bypass replication. *Cell*, 107, 91–102.

Liu, G. and Chen, X. (2006) DNA polymerase eta, the product of the xeroderma pigmentosum variant gene and a target of p53, modulates the DNA damage checkpoint and p53 activation. *Mol Cell Biol*, 26, 1398–1413.

Liu, V. F. and Weaver, D. T. (1993) The ionizing radiation-induced replication protein A phosphorylation response differs between ataxia telangiectasia and normal human cells. *Mol Cell Biol*, 13, 7222–7231.

Masuda, K., Ouchida, R., Hikida, M., Kurosaki, T., Yokoi, M., Masutani, C., Seki, M., Wood, R. D., Hanaoka, F., and O-Wang, J. (2007) DNA polymerases eta and theta function in the same genetic pathway to generate mutations at A/T during somatic hypermutation of Ig genes. *J Biol Chem*, 282, 17387–17394.

Masutani, C., Araki, M., Yamada, A., Kusumoto, R., Nogimori, T., Maekawa, T., Iwai, S., and Hanaoka, F. (1999a) Xeroderma pigmentosum variant (XP-V) correcting protein from HeLa cells has a thymine dimer bypass DNA polymerase activity. *EMBO J*, 18, 3491–3501.

Masutani, C., Kusumoto, R., Iwai, S., and Hanaoka, F. (2000) Mechanisms of accurate translesion synthesis by human DNA polymerase eta. *EMBO J*, 19, 3100–3109.

Masutani, C., Kusumoto, R., Yamada, A., Dohmae, N., Yokoi, M., Yuasa, M., Araki, M., Iwai, S., Takio, K., and Hanaoka, F. (1999b) The XPV (xeroderma pigmentosum variant) gene encodes human DNA polymerase eta. *Nature*, 399, 700–704.

Matsuoka, S., Ballif, B. A., Smogorzewska, A., McDonald, E. R., III, Hurov, K. E., Luo, J., Bakalarski, C. E., Zhao, Z., Solimini, N., Lerenthal, Y., Shiloh, Y., Gygi, S. P., and Elledge, S. J. (2007) ATM and ATR substrate analysis reveals extensive protein networks responsive to DNA damage. *Science*, 316, 1160–1166.

McCulloch, S. D., Kokoska, R. J., Masutani, C., Iwai, S., Hanaoka, F., and Kunkel, T. A. (2004) Preferential cis-syn thymine dimer bypass by DNA polymerase eta occurs with biased fidelity. *Nature*, 428, 97–100.

McCulloch, S. D. and Kunkel, T. A. (2008) The fidelity of DNA synthesis by eukaryotic replicative and translesion synthesis polymerases. *Cell Res*, 18, 148–161.

McDonald, J. P., Levine, A. S., and Woodgate, R. (1997) The *Saccharomyces cerevisiae* RAD30 gene, a homologue of *Escherichia coli* dinB and umuc, is DNA damage inducible and functions in a novel error-free postreplication repair mechanism. *Genetics*, 147, 1557–1568.

McDonald, J. P., Rapic-Otrin, V., Epstein, J. A., Broughton, B. C., Wang, X., Lehmann, A. R., Wolgemuth, D. J., and Woodgate, R. (1999) Novel human and mouse homologs of *Saccharomyces cerevisiae* DNA polymerase eta. *Genomics*, 60, 20–30.

McIlwraith, M. J., Vaisman, A., Liu, Y., Fanning, E., Woodgate, R., and West, S. C. (2005) Human DNA polymerase eta promotes DNA synthesis from strand invasion intermediates of homologous recombination. *Mol Cell*, 20, 783–792.

Minko, I. G., Washington, M. T., Kanuri, M., Prakash, L., Prakash, S., and Lloyd, R. S. (2003) Translesion synthesis past acrolein-derived DNA adduct, gamma-hydroxypropano-deoxyguanosine, by yeast and human DNA polymerase eta. *J Biol Chem*, 278, 784–790.

Minko, I. G., Washington, M. T., Prakash, L., Prakash, S., and Lloyd, R. S. (2001) Translesion DNA synthesis by yeast DNA polymerase eta on templates containing N2-Guanine adducts of 1,3-Butadiene metabolites. *J Biol Chem*, 276, 2517–2522.

Nasheuer, H. P., Pospiech, H., and Syväoja, J. (2007) Progress towards the anatomy of the eukaryotic DNA replication fork. In: Lankenau, D. H. (Ed.) *Genome Integrity: Facets and Perspectives*, Genome Dynamics & Stability, Vol. 1, Springer, Berlin, Heidelberg, New York, pp. 27–68.

Nasheuer, H. P., Smith, R., Bauerschmidt, C., Grosse, F., and Weisshart, K. (2002) Initiation of eukaryotic DNA replication: regulation and mechanisms. *Prog Nucleic Acid Res Mol Biol*, 72, 41–94.

Nelson, J. R., Lawrence, C. W., and Hinkle, D. C. (1996) Deoxycytidyl transferase activity of yeast REV1 protein. *Nature*, 382, 729–731.

Oakley, G. G., Loberg, L. I., Yao, J., Risinger, M. A., Yunker, R. L., Zernik-Kobak, M., Khanna, K. K., Lavin, M. F., Carty, M. P., and Dixon, K. (2001) UV-induced hyperphosphorylation of replication protein A depends on DNA replication and expression of ATM protein. *Mol Biol Cell*, 12, 1199–1213.

Oakley, G. G., Patrick, S. M., Yao, J., Carty, M. P., Turchi, J. J., and Dixon, K. (2003) RPA phosphorylation in mitosis alters DNA binding and protein–protein interactions. *Biochemistry*, 42, 3255–3264.

Ogi, T., Kato, T. J., Kato, T., and Ohmori, H. (1999) Mutation enhancement by DINB1, a mammalian homologue of the *Escherichia coli* mutagenesis protein DinB. *Genes Cells*, 4, 607–618.

Olson, E., Nievera, C. J., Klimovich, V., Fanning, E., and Wu, X. (2006) RPA2 is a direct downstream target for ATR to regulate the S-phase checkpoint. *J Biol Chem*, 281, 39517–39533.

Pan, Q., Fang, Y., Xu, Y., Zhang, K., and Hu, X. (2005) Down-regulation of DNA polymerases kappa, eta, iota, and zeta in human lung, stomach, and colorectal cancers. *Cancer Lett*, 217, 139–147.

Patrick, S. M., Oakley, G. G., Dixon, K., and Turchi, J. J. (2005) DNA damage induced hyperphosphorylation of replication protein A. 2. Characterization of DNA binding activity, protein interactions, and activity in DNA replication and repair. *Biochemistry*, 44, 8438–8448.

Paulsen, R. D. and Cimprich, K. A. (2007) The ATR pathway: fine-tuning the fork. *DNA Repair*, 6, 953–966.

Plosky, B. S., Vidal, A. E., Fernandez de Henestrosa, A. R., McLenigan, M. P., McDonald, J. P., Mead, S., and Woodgate, R. (2006) Controlling the subcellular localization of DNA polymerases iota and eta via interactions with ubiquitin. *EMBO J*, 25, 2847–2855.

Prakash, S., Johnson, R. E., and Prakash, L. (2005) Eukaryotic translesion synthesis DNA polymerases: specificity of structure and function. *Annu Rev Biochem*, 74, 317–353.

Sarkaria, J. N., Busby, E. C., Tibbetts, R. S., Roos, P., Taya, Y., Karnitz, L. M., and Abraham, R. T. (1999) Inhibition of ATM and ATR kinase activities by the radiosensitizing agent, caffeine. *Cancer Res*, 59, 4375–4382.

Sarkaria, J. N., Tibbetts, R. S., Busby, E. C., Kennedy, A. P., Hill, D. E., and Abraham, R. T. (1998) Inhibition of phosphoinositide 3-kinase related kinases by the radiosensitizing agent wortmannin. *Cancer Res*, 58, 4375–4382.

Shachar, S., Ziv, O., Avkin, S., Adar, S., Wittschieben, J., Reiszner, T., Chaney, S., Friedberg, E. C., Wang, Z., Carell, T., Geacintov, N., and Livneh, Z. (2009) Two-polymerase mechanisms dictate error-free and error-prone translesion DNA synthesis in mammals. *EMBO J*, 28, 383–393.

Shrivastav, M., de Haro, L. P., and Nickoloff, J. A. (2008) Regulation of DNA double-strand break repair pathway choice. *Cell Res*, 18, 134–147.

Skoneczna, A., McIntyre, J., Skoneczny, M., Policinska, Z., and Sledziewska-Gojska, E. (2007) Polymerase eta is a short-lived, proteasomally degraded protein that is temporarily stabilized following UV irradiation in *Saccharomyces cerevisiae*. *J Mol Biol*, 366, 1074–1086.

Stary, A., Kannouche, P., Lehmann, A. R., and Sarasin, A. (2003) Role of DNA polymerase eta in the UV mutation spectrum in human cells. *J Biol Chem*, 278, 18767–18775.

Stelter, P. and Ulrich, H. D. (2003) Control of spontaneous and damage-induced mutagenesis by SUMO and ubiquitin conjugation. *Nature*, 425, 188–191.

Szuts, D., Marcus, A. P., Himoto, M., Iwai, S., and Sale, J. E. (2008) REV1 restrains DNA polymerase zeta to ensure frame fidelity during translesion synthesis of UV photoproducts in vivo. *Nucleic Acids Res*, 36, 6767–6780.

Thakur, M., Wernick, M., Collins, C., Limoli, C. L., Crowley, E., and Cleaver, J. E. (2001) DNA polymerase eta undergoes alternative splicing, protects against UV sensitivity and apoptosis, and suppresses Mre11-dependent recombination. *Genes Chromosomes Cancer*, 32, 222–235.

Trincao, J., Johnson, R. E., Escalante, C. R., Prakash, S., Prakash, L., and Aggarwal, A. K. (2001) Structure of the catalytic core of *S. cerevisiae* DNA polymerase eta: implications for translesion DNA synthesis. *Mol Cell*, 8, 417–426.

Tung, B. S., McGregor, W. G., Wang, Y. C., Maher, V. M., and McCormick, J. J. (1996) Comparison of the rate of excision of major UV photoproducts in the strands of the human HPRT gene of normal and xeroderma pigmentosum variant cells. *Mutat Res*, 362, 65–74.

Vaisman, A., Lehmann, A. R., and Woodgate, R. (2004) DNA polymerases eta and iota. *Adv Protein Chem*, 69, 205–228.

Vaisman, A., Masutani, C., Hanaoka, F., and Chaney, S. G. (2000) Efficient translesion replication past oxaliplatin and cisplatin GpG adducts by human DNA polymerase eta. *Biochemistry*, 39, 4575–4580.

Vreeswijk, M. P., van Hoffen, A., Westland, B. E., Vrieling, H., van Zeeland, A. A., and Mullenders, L. H. (1994) Analysis of repair of cyclobutane pyrimidine dimers and pyrimidine 6-4 pyrimidone photoproducts in transcriptionally active and inactive genes in Chinese hamster cells. *J Biol Chem*, 269, 31858–31863.

Wang, Y., Woodgate, R., McManus, T. P., Mead, S., McCormick, J. J., and Maher, V. M. (2007) Evidence that in xeroderma pigmentosum variant cells, which lack DNA polymerase eta, DNA polymerase iota causes the very high frequency and unique spectrum of UV-induced mutations. *Cancer Res*, 67, 3018–3026.

Wu, X., Yang, Z., Liu, Y., and Zou, Y. (2005) Preferential localization of hyperphosphorylated replication protein A to double-strand break repair and checkpoint complexes upon DNA damage. *Biochem J*, 391, 473–480.

Xiao, Z., Chen, Z., Gunasekera, A. H., Sowin, T. J., Rosenberg, S. H., Fesik, S., and Zhang, H. (2003) Chk1 mediates S and G2 arrests through Cdc25A degradation in response to DNA-damaging agents. *J Biol Chem*, 278, 21767–21773.

Yamada, A., Masutani, C., Iwai, S., and Hanaoka, F. (2000) Complementation of defective translesion synthesis and UV light sensitivity in xeroderma pigmentosum variant cells by human and mouse DNA polymerase eta. *Nucleic Acids Res*, 28, 2473–2480.

Yamada, K., Takezawa, J., and Ezaki, O. (2003) Translesion replication in cisplatin-treated xeroderma pigmentosum variant cells is also caffeine-sensitive: features of the error-prone DNA polymerase(s) involved in UV-mutagenesis. *DNA Repair (Amst)*, 2, 909–924.

Yang, W. and Woodgate, R. (2007) What a difference a decade makes: insights into translesion DNA synthesis. *Proc Natl Acad Sci*, 104, 15591–15598.

Yao, J., Dixon, K., and Carty, M. P. (2001) A single (6-4) photoproduct inhibits plasmid DNA replication in xeroderma pigmentosum variant cell extracts. *Environ Mol Mutagen*, 38, 19–29.

Yuasa, M., Masutani, C., Eki, T., and Hanaoka, F. (2000) Genomic structure, chromosomal localization and identification of mutations in the xeroderma pigmentosum variant (XPV) gene. *Oncogene*, 19, 4721–4728.

Zernik-Kobak, M., Vasunia, K., Connelly, M., Anderson, C. W., and Dixon, K. (1997) Sites of UV-induced phosphorylation of the p34 subunit of replication protein A from HeLa cells. *J Biol Chem*, 272, 23896–23904.

Zhang, Y., Wu, X., Guo, D., Rechkoblit, O., Geacintov, N. E., and Wang, Z. (2002) Two-step error-prone bypass of the (+)- and (–)-trans-anti-BPDE-N2-dG adducts by human DNA polymerases eta and kappa. *Mutat Res Fundam Mol Mech Mutagen*, 510, 23–35.

Zhou, B. B. and Elledge, S. J. (2000) The DNA damage response: putting checkpoints in perspective. *Nature*, 408, 433–439.

Zhuang, Z., Johnson, R. E., Haracska, L., Prakash, L., Prakash, S., and Benkovic, S. J. (2008) Regulation of polymerase exchange between Pol eta and Pol delta by monoubiquitination of PCNA and the movement of DNA polymerase holoenzyme. *Proc Natl Acad Sci USA*, 105, 5361–5366.

Zou, L. and Elledge, S. J. (2003) Sensing DNA damage through ATRIP recognition of RPA-ssDNA complexes. *Science*, 300, 1542–1548.